THERMO-FLUID SIMULATION OF A ROTATING DISC WITH RADIAL COOLING PASSAGES

Francois Holtzhausen

B.Eng. (Mechanical)

Dissertation submitted in partial fulfilment of the requirements of the degree
Magister Ingeneria
in the
School of Mechanical and Materials Engineering,
Faculty of Engineering
at the
Potchefstroom University for Christian Higher Education

Promoter: Prof. P.G. Rousseau
Co-Promoter: M. van Eldik
POTCHEFSTROOM, SOUTH AFRICA
2003

ACKNOWLEDGEMENTS

First and foremost I would like to thank my study leader Prof. P.G. Rousseau for his great contribution to this study, without his guidance this thesis would not have been possible. Secondly I would like to thank my co-promoter Mr. M. van Eldik for his technical and theoretical assistance throughout this study.

I am also indebted to Bennie du Toit for his help with the formulation of the equations used in this study. I am also very grateful for the guidance of Robbie Arrow during the construction and operation of the experimental test bench, his technical wisdom was greatly appreciated.

I also thank my heavenly father for the unseen spiritual love and guidance he bestowed upon me. I would also like to thank my mother and my sister for their emotional support during rough times. Last but not least thanks to all my friends, Gert, Bossi, Hans, Jo, Philip, Thys, Grant, Rian, Leanda, Jaco and Lourens for all their help and support.

ABSTRACT

Turbine blade cooling via internal cooling channels is a very important aspect in modern-day gas turbine cycles. The need for blade cooling stems from the fact that higher cycle efficiencies requires higher maximum temperatures and therefore also higher turbine inlet temperatures. In order to evaluate the effects of these cooling flows on the cycle as a whole under various load conditions, it is necessary to simulate the compressible flow with heat transfer within the channels. The main objective of this study is to develop a mathematical model to simulate the steady-state compressible flow in the radial cooling channels of a simple rotating disc and to determine a temperature distribution in the disc. The disc's axis of rotation is vertical and it contains six equally spaced cooling channels through which air is dispersed radially outward.

The steady-state compressible equations for the fluid flow in a rotating pipe were derived from first principals. The generated heat transfer in the rotating pipe was then coupled incrementally to a system of temperature conduction equations. It was then possible to determine a three dimensional temperature distribution in the rotating disc. The study also included an experimental validation of the flow model under adiabatic conditions.

An inlet loss factor was empirically determined from data obtained from the experimental test bench. It was found that the inlet loss factor is a function of the inlet radial velocity component divided by the inlet tangential velocity component. Finally, it was shown that the results obtained from the theoretical model are in good agreement with the data obtained from the experimental test bench.

OPSOMMING

Turbine lem verkoeling deur middel van interne verkoelings kanale is 'n baie belangrike aspek in moderne gas turbine siklusse. Hoër siklus effektiwiteite benodig hoër maksimum temperature en dus ook hoër turbine inlaat temperature. Turbine lem verkoeling word dus benodig om turbine lem faling as gevolg van oorverhitting te voorkom. Dus, om die effekte van die verkoelings vloei, onderwerp aan verskeie las kondisies op die siklus as 'n geheel te evalueer, is dit nodig om die saamdrukbare vloei met hitte oordrag in die kanale te simuleer. Die doel van die studie is om 'n wiskundige model te ontwikkel om die gestadige saamdrukbare vloei in radiale verkoelings kanale van 'n eenvoudige roterende skyf te simuleer. Verder moet die model ook in staat wees om 'n temperatuur verspreiding in die skyf te bepaal.

Die gestadige saamdrukbare vergelykings vir die vloei in 'n roterende pyp is van eerste beginsels afgelei. Die gegenereerde hitte oordrag in die roterende pyp is per inkrement aan 'n stelsel hitte geleiding vergelykings gekoppel. Die vergelykings het dit dan moontlik gemaak om 'n drie dimensionele hitte verspreiding in die skyf te bepaal. Die studie het ook 'n eksperimentele validasie van die adiabatiese vloei in die roterende kanale ingesluit.

'n Inlaat verlies faktor is empiries bepaal uit die eksperimentele resultate. Daar is gevind dat die inlaat verlies faktor 'n funksie was van die inlaat radiale snelheid komponent gedeel deur die inlaat tangensiële snelheid komponent. Dit is ook bevestig dat die eksperimentele en teoretiese waardes goed met mekaar ooreenstem.

TABLE OF CONTENTS

NOMENCLATURE

A	Cross sectional area of the rotating pipe	m^2
B	Body forces	-
C	Absolute velocity	m/s
C_1	Integration constant number one	-
C_2	Integration constant number two	-
c_p	Specific heat at constant pressure	$J/kg \bullet K$
c_v	Specific heat at constant volume	$J/kg \bullet K$
D	Diameter of the rotating pipe	m
f	Friction factor of a rotating pipe	-
g	Gravitational acceleration	m/s^2
h	Enthalpy	$J/kg \bullet K$
h_{inside}	Rotating cylindrical cavity convection heat transfer coefficient	$W/m^2 \bullet K$
h_{bottom}	Outer edge of the disc convection heat transfer coefficient	$W/m^2 \bullet K$
h_o	Total enthalpy	$J/kg \bullet K$
HTA	Heat transfer area	m^2
$inlet\ velocity_{ratio}$	Radial inlet velocity divided by the tangential inlet velocity	-
K	Secondary loss factor	-
k	Thermal conductivity	$W/m \bullet K$
k_i	Thermal conductivity for node block (i=1,2,3,...7)	$W/m \bullet K$
L	Length of the control volume	m
M	Mach number	-
M_z	Total torque exerted due to the pipe walls	W

$\dot{m}$	Mass flow	kg/s
NTU	Number of transfer units	-
P, p	Static pressure	Pa
P_o, p_o	Total pressure	Pa
Q	Heat transfer	W
Q_h	Heat transfer from the pipe walls	W
r	Radius	m
r_i	Radius at radial increment (i=1,2,3...9)	m
$ratio$	Friction factor of a rough stationary pipe divided by the friction factor of a smooth stationary pipe	-
$R_{t,cond}$	Conduction resistance	-
$\hat{s}$	Unit vector parallel to the flow direction at the inlet and outlet	-
S_r	Source term for the conduction equations in the radial direction	-
S_θ	Source term for the conduction equations in the theta direction	-
S_z	Source term for the conduction equations in the axial direction	-
T	Static temperature	K
T_o	Total temperature	K
Tf	Environmental temperature	K
$T_{i,j}$	Disc nodal temperature (i=block=1,2,3...7) and (j=node=1,2,3...27)	K
t	Time	s
U	Overall heat transfer coefficient	$W/m^2 \cdot K$
u	Internal energy	$J/kg \cdot K$
V	Velocity	m/s
$\forall$	Volume of the control volume	m^3

W	Total rate of work done on the fluid	W
z	Axial direction	-
z_i	Axial position (i=1,2,3)	m

Greek symbols

α	Thermal diffusivity	m^2/s
θ	Tangential direction	-
γ	Ratio of specific heats	-
Δ	Difference	-
ρ	Density	kg/m^3
ρ_i	Density at radial increment (i=1,2,3,...9)	kg/m^3
τ	Shear forces	-
ω	Rotational speed	rad/s
$\dot{\omega}$	Rotational acceleration	rad/s^2
μ	Dynamic viscosity or absolute viscosity	$kg/m \cdot s$
υ	Kinematic viscosity $(\upsilon = \frac{\mu}{\rho})$	m^2/s
ε	Effectiveness	-
Ω	Rotational speed	rad/s

Subscripts

e	Outlet to the control volume	-
i	Inlet to the control volume	-
in	Inlet / rotating cylindrical cavity	-

out	Outlet / outer edge of the disc	-
0	Inner	-
θ	Tangential component	-
r	Radial component	-
z	Axial component	-
max	Maximum	-
w	Wall	-
m	Medium	-
av	Average	-
iso	Isothermal	-
quad	Quadratic	-
D	Diameter	-
H	Heat transfer conditions	-
∞	Free stream conditions	-
sl	Stationary straight pipe, laminar flow	-
st	Stationary straight pipe, turbulent flow	-
s	Surface	-
crit	Critical value	-
top	Top side of the disc	-
bottom	Bottom side of the disc	-
ri,j	i=radial position (i=1,2,...9) and j=node block (j=1,2,...7)	-
zi,j	i=axial position (i=1,2,3) and j=node block (j=1,2,...7)	-
W	West node	-

E	East node	-
P	Central node	-

Superscripts

$\bar{}$	Vector	-
$\hat{}$	Unit vector	-
$\tilde{}$	Average value	-
*	Local value	-

Dimensionless groups

Re	Reynolds number based on the radial velocity component	-
Re_Ω	Rotational Reynolds number ($Re_\Omega = \frac{\rho\Omega r^2}{\mu}$)	-
$Re_\Omega^{'}$	Augmented rotational Reynolds number ($Re_\Omega^{'} = \frac{\Omega D_0^{\,2}\rho}{2\mu}$)	-
Nu	Nusselt number	-
Pr	Prandtl number	-
K_l	Dimensionless parameter for laminar flow	-
K_t	Dimensionless parameter for turbulent flow	-

Physical constants

R	Universal gas constant for air	=	287	$J/kg{\bullet}K$

LIST OF FIGURES

temperature of 55°C.

Figure G.12: Rotating pipe velocity distribution for various rotational speeds at an inlet temperature of 55°C.

LIST OF TABLES

CHAPTER 1

1. INTRODUCTION

1.1. Background

It is well-known that maximum cycle temperatures in the modern gas turbine are primarily limited by the high-temperature failure characteristics of the turbine blades. The turbine blades operate under high centrifugal loading and are subject to gas-bending, vibratory and thermal stressing. Thus one of the most important problems encountered in increasing maximum cycle temperatures, and therewith in obtaining the indicated large improvements in gas-turbine performance, is that of providing some means of preventing turbine-blade failure due to overheating.

A solution to this problem appears to lie in one of two possibilities: either the improvement of turbine-blade materials capable of extended operation under severe conditions of temperature and stress, or the use of direct or indirect methods of cooling blades made of currently available materials. Several artificial cooling methods involve the use of radiation exchange between the high-temperature blades and adjacent low-temperature shields, or the use of blades coated with a suitable heat-resistant ceramic (thermal barrier).

Turbine blades may also be cooled directly by forcing a cooling fluid through passages within the blade, bled from the compressor (figure 1.1), or indirectly by conducting heat from the blades to an internally cooled turbine rotor. The coolant reduces the metal temperatures to below the material melting temperature and thereby increases the durability of the blade. The coolant passages are of complex shape and tend to have transverse ribs and pin-fins to enhance the heat transfer process. A better heat transfer prediction capability would enable the minimisation of the amount of flow taken from the

compressor to cool the turbine blades. This will reduce the thermodynamic penalties, thus improving the overall gas turbine cycle efficiency.

It has been demonstrated (Morris and Chang (1997)) that an uncertainty of ± 10% in the heat transfer coefficients distributions result in an uncertainty of ± 2% in the metal temperature. This produces an uncertainty of ± 50% of the predicted blade life. Thus it is imperative to accurately predict the blade life to ensure a safe and reliable gas-turbine system.

Figure 1.1 illustrates the complexity of the coolant passages inside a rotor blade. A combination of film cooling, impingement cooling and convection cooling is used to satisfy the design requirements. Convection cooling channels are mainly orthogonal to the axis of the turbine with the coolant flowing in a root-to-tip or tip-to-root direction as shown in figure 1.1. Prediction of the coolant flow field and the heat transfer coefficient distribution in these passages is extremely difficult due to the geometric features of the passages and also because the coolant rotates with the blade.

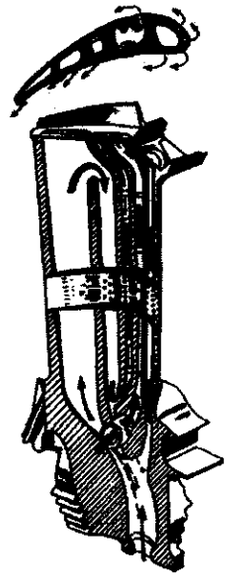

Figure 1.1: Typical turbine rotor blade cooling channel network.

1.2. Problem statement and objectives

To improve the design capability of high temperature turbines, a detailed understanding of the three-dimensional flow and heat transfer in turbine blade cooling passages is necessary. The geometries of turbine blades in real gas-turbine engines are very complicated. In order to understand the fluid-flow in internal cooling passages of turbine blades a simplification needs to be made to simulate the geometries by using plane rotating-disc systems.

Rotating-disc systems provide simplified experimental or computational models of the complex internal cooling air systems of gas-turbine engines. The reason for this is that the governing equations that describe the flow and heat transfer in a rotating disc can be readily transformed to simulate more complex rotating turbine blade scenarios. The gas turbine provides many examples of this: an air-cooled turbine disc rotating near a casing can be modelled by a simple rotor-stator system; two co-rotating discs can be modelled by a rotating cylindrical cavity. In fact, many rotating flows of practical importance can be considered in terms of the rotor-stator system or of the rotating cavity.

In this study a rotating-disc system with radial outflow of fluid (air) will be used to simulate the fluid flow and heat transfer using a cylindrical coordinate approach. The fluid enters the disc axially and is dispersed radially outwards through passages due to the centrifugal force of the rotating disc (figure 1.2).

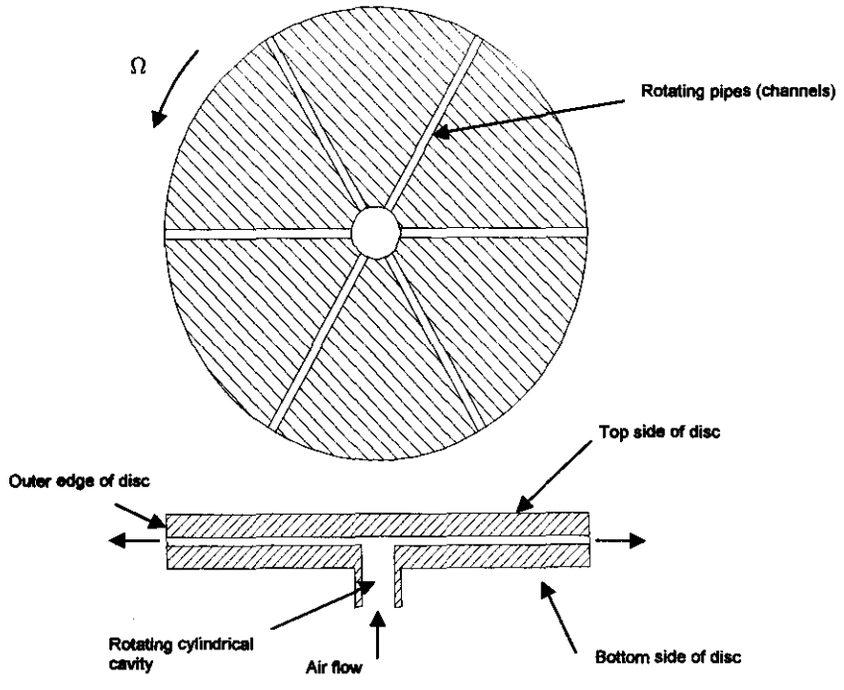

Figure 1.2: Schematic presentation of a rotating disc with internal radial passages.

Thus the primary objective of this study is to validate the theory behind steady-state compressible fluid-flow in a rotating disc with internal radial passages by means of an experimental test bench. A secondary objective will be to investigate the behaviour of the fluid flow and thermal parameters at various rotational speeds of the disc. The final goal is to determine a temperature distribution in the rotating disc at various rotational speeds.

The fluid flow in the radial cooling passages will be modelled by using a rotating pipe model (see figure 1.3). By employing the energy conservation equation, the generated heat flux will then be used to solve a network of conduction heat transfer equations within the disc. The model will then be capable of determining the temperature distributions of the rotating disc at various rotational speeds. The temperature distribution of the disc is of utmost importance to identify local hotspots in the disc.

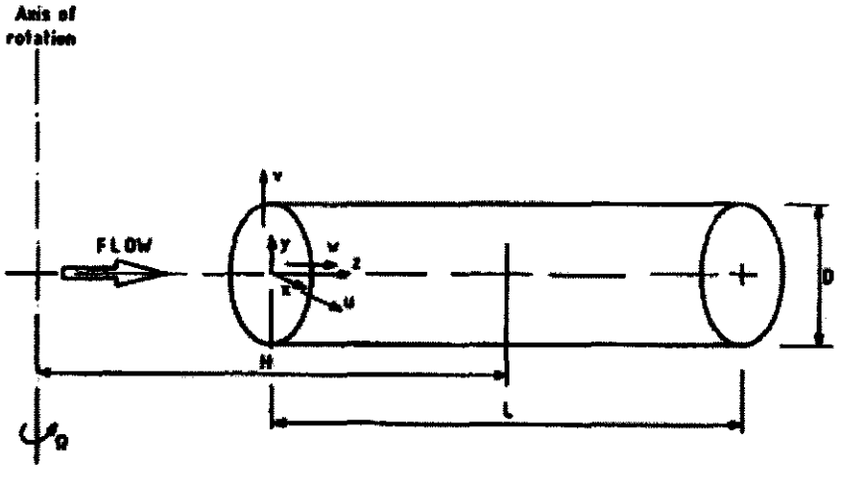

Figure 1.3: Representation of a rotating pipe.

A great deal of uncertainty exists about the behaviour of the three-dimensional vortex flow structure at the inlet (rotating cylindrical cavity) of the rotating disc. The inlet loss factor will be determined empirically by using measurements from the experimental test bench. The outlet loss factor will be modelled by using an inviscid free vortex.

1.3. Scope of the thesis

The problem of validating the theory associated with steady-state compressible fluid-flow as described in 1.2 above, will be addressed in this thesis in the following manner.

In Chapter 2 a detailed literature survey will be conducted to obtain relevant information on the research conducted previously on rotating-disc systems. The survey will be conducted to obtain relevant information to aid in the simulation of the fluid-flow and heat transfer in rotating-disc/ cavity systems.

Special attention will be given to rotating-disc systems with radial outflow of fluid as well as the correlations for the heat transfer coefficients in rotating flows.

In Chapter 3 the process of obtaining the correct equations for the various types of heat transfer in the rotating disc, such as conduction and convection, will be explained in detail. The theory behind the behaviour of the fluid-flow in the radial cooling passages in the rotating disc will be investigated.

The one property that distinguishes the heat transfer found in rotating systems from stationary systems is the heat transfer coefficients. As stated above, rotation has a significant impact on the heat transfer, thus appropriate correlations need to be found in order to accurately simulate the rotating-disc system.

In Chapter 4 the EES *(Engineering Equation Solver)* simulation process of the rotating- disc system and all the relevant assumptions will be discussed in detail. The mathematical equations and correlations for both the fluid flow and the heat transfer will be incorporated in a computer programme to simulate the steady-state behaviour of the rotating disc.

In Chapter 5 the configuration and the operation of the experimental assembly will be discussed in detail. At the end of the chapter the data obtained from the experimental test assembly will be presented. The validity of the results will also be investigated. At the end of Chapter 5 the results obtained from the EES simulation model and the experimental test bench will be compared. This is necessary to verify and validate the study.

All of the results obtained from the simulation model will be given in Chapter 6. The results include temperature, pressure and velocity distributions for various rotational speeds and inlet temperatures of the disc.

The mass flow through the rotating channels in the disc will also be investigated for various disc rotational speeds and inlet temperatures. Finally, various graphs will illustrate the disc temperature distribution for various rotational speeds.

This study only focuses on a rotating disc with internal radial passages. In Chapter 7 recommendations for future research will be given to accurately simulate a more complex body. This includes a more complex form of heat transfer and fluid-flow in a rotating body with cylindrical coordinates.

1.4. Summary

To accurately simulate the fundamental three-dimensional, steady-state flow and heat-transfer phenomena that control the performance of advanced turbines, the main parameters that affect the distributions of the local heat transfer coefficient must be known. These parameters include coolant flow rate, disc temperature, rotational speed and cavity configuration.

Effects of coolant passage cross-section and orientation on rotating heat transfer are also important. Furthermore, it is also essential to determine the associated coolant passage pressure losses for a given internal cooling design. This can help in designing an efficient cooling system and prevent local hotspot overheating of the rotor blade.

In the following chapter an extensive literature survey will be conducted to obtain relevant information on rotating-disc systems.

CHAPTER 2

2. LITERATURE SURVEY

2.1. Introduction

The main objective of the literature survey is to compare previously conducted research on the topic of rotating disc and rotating pipe systems to the current study. Various topics will be addressed, with the emphasis on rotation. These topics will include flow and heat transfer in rotating channels, rotating cavities, rotor-stator systems, rotating discs and rotating cylinders. All of these issues will be investigated to aid the current study.

2.2. Previous Work

2.2.1. Flow and heat transfer in rotating channels

Kotbra (1990) conducted an empirical study of the hydraulic-thermal phenomena in rotating radial channels of electric machines. The experiment was made up of a heated internal rotor and external stator configuration with radial cooling channels separated by an air gap. The most important element of the research by Kotbra (1990) was the influence of rotation and air flow on the heat transfer coefficient. The non-rotating heat transfer coefficients were compared to rotating heat transfer coefficients. This resulting data were then adapted to form non-dimensional variables.

The results showed that the heat transfer increase was greater in the laminar region than in the turbulent region. This smaller influence in the turbulent region of the flow can be explained by the fact that the heat transfer effectiveness was higher in turbulent flow than in laminar flow. Thus the influence of rotation on the heat transfer coefficients was less pronounced for

the turbulent flow region. The heat transfer increase for both the turbulent and the laminar flow were less than expected. This was due to the fact that the heat transfer increase due to rotation is not caused by transverse Coriolis forces, but to a large extent, by pulsations of the flow. The formation of transverse secondary flow induced by the action of the Coriolis forces requires much longer channels.

A detailed evaluation of the theory behind the complex motion of rotating flows is addressed in the book by Greenspan (1968). The author addresses certain topics associated with linear and non-linear contained rotating fluid motion. These topics include rigid rotation, The Ekman layer, spin-up, viscous dissipation, motion in a cylinder, boundary layer theories, moment-integral methods and vortex flows.

The author also describes the theory behind an unbounded rotating fluid (encountered in the free-disc scenario) such as plane inertial waves, oscillatory motion and slow motion along the axis of rotation. The theory described in the book by Greenspan (1968) is vital for the analysis of the flow inside rotating channels or discs. The literature highlights important aspects of the current study which needs to be addressed, especially the motion in a cylinder, vortex flows and boundary layer assumptions.

Wagner et al. (1991a) conducted experiments to determine the effects of rotation on heat transfer in turbine blade internal coolant passages. The objective of the study was to obtain the heat transfer data required to develop heat transfer correlations and to asses computational fluid dynamic techniques for rotating coolant passages (figure 2.1).

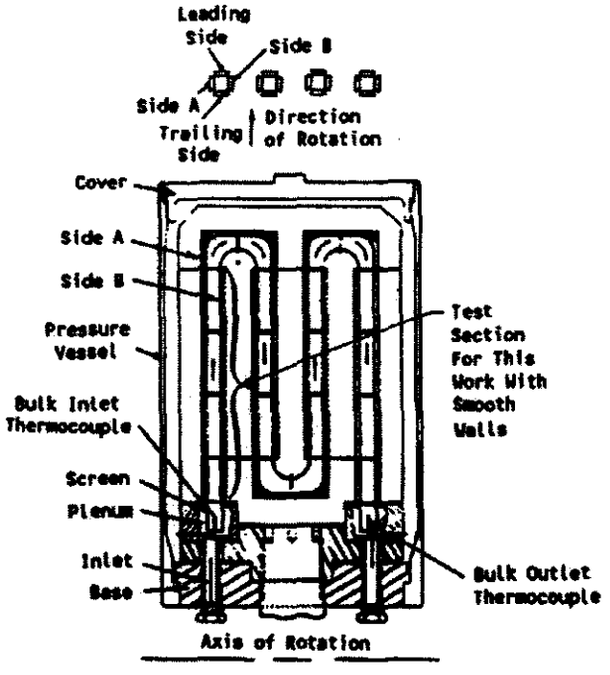

Figure 2.1: Cross-section view of coolant passage heat transfer model assembly.

(Wagner et al., 1991).

An analysis of the governing equations showed that four parameters influenced the heat transfer in rotating passages: coolant density ratio, Rossby number, Reynolds number, and radius ratio. Rotation affected the heat transfer coefficients differently for different locations in the coolant passage. The heat transfer increased at some locations with rotation, but decreased and then increased again at other locations. The difference in heat transfer was attributed to the strength of secondary flow cells associated with a Coriolis force and the buoyancy effects.

Wagner et al. (1991b) extended his research to determine the effects of buoyancy and Coriolis forces on the heat transfer in a multi-pass coolant passage. The results for outward flow in the first passage were previously presented by Wagner et al. (1991a) (figure 2.1). The flow in the first and third passage was radially outward. The flow of the connecting second passage was radially inward. The main focus of the research was to determine the

effects of the flow direction on the heat transfer in rotating coolant passages. The results showed that both Coriolis and buoyancy effects must be considered in turbine blade cooling designs and that the effect of rotation on the heat transfer coefficients were markedly different depending on the flow direction.

An analysis of the governing flow equations showed that four parameters influenced the heat transfer in rotating passages: coolant-to-wall temperature ratio, Rossby number, Reynolds number, and radius-to-passage hydraulic diameter ratio. Local heat transfer coefficients were found to decrease by as much as 60 percent and to increase by 250 percent from no-rotation levels.

Harasgama and Morris (1988) investigated the influence of Coriolis-induced secondary flow and centripetal buoyancy on the heat transfer within typical rotor blade cooling passages. The experimental results obtained indicated that for through-flow Reynolds numbers up to 30 000, increasing rotational speeds tend to increase the mean levels of heat transfer relative to a stationary case when the flow is radially outward. This trend is reversed when the flow is radially inward.

They also found that increasing the centripetal buoyancy even further for radially outward flow tends to decrease the mean level of heat transfer and in some cases these levels fall below the equivalent stationary values. The trailing (pressure) side heat transfer is usually higher than that on the leading (suction) side due to secondary flows.

Harasgama and Morris (1988) also tested earlier correlations on the leading side of rotating circular, triangular and square ducts. The correlation did not predict the Nusselt number for the trailing side of the rotating duct. It was proposed that the correlation only be used in the preliminary stages of the design of turbine rotor blade cooling passages.

Medwell et al. (1991) presented a numerical method to determine the heat transfer in a cylindrical cooling duct within turbine blades that rotate about an axis orthogonal to its own axis of symmetry. The predicted results were compared to experimental data and it was demonstrated that conduction in the solid boundary must be taken into account if satisfactory agreement is to be achieved. Excluding the effect of conduction can lead to an overestimation of 50% of the maximum wall temperature.

Fann and Yang (1992) performed a three-dimensional study of hydrodynamically and thermal developing laminar flow in a long rotating channel with uniform wall temperature. The velocity-vorticity method was used in the formulation and numerical results were obtained by means of a finite-difference technique. The Nusselt number, friction factor, temperature and velocity distributions were determined. The role of the Coriolis force in the transport phenomena was also investigated.

It was found that the flow patterns changed along the channels due to the viscous effect, the Coriolis force, and their interaction. The effects of rotation included an enhancement of the Nusselt number on the trailing wall, a moderate increase in the Nusselt number on the side walls, a degradation of the Nusselt number on the leading wall and fluctuations of the friction factor and the Nusselt number along the flow. It was also found that in general both the friction factor and the Nusselt number were augmented with an increase in the rotational speed and the through-flow rate and a decrease in the aspect ratio of the channel.

Morris and Chang (1997) described an experimental investigation of the heat transfer inside a simulated cooling channel for a gas turbine rotor blade. The cooling channel was circular in cross-section and rotated about an axis which is orthogonal to its centre line. The main focus of the study was aimed at the

Medwell et al. (1991) presented a numerical method to determine the heat transfer in a cylindrical cooling duct within turbine blades that rotate about an axis orthogonal to its own axis of symmetry. The predicted results were compared to experimental data and it was demonstrated that conduction in the solid boundary must be taken into account if satisfactory agreement is to be achieved. Excluding the effect of conduction can lead to an overestimation of 50% of the maximum wall temperature.

Fann and Yang (1992) performed a three-dimensional study of hydrodynamically and thermal developing laminar flow in a long rotating channel with uniform wall temperature. The velocity-vorticity method was used in the formulation and numerical results were obtained by means of a finite-difference technique. The Nusselt number, friction factor, temperature and velocity distributions were determined. The role of the Coriolis force in the transport phenomena was also investigated.

It was found that the flow patterns changed along the channels due to the viscous effect, the Coriolis force, and their interaction. The effects of rotation included an enhancement of the Nusselt number on the trailing wall, a moderate increase in the Nusselt number on the side walls, a degradation of the Nusselt number on the leading wall and fluctuations of the friction factor and the Nusselt number along the flow. It was also found that in general both the friction factor and the Nusselt number were augmented with an increase in the rotational speed and the through-flow rate and a decrease in the aspect ratio of the channel.

Morris and Chang (1997) described an experimental investigation of the heat transfer inside a simulated cooling channel for a gas turbine rotor blade. The cooling channel was circular in cross-section and rotated about an axis which is orthogonal to its centre line. The main focus of the study was aimed at the

development of an experimental procedure and method of data processing to determine the full axial and circumferential heat transfer data over the tube's inner surface.

The strategic aim of the research was to determine the combined effect of Coriolis and centripetal buoyancy forces on the forced convection mechanism inside the tube. The experimental technique involved the determination of the inside surface temperature and heat flux distribution using a solution of the channel wall heat conduction equation.

The prediction of circumferential wall temperatures using the measured temperatures on the leading and trailing edges gave very good agreement with the independently measured values. The method produced was capable to discern systematic changes in the strength of the Coriolis-driven secondary flow and the centripetal buoyancy.

The authors also concluded with the help of experiments that the use of a forced convection Reynolds number effect, in the form of a 0.8 exponent of Reynolds number, is a valid assumption. Thus the Dittus Boelter (see Incropera and DeWitt (1996)) equation for turbulent flow in a pipe can be used to correlate the Nusselt number in a rotating radial cooling passage.

2.2.2. Rotating cavities

Owen & Bilimoria (1977) modelled the flow and heat transfer in rotating cylindrical cavities. The main purpose of their study involved the measurements of mean and local Nusselt numbers on a heated experimental rotating-disc assembly. The experimental rotating-disc assembly consisted of a rotating cylindrical cavity where both axial through-flow and radial outflow of air could be achieved.

Various flow patterns inside the cylindrical cavity were identified for both the axial and radial through-flow scenarios. They consisted of laminar and turbulent flow where measurements were done for non-rotating and rotating cases. The main results for the two types of flow scenarios will be briefly described.

Axial through-flow of air

For laminar flow, a weak toroidal vortex was formed inside the cavity. In the stationary case, the vortex was not axisymmetric and was influenced by gravitational buoyancy effects. The flow inside the cavity became turbulent as soon as the axial jet became turbulent. For the stationary cavity, turbulent flow produced a powerful axisymmetric toroidal vortex. For turbulent flow with low rotational speeds and a high Rossby number (> 100) the tangential velocity in the cavity tended towards that of a free vortex. For a lower Rossby number (< 21) the tangential velocity conformed to a forced vortex.

The local Nusselt number breakdown was strongly influenced by gap ratios. During spiral vortex breakdown, the local Nusselt number increased with both increasing through-flow and rotational Reynolds numbers. Owen & Bilimoria (1977) found that a complex interaction of disc temperature distribution and the recirculating flow within the cavity makes the heat transfer results for axial through-flow extremely difficult to interpret.

Radial outflow of air

At low rotational speeds (rotational Reynolds number < 2500) the laminar jet oscillates, shedding vorticity into the cavity via the wall jet. This includes a turbulent core of recirculating fluid which fills the remainder of the cavity. At higher speeds (rotational Reynolds number > 6000) the turbulent core begins to decrease in radial extent, and Ekman layers appear on each disc.

Increasing the rotational speed further (rotational Reynolds number $>5\times10^4$) forces the core towards the centre of the cavity, leaving thin Ekman layers on the discs.

Spiral vortex breakdown was also observed over a range of Rossby numbers similar to that in the axial through-flow case, although the effects were far less dramatic and the termination far less definite than for the axial case. Like the laminar case and unlike the axial through-flow case the radius of the core decreases with increasing rotational speed once a critical value of the rotational Reynolds number is exceeded. As the rotational Reynolds number further increased, the core reduces in size, allowing an Ekman layer to form on the downstream disc. There are three important regimes in the turbulent case:

1. The core dominating regime.
2. The developing Ekman layer regime.
3. The fully developed Ekman layer regime.

The reduction of the turbulent core with increasing rotational Reynolds number has a large influence on the heat transfer in the rotating cavity. In contrast with the heat transfer results for axial through-flow, the results for the radial outflow showed little gap ratio dependency for the three values tested. Nusselt numbers increase in magnitude with increasing rotational speed up to a rotational Reynolds number $\approx 10^6$. After this value the Nusselt numbers were seen to flatten off. The Nusselt numbers were also seen to increase with increasing through-flow Reynolds number. It was also established that the influence of vortex breakdown on the heat transfer is less profound for the radial outflow case.

At low values of the rotational Reynolds number the effect of rotational speed on the heat transfer is small, but the effect of the through-flow Reynolds number is significant. This is consistent with regime 1. At Rossby numbers of order 10, the heat transfer increases significantly with both through-flow and rotational Reynolds number, which is consistent with regime 2. At Rossby numbers of unity, the heat transfer increases only slightly with increasing rotational Reynolds number, which is consistent with regime 3.

The study by Owen & Bilimoria (1977) on the heat transfer in rotating cylindrical cavities highlights the importance of the complex flow structure and the effects it has on the convection coefficients. It is also important to notice the difference between the geometries of the rotating cylindrical cavity assembly by Owen & Bilimoria (1977) and the rotating disc with radial cooling passages of the current study.

Northrop & Owen (1988a) compared theoretical and experimental results for the flow and heat transfer in a rotating cavity with radial outflow of cooling air for a range of rotational Reynolds numbers and dimensionless flow rates. Flow visualisation confirmed that the flow structure comprised of a source region, Ekman layers, a sink layer, and an interior core of rotating fluid (figure 2.2). Measured values of the size of the source region were in good agreement with a simple theoretical model.

They found that, except at high flow rates and low rotational speeds, where the source region fills the entire cavity, the agreement between the measured and theoretically determined Nusselt numbers is mainly good. A few important results from the study of Northrop & Owen (1988a) will be discussed briefly below.

1. A maximum value of Nusselt number occurred near the edge of the source region, and the Nusselt number increased with increasing non-dimensional flow rate and rotational Reynolds number.
2. It was also shown that Nusselt numbers were strongly influenced by the radial distribution of surface temperature, particularly for the outer part of the disc covered by the Ekman layers.
3. If the flow rate is large enough for the source region to fill the entire cavity, a wall jet forms on the downstream disc, resulting in higher rates of heat transfer at the smaller radii.
4. If Coriolis forces dominate the inertial forces in a rotating fluid, Ekman layers form on the rotating discs.
5. Under some conditions negative values for the Nusselt numbers have been predicted and measured.

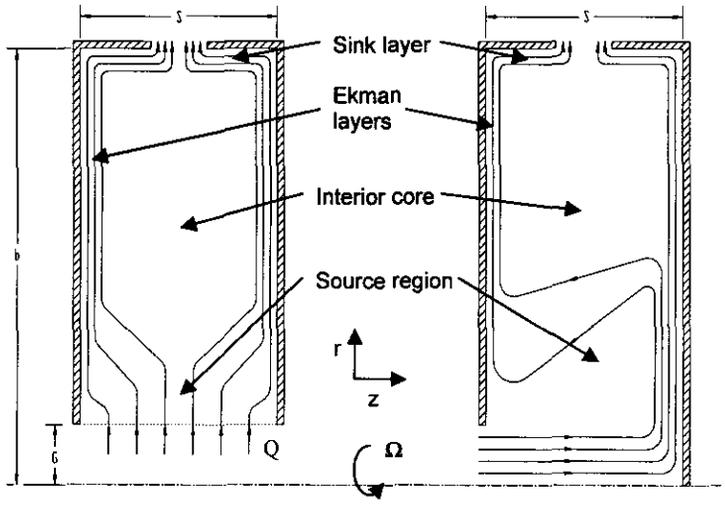

(a) radial inlet (b) axial inlet

Figure 2.2: Schematic diagram of the flow structure inside a rotating cavity with radial outflow of fluid. (Northrop & Owen, 1988a).

Owen and Rogers (1995) describe the theory behind flows in rotating cavity systems. The basic equations and boundary layer theory governing the heat transfer and fluid flow inside rotating cavities are publicised. Some attention is given to the Ekman boundary layer occurrence as well as vortex flows in

viscous fluids. The authors were especially concerned with the complex flow structures occurring inside rotating cavities subjected to superimposed radial inflow and outflow of fluid.

In the latter part of their publication Owen and Rogers (1995) investigate turbulent and laminar heat transfer for radial inflow and outflow of fluid in rotating cavities. The buoyancy-induced flow and heat transfer occurring in rotating cavities are also described for both isothermal and non-isothermal flow scenarios.

Tucker and Long (1998) presented a study of radial and circumferential temporal variations of cavity air temperature for a rotating cavity with an axial through-flow of cooling air. Results showed that the cavity air radial and circumferential temperature distributions were both strongly influenced by cavity surface temperatures. When the discs were heated significant circumferential cavity air temperature variations were observed, showing the flow to be three-dimensional. The study also showed that when the shroud was heated and the discs unheated, no circumferential temperature variations were observed.

Flow visualisation and heat transfer measurements have been made by Owen and Onur (1983) in a rotating cavity with either axial through-flow or radial outflow of coolant. For axial through-flow, flow visualisations revealed the presence of spiral vortex breakdown. The occurrence and scale of this breakdown depends on the Rossby number. A correlation has been obtained for the mean Nusselt number in terms of cavity gap ratio, the axial Reynolds number, and rotational Grashof number.

For the radial outflow tests it was found that Ekman layers formed on the discs and a central core of inviscid fluid occurred between the Ekman layers and the source and sink layers. This flow structure is consistent with the

research done by Owen & Bilimoria (1977) and Pilbrow et al. (1999). The mean Nusselt numbers have been correlated, for the radial outflow case, over a wide range of gap ratios, coolant flow rates, rotational Reynolds numbers and Grashof numbers.

In addition to the three forced convection regimes, a fourth free convection regime has been identified. This fourth free convection regime was formed when a constant flow rate was introduced and the rotational speed reached a critical point. At this point the inner layer began to oscillate and the "classic structure" broke down into a "chaotic structure". This "chaotic structure" was the reason for the free convection regime.

Ong and Owen (1991) developed a boundary-layer method to compute the heat transfer for compressible flow of fluid in a rotating cavity with radial outflow of fluid (figure 2.2). Their results were compared to the experimental data of Northrop & Owen (1988) for an air-cooled rotating cavity. For the range of temperatures and flows considered, property variation had a negligible influence on the computed Nusselt numbers. However, for turbulent flow at large Eckert numbers, viscous dissipation could have a significant effect on the Nusselt number.

They also found that in the source region, the measured and computed Nusselt numbers increased in magnitude with increasing radius. In the Ekman layers outside the source region, the Nusselt numbers decreased with increasing radius. In the case where the temperature of the disc decreased radially, negative Nusselt numbers could occur near the outer edge of the disc.

Their results compared well with the experimental results of Northrop & Owen (1988) and it was concluded that the boundary-layer equations would provide accurate enough solutions for application to air-cooled gas turbine discs.

Long and Owen (1986) conducted experiments to determine the effect of inlet conditions on the flow and heat transfer in a rotating cavity with radial outflow of air (figure 2.2). Flow visualisation was used to study the isothermal flow structure. The flow structure comprised of a source region, Ekman layers on each disc, a sink layer, and an interior core. These observations were the same as the observations made by Northrop & Owen (1988), Pilbrow et al. (1999), Owen and Onur (1983) and Ong and Owen (1991).

The authors also presented a simple model for the flow and heat transfer in a rotating cavity with a radial outflow of fluid. They formulated equations to correlate the local volumetric flow rate in each Ekman layer and the local Nusselt number for a rotating cavity for radial outflow of air. An equation to calculate the radial extent of the source region for impinging and non-impinging fluids was also presented.

Heat transfer measurements were made by heating the downstream disc and allowing it to cool. The Nusselt numbers were determined from the numerical solution of Fourier's conduction equation. They found that the local Nusselt numbers reached a maximum value at a radial location corresponding to the edge of the source region. This corresponds to the research done by Northrop & Owen (1988) and Pilbrow et al. (1999). The magnitude of the Nusselt number increased with increasing rotational speed and increasing coolant flow rate. The measured Nusselt numbers tended to be significantly higher than the theoretical values when the flow rate were too high and Ekman layers formed on the discs. This was attributed to the formation of a wall jet on

the heated disc, and the resulting heat transfer was virtually independent of rotational speed.

Karabay et al. (2000) theoretically studied the fluid flow and heat transfer in a simplified model of a pre-swirl rotating disc system. The main aim of the study was to provide a theoretical framework for pre-swirl systems and to show the effects of the flow parameters on the velocity, pressure and Nusselt numbers in the rotating cavity. The Reynolds analogy (see Owen and Rogers (1995)) together with a low-Reynolds-number k-ε turbulence model has been used to solve the pressure distribution, adiabatic disc temperature and local Nusselt numbers in a pre-swirl rotating disc system.

Mirzaee et al. (1998) described a combined computational end experimental study of the heat transfer in a rotating cavity with a peripheral inflow and outflow of cooling air. Measured values for the tangential component of velocity exhibited a Rankine vortex behaviour. Both the computed and measured values for the radial component of velocity confirmed the recirculating nature of the flow.

The measured and computed Nusselt numbers showed that the Nusselt number increased as the magnitudes of the flow rate and the rotational speed increased.

2.2.3. Rotor-stator systems

Nesreddine et al. (1994) investigated the problem of axisymmetric laminar flow between a stationary and a rotating disk subject to a uniform radial through-flow. Results have shown in particular that the through-flow Reynolds number has a strong influence on the complex structure of the flow field. Multiple solutions have been obtained for the flow field. This phenomenon can

be attributed to the nonlinear nature of the governing equations as well as the strong coupling between them. In general a basic unicell structure has been observed for a low through-flow Reynolds number.

An increase in the through-flow rate may result in a cyclic behaviour of a multicell structure. The radial gradient of the wall pressure of the fixed disk increases considerably with an increase of the through-flow Reynolds number, in particular within a narrow region near the orifice. The starting conditions have an important influence on the final converged solution. This influence becomes drastically more profound for cases with high rotational Reynolds and/or high through-flow Reynolds numbers. The effects of the starting conditions on the flow stability have been presented and discussed for four different ranges of the flow parameters.

The information obtained here stresses the importance of the flow parameters, especially the rotational and through-flow Reynolds numbers and the effect that these flow parameters have on the interaction between the flow structure and the heat transfer.

Chen et al. (1994) used an elliptic finite-element solver, together with a low-Reynolds-number k-ε turbulence model, to solve the Reynolds-average Navier-Stokes equations, for the flow and heat transfer in enclosed rotor-stator systems. Correlations were made for possible Couette turbulent-flow (merge of boundary layers) to adjust computed velocity distributions. It was also shown that the author's definition of Nusselt number increased as the rotational Reynolds number increased and the Gap ratio decreased. This is in contradiction to the application of the Reynolds analogy (see Owen and Rogers (1989)) to the computed moment coefficients.

2.2.4. Rotating discs

The book by Owen and Rogers (1989) can be viewed as the most important literature available for the modelling of rotating-disc systems. In this book the authors describe the complicated theory behind the flow and heat transfer for rotating disc systems. Owen and Rogers (1989) derived the basic fluid flow and heat transfer equations related to rotating disc systems, including boundary-layer (Ekman-layer) equations. Further literature includes laminar and turbulent flow over a single disc and the theory behind the fluid flow and heat transfer associated with rotor-stator systems.

It is well-known that the most important factor for the accurate prediction for the heat transfer in rotating-disc systems is a good correlation for the various Nusselt numbers. The accurate modelling of the heat transfer in a rotating disc with internal radial passages also depends on a precise correlation of the various Nusselt numbers. The appropriate correlations for the Nusselt numbers can be found in the book by Owen and Rogers (1989). These correlations are supported by previously conducted experimental tests and measurements done on rotating disc systems.

Pilbrow et al. (1999) modelled and experimentally measured the flow and Nusselt numbers for a pre-swirl rotating cavity. The rotating cavity was situated between the cover-plate and rotor of the rotating disc assembly (figure 2.3). The air enters via the pre-swirl nozzles and the swirling air flows radially outward in the cavity and exits through the blade cooling passage.

The main interests of the study by Pilbrow et al. (1999) involved a parametric study of the effects of the rotational Reynolds number, non-dimensional flow rate, a turbulent flow parameter and pre-swirl ratio on the flow and heat transfer in a simple rotating cavity. A few of the important observations made in the study of Pilbrow et al. (1999) will be briefly discussed below.

The flow structure inside the rotating cavity comprised of a number of regions. There were boundary layers on the two discs and the outer shroud, between which there were a core of rotating fluid. For a low flow rate the core comprised of two regions: a source region at the smaller radii and a non-viscous core between the Ekman-type boundary layers. The source region extended radially to the point where all superposed flow has been entrained into the boundary layers. For larger flow rates the source region filled the entire space between the boundary layers in the cavity. Inside the source region, angular momentum was conserved and a free vortex was formed outside the boundary layers. This flow structure was consistent with the study of the fluid flow in rotating cavities by Owen & Bilimoria (1977).

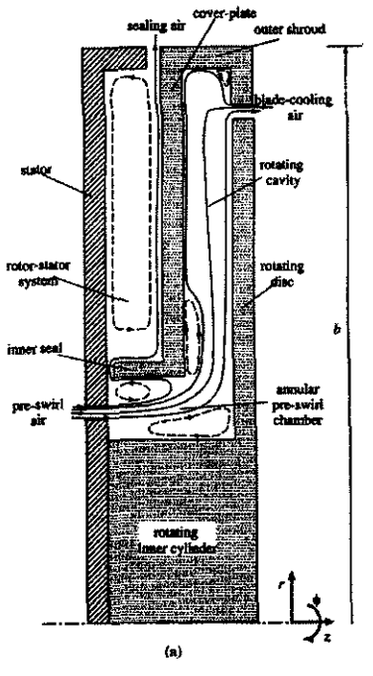

Figure 2.3: Simplified diagram of the cover-plate pre-swirl system.

The study by Pilbrow et al. (1999) highlights the importance of certain flow parameters and the influence these parameters has on the heat transfer of a rotating cavity. Pilbrow et al. (1999) observed that a turbulent flow parameter and a pre-swirl ratio had a major impact on the flow structure inside a rotating

cavity. They further found that the Nusselt numbers depended largely on the rotational Reynolds number.

Mirzaee et al. (1999) conducted experiments on a system where co-rotating discs were cooled by air supplied at the periphery of the system. Cooling air leaved through the clearances between the outer casing and the discs (figure 2.4). Thermocouples and flux-meters attached to the heated disc enabled the Nusselt numbers to be determined for a wide range of rotational speeds and coolant flow rates. The flow structure was shown to be complex and depended strongly on the turbulent flow parameter (rotational speed, flow rate). The same dependency was also established by Pilbrow et al. (1999). For a given turbulent flow parameter, the computations showed that Nusselt numbers increased as the rotational Reynolds number increased.

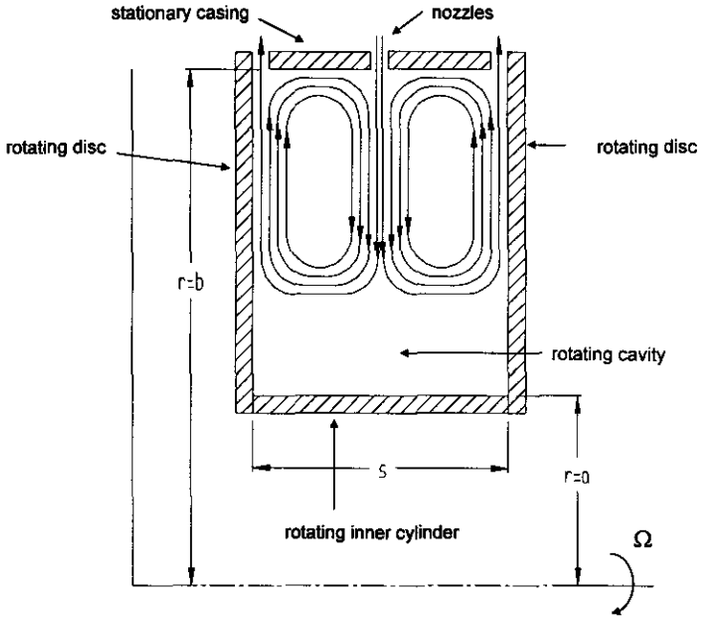

Figure 2.4: Rotating cavity with a peripheral flow of cooling air. (Mirzaee et al., 1999).

Soong et al. (2000) studied the flow structure and temperature distribution in ventilated and non-ventilated rotating disk passages. Two computational methods were used, namely the finite volume method (FVM) and finite element method (FEM). Both were based on the Navier-Stokes partial

differential equations (PDEs) but with different algorithms and meshes. The following important parameters were considered: inlet Reynolds number, rotational speed, shroud clearance, and wall temperature.

It was found that both the Coriolis force and centrifugal buoyancy had important effects on the flow structure and heat transfer because of the rotational speed and inlet velocity. In other words, the relative rotation rate of the disc affects the cell structure in the flow field. The two-cell structure formed from the centrifugal force was weak for high rotational flow and degraded the total heat transfer performance. The same results were obtained by Nesreddine et al. (1994). The Nusselt number decreased along the radius, especially near the disc outer edge, and the absolute value was much greater for non-ventilated discs. The predicted friction coefficient was very different in both cases. For the ventilated case, the friction coefficient varied rapidly, but for the non-ventilated case the friction coefficient was rather constant when rotational speed was low (< 100 rpm). However, when the rotational speed was higher (> 800 rpm) the friction coefficient varied noticeably along the radius. Finally, the shroud clearance had a prominent effect only in the high Reynolds number flow.

The equations of motion for forced and free convection for non-isothermal flow is given in the book by Bird et al. (1960). The authors formulated the equations in terms of three coordinate systems: rectangular, cylindrical and spherical coordinates. The cylindrical coordinate system equation will be used to determine the steady state temperature distribution of the rotating disc of the current study. Various literature sources will be consulted to obtain accurate correlations for the heat transfer coefficients associated with rotating discs or cylinders.

Northrop and Owen (1988b) have conducted heat transfer tests on a free-disc of a diameter of 950mm rotating at speeds up to 3000 rpm. The radial

temperature distribution could be altered by means of five electric heaters embedded inside the disc. The tests were carried out for four different distributions: the temperature distributions increased with radius in three of the tests and decreased in the fourth. The heat fluxes were obtained from the numerical solution of Laplace's conduction equation and from flux-meters mounted in one of the surfaces of the disc. The temperature distributions on the disc were approximated by a power-law. The same temperature distribution technique was used by Owen and Rogers (1995).

The experiments showed that apart from near the centre of the disc, where radiation and free convection effects were significant, and near the outer part of the disc, where the conduction solution was inaccurate, the measured local Nusselt numbers were in reasonable agreement with previously conducted research. The theoretical Nusselt number correlations used by the authors for a rotating disc can be found in the next chapter.

Qureshi et al. (1989) conducted an experimental investigation to measure the rates of convective heat transfer of rotating discs. The constant temperature steady-state technique was used to determine the local and average heat transfer coefficients on the sides of rotating discs. The effects of the coolant flow rates, cavity inflow conditions and rotational speeds on the heat transfer were studied and correlations were developed.

It was found that for rotating-disc systems in confined cavities with superimposed coolant flows, Nusselt numbers were found to be higher than those for free rotating discs without confinement. In general it was found that the Nusselt number increased along the discs radii with an increase in the rotational speed. The increase in the Nusselt number along the disc face was in some instances dependent on the coolant flow rate, especially for low rotational speeds.

Greyvenstein (2002) used a rotating-pipe model to simulate the outflow of fluid in radial passages of a rotating aluminium disc. The results from the mathematical model were compared to data obtained through an experimental test bench. The results obtained from the rotating-pipe model were in good agreement with the measured results. On the other hand, Greyvenstein (2002) did not take into account the effects of vortex behaviour and heat transfer. Furthermore, mass flow measurements were done using an anemometer. This method of measuring air velocity and converting it to mass flow is not a suitable method to accurately measure the mass flow.

The study below will focus on an extension of the research done by Greyvenstein (2002). A better approximation for the inlet and outlet loss coefficients will be presented by using vortex theory. The rotating-pipe model will also be improved and the effects of heat transfer will be incorporated in the model to predict a temperature distribution of the entire disc. Finally, the experimental test bench will be upgraded to make more intensive and accurate measurements possible.

2.2.5. Rotating cylinders

Yang et al. (1988) investigated the rotational effects on the natural convection in a horizontal cylinder. The rotational effect was examined as a function of Grashof and Reynolds number. The study showed that at low rotational speeds, the rotation tilted the temperature fields in the lateral planes as a result of the Coriolis force. With increasing rotational speeds the temperature became more uniform, and the strength of the flow due to buoyancy in the vertical plane reduced. At very high rotational speeds, the flow acted as a rigid body.

At small rotational speeds the spatial heat flux distributions were more uniform. At high rotational speeds the heat transfer rate was lower due to reduced buoyancy driving forces. Thus, at lower rotational speeds the buoyancy force dominated the flow structure inside the rotating cylinder. At higher rotational speeds the buoyancy forces subsided and the Coriolis force governed the flow structure.

The results obtained from the study by Yang et al. (1988) stresses the importance of the impact of rotational speed on the convection coefficients this is also significant for the rotating cylindrical cavity of the current study.

Kendoush (1996) obtained an approximate analytical solution for the convective heat transfer rates through a laminar boundary layer over the surface of an isothermal rotating cylinder. The average Nusselt number for the forced convection of a rotating cylinder has been correlated by using the rotational Reynolds number and the Prandtl number and by solving appropriate velocity components in the energy equation. This correlation is only valid for fluids of low Prandtl numbers (e.g. gases and light fluids) and scenarios where the heat transfer is predominated by forced convection.

Ozerdem (2000) derived a correlation for the convective heat transfer from a horizontal cylinder rotating in ambient air. The average convective heat transfer coefficients have been measured by using a radiation pyrometer. The correlation has been established as a function of rotational Reynolds number (from 2000 to 40000) with a constant Prandtl number of 0.72 (for air). It has been found that the Nusselt number increased with an increase in rotating speed. The correlation of the Nusselt number can be used to estimate the heat transfer coefficients of the rotating cylindrical cavity and the outer edge of the rotating disc.

Other research has been done on the topic of convective heat transfer from a horizontal rotating cylinder in ambient air. Anderson and Saunders (1953) found that the average Nusselt number was independent of the rotating Reynolds number up to a critical value. Above this critical value, it was found that the average Nusselt number increased with the rotating Reynolds number. Dropkin and Carmi (1957) determined the heat transfer rate from a horizontal rotating cylinder to ambient air for rotating Reynolds numbers up to 433 000. Becker (1963) first studied the heat transfer from a horizontal cylinder rotating in water. He then extrapolated the data to a Prandtl number valid for air. Schimada et al. (1991) measured local and average coefficients of heat transfer from a rotating cylinder with and without flow conditions. Etemad and Buffalo (1955) obtained a free-convection heat-transfer correlation for a rotating horizontal cylinder in air for a range of Reynolds numbers from 0 to 65 000. The heat transfer data obtained agreed well with the experimental results of Anderson and Saunders (1953). The resulting Nusselt number correlations obtained by these researchers can be found in the theoretical chapter.

Abu-Hijleh (1998) numerically solved the problem of laminar-mixed convection from a rotating isothermal cylinder. A correlation for the average Nusselt number is proposed as a function of the Reynolds number and a buoyancy parameter. The results compared extremely well to other correlations in the literature.

2.3. Identified shortcomings

There exist complex three dimensional vortex flow structures inside the rotating cylindrical cavity and at the outlet of the rotating pipe. It was decided that complex modelling of vortex flows falls outside of the scope of this study. The inlet loss factor will be experimentally determined and an analytical

solution will be used for the vortex at the outlet of the rotating pipes. The vortices will be modelled as incompressible and inviscid. Some research has been done on vortex flows and associated rotating disc systems.

The study by Karaby et al. (2000) and the book by Owen and Rogers (1995) contains expressions to describe the complex interactions of vortex flows on the flow parameters and the heat transfer in rotating disc systems. Owen and Rogers (1995) showed that for a rotating cavity with a radial outflow of fluid, the flow structure is mainly controlled by two parameters: the pre-swirl ratio and the turbulent flow parameter.

Ong and Owen (1991) and Long and Owen (1986) introduced an equation to determine the tangential velocity in the source region of a rotating cavity for free-vortex flow. The tangential velocity is dependent on a swirl fraction and a non-dimensional radius. The swirl fraction is related to the initial swirl of the fluid entering the cavity.

Mirzaee et al. (1998) approximated the velocity components in a rotating cavity under the influence of a free and forced vortex (Rankine vortex (see Owen and Rogers (1995)).

Lastly, the experimental measurements will not include any temperature measurements. The only measurements that will be done are volume flow rates and inlet pressures at various rotational speeds and valve openings. Thus the heat transfer results obtained from the simulation model cannot be verified using the experimental test bench.

2.4. Conclusion

The literature contained in this chapter focuses on the research conducted previously on rotating disc systems. The literature survey reveals that the simulation of rotating-disc systems is a relatively recent development and that contributions in this field will act as building blocks for any future research.

The next chapter focuses on the relevant theory and correlations needed to accurately simulate a rotating disc with internal radial passages.

The first term of Equation (3.1) may be omitted because only steady-state conditions apply.

For the infinitesimal control volume and applying mathematical manipulation the equation may be written in its differential form as:

$$\frac{1}{A}\frac{\partial}{\partial s}(\rho V A) = 0$$

The preceding equation may now be integrated over a pipe with finite length L resulting in the final integral form:

$$(\rho_e V_e A_e - \rho_i V_i A_i) = 0$$

or

$$\dot{m}_e - \dot{m}_i = 0 \tag{3.2}$$

3.2.2. Linear momentum conservation

The integral form of the linear momentum conservation equation for a finite non-inertial control volume of which the origin has no linear acceleration is given by Shames (1992):

$$\begin{aligned} &\oiint \tau \overline{dA} + \iiint \overline{B}\rho d\forall \\ &-\iiint \left(\left(2\overline{\omega} \times \overline{V}\right) + \left(\dot{\overline{\omega}} \times \overline{r}\right) + \left(\overline{\omega} \times \left(\overline{\omega} \times \overline{r}\right)\right) \right) \rho d\forall \\ &= \frac{\partial}{\partial t}\left(\iiint \overline{V} \rho d\forall \right) + \oiint \overline{V}\left(\rho \overline{V} \bullet \overline{dA}\right) \end{aligned} \tag{3.3}$$

For the infinitesimal control volume and applying mathematical manipulation the equation for compressible flow may be written in its differential form as:

$$\rho\omega^2 r ds + \frac{1}{2}\rho\omega^2 \frac{\partial}{\partial s}\left(r^2\right) ds = \frac{p}{p_o}\frac{\partial p_o}{\partial s} ds + \frac{f}{D}\frac{1}{2}\rho|V|V ds$$
$$+\frac{1}{2}\rho C^2 \frac{1}{T_o}\frac{\partial T_o}{\partial s} ds$$

which, after integration over a finite pipe length L, leads to

$$\frac{1}{2}\tilde{\rho}\omega^2\left(r_e^2 - r_i^2\right) + \frac{1}{2}\tilde{\rho}\omega^2\left(r_e^2 - r_i^2\right) = \frac{\tilde{p}}{\tilde{p}_o}\left(p_{oe} - p_{oi}\right) + \frac{\tilde{f}L}{\tilde{D}}\frac{1}{2}\tilde{\rho}\left|\tilde{V}\right|\tilde{V}$$
$$+\frac{1}{2}\tilde{\rho}C^2\frac{1}{\tilde{T}_o}\left(T_{oe} - T_{oi}\right)$$

Terms for the change in total pressure due to secondary losses within the pipe at the inlet and outlet, may now be added.

The coefficient of friction for a rotating pipe will be discussed in section 3.5.

The final integral form of the equation is as follows:

$$\tilde{\rho}\omega^2\left(r_e^2 - r_i^2\right) = \frac{\tilde{p}}{\tilde{p}_o}\left(p_{oe} - p_{oi}\right) + \frac{1}{2}\tilde{\rho}C^2\frac{1}{\tilde{T}_o}\left(T_{oe} - T_{oi}\right)$$
$$+\left(\frac{\tilde{f}L}{\tilde{D}} + \sum K\right)\frac{\left|\tilde{\dot{m}}\right|\tilde{\dot{m}}}{2\tilde{\rho}\tilde{A}^2} + K_i p_i\left(\left(1 + \frac{\gamma-1}{2}M_i^2\right)^{\frac{\gamma}{\gamma-1}} - 1\right) \qquad (3.4)$$
$$+K_e p_e\left(\left(1 + \frac{\gamma-1}{2}M_e^2\right)^{\frac{\gamma}{\gamma-1}} - 1\right)$$

3.2.3. Angular momentum conservation

The integral form of the angular momentum conservation equation for a finite non-inertial control volume of which the origin has no linear acceleration is given by Shames (1992):

$$\oiint \bar{r} \times \tau \overline{dA} + \iiint \bar{r} \times \bar{B} \rho d\forall - \iiint \left(\bar{r} \times \left(2\bar{\omega} \times \bar{V} \right) + \bar{r} \times \left(\dot{\bar{\omega}} \times \bar{r} \right) + \bar{r} \times \left(\bar{\omega} \times \left(\bar{\omega} \times \bar{r} \right) \right) \right) \rho d\forall = \frac{\partial}{\partial t} \left(\iiint \bar{r} \times \bar{V} \rho d\forall \right) + \oiint \bar{r} \times \bar{V} \left(\rho \bar{V} \bullet \overline{dA} \right) \quad (3.5)$$

The first term of Equation (3.5) represents the torque exerted on the fluid by all forces acting on the surface of the fluid control volume. This therefore includes the tangential (shear) and normal (pressure) forces exerted by the pipe walls as well as the pressures acting perpendicular to the inlet and outlet areas of the pipe. For the infinitesimal control volume and applying mathematical manipulation the equation may be written in its differential form as:

$$dM_z = \left| \frac{\partial r}{\partial s} \right| 2\rho V A \omega r ds$$

which after integration over a finite pipe length L leads to:

$$M_z = \tilde{\rho} \tilde{V} \tilde{A} \omega \left(r_e^2 - r_i^2 \right)$$

This then leads to the final integral form of the equation in terms of the mass flow rate as follows:

$$M_z = \dot{\tilde{m}} \omega \left(r_e^2 - r_i^2 \right) \quad (3.6)$$

3.2.4. Energy conservation

The integral form of the energy conservation equation for a finite control volume is given by Shames (1992):

$$\sum Q + \sum W = \frac{\partial}{\partial t}\left(\iiint\left(u + \frac{1}{2}C^2 + gz\right)\rho d\forall\right) + \oiint\left(h + \frac{1}{2}C^2 + gz\right)\rho\overline{V}\bullet\overline{dA} \tag{3.7}$$

$\sum Q$ is the total rate of heat transfer to the fluid and $\sum W$ the total rate of work done on the fluid. The rate of change of energy within the infinitesimal control volume will be taken as zero because of the steady-state conditions considered here. For the infinitesimal control volume and applying mathematical manipulation the equation may be written in its differential form as:

$$\sum dQ + \sum dW = \rho VA\frac{\partial}{\partial s}(h_o)ds$$

The preceding equation may now be integrated over a pipe with finite length L, resulting in the final integral form as follows:

$$\sum Q + \sum W = \tilde{\rho}\tilde{V}\tilde{A}(h_{oe} - h_{oi})$$

For a rotating pipe the total heat transfer to the fluid is simply equal to the heat transfer from the pipe walls Q_h, while the total work done on the fluid is equal to the torque exerted by the pipe walls M_z (as defined by Equation (3.6)) times the angular velocity ω. Therefore:

$$Q_h + M_z\omega = \tilde{\dot{m}}(h_{oe} - h_{oi}) \tag{3.8}$$

3.2.5. Summary

The final integral forms of the conservation equations for a purely radial rotating pipe may be summarised as follows:

Mass conservation

$$\dot{m}_e - \dot{m}_i = 0$$

Linear momentum conservation (compressible flow)

$$\tilde{\rho}\omega^2\left(r_e^2 - r_i^2\right) = \frac{\tilde{p}}{p_o}\left(p_{oe} - p_{oi}\right) + \frac{1}{2}\tilde{\rho}C^2\frac{1}{\tilde{T}_o}\left(T_{oe} - T_{oi}\right)$$
$$+\left(\frac{\tilde{f}L}{\tilde{D}} + \sum K\right)\frac{\left|\tilde{\dot{m}}\right|\tilde{\dot{m}}}{2\tilde{\rho}\tilde{A}^2} + K_i p_i\left(\left(1 + \frac{\gamma-1}{2}M_i^2\right)^{\frac{\gamma}{\gamma-1}} - 1\right)$$
$$+K_e p_e\left(\left(1 + \frac{\gamma-1}{2}M_e^2\right)^{\frac{\gamma}{\gamma-1}} - 1\right)$$

Angular momentum conservation

$$M_z = \tilde{\dot{m}}\omega\left(r_e^2 - r_i^2\right)$$

Energy conservation

$$Q_h + M_z\omega = \tilde{\dot{m}}\left(h_{oe} - h_{oi}\right)$$

3.3. Solid disc

3.3.1. Conduction equations

The heat transfer or temperature distribution of the rotating disc with radial cooling passages will be modelled using the equations formulated by Bird et al. (1960:319). A temperature distribution will be given in a cylindrical coordinate system. The partial differential equation will be integrated over a control volume using the finite difference method. This resulting equation will then be incorporated in an EES model to simulate the steady state temperature distribution of a rotating disc with radial cooling passages. The heat generated by the pumping power in the fluid will be connected to the solid conduction equations with the aid of the effectiveness-NTU heat exchanger calculation method. Finally the equation of energy in terms of the transport properties for Newtonian fluids of a constant density and conduction coefficient may be given in the form:

$$\rho \hat{C}_v \left(\frac{\partial T}{\partial t} \right) = k \left[\frac{1}{r} \frac{\partial}{\partial r} \left(r \frac{\partial T}{\partial r} \right) + \frac{1}{r^2} \frac{\partial^2 T}{\partial \theta^2} + \frac{\partial^2 T}{\partial z^2} \right] + Q \qquad (3.9)$$

The objective of this study is to construct a steady-state model for the fluid flow and heat transfer of a rotating disc with radial cooling passages. Thus, the transient term will be omitted. This then yields:

$$k \left[\frac{1}{r} \frac{\partial}{\partial r} \left(r \frac{\partial T}{\partial r} \right) + \frac{1}{r^2} \frac{\partial^2 T}{\partial \theta^2} + \frac{\partial^2 T}{\partial z^2} \right] + Q = 0 \qquad (3.10)$$

The result of the simplification of the equation makes it possible to accurately determine the temperature distribution of a solid cylindrical body in terms of a cylindrical coordinate system (r, θ, z).

By discretisation of the differential equation by using the finite difference method the equation may now be written in its final general integral form for a single node.

$$\left(\frac{2}{\rho_i \bar{C}\left(\left(r+\frac{\Delta r}{2}\right)^2-\left(r-\frac{\Delta r}{2}\right)^2\right)}\bullet S_r\right)+\left(\frac{1}{\rho_i \bar{C}\Delta\theta}\bullet S_\theta\right)+\left(\frac{2}{\rho_i \bar{C}\Delta z}\bullet S_z\right)+Q=0 \tag{3.11}$$

The source terms in the radial, theta and axial directions differ depending on the location of the associated node. The source terms for a side, corner and central node can be found in chapter 4. The complete discretisation process of the conduction equations can be found in appendix E.

3.3.2. Conduction resistance

Bird et al. (1960) introduced the temperature distribution equations in cylindrical coordinates. The following is true for an internal node in the r-coordinate component:

$$\rho \forall C_p \frac{\partial T}{\partial t} = Q_{in} - Q_{out} \tag{3.12}$$

and

$$\rho \forall C_p \frac{\partial T}{\partial t} = \frac{T_E - T_P}{R_E} + \frac{T_W - T_P}{R_W} \tag{3.13}$$

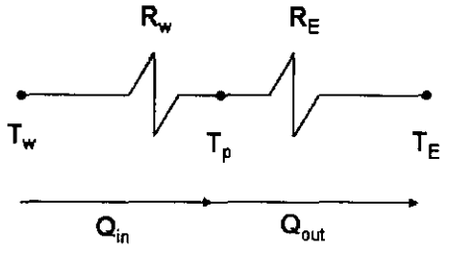

Figure 3.2: Conduction resistance for an internal node.

Incropera and De Witt (1996:92) describe the conduction resistance for a cylindrical wall as follows:

$$R_{t,cond} = \frac{\ln \frac{r_2}{r_1}}{2\pi k} \tag{3.14}$$

Thus the following is true after integration over the control volume:

$$\frac{\rho C_p}{2k}\left(r_e^2 - r_w^2\right)\frac{\partial T}{\partial t} = \frac{T_E - T_P}{\ln \frac{r_E}{r_P}} - \frac{T_W - T_P}{\ln \frac{r_W}{r_P}} \tag{3.15}$$

The equations formulated in appendix E state the following for the same conditions:

$$\frac{\rho C_p}{2k}\left(r_e^2 - r_w^2\right)\frac{\partial T}{\partial t} = \frac{r_e}{r_E - r_P}\left(T_E - T_P\right) - \frac{r_w}{r_W - r_P}\left(T_W - T_P\right) \tag{3.16}$$

Thus it should be determined if: $\ln \frac{r_E}{r_P} \approx \frac{r_e}{r_E - r_P}$

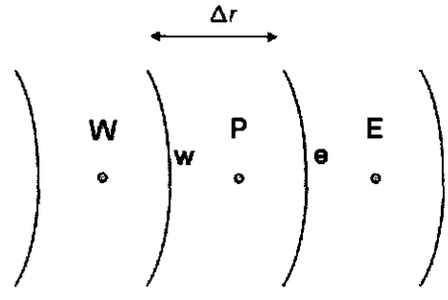

Figure 3.3: Node distribution for a cylindrical coordinate system.

$$\frac{r_e}{r_E - r_P} = \frac{\left(r_P + \frac{1}{2}\Delta r\right)}{\left(r_P + \Delta r\right) - r_P} = \frac{r_P + \frac{1}{2}\Delta r}{\Delta r} = \frac{r_P}{\Delta r} + \frac{1}{2}$$

$$\frac{1}{\ln\frac{r_E}{r_P}} = \frac{1}{\ln\frac{r_P+\Delta r}{r_P}} = \frac{1}{\ln\left(1+\frac{\Delta r}{r_P}\right)}$$

$\frac{\Delta r}{r_P}$	$\frac{r_P}{\Delta r}+\frac{1}{2}$	$\frac{1}{\ln\left(1+\frac{\Delta r}{r_P}\right)}$	error
1	1.500	1.443	3.950%
0.75	1.833	1.786	2.632%
0.50	2.500	2.469	1.256%
0.25	4.500	4.484	0.357%
0.10	10.50	10.492	0.075%
0.05	20.50	20.496	0.020%
0.01	100.5	100.499	0.001%

Table 3.1: Comparison table for two terms used in the temperature distribution equations.

Table 3.1 therefore shows that for small $\frac{\Delta r}{r_p}$ values the derived equations will give the same values as the equation containing the conduction resistance term stated by Incropera and DeWitt (1996).

3.3.3. Heat transfer connection

As stated above, the heat flux generated by the fluid flow in the rotating radial cooling channels will be connected to the heat transfer conduction model of the solid disc via the effectiveness-NTU method (Incropera and DeWitt (1996:599)). The reason for using the effectiveness-NTU method is to prevent temperature cross-over when a relatively course grid is employed. The effectiveness-NTU method includes the integration of the temperature profile over the length of the increment to be used. Therefore it will not be necessary

to use very small increments in the model to obtain a reasonable degree of accuracy.

If it is assumed that for an increment the wall temperature is constant, the effectiveness of the heat transfer over the wall of the cooling passages is defined as:

$$\varepsilon = 1 - e^{-NTU} \tag{3.17}$$

$$\varepsilon = \frac{Q}{Q_{max}} \tag{3.18}$$

$$NTU = \frac{UA}{\dot{m}C_p} \tag{3.19}$$

$$UA = hHTA \tag{3.20}$$

Finally, the actual heat transfer over the wall of the rotating radial channel is:

$$Q = \varepsilon \dot{m} C_p (T_w - T_m) \tag{3.21}$$

3.4. Nusselt number correlations

3.4.1. Top and bottom of the disc

To accurately predict the heat transfer of a rotating body one needs to find the proper correlation for the heat transfer coefficient (Nusselt number). In most cases the correlation is given as a function of the Reynolds number and the Prandtl number, such as the famous *Dittus-Boelter* equation for the turbulent flow in circular tubes.

The Nusselt number on the top and bottom of the rotating disc in the current study may be correlated using the results from the experiments conducted by Cobb and Saunders (1956). The experiments were conducted on a 457mm disc with a built-in electric heater rotating around a horizontal axis in air.

Average Nusselt numbers were determined over the range $10^4 < Re_\Omega < 6\times10^5$, and transition from laminar to turbulent flow occurred at $Re_\Omega \approx 2.4\times10^5$. For $Re_\Omega < 2\times10^5$ and $Pr = 0.71$ the Nusselt number was correlated by:

$$Nu_{av} = 0.36 Re_\Omega^{0.5} \quad (3.22)$$

For turbulent flow and $Pr = 0.71$ the Nusselt number was correlated by:

$$Nu_{av} = 0.015 Re_\Omega^{0.8} \quad (3.23)$$

where:

$$Re_\Omega = \frac{\rho \Omega r^2}{\mu} \quad (3.24)$$

Another Nusselt number correlation for a rotating free disc is given by Owen et al. (1974). The 762mm disc was heated by stationary radiant heaters, and this resulted in a uniform temperature distribution on the disc surface.

Using the measured surface temperatures as boundary conditions, they solved Laplace's conduction equation to determine the temperature distribution inside the disc. This was then used to calculate the surface heat flux. There were no sign of transition from laminar to turbulent flow, even at rotational Reynolds numbers as low as $Re_\Omega = 2.1\times10^5$. The resulting correlation for the Nusselt number ($Pr = 0.72$) may be written as:

$$Nu_{av} = 0.0171 Re_\Omega^{0.814} \quad (3.25)$$

Owen and Rogers (1989) presented the Nusselt number correlation for a rotating disc with an isothermal and a purely quadratic disc-temperature distribution on the disc's surface.

For small dissipative effects the Nusselt correlation may be given as:

$$Nu_{av,iso} = 0.32586 \mathrm{Re}_{\Omega}^{0.5} \quad (3.26)$$

and

$$Nu_{av,quad} = 0.51848 \mathrm{Re}_{\Omega}^{0.5} \quad (3.27)$$

Northrop and Owen (1988) correlated the Nusselt numbers for a rotating disc in air. For an isothermal disc with a power law index (n=0) and a Prandtl number of 0.72 the local and average Nusselt number correlations are:

Local Nusselt number

$$Nu = 0.0196 \mathrm{Re}_{\Omega}^{*0.8} \quad (3.28)$$

for $\mathrm{Re}_{\Omega}^{*} > 2.4 \times 10^{5}$.

McComas and Hartnett (1970) obtained a value of 0.0138 rather than 0.0151 for the constant of proportionality.

Average Nusselt number:

$$Nu_{av} = 0.0151 \mathrm{Re}_{\Omega}^{0.8} \quad (3.29)$$

For air with a quadratic (n=2) temperature rise on the disc the average Nusselt number becomes:

$$Nu_{av} = 0.0191 \mathrm{Re}_{\Omega}^{0.8} \quad (3.30)$$

For a detailed explanation of the power-law method the reader is referred to Northrop and Owen (1988) and Owen and Rogers (1995).

Qureshi et al. (1989) correlated the Nusselt number for the surface of a rotating disc. The Nusselt number increased with increasing rotational Reynolds number and the dependence of the disc face local Nusselt number on the coolant flow rate becomes less pronounced at high values for the rotational Reynolds number. The correlations are given for laminar and turbulent flow:

$$Nu_r = 0.8\mathrm{Re}_{\Omega}^{0.5} \tag{3.31}$$

for $(3\times10^4 \le \mathrm{Re}_{\Omega} \le 2\times10^5)$

$$Nu_r = 0.0274\mathrm{Re}_{\Omega}^{0.8} \tag{3.32}$$

for $(2\times10^5 \le \mathrm{Re}_{\Omega} \le 1.2\times10^6)$

The transition between laminar and turbulent flow was found to occur at $\mathrm{Re}_{\Omega} = 2\times10^5$.

Kreith et al. (1959) experimentally investigated the heat transfer from an isothermal disc and correlated the average Nusselt number for laminar flow conditions as:

$$Nu_{av} = 0.345\mathrm{Re}_{\Omega}^{0.5} \tag{3.33}$$

3.4.2. Inside and outside of the disc

The Nusselt number of the rotating cylindrical cavity (axial inlet of the cooling passages) (figure 3.4) may be correlated using the analytical solution presented by Kendoush (1996). The same correlation will also be used for the outside edge of the rotating disc of the current study (figure 3.4).

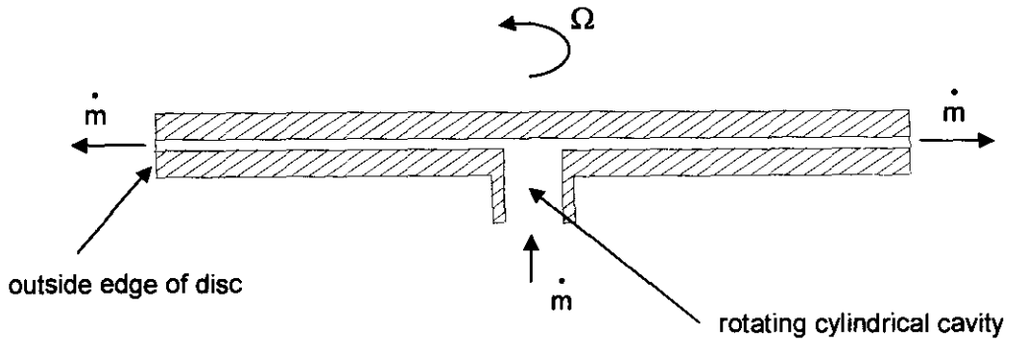

Figure 3.4: Schematic representation of the rotating disc.

The correlation is valid for fluids of small viscosity and low Prandtl numbers (gases and light fluids). It is also important to mention that the presented correlations may only be used for fluid flows dominated by forced convection. Thus for convective heat transfer from an isothermal rotating cylinder the Nusselt number may be approximated by:

$$Nu_{av} = 0.6366\left(\mathrm{Re}_{\Omega}^{'}\,\mathrm{Pr}\right)^{0.5} \tag{3.34}$$

where:

$$\mathrm{Re}_{\Omega}^{'} = \frac{\Omega D_0^{\,2}\rho}{2\mu} \tag{3.35}$$

and

$$\mathrm{Pr} = \frac{\upsilon}{\alpha} \tag{3.36}$$

subjected to: $\mathrm{Re}_{\Omega}^{'} > 10^3$.

Other correlations for the Nusselt number for the inside cylindrical rotating cavity and outside edge of the disc (figure 3.4) are presented by Ozerdem (2000), Anderson and Saunders (1953), Etemad and Buffalo (1955) and Becker (1963). They correlated the Nusselt number for the convective heat transfer from a horizontal cylinder rotating in ambient air. These correlations

are given as a function of the rotational Reynolds number and Prandtl number (0.72):

Author	Equation	Remark
Anderson and Saunders (1953)	$Nu_{av} = 0.1\mathrm{Re}_{\Omega}^{'2/3}$ (3.37)	Analogy solution
Etemad and Buffalo (1955)	$Nu_{av} = 0.076\mathrm{Re}_{\Omega}^{'0.7}$ (3.38)	$8000 \le \mathrm{Re}_{\Omega}^{'} \le 65400$
Dropkin and Carmi (1957)	$Nu_{av} = 0.073\mathrm{Re}_{\Omega}^{'2/3}$ (3.39)	$15000 \le \mathrm{Re}_{\Omega}^{'} \le 43300$
Becker (1963)	$Nu_{av} = 0.119\mathrm{Re}_{\Omega}^{'2/3}$ (3.40)	$800 \le \mathrm{Re}_{\Omega}^{'} \le 100000$
Ozerdem (2000)	$Nu_{av} = 0.318\mathrm{Re}_{\Omega}^{'0.571}$ (3.41)	$2000 < \mathrm{Re}_{\Omega}^{'} < 40000$

Due to the nature of the flow structure inside the rotating cavity (vortex dominated) the previously noted correlations may be inaccurate. The Nusselt number correlation for a rotating cylindrical cavity with radial outflow was presented by Owen and Onur (1983).

They identified various heat transfer structures inside the rotating cavity. The Nusselt number may be estimated using the 'core dominating' regime for radial outflow of fluid of a rotating cylindrical cavity (see Owen and Onur (1983)).

3.4.3. Rotating passages

The Nusselt correlation for the internal radial passages will be correlated using the 'Dittus-Boelter' equation for the turbulent flow in circular tubes. The equation was taken from Incropera and DeWitt (1996).

$$Nu_D = 0.023\mathrm{Re}^{0.8}\mathrm{Pr}^n \tag{3.42}$$

where $n = 0.4$ for heating ($T_s > T_m$) and $n = 0.3$ for cooling ($T_s < T_m$)

The equation has been confirmed experimentally for the following range of conditions:

1. $0.7 \le \mathrm{Pr} \le 160$
2. $\mathrm{Re} \ge 10000$
3. $\frac{L}{D} \ge 10$

and

$$\mathrm{Re} = \frac{4\dot{m}}{\pi D\mu} \tag{3.43}$$

The heat transfer coefficient for the internal radial passages can also be correlated using the constant heat flux Colburn equation contained in the study by Wagner et al. (1991). The Nusselt number correlation is given for fully developed turbulent flow in a smooth tube and for a constant wall temperature. The correlation is given by:

$$Nu_H = 0.022\mathrm{Re}^{0.8}\mathrm{Pr}^{0.6} \tag{3.44}$$

with $\mathrm{Pr} = 0.72$

$$Nu_\infty = 0.0176\mathrm{Re}^{0.8} \tag{3.45}$$

3.5. Friction factor correlation

For a rough[1] non-rotating pipe the friction factor for laminar flow is given by the equation found in Shames (1992:362) and for turbulent flow in Shames (1992:366). The equations are:

Laminar flow

$$\tilde{f}_{stationary,rough} = \frac{64}{\mathrm{Re}} \tag{3.46}$$

Turbulent flow

$$\tilde{f}_{stationary,rough} = \frac{0.25}{\left\{\log\left[\left(\frac{e}{3.7D}\right)+\left(\frac{5.74}{\mathrm{Re}^{0.9}}\right)\right]\right\}^2} \tag{3.47}$$

Ito and Nanbu (1971) presented results and formulas for friction factors for laminar and turbulent flow in smooth[2] rotating straight pipes of circular cross section. The friction factor for laminar flow in a smooth rotating straight pipe is given by:

Laminar flow

$$\frac{\tilde{f}_{rotating,smooth}}{f_{sl}} = 0.0883K_l^{0.25}\left(1+11.2K_l^{-0.325}\right) \tag{3.48}$$

$$f_{sl} = \frac{64}{\mathrm{Re}} \tag{3.49}$$

$$K_l = \mathrm{Re}_\Omega \mathrm{Re} \tag{3.50}$$

[1] The relative roughness of the pipe is taken into account when calculating the pressure loss.
[2] The relative roughness of the pipe is omitted when determining the pressure loss.

This equation gives good agreement with experimental results obtained by Ito and Nanbu (1971) in the range:

$$2.2\times10^2 < K_l < 10^7 \text{ and } \frac{\mathrm{Re}_\Omega}{\mathrm{Re}} < 0.5$$

Below $K_l = 2.2\times10^2$, the friction factor for a rotating straight pipe practically coincides with that for a stationary straight pipe.

The friction factor for turbulent flow in a smooth rotating straight pipe is given by:

Turbulent flow

$$\frac{\tilde{f}_{rotating,smooth}}{f_{st}} = 0.942 + 0.058K_t^{0.282} \quad (3.51)$$

$$f_{st} = 0.3164\mathrm{Re}^{-0.25} \quad (3.52)$$

$$K_t = \frac{\mathrm{Re}_\Omega^2}{\mathrm{Re}} \quad (3.53)$$

This equation gives good agreement with experimental results obtained by Ito and Nanbu (1971) in the range:

$$1 < K_t < 5\times10^2$$

Below $K_t = 1$, the friction factor for a rotating straight pipe practically coincides with that for a stationary straight pipe.

The transition from laminar to turbulent flow occurs above a critical value of the Reynolds number. The critical Reynolds number is:

$$R_{crit} = 1070\mathrm{Re}_\Omega^{0.23} \quad (3.54)$$

To obtain the correct value for the friction factor for a rough rotating straight pipe one needs to determine the effect that the relative roughness has on the friction factor.

This can be done by determining a scaling factor:

$$ratio = \frac{\tilde{f}_{stationary,rough}}{\tilde{f}_{stationary,smooth}} \quad (3.55)$$

This ratio can be used to scale the friction factor for a smooth rotating straight pipe.

$$\tilde{f}_{rotating,rough} = ratio \times \tilde{f}_{rotating,smooth} \quad (3.56)$$

3.6. Inlet and outlet conditions

Due to the rotation of the disc the air entering the rotating cylindrical cavity will have a swirling motion. This swirling motion of the air can be attributed to the formation of vortex flows. Near the centre of the rotating cylindrical cavity a forced vortex can be identified. Further from the centre a free vortex will dominate the flow structure. As stated above, the effect that the inlet vortex has on the fluid-flow will be incorporated into the simulation model via an empirically determined inlet loss factor. At the outlet of the rotating pipe a free vortex will aid in pressure recuperation. The formation of vortex flows will have a major impact on the pressure gradient and the mass flow through the rotating pipe.

3.6.1. Inlet loss coefficient

The inlet loss factor will be empirically determined from experimental measurements. The procedure followed to calculate the inlet loss factor (K_{in}) will be discussed in section 5.8.

3.6.2. Outlet loss coefficient

With respect to the complex three-dimensional flow patterns associated with vortex flows, the current study will contain a simplified model for the modelling of the vortex flows at the outer edge of the rotating disc. The free vortex at the outlet of the rotating pipe will be modelled as incompressible and inviscid. Therefore it is clear that the total pressure must remain constant in the free vortex at the outside of the rotating disc.

Thus:

$$P_{0e} = P_{0i} \tag{3.57}$$

Thus the outlet loss factor is defined as follows:

$$K_{out} = 0 \tag{3.58}$$

The full derivation process followed to obtain the result mentioned in equation (3.57) can be found in appendix C.

3.7. Conclusion

It is now possible to simulate the rotating disc with internal radial passages. All the relevant conservation equations and correlations have been formulated. The following chapter will describe in detail the algorithm that was developed to produce the simulation model.

CHAPTER 4

4. SIMULATION MODEL

4.1. Introduction

Now that all the conservation equations and correlations have been derived (see chapter 3), an algorithm may be formulated to simulate the steady-state fluid flow and heat transfer of a rotating disc with radial cooling passages. Thus the main objective of this chapter will be to formulate an algorithm that will be used to simulate the rotating-disc system. A secondary objective will be to clarify all the assumptions made in developing the simulation. In the latter part of the chapter the heat transfer correlations obtained in the literature will be compared with each other to acquire the most appropriate correlations for the current study. The above objectives will be pursued by focusing on the EES model (4.2) and on general assumptions (4.3).

4.2. EES model

The main EES model will be solved implicitly by using equations of continuity, momentum and energy in their integral form. The flow is solved for a given rotational speed, inlet temperature, pressure ratio and pipe geometry (see appendix D for a copy of the complete simulation model). A mathematical model has also been presented by Greyvenstein (2002) for the same rotating disc assembly.

4.2.1. Theory

4.2.1.1. Rotating pipe

The rotating pipe is a purely radial pipe (with no deviation in the theta or axial directions). The rotating pipe is also a straight pipe with constant cross-sectional area from the inlet to the outlet.

The rotating pipe will be divided into nine increments (figure 4.1). This is necessary to obtain a distribution of various simulated parameters lengthwise in the pipe. Only one of the six rotating pipes will be modelled. This is a valid assumption because of the symmetry of the rotating pipes.

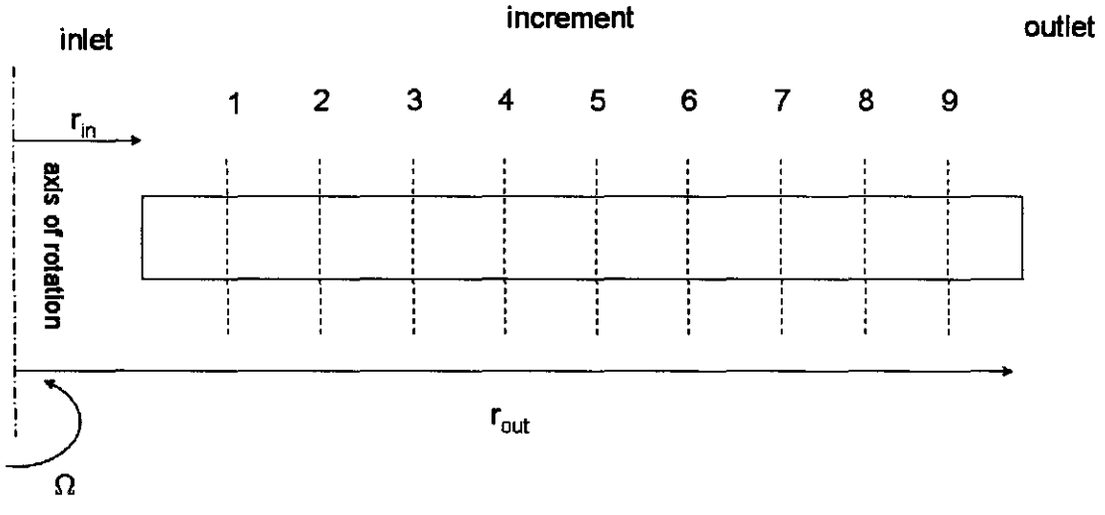

Figure 4.1: Rotating pipe incrementation.

4.2.1.2. Solid disc temperature distribution

To obtain a temperature distribution an axisymmetric segment of the disc will be divided into seven node blocks (figure 4.3). A node block is made up of twenty seven nodes (figure 4.4), each connected to their neighbours with the equations described in the theory chapter. There are three axial (z), nine radial (r) and seven theta (θ) component nodes. The reason for the chosen nodal distribution is the thin nature of the disc. The disc has a diameter of 600mm and a width of 14mm; thus a greater temperature gradient is expected in the radial direction than in the axial direction. The nodes in block one are connected to the nodes in block two and so on; therefore a totally three-dimensional temperature distribution of 189 points distributed equally in the segment is possible.

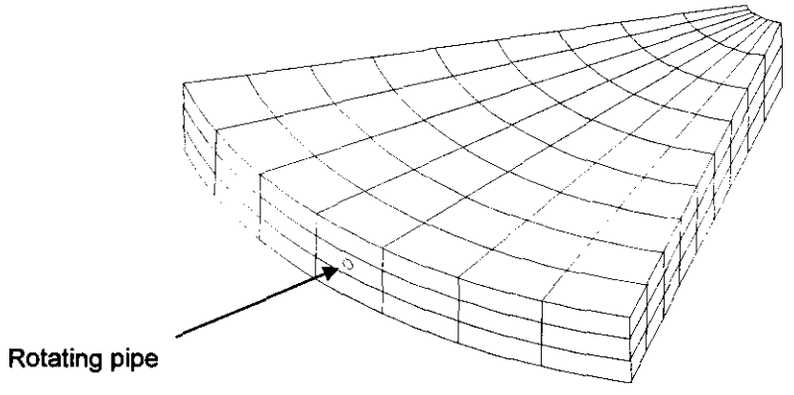

Figure 4.2: Axisymmetric segment to be simulated.

The outer boundaries of blocks one and seven are considered to be adiabatic walls. Block one is connected to block two and has no other neighbours in the theta direction; the same applies to block seven. This assumption is relevant because of the axisymmetric nature of the rotating disc. The rotating pipe is located in the middle of block four (nodes 2,5,8,11,14,17,20,23,26 of block four).

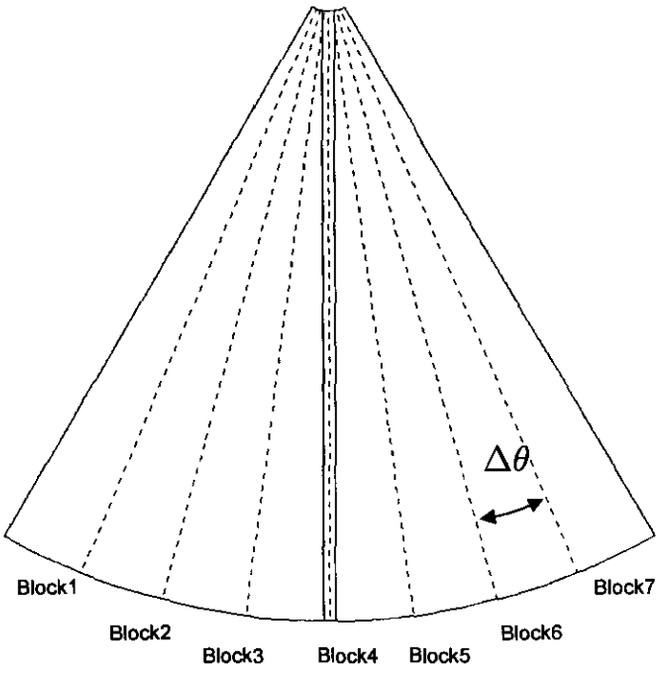

Figure 4.3: Axisymmetric segment and node blocks used to produce a temperature distribution within the disc.

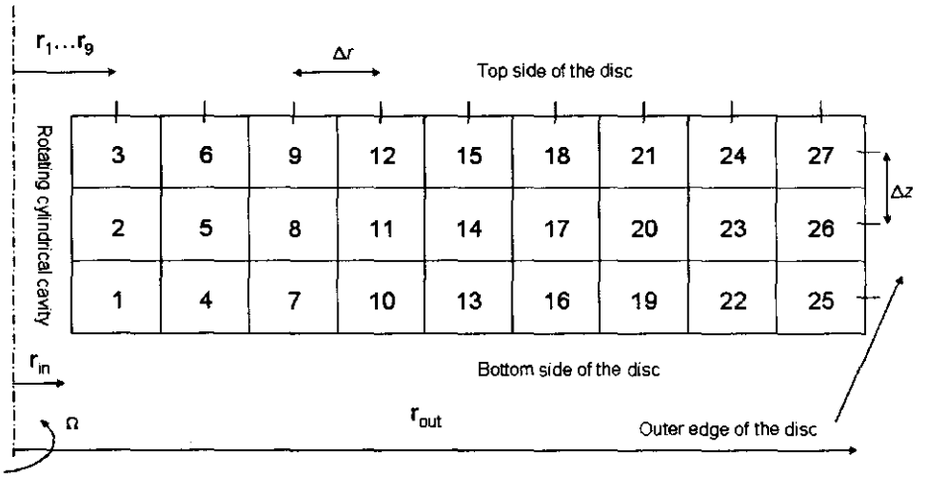

Figure 4.4: Representation of a Node block.

with the source terms:

$$S_r = r_{in} h_{inside} \left(Tf_{in} - T_{2,1}\right) + k_2 \left(r_1 + \frac{\Delta r}{2}\right)\left(\frac{T_{2,4} - T_{2,1}}{\Delta r}\right)$$

$$S_\theta = \frac{k_2}{\Delta\theta}\left[\frac{T_{1,1} - T_{2,1}}{r_1^2}\right] - \frac{k_2}{\Delta\theta}\left[\frac{T_{2,1} - T_{3,1}}{r_1^2}\right]$$

$$S_z = \frac{k_2}{\Delta z}\left(T_{2,2} - T_{2,1}\right) + h_{bottom}\left(Tf_{bottom} - T_{2,1}\right)$$

Side Node

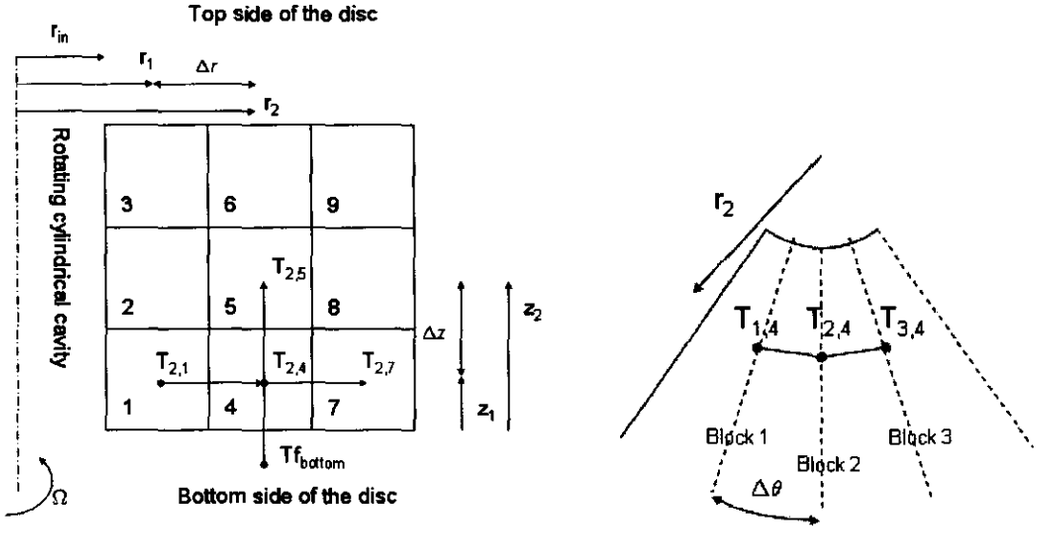

Figure 4.6: Side node and neighbours.

The final general integral form of the conduction equation for block 2 node 4 may now be written as (see section 3.3.1 and appendix E):

The final general integral form of the conduction equation for block 2 node 5 may now be written as (see section 3.3.1 and appendix E):

$$\left(\frac{2k_2}{\rho_2\overline{C}_{pr2,2}\left(\left(r_2+\frac{\Delta r}{2}\right)^2-\left(r_2-\frac{\Delta r}{2}\right)^2\right)}\bullet S_r\right)+\left(\frac{1}{\rho_2\overline{C}_{pr2,2}\Delta\theta}\bullet S_\theta\right)+\left(\frac{2}{\rho_2\overline{C}_{pz2,2}\Delta z}\bullet S_z\right)+Q=0 \tag{4.3}$$

with the source terms:

$$S_r=\left(r_2+\frac{\Delta r}{2}\right)\left(\frac{T_{2,8}-T_{2,5}}{\Delta r}\right)-\left(r_2-\frac{\Delta r}{2}\right)\left(\frac{T_{2,5}-T_{2,2}}{\Delta r}\right)$$

$$S_\theta=\frac{k_2}{\Delta\theta}\left[\frac{T_{1,5}-T_{2,5}}{r_2^2}\right]-\frac{k_2}{\Delta\theta}\left[\frac{T_{2,5}-T_{3,5}}{r_2^2}\right]$$

$$S_z=\frac{k_2}{\Delta z}\left(T_{2,6}-T_{2,5}\right)-\frac{k_2}{\Delta z}\left(T_{2,5}-T_{2,4}\right)$$

4.2.2. Algorithm

Table 4.1 describes the layout of the EES simulation programme used to simulate the rotating disc system. It should be stated that all the equations form an integrated solution and all the equations will be solved simultaneously to produce accurate simulation results.

INPUT CONDITIONS
Pipe and disc geometry
Temperatures
Pressures
Fluid (air) properties
Aluminium disc material properties
Disc rotation speed

COMPRESSIBLE PIPE FLOW (Inlet)	EQUATIONS USED
Air total inlet temperature	A.22
Air total inlet pressure	A.24
Air inlet density	A.25
Air inlet mach number	A.23
Air total inlet velocity component	A.19

COMPRESSIBLE PIPE FLOW (Outlet)	EQUATIONS USED
Air total outlet temperature	A.22
Air total outlet pressure	A.24
Air outlet density	A.25
Air outlet mach number	A.23
Air total outlet velocity component	A.19

COMPRESSIBLE PIPE FLOW (Average)	EQUATIONS USED
Air total average temperature	A.22
Air total average pressure	A.24
Air average density	A.25
Air average mach number	A.23
Air total average velocity component	A.19

FRICTION FACTORS	EQUATIONS USED
Friction factor for a rotating pipe	3.48 to 3.56
Friction factor for a stationary pipe	3.46 and 3.47

LOSS FACTORS	EQUATIONS USED
Inlet loss factor (K_in)	5.1
Outlet loss factor (K_out)	A.26

CONSERVATION EQUATIONS	EQUATIONS USED
Mass conservation	3.2
Linear momentum conservation	3.4
Momentum of momentum conservation	3.6
Energy conservation	3.8

EFFECTIVENESS NTU FOR A PIPE	EQUATIONS USED
Effectiveness	3.17
NTU	3.19
UA	3.20
Actual heat transfer rate (Q)	3.21

NUSSELT NUMBERS	EQUATIONS USED
Rotating cylindrical cavity Nusselt number	3.34
Outer edge of disc Nusselt number	3.34
Top side of disc Nusselt number	3.25
Bottom side of the disc Nusselt number	3.25
Rotating pipe Nusselt number	3.42

NODE TEMPERATURE DISTRIBUTION EQUATIONS	EQUATIONS USED
Block 1 (27 equations)	4.1 to 4.3
Block 2 (27 equations)	4.1 to 4.3
Block 3 (27 equations)	4.1 to 4.3
Block 4 (27 equations)	4.1 to 4.3
Block 5 (27 equations)	4.1 to 4.3
Block 6 (27 equations)	4.1 to 4.3
Block 7 (27 equations)	4.1 to 4.3

Table 4.1: Layout of the EES algorithm.

4.3. General assumptions

4.3.1. Boundary conditions

It will be assumed that the rotating pipe acts as a heat flux source term (at nine increment points) which will be used in the determination of the temperature distribution of the disc.

4.3.2. Compressible fully developed fluid flow

The inlet pressure to the rotating pipe will be experimentally measured with the help of the experimental test bench, while the outlet pressure will be taken as ambient (87.5 kPa at 25°C, atmospheric conditions in Potchefstroom, South Africa).

4.3.3. Heat transfer correlations

The Nusselt numbers for a rotating disc have been calculated using various correlations in the literature. Graphic representations of the calculations are given in figures 4.8 to 4.10. It can be seen that the Nusselt numbers increase with increasing rotational speed.

It is important to note that some of the correlations are not valid for the full range of rotational speeds. It can also be seen that not all the correlations are valid for both the rotating cylindrical cavity and the outside edge of the disc. This is due to the high rotational Reynolds number located on the outside edge of the disc. Finally, it is also important to point out that some of the correlations deviate from the expected trend. This phenomenon can be attributed to a transition zone caused by the connection between equations. It is also evident from the graphs that the Nusselt numbers differ by huge margins therefore it is imperative to choose the most suitable correlation for the current study.

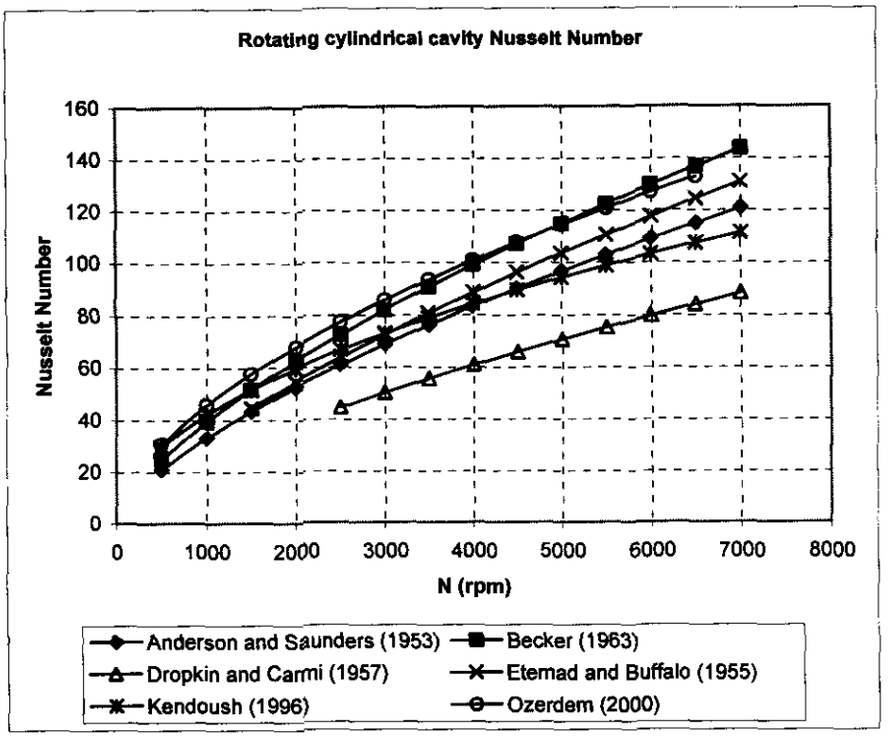

Figure 4.8: Rotating cylindrical cavity Nusselt number.

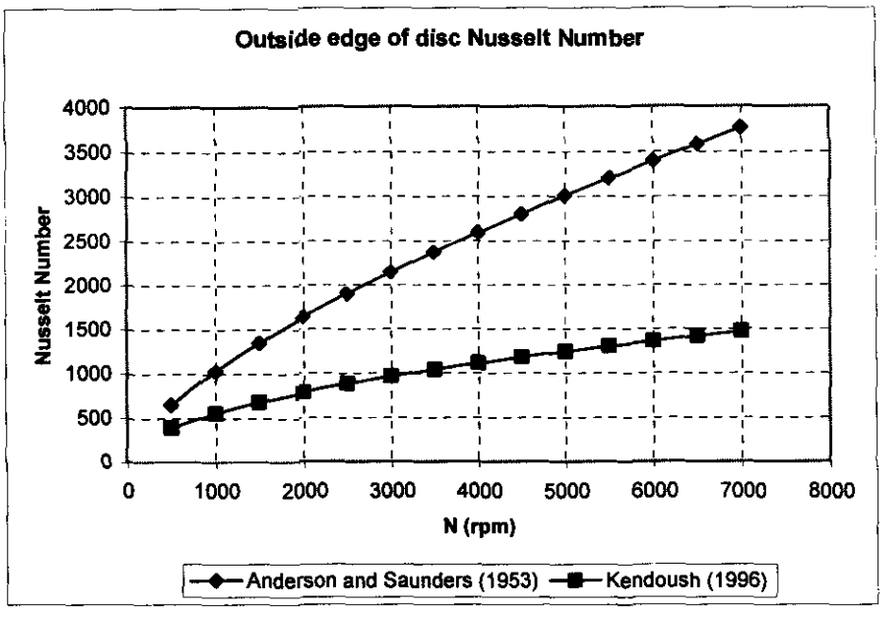

Figure 4.9: Outside edge of the disc Nusselt Number.

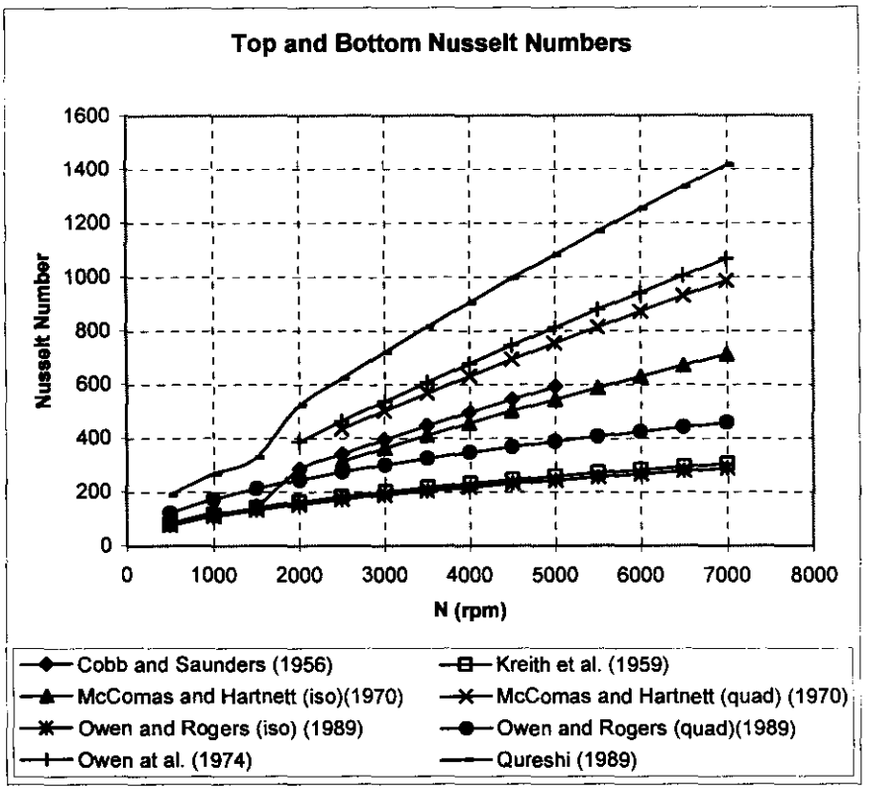

Figure 4.10: Top and bottom side of the disc Nusselt number.

It was decided to use the correlation presented by Kendoush (1996) for the rotating cylindrical cavity and the outside edge of the disc. This is a valid assumption because the correlation by Kendoush (1996) is the only general analytical correlation that could be found for the convective heat transfer from an isothermal rotating cylinder. The correlations presented by the other authors are very scenario specific.

For the top and bottom of the disc it was decided to use the correlation presented Owen et al. (1974). This assumption is valid because the correlation by Owen et al. (1974) is the best known and most widely used correlation for free discs.

4.4. Conclusion

This chapter described the development of an EES computer programme (see appendix D) to simulate a rotating disc with internal radial cooling channels. The various aspects that were looked at included the definition of a grid to solve the temperature distribution of the disc and an outline of the EES computer program algorithm. In section 4.3.3 of the chapter the various heat transfer coefficients obtained from the literature were compared to each other and the most suitable Nusselt number correlation were selected. The following chapter will discuss the experimental test bench that was used to verify the results obtained from the EES simulation model.

CHAPTER 5

5. EXPERIMENTAL TEST BENCH

5.1. Introduction

The current chapter will describe the layout, operation and the results obtained from the experimental test bench capable of measuring the volumetric flow rate and inlet pressures at various rotational speeds. At the end of the chapter the results from the simulation model will be compared to the measurements obtained from the experimental test bench. This is necessary to verify the accuracy of the theoretical results acquired from the simulation model.

5.2. Experimental objectives

The experimental test bench will be used to measure the volumetric flow rate through the rotating channels for various pressure ratios and rotational speeds of the disc. The experimental test bench must therefore be able to measure the inlet pressure in the rotating cylindrical cavity (inlet to the rotating pipe) and the volumetric flow rate through the system. It is not within the scope of this study to do any heat transfer measurements, although the test bench will be capable of this.

5.3. Experimental apparatus

The rotating disc test bench facility used in this study has been previously described. (see Greyvenstein (2002)). To produce more accurate measurements,

the rotating-disc test bench has been upgraded. In the interest of completeness a description of this facility will be presented here, together with a detailed description of the add-ons to the earlier test bench.

The original test bench consisted solely of a rotating disc. The rotating-disc test bench was upgraded by adding a centrifugal fan, electrical heater, ball valves, a more accurate flowmeter, temperature probes and a pressure transmitter. A schematic of the new test bench facility is shown in figure 5.1. With the help of the ball valves it is possible to accurately adjust the pressure ratio (volume flow rate) across the rotating pipes.

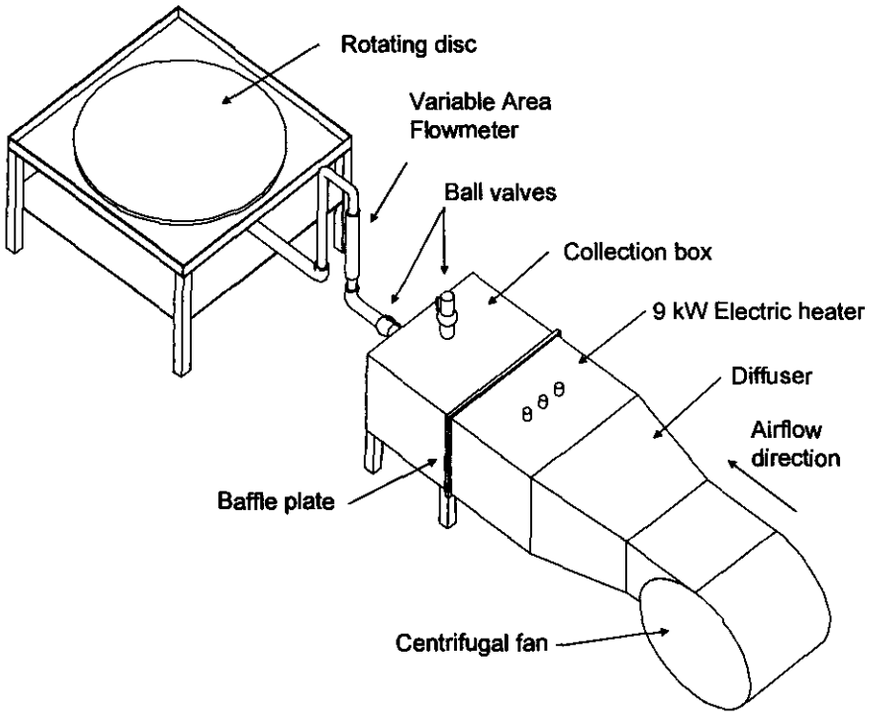

Figure 5.1: Experimental test bench.

Air is pumped through the system with the help of the centrifugal fan and the centrifugal pumping motion of the rotating disc. The rotating disc is driven by a

variable speed DC motor via a toothed belt drive. The speed of the rotating disc can be adjusted by using a frequency inverter.

Although no temperature measurements will be done the experimental test bench is capable of controlling and measuring the inlet and outlet temperatures to the rotating pipes. The air can be heated with a 9 kW electrical heater which consists of three 3kW coils. The inlet air temperature could be controlled by using a TOHO CN-40-R microprocessor-based digital temperature controller with full PID-control. The controller consists of a temperature sensor that measures the temperature at the inlet of the rotating disc (figure 5.2). The digital temperature controller controls a contactor which switches the electrical coils on and off. The baffle plate mixes the air to ensure a homogeneous air temperature distribution.

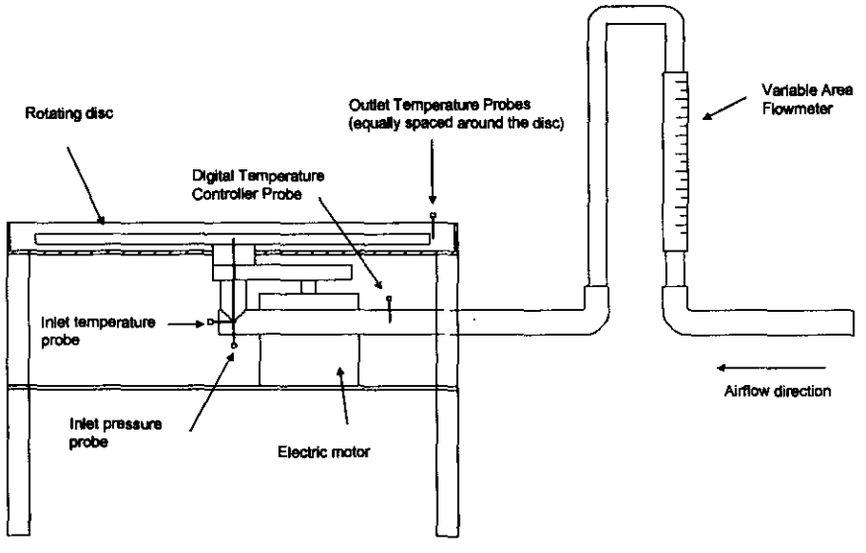

Figure 5.2: Side view of experimental test bench showing probe positions.

5.4. Design parameters

The rotational speed of the rotating disc model will be limited to between 2000 and 5000 rpm. The experimental rotating disc is capable of speeds no higher than 6000 rpm. The disc experiences a resonant zone between 5000 and 6000 rpm. Because of safety reasons the disc will therefore not be subjected to rotational speeds higher than 5000 rpm.

The experimental test bench has been designed to be able to raise the air inlet temperature to at least 50 °C. However, for the purpose of this study it will not be necessary to raise the temperature any higher than the ambient temperature (25°C).

5.5. Flow and heat transfer measurements

The volume flow rate was controlled by using two ball valves. The horizontal ball valve influenced the flow rate directly and the vertical ball valve acted as a blow-off (vent). The volume flow rate was measured by using a Fischer & Porter Extruded body Flowrator (glass tube variable-area flowmeter). The flowmeter consists of a float that measures a percentage of maximum flow. The flowmeter is capable of measuring a maximum flow of 1280 L/min and a minimum of 8 L/min.

The pressure at the inlet of the rotating disc was measured using a pressure probe (figure 5.2). The probe consisted of a long tube positioned to measure the pressure inside the rotating cylindrical cavity (inlet to the rotating channels). The pressure probe was connected to a VEGABAR 42 pressure transmitter.

Temperature measurements can be taken by using Pyrotemp probes (two-wire type T thermocouples). The inlet and outlet temperature probe positions are shown in figure 5.2. Four probes were situated one centimetre from the exit of the rotating pipes (figure 5.2). These probes are capable of measuring the outlet temperature of the rotating channels.

The signals from the thermocouples and the pressure transmitter were transmitted to ADAM modules. The five signals (mV) from the Pyrotemp probes were fed to an ADAM 4018, 8 channel thermocouple input module. Similarly, the signals (mA) from the pressure transmitter were fed to an ADAM 4017, 8 channel analog input module. The ADAM 4018 and 4017 modules were connected to an ADAM 4520 isolated converter. The data was then logged using Visidaq data acquisition software. Only the data obtained from the pressure probe will be used in this study.

5.6. Data acquisition method

The method that was followed to obtain the experimental data will be briefly described. The centrifugal fan was first switched on (full power or 10 L/min). The blow-off (vent) ball valve was fully closed and the in-line ball valve was fully opened. The frequency inverter was then used to adjust the rotational speed of the rotating disc. The maximum volume flow rate for the set rotational speed was then measured with the help of the variable area flowmeter. The VEGABAR 42 pressure transmitter then measured the pressure in the rotating cylindrical cavity.

The in-line ball valve was then used to reduce the volume flow rate by two percent. At this condition the pressure transmitter again measured the inlet

pressure. This procedure was repeated until the flowmeter could no longer register a value (< 8 L/min).Thereupon the ball valve was fully opened and the rotational speed was adjusted. The whole procedure was repeated for all the rotational speeds. The pressure ratios could be determined with the help of the measured inlet pressures and the ambient pressure.

5.7. Experimental results and discussion

The following graph (figure 5.3) shows the results obtained from the experimental test bench. The experiment has been carried out at a constant inlet temperature of 25°C.

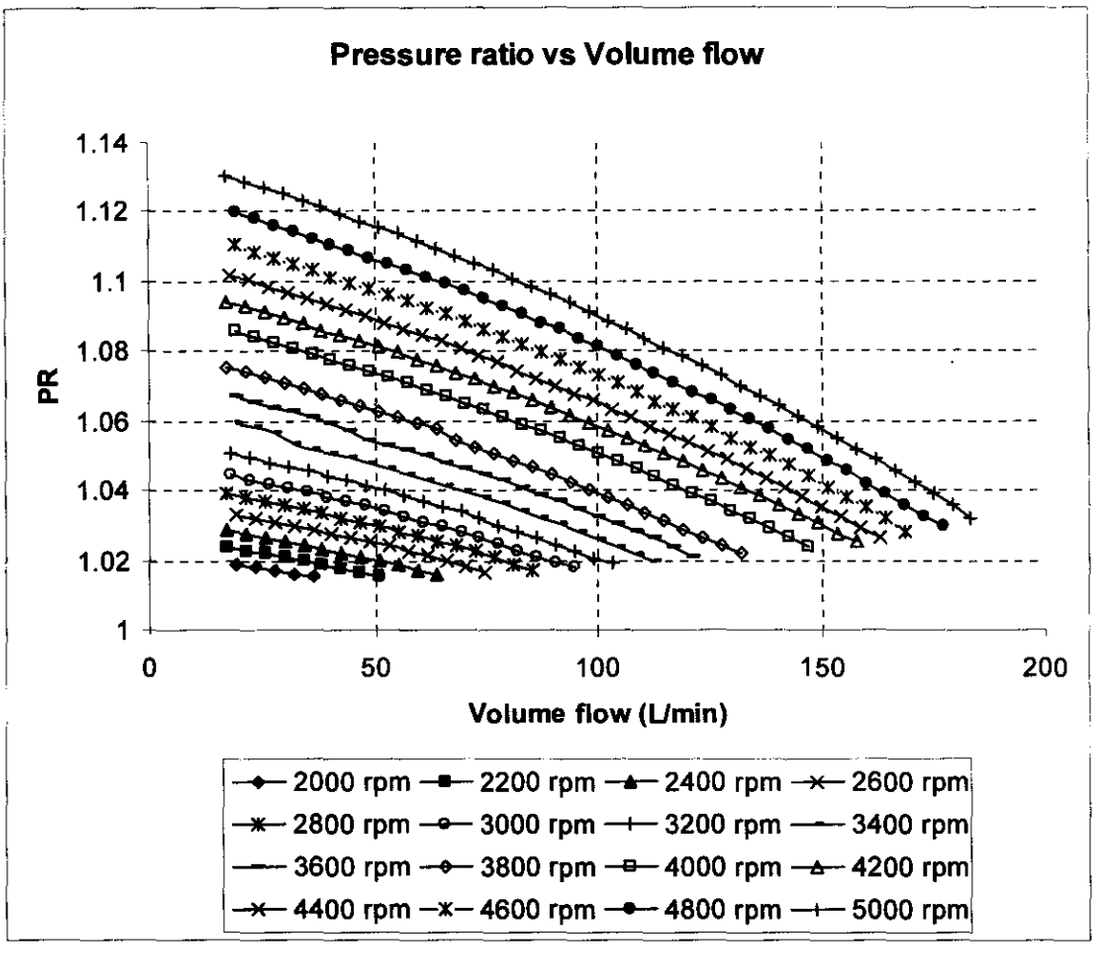

Figure 5.3: Experimental results showing pressure ratio versus volume flow for an inlet temperature of 25 °C.

It can be seen from figure 5.3 that the pressure ratio falls as the volumetric flow rate increases for all rotational speeds. Thus the inlet pressure is reduced even more each time the ball valve is closed increasingly. This in turn raises the pressure ratio, which reduces the volume flow rate. This trend could have been expected, owing to the fact that the rotating disc with radial cooling channels has very similar performance characteristics as a centrifugal compressor, hence the similarities between a non-dimensional compressor chart and the obtained results. See appendix F for a tabulation of all the experimental data.

5.8. Inlet loss factor

The vortex in the rotating cylindrical cavity gives rise to an inlet loss factor. The accuracy of the simulation model will be strongly influenced by the precision of the inlet loss factor. The inlet loss factors have been empirically determined by using the data obtained from the experimental test bench. The mass flow and pressure ratio in the simulation model was set to the mass flow and pressure ratio measurements obtained from the experimental test bench. Thus, an inlet loss factor could be calculated, for a given mass flow and pressure ratio.

With the help of the experimental data an analytical formula could be derived for the inlet loss factor. It was decided to determine if the inlet loss factor could be calculated from an inlet velocity ratio. The inlet velocity ratio was defined as the inlet radial velocity component divided by the inlet tangential velocity component. Figure 5.4 illustrates this relationship.

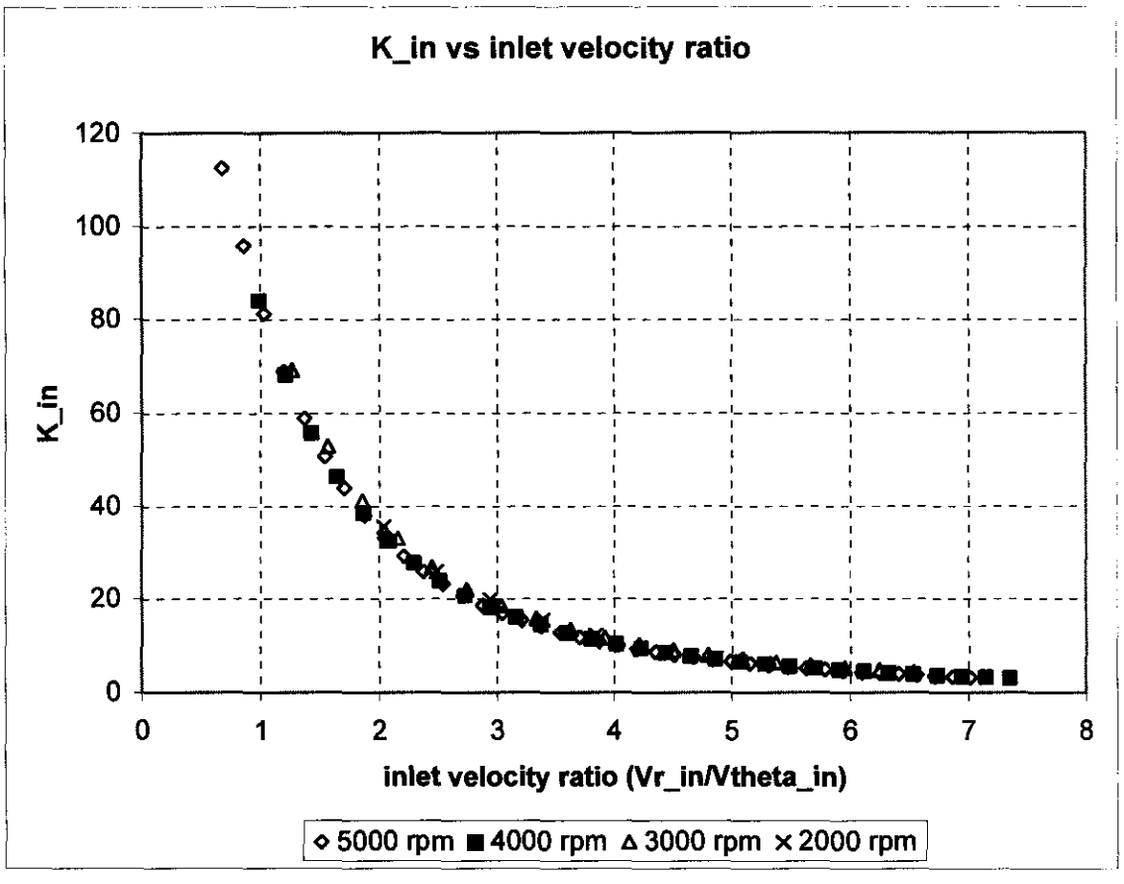

Figure 5.4: Graph showing relationship between the inlet loss factor and the inlet velocity ratio.

Figure 5.4 shows the inlet loss factor as a function of the inlet velocity ratio for various pressure ratios and rotational speeds of the disc. It is evident from figure 5.4 that the inlet loss factor was indeed only a function of the defined inlet velocity ratio. The inlet tangential velocity component remains constant for a specified rotational speed of the disc. The inlet loss factor will therefore increase as the inlet radial velocity component decreases. Practically the data points of figure 5.4 make perfect sense. At a low radial velocity the fluid will find it difficult to enter the rotating channels because of the strong vortex that will form at the inlet. The vortex in the rotating cylindrical cavity is mainly driven by the tangential velocity component. The vortex will weaken as the radial velocity increases,

aiding the flow through the rotating channels and in turn lessening the inlet loss factor. Thus the higher the inlet radial velocity component the lower the inlet loss factor tends to be and vice versa. It is also interesting to note that as $\frac{Vr_{in}}{V\theta_{in}} \rightarrow \infty$ the inlet loss factor approaches 0.5 which is the standard inlet loss factor for the flow through a t-piece in a stationary pipe.

A curve fit of the experimental data presented in figure 5.4 was done in order to establish an analytical formula to calculate the inlet loss factor. The following sixth-order polynomial was found to produce the best fit for the data:

$$\begin{aligned} K_{in} = {} & 217.037756 - 206.440104(\text{inlet velocity}_{ratio}) \\ & + 94.1341751(\text{inlet velocity}_{ratio})^2 - 24.3646525(\text{inlet velocity}_{ratio})^3 \\ & + 3.63608919(\text{inlet velocity}_{ratio})^4 - 0.290970438(\text{inlet velocity}_{ratio})^5 \\ & + 0.00965448459(\text{inlet velocity}_{ratio})^6 \end{aligned} \quad (5.1)$$

Equation 5.1 will be used in the simulation model to determine the inlet loss factor.

The deviation of the simulation results from the experimental results is due to the sensitivity of equation 5.1. Small differences between the exact inlet loss value and the inlet loss value determined by equation 5.1 had significant impact on the mass flow rate. Thus the accuracy of the simulation model is strongly influenced by the inlet loss factor.

5.10. Conclusion

The layout, operation and the results of the experimental test bench has been presented in this chapter. Although no heat transfer measurements were made, adequate results have been obtained showing the performance characteristics of the rotating disc with radial cooling channels. The results obtained from the simulation model compared well with the data obtained from the experimental test bench. It was found that the inlet loss factor is a function of the inlet radial velocity divided by the inlet tangential velocity. With the help of experimental data it was possible to formulate an equation to calculate the inlet loss factor. Although a satisfactory comparison between the simulation model and the experimental data could be made, the simulation model was found to be very sensitive for minute variations of the inlet loss factor. The following chapter will contain all the results from the simulation model. The results will include the temperature, pressure, density and velocity distributions in the rotating pipe and disc at various rotational speeds.

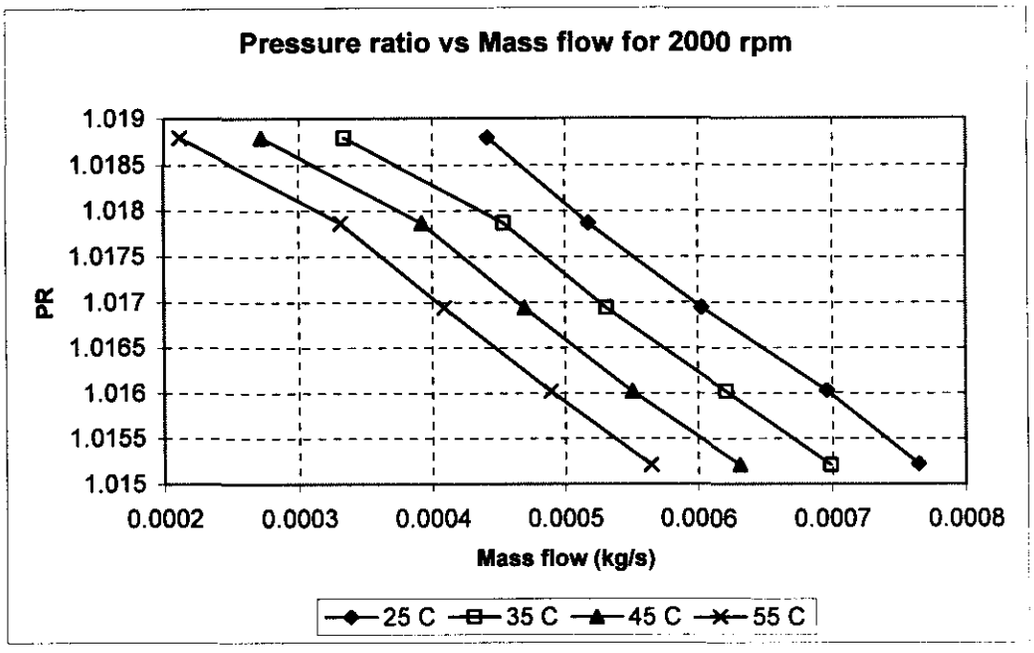

Figure 6.1: Pressure ratio versus mass flow for 2000 rpm at various inlet temperatures.

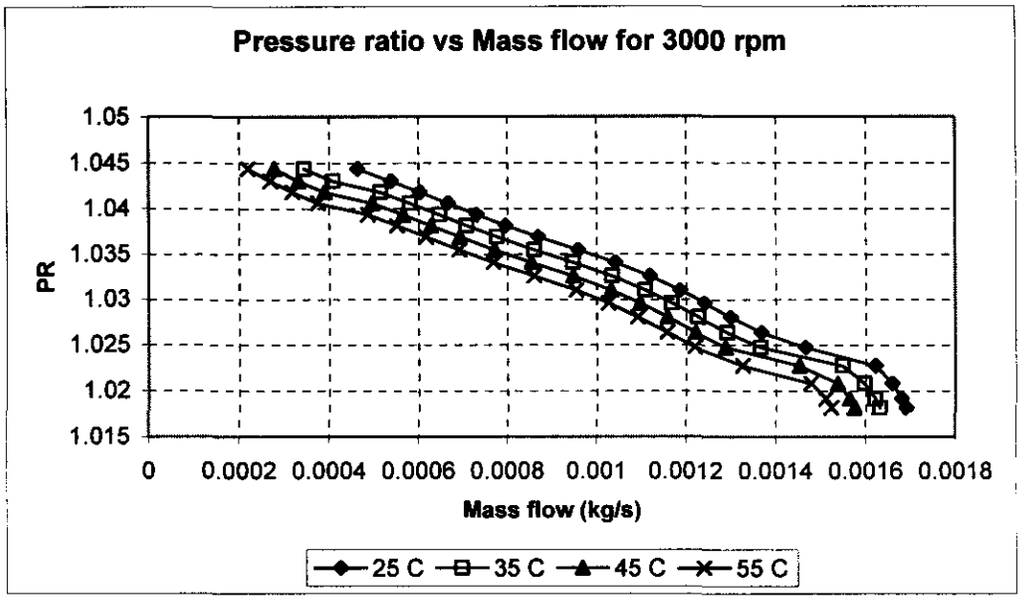

Figure 6.2: Pressure ratio versus mass flow for 3000 rpm at various inlet temperatures.

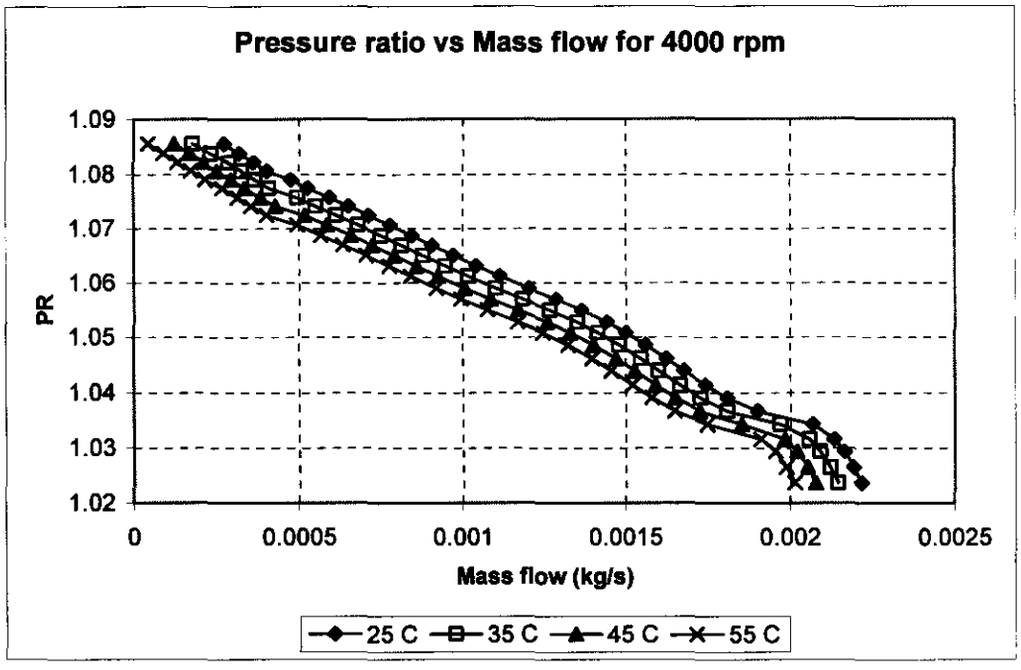

Figure 6.3: Pressure ratio versus mass flow for 4000 rpm at various inlet temperatures.

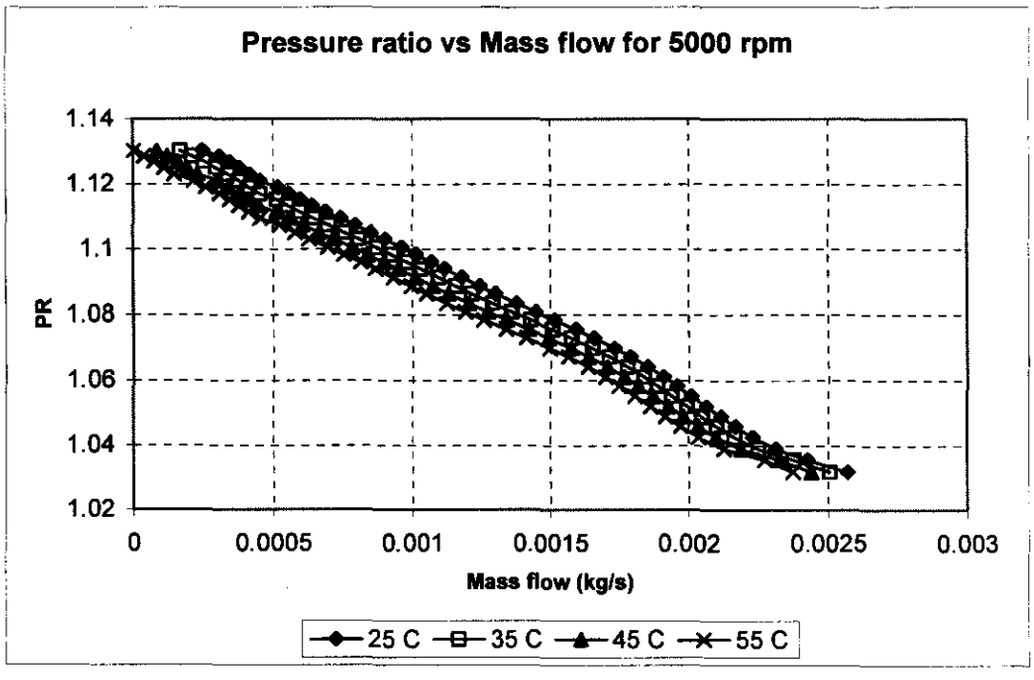

Figure 6.4: Pressure ratio versus mass flow for 5000 rpm at various inlet temperatures.

It is evident from figure 6.1 to 6.4 that as the mass flow decreases the pressure ratio increases. The same occurrence is also true for a centrifugal compressor. Another observation that can be made is that the mass flow rate decreases as the inlet temperature increases. This behaviour can be explained with the help of equation 3.8. The second term (torque exerted on the pipe walls times the angular velocity) remains constant for a specific rotational speed. Thus, as the inlet temperature increases, the total enthalpy increases as well. Therefore the mass flow rate must decrease in order for the heat transfer from the pipe walls to remain constant for a specified rotational speed of the disc.

$$Q_h + M_z\omega = \dot{\tilde{m}}(h_{oe} - h_{oi})$$

Another way to describe the decrease of mass flow for an increase of inlet temperature is the fact that the density decreases as the inlet temperature increases. A decrease of density will force the velocity to increase. An increase of velocity will result in a large increase of the friction resistance in the rotating pipe. The density decreases and the velocity increases but the influence that an increase of velocity has on the friction factor dominates the behaviour of the mass flow. For a raised inlet temperature the mass flow will therefore decrease.

There exists an inconsistency in the graphs at low pressure ratios and high mass flow rates for rotational speeds of 3000 to 4000 rpm. These inconsistencies can be attributed to the simulation model's sensitivity to the calculated inlet loss factor.

6.3. Temperature distribution in the rotating pipe

The following figure shows the total temperature distribution in the rotating pipe for various rotational speeds.

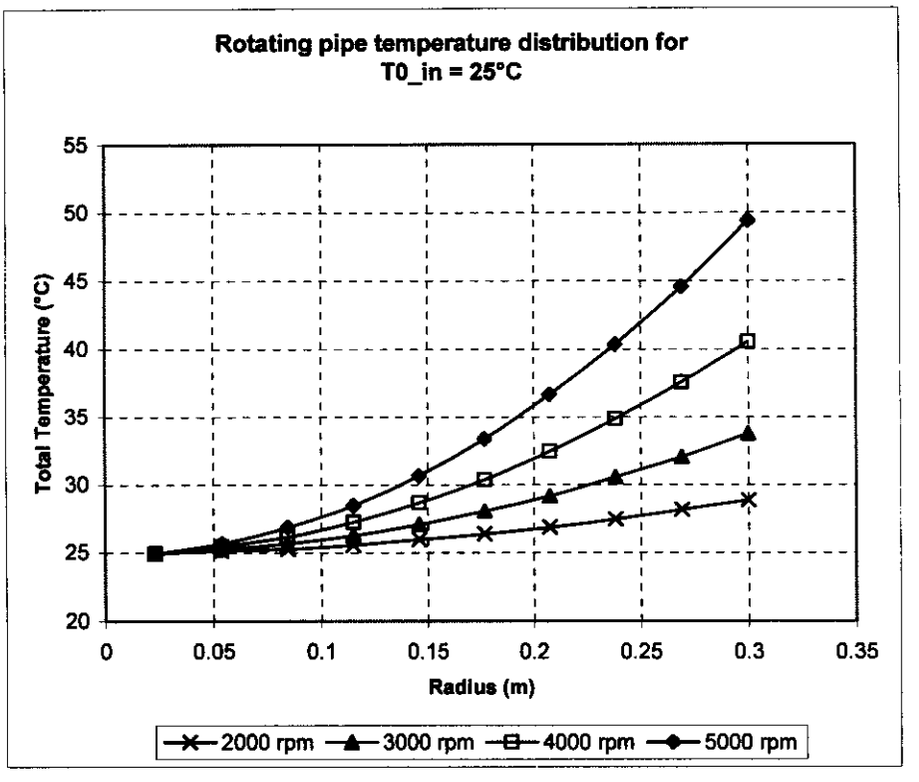

Figure 6.5: Rotating pipe temperature distribution for various rotational speeds at an inlet temperature of 25°C.

It is clear from figure 6.5 that as the rotational speed of the disc increases the temperature gradient in the rotating pipe also increases. The trend illustrated in figure 6.5 could have been expected. The higher the rotational speed of the disc, the more work is being done on the fluid by the pipe walls.

Thus, with an increase of the torque exerted by the pipe walls on the fluid, due to a higher rotational speed, the enthalpy will increase. It is therefore understandable that the temperature must also increase. The inlet temperature was varied from 25°C to 55°C. It was found that at higher inlet temperatures the graph stays exactly the same, except that it is raised by 10°C. The graphs showing the temperature distributions at higher inlet temperatures can be found in appendix G.

6.4. Pressure distribution in the rotating pipe

The following figure shows the total pressure distribution in the rotating pipe for various rotational speeds.

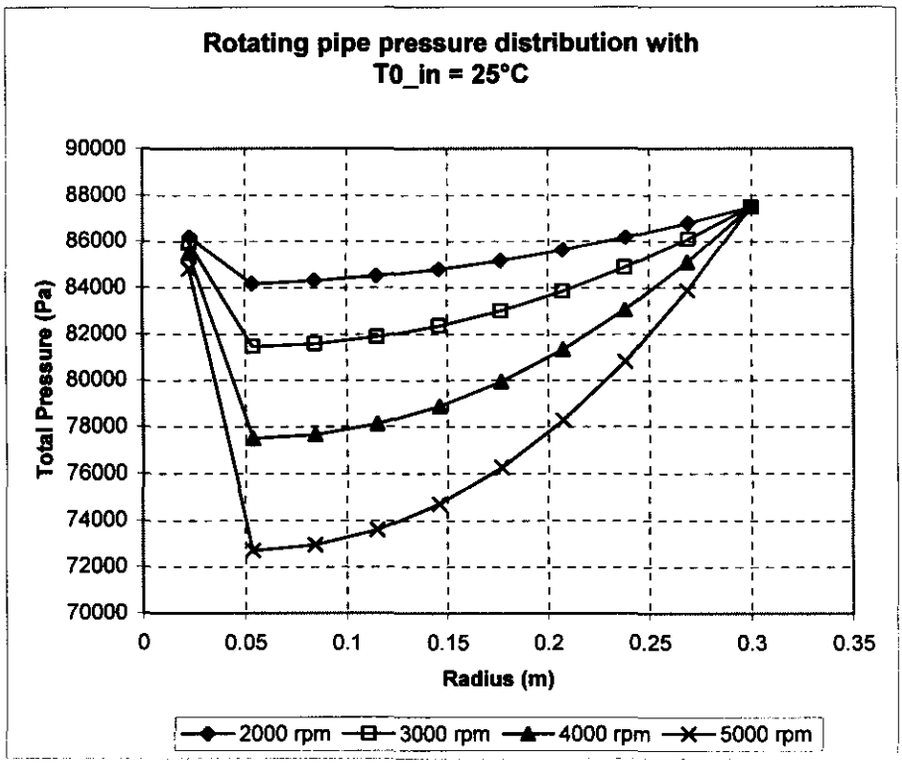

Figure 6.6: Rotating pipe pressure distribution for various rotational speeds at an inlet temperature of 25°C.

Figure 6.6 shows that there is a massive decline in the pressure at the inlet of the rotating pipe. This phenomenon can be accredited to the calculated inlet loss factor. It is also clear from figure 6.6 that the inlet loss factor has a much greater effect as the rotational speed of the disc increases. The outlet loss factor is taken as zero; the reason for this has been explained above.

Therefore the total outlet pressure must equal the ambient pressure (87.5 kPa), as illustrated in figure 6.6. For each of the rotational speeds the total inlet pressure has been experimentally determined from the experimental test bench. The final observation that can be made from figure 6.6 is that the pressure increases from the inlet to the outlet of the rotating pipe. A pressure ratio can therefore be identified. The higher the rotational speed of the disc, the higher the pressure ratio.

It was found that at higher inlet temperatures the graph stays exactly the same, except that it is slightly raised. The graphs showing the pressure distributions at higher inlet temperatures can be found in appendix G.

6.5. Density distribution in the rotating pipe

The following figure shows the total density distribution in the rotating pipe for various rotational speeds.

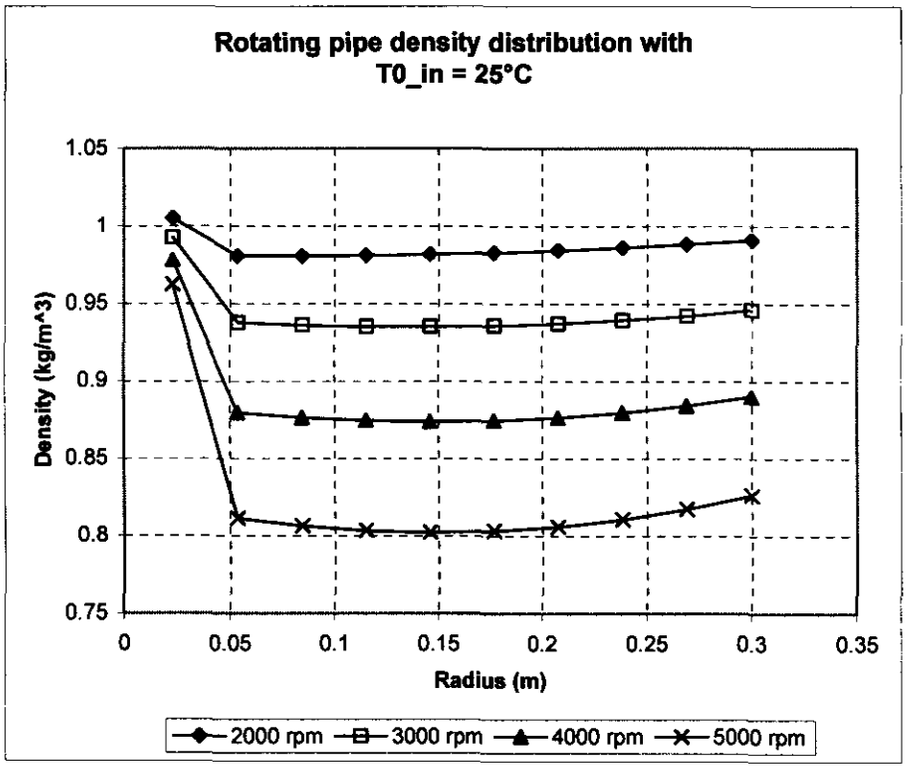

Figure 6.7: Rotating pipe density distribution for various rotational speeds at an inlet temperature of 25°C.

The preceding figure illustrates that there is a massive decline in the density at the inlet to the rotating pipe. The reason for this is again due to inlet loss factor. It is also apparent that the inlet loss has a more noticeable effect the higher the rotational speed. At a radial position of about 0.05m the density starts to increase. The temperature and the velocity increases in the rotating-pipe, which

in turn decreases the density. However, due to the compression of the air in the rotating pipe these lowering effects of the density is overcome. Therefore the density increases in the radial direction. It was found that for higher inlet temperatures the graph exhibits the same trend, except that it is slightly lowered. These graphs at higher inlet temperatures may be found in appendix G.

6.6. Velocity distribution in the rotating pipe

The following figure shows the total velocity distribution in the rotating pipe for various rotational speeds.

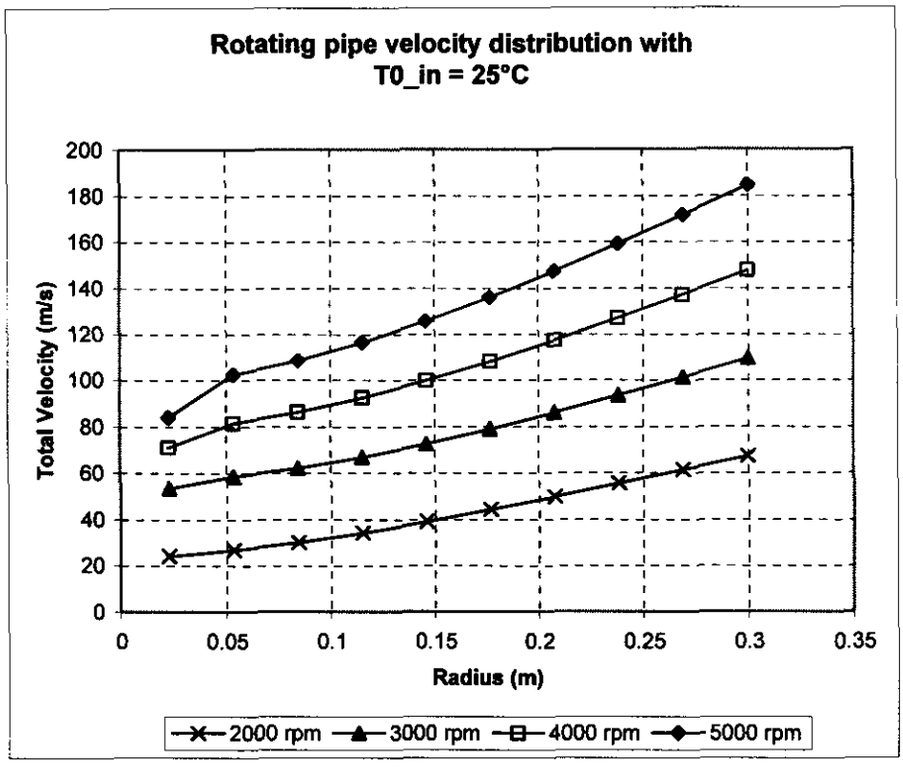

Figure 6.8: Rotating pipe velocity distribution for various rotational speeds at an inlet temperature of 25°C.

The trend illustrated in figure 6.8 could have been expected. For higher rotational speeds the velocity distribution tends to be higher. The radial velocity increases significantly at the inlet due to major decrease of the density at the inlet. But, because of the combination of the tangential velocity component the graphs are smoothed. Therefore the total velocity component will increase in the radial direction due to the increasing tangential velocity component. It was found that the trend of the graphs for higher inlet temperatures stays the same, except that they are again slightly lowered. The graphs showing the velocity distributions in the rotating pipe for higher inlet temperatures may be found in appendix G.

6.7. Temperature distribution of the solid disc

The temperature distribution of an axisymmetric sixty degree segment (figure 6.9) of the rotating disc has been calculated for various rotational speeds of the disc. The inlet temperature was set to 25°C and the environmental temperature to 55°C. This was done in order to illustrate the cooling effect of the rotating passages.

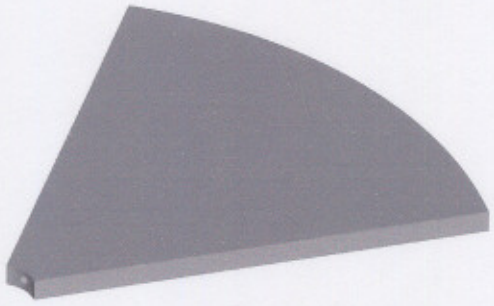

Figure 6.9: Axisymmetric 60° segment of the rotating disc.

To illustrate the three-dimensional temperature distribution in the segment, it was decided to display the temperature profile of various sections of the segment (figure 6.10). Section A is a horizontal section through the middle of the internal channel. Section B is a vertical section, again through the middle of the internal

channel. Section C depicts the temperature profile of the wall of the rotating cylindrical cavity. Section D is a vertical section halfway in the radial direction of the disc. Section E illustrates the temperature profile of the outer edge of the rotating disc.

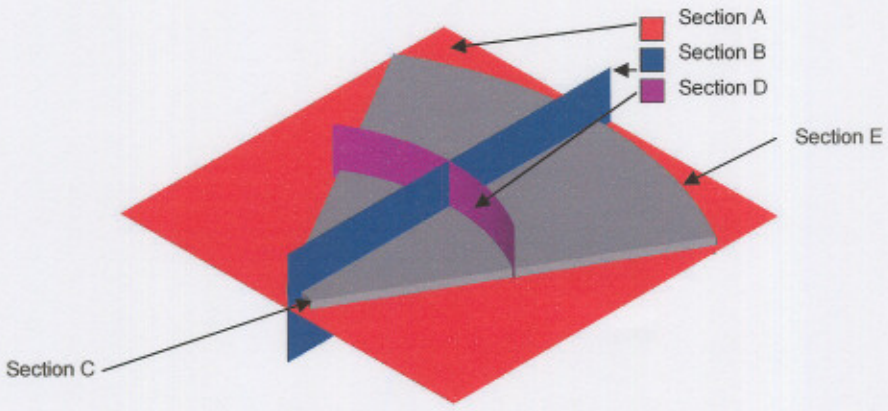

Figure 6.10: Sectioning of an axisymmetric segment of the rotating disc.

A grid containing nodes and a temperature contour of the various sections is given to simplify the visualisation of the temperature distribution.

6.7.1. Temperature distribution at 2000 rpm

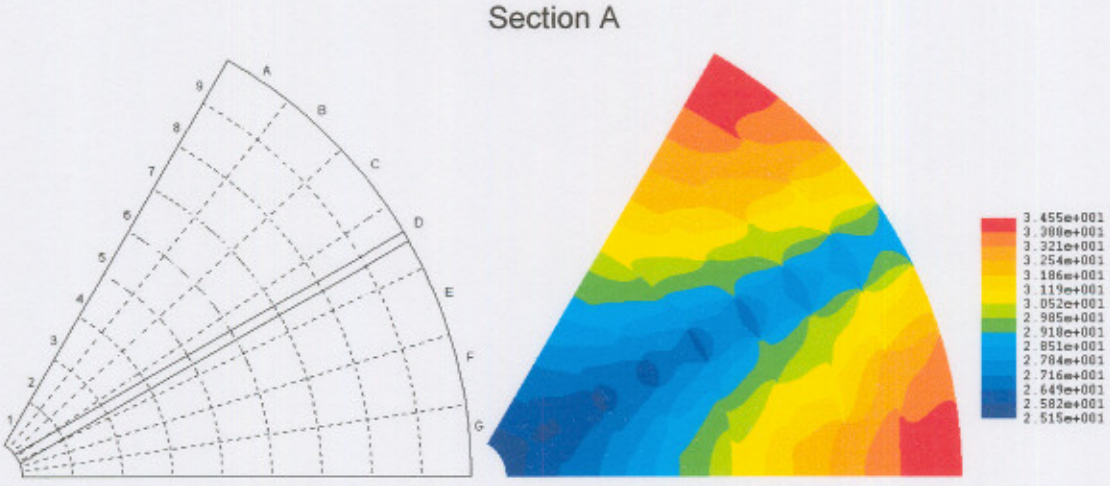

Figure 6.11: Grid and temperature contour of Section A at 2000 rpm.

Node	1	2	3	4	5	6	7	8	9
A	25.65	26.55	27.75	29.15	30.55	31.85	32.95	33.95	34.55
B	25.55	26.35	27.35	28.65	29.85	31.05	32.15	33.05	33.65
C	25.45	25.95	26.65	27.55	28.45	29.45	30.35	31.15	31.85
D	25.15	25.25	25.55	25.95	26.35	26.85	27.45	28.15	28.85
E	25.45	25.95	26.65	27.55	28.45	29.45	30.35	31.15	31.85
F	25.55	26.35	27.35	28.65	29.85	31.05	32.15	33.05	33.65
G	25.65	26.55	27.75	29.15	30.55	31.85	32.95	33.95	34.55

Table 6.1: Nodal temperature distribution of Section A at 2000 rpm.

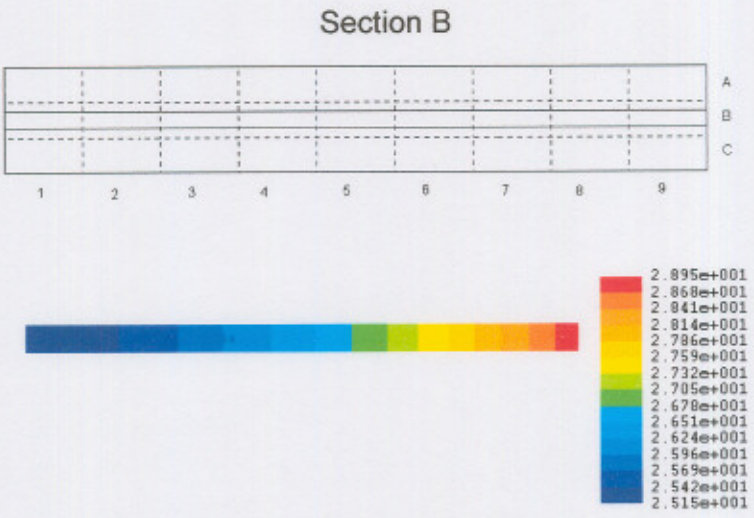

Figure 6.12: Grid and temperature contour of Section B at 2000 rpm.

Node	1	2	3	4	5	6	7	8	9
A	25.25	25.35	25.65	26.05	26.45	26.95	27.55	28.25	28.95
B	25.15	25.25	25.55	25.95	26.35	26.85	27.45	28.15	28.85
C	25.25	25.35	25.65	26.05	26.45	26.95	27.55	28.25	28.95

Table 6.2: Nodal temperature distribution of Section B at 2000 rpm.

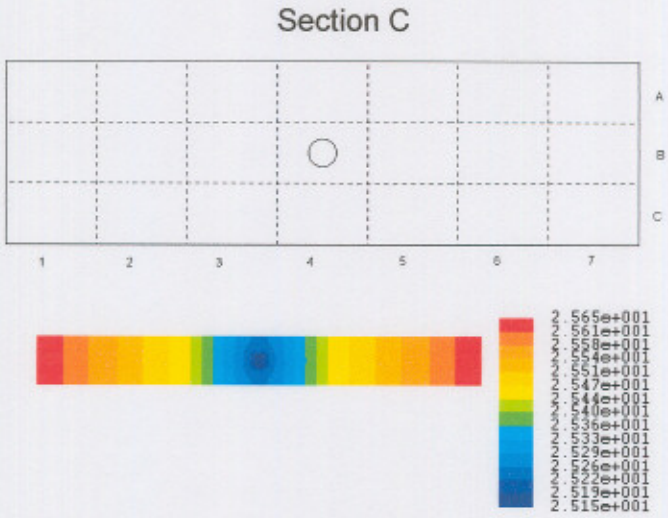

Figure 6.13: Grid and temperature contour of Section C at 2000 rpm.

Node	1	2	3	4	5	6	7
A	25.65	25.55	25.45	25.25	25.45	25.55	25.65
B	25.65	25.55	25.45	25.15	25.45	25.55	25.65
C	25.65	25.55	25.45	25.25	25.45	25.55	25.65

Table 6.3: Nodal temperature distribution of Section C at 2000 rpm.

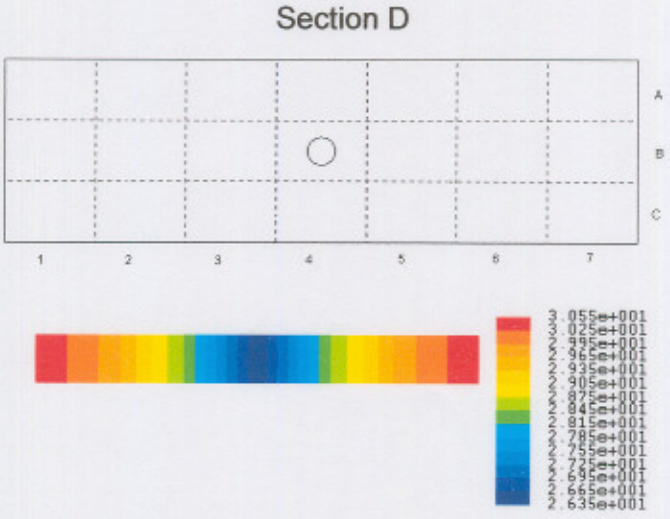

Figure 6.14: Grid and temperature contour of Section D at 2000 rpm.

Node	1	2	3	4	5	6	7
A	30.55	29.85	28.45	26.45	28.45	29.85	30.55
B	30.55	29.85	28.45	26.35	28.45	29.85	30.55
C	30.55	29.85	28.45	26.45	28.45	29.85	30.55

Table 6.4: Nodal temperature distribution of Section D at 2000 rpm.

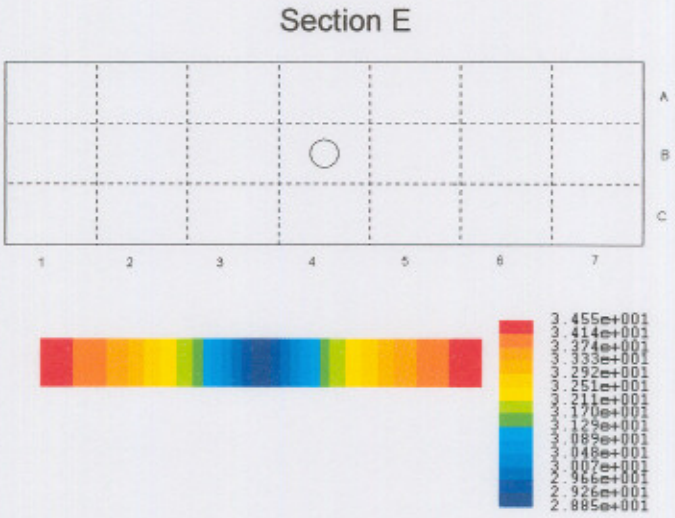

Figure 6.15: Grid and temperature contour of Section E at 2000 rpm.

Node	1	2	3	4	5	6	7
A	34.55	33.65	31.85	28.95	31.85	33.65	34.55
B	34.55	33.65	31.85	28.85	31.85	33.65	34.55
C	34.55	33.65	31.85	28.95	31.85	33.65	34.55

Table 6.5: Nodal temperature distribution of Section E at 2000 rpm.

6.7.2. Temperature distribution at 3000 rpm

Section A

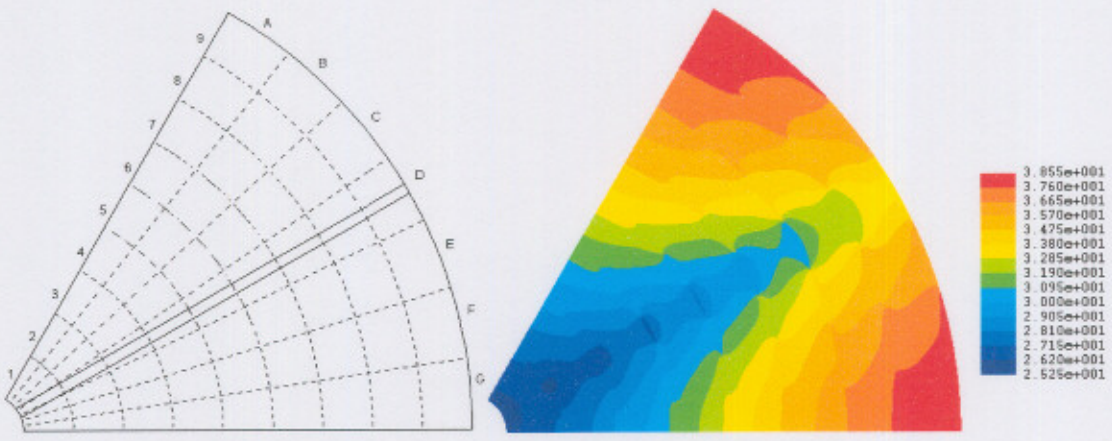

Figure 6.16: Grid and temperature contour of Section A at 3000 rpm.

Node	1	2	3	4	5	6	7	8	9
A	26.05	27.45	29.25	31.25	33.25	35.05	36.65	37.85	38.55
B	25.85	27.15	28.75	30.55	32.45	34.15	35.75	36.95	37.75
C	25.65	26.55	27.75	29.25	30.75	32.25	33.85	35.15	36.15
D	25.25	25.65	26.25	27.05	28.05	29.15	30.55	32.05	33.75
E	25.65	26.55	27.75	29.25	30.75	32.25	33.85	35.15	36.15
F	25.85	27.15	28.75	30.55	32.45	34.15	35.75	36.95	37.75
G	26.05	27.45	29.25	31.25	33.25	35.05	36.65	37.85	38.55

Table 6.6: Nodal temperature distribution of Section A at 3000 rpm.

Section B

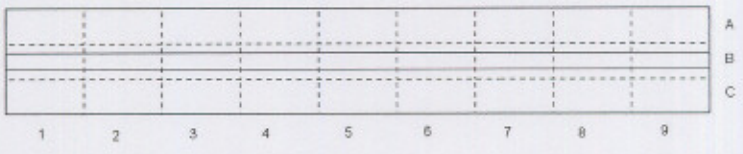

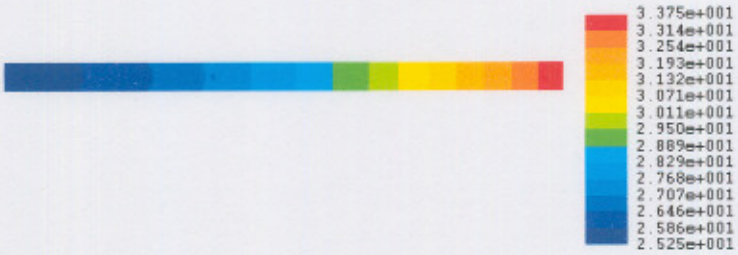

Figure 6.17: Grid and temperature contour of Section B at 3000 rpm.

Node	1	2	3	4	5	6	7	8	9
A	25.45	25.85	26.45	27.25	28.15	29.25	30.65	32.15	33.75
B	25.25	25.65	26.25	27.05	28.05	29.15	30.55	32.05	33.75
C	25.45	25.85	26.45	27.25	28.15	29.25	30.65	32.15	33.75

Table 6.7: Nodal temperature distribution of Section B at 3000 rpm.

Section C

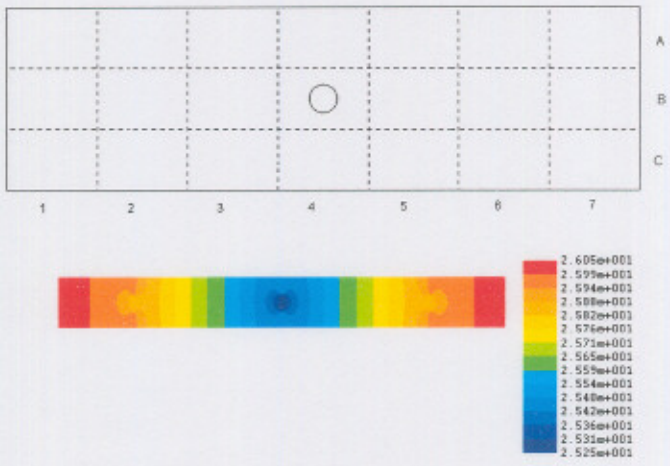

Figure 6.18: Grid and temperature contour of Section C at 3000 rpm.

Node	1	2	3	4	5	6	7
A	26.05	25.95	25.65	25.45	25.65	25.95	26.05
B	26.05	25.85	25.65	25.25	25.65	25.85	26.05
C	26.05	25.95	25.65	25.45	25.65	25.95	26.05

Table 6.8: Nodal temperature distribution of Section C at 3000 rpm.

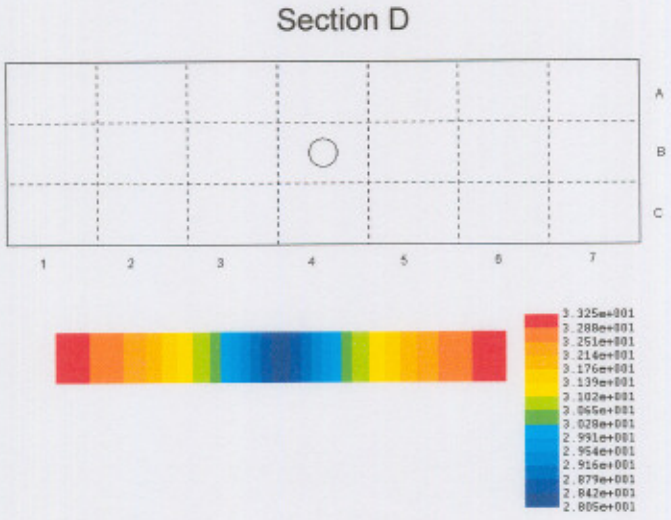

Figure 6.19: Grid and temperature contour of Section D at 3000 rpm.

Node	1	2	3	4	5	6	7
A	33.25	32.45	30.75	28.15	30.75	32.45	33.25
B	33.25	32.45	30.75	28.05	30.75	32.45	33.25
C	33.25	32.45	30.75	28.15	30.75	32.45	33.25

Table 6.9: Nodal temperature distribution of Section D at 3000 rpm.

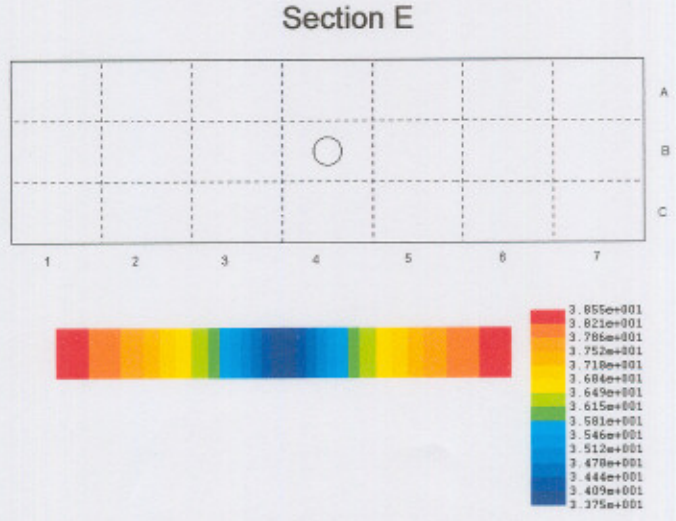

Figure 6.20: Grid and temperature contour of Section E at 3000 rpm.

Node	1	2	3	4	5	6	7
A	38.55	37.75	36.15	33.75	36.15	37.75	38.55
B	38.55	37.75	36.15	33.75	36.15	37.75	38.55
C	38.55	37.75	36.15	33.75	36.15	37.75	38.55

Table 6.10: Nodal temperature distribution of Section E at 3000 rpm.

6.7.3. Temperature distribution at 4000 rpm

Section A

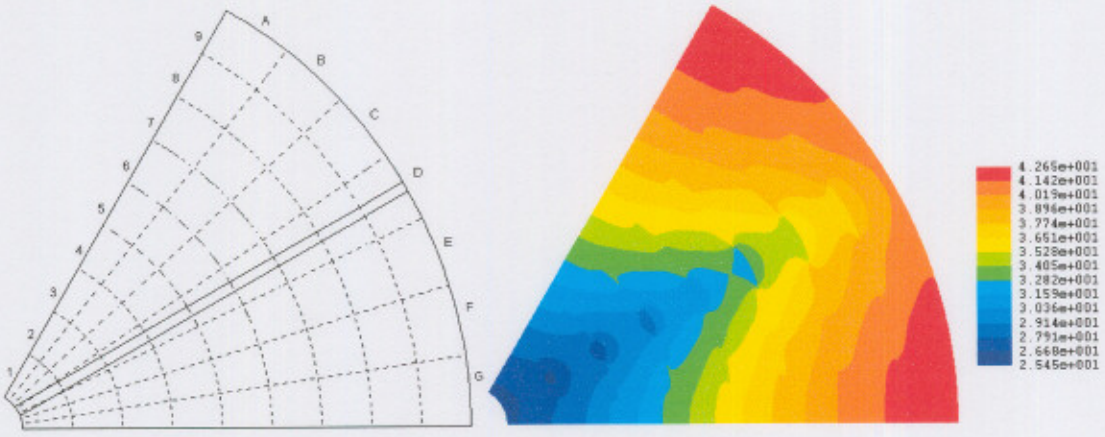

Figure 6.21: Grid and temperature contour of Section A at 4000 rpm.

Node	1	2	3	4	5	6	7	8	9
A	26.45	28.45	30.95	33.55	36.15	38.45	40.45	41.85	42.65
B	26.35	28.05	30.35	32.85	35.25	37.65	39.65	41.15	42.15
C	25.95	27.35	29.15	31.25	33.45	35.75	37.95	39.85	41.25
D	25.45	26.15	27.25	28.65	30.35	32.45	34.85	37.55	40.55
E	25.95	27.35	29.15	31.25	33.45	35.75	37.95	39.85	41.25
F	26.35	28.05	30.35	32.85	35.25	37.65	39.65	41.15	42.15
G	26.45	28.45	30.95	33.55	36.15	38.45	40.45	41.85	42.65

Table 6.11: Nodal temperature distribution of Section A at 4000 rpm.

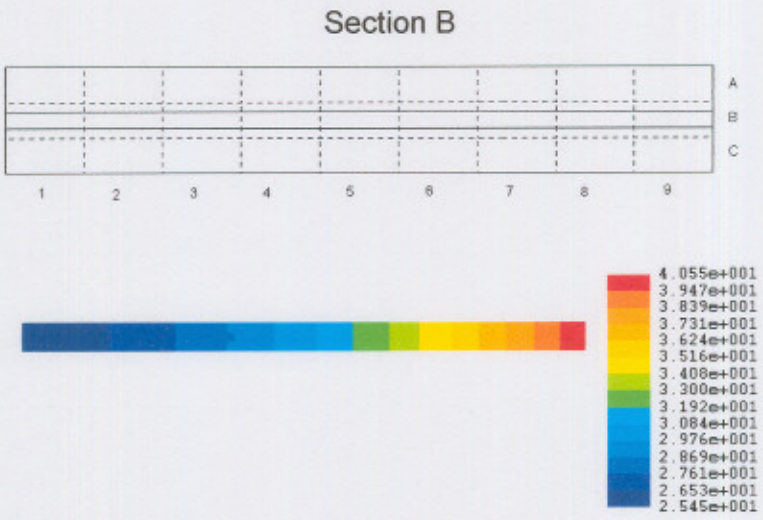

Figure 6.22: Grid and temperature contour of Section B at 4000 rpm.

Node	1	2	3	4	5	6	7	8	9
A	25.75	26.35	27.45	28.85	30.55	32.55	34.95	37.65	40.55
B	25.45	26.15	27.25	28.65	30.35	32.45	34.85	37.55	40.55
C	25.75	26.35	27.45	28.85	30.55	32.55	34.95	37.65	40.55

Table 6.12: Nodal temperature distribution of Section B at 4000 rpm.

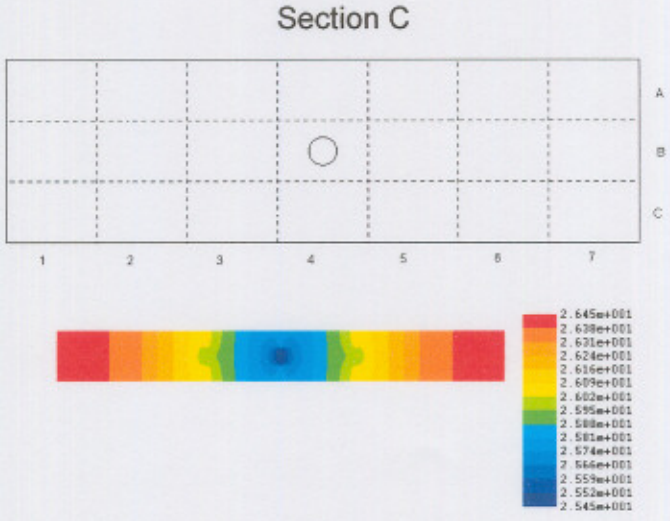

Figure 6.23: Grid and temperature contour of Section C at 4000 rpm.

Node	1	2	3	4	5	6	7
A	26.45	26.35	26.05	25.75	26.05	26.35	26.45
B	26.45	26.35	25.95	25.45	25.95	26.35	26.45
C	26.45	26.35	26.05	25.75	26.05	26.35	26.45

Table 6.13: Nodal temperature distribution of Section C at 4000 rpm.

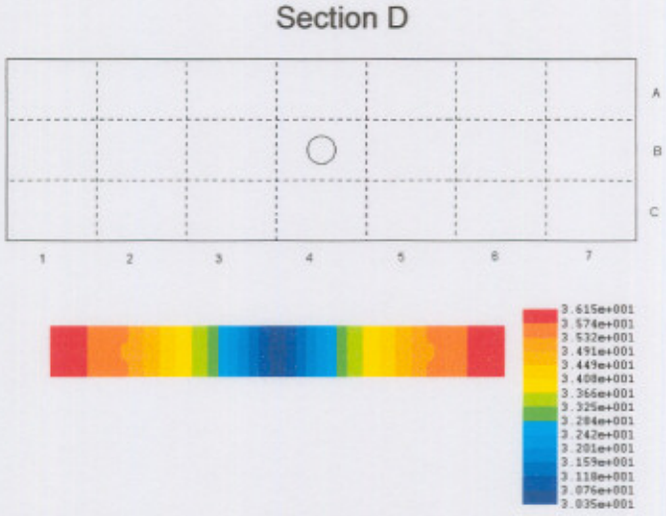

Figure 6.24: Grid and temperature contour of Section D at 4000 rpm.

Node	1	2	3	4	5	6	7
A	36.15	35.35	33.45	30.55	33.45	35.35	36.15
B	36.15	35.25	33.45	30.35	33.45	35.25	36.15
C	36.15	35.35	33.45	30.55	33.45	35.35	36.15

Table 6.14: Nodal temperature distribution of Section D at 4000 rpm.

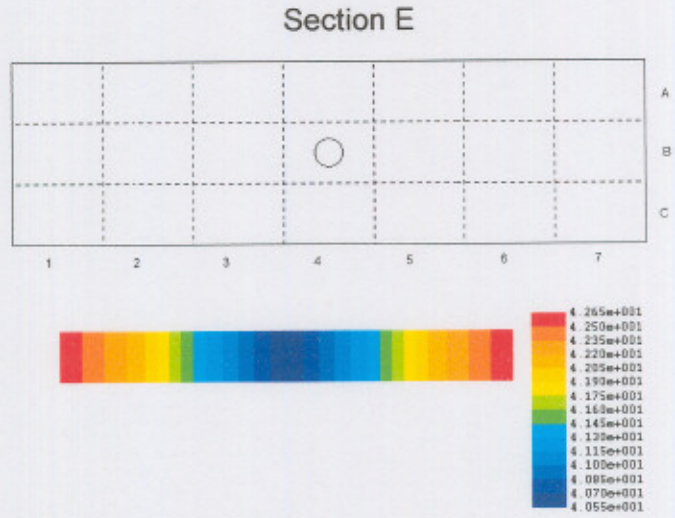

Figure 6.25: Grid and temperature contour of Section E at 4000 rpm.

Node	1	2	3	4	5	6	7
A	42.65	42.15	41.25	40.55	41.25	42.15	42.65
B	42.65	42.15	41.25	40.55	41.25	42.15	42.65
C	42.65	42.15	41.25	40.55	41.25	42.15	42.65

Table 6.15: Nodal temperature distribution of Section E at 4000 rpm.

6.7.4. Temperature distribution at 5000 rpm

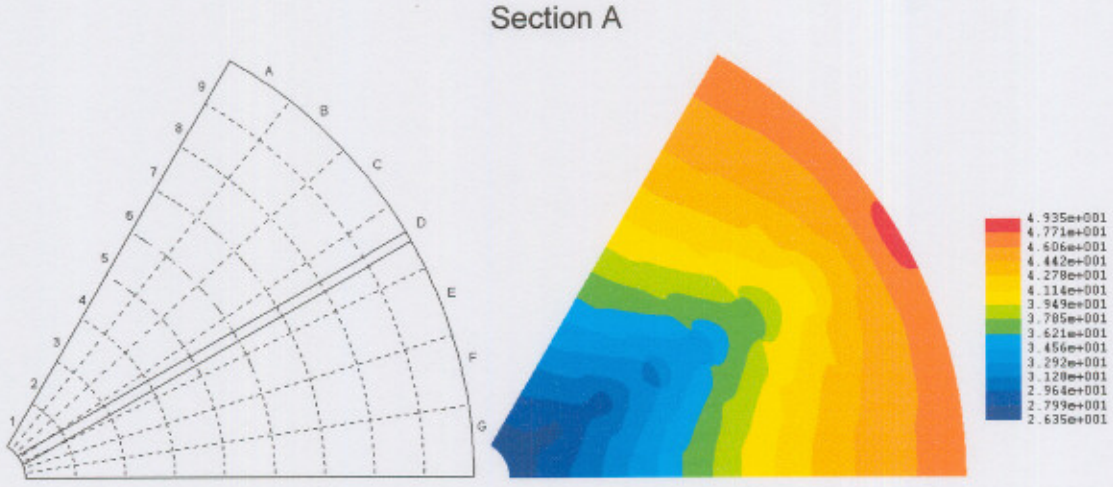

Figure 6.26: Grid and temperature contour of Section A at 5000 rpm.

Node	1	2	3	4	5	6	7	8	9
A	26.95	29.55	32.75	36.15	39.35	42.15	44.35	45.95	46.85
B	26.75	29.15	32.05	35.25	38.45	41.35	43.85	45.75	46.75
C	26.35	28.25	30.65	33.55	36.55	39.75	42.65	45.35	47.15
D	25.65	26.85	28.45	30.65	33.35	36.65	40.35	44.55	49.35
E	26.35	28.25	30.65	33.55	36.55	39.75	42.65	45.35	47.15
F	26.75	29.15	32.05	35.25	38.45	41.35	43.85	45.75	46.75
G	26.95	29.55	32.75	36.15	39.35	42.15	44.35	45.95	46.85

Table 6.16: Nodal temperature distribution of Section A at 5000 rpm.

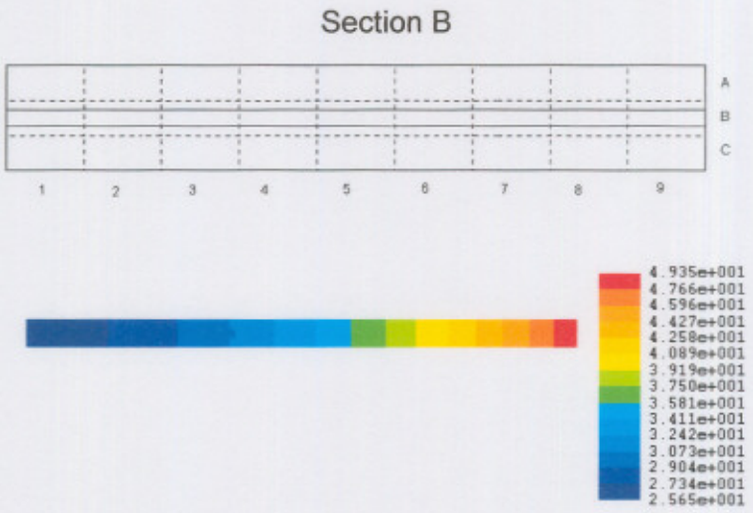

Figure 6.27: Grid and temperature contour of Section B at 5000 rpm.

Node	1	2	3	4	5	6	7	8	9
A	25.95	27.15	28.75	30.85	33.55	36.75	40.45	44.55	49.25
B	25.65	26.85	28.45	30.65	33.35	36.65	40.35	44.55	49.35
C	25.95	27.15	28.75	30.85	33.55	36.75	40.45	44.55	49.25

Table 6.17: Nodal temperature distribution of Section B at 5000 rpm.

Section C

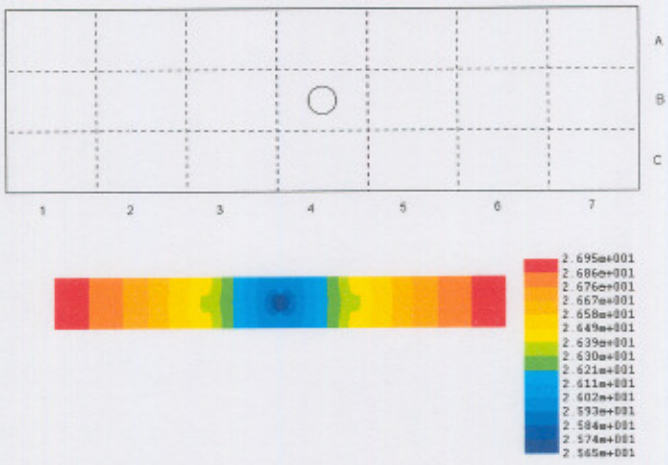

Figure 6.28: Grid and temperature contour of Section C at 5000 rpm.

Node	1	2	3	4	5	6	7
A	26.95	26.75	26.45	25.95	26.45	26.75	26.95
B	26.95	26.75	26.35	25.65	26.35	26.75	26.95
C	26.95	26.75	26.45	25.95	26.45	26.75	26.95

Table 6.18: Nodal temperature distribution of Section C at 5000 rpm.

Section D

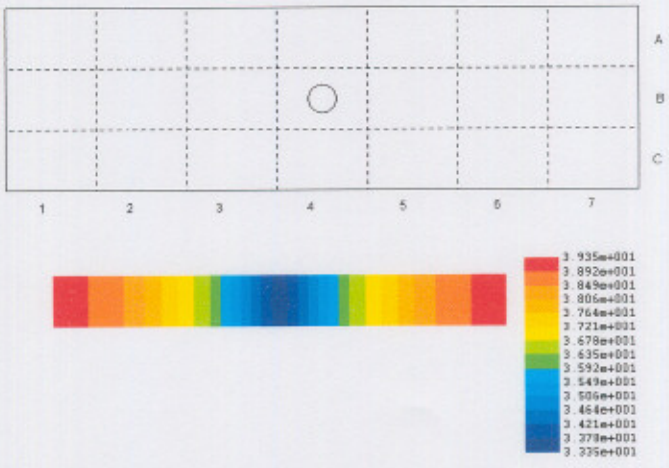

Figure 6.29: Grid and temperature contour of Section D at 5000 rpm.

Node	1	2	3	4	5	6	7
A	39.35	38.45	36.55	33.55	36.55	38.45	39.35
B	39.35	38.45	36.55	33.35	36.55	38.45	39.35
C	39.35	38.45	36.55	33.55	36.55	38.45	39.35

Table 6.19: Nodal temperature distribution of Section D at 5000 rpm.

Section E

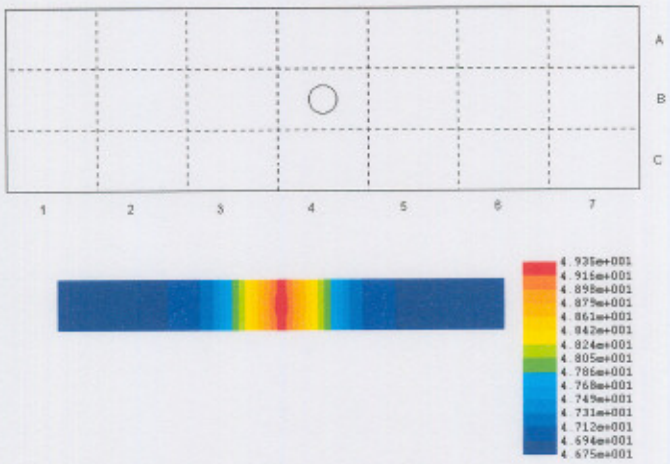

Figure 6.30: Grid and temperature contour of Section E at 5000 rpm.

Node	1	2	3	4	5	6	7
A	46.85	46.75	47.15	49.25	47.15	46.75	46.85
B	46.85	46.75	47.15	49.35	47.15	46.75	46.85
C	46.85	46.75	47.15	49.25	47.15	46.75	46.85

Table 6.20: Nodal temperature distribution of Section E at 5000 rpm.

6.7.5. Discussion of temperature distribution results

Figures 6.11 to 6.30 illustrate the temperature profiles of a segment of the rotating disc with an internal radial channel for various rotational speeds. The environmental temperature of the disc was raised to 55°C and the inlet temperature to the rotating channel was kept at 25°C. This was done in order to

calculate the cooling effect of the rotating channel. It is clear from figures 6.11 to 6.30 that the disc is indeed cooled by the rotating channel. For all rotational speeds the disc tends to be cooler at smaller radii. Then, as the temperature in the internal rotating pipe increases, the disc temperature rises. It should also be mentioned that as the rotational speed of the disc increases, the cooling effect is lessened due to the increasing temperature in the rotating channel. The material furthest from the internal channel tends to be the hottest, as could be expected.

An inconsistency occurred at the outer edge of the rotating disc at 5000 rpm. The hotspots encountered at rotational speeds of 2000 rpm to 4000 rpm disappear. This happens because the temperature inside the rotating channel is raised above the local disc temperature. Therefore the maximum temperature of the disc at a rotational speed of 5000 rpm is located at the outlet of the rotating channel.

6.8. Conclusion

This chapter contained all of the results generated by the EES simulation program. There were no unexpected results obtained from the simulation model and the trends of the graphs could be easily explained. A temperature distribution of a segment of the rotating disc has been presented and this shows the cooling effects of the internal rotating channel for various rotational speeds of the disc. The next chapter will present a conclusion of the conducted research and will provide recommendations for future research on the current topic.

CHAPTER 7

7. CONCLUSIONS AND RECOMMENDATIONS

7.1. Summary

The primary objective of this study was to validate the theory behind steady-state compressible fluid-flow in a rotating disc with internal radial passages by means of an experimental test bench. The secondary objective was to investigate the behaviour of the fluid flow and thermal parameters at various rotational speeds. The final goal was to determine a temperature distribution in the rotating disc at various rotational speeds.

Chapter 1 gave a short introduction on the workings of turbine blade cooling and the need to transform the complex turbine blade geometry into a more workable rotating disc system. In Chapter 2 an extensive literature survey was conducted to obtain relevant information on the behaviour of rotating disc systems. Chapter 3 focused on the theory and correlations needed to accurately simulate a rotating disc with internal radial passages. Chapter 4 described the development of an EES computer programme to simulate a rotating disc with internal radial cooling channels. At the end of Chapter 4 the various heat transfer coefficients obtained from the literature were compared and the most suitable Nusselt number correlation was selected. Chapter 5 discussed the experimental test bench that was used to verify the results obtained from the EES simulation model. At the end of Chapter 5 the results obtained from the experimental test bench was compared to a mathematical simulation model. This was necessary to verify the accuracy of the theoretical results acquired from the simulation model. Chapter 6 contained all the results obtained from the EES simulation model. The

results included the temperature, pressure, density and velocity distributions in the rotating pipe and disc at various rotational speeds.

With the aid of the experimental test bench, fluid-flow measurements through the rotating passages in a rotating disc were possible. The results obtained from the experimental test bench were presented in a graph showing pressure ratio versus mass flow. In chapter 5 the results obtained from the test bench was compared to an EES simulation model. The simulation model is capable of determining the steady-state compressible fluid-flow in a rotating disc with internal radial passages. The results from the test bench and the simulation model compared well. Therefore it is plausible to say that the primary goal to validate the theory behind steady-state compressible fluid-flow in a rotating disc with internal radial passages by means of an experimental test bench was successfully achieved.

In Chapter 6 the results obtained from the EES simulation model were presented in graphs. An explanation could be given for each graph. Thus the second objective, to investigate the behaviour of the fluid-flow and thermal parameters of the rotating disc at various rotational speeds, was also achieved.

In Section 6.7 a detailed presentation of the temperature distribution of the rotating disc at various rotational speeds was given. In so doing, the final objective of this study was also achieved.

7.2. Shortcomings of this study

The following shortcomings were identified in this study:

- No analytical solution for the vortex in the rotating cylindrical cavity could be obtained. The reason for this is that it is not clear if a free or forced vortex or a combination of both will dominate the fluid domain at the inlet. The inlet loss factor of the rotating pipe was empirically determined from experimental measurements.
- The results obtained from the EES simulation model concerning any temperature-related results could not be verified. The reason for this is that no temperature measurements have been done on the rotating-disc. Furthermore, due to the rotation and the geometry of the rotating-pipe, the pressure, density or velocity distribution could not be experimentally measured. Therefore the simulation results concerning these parameters could not be verified using the experimental test bench.
- The experimental test bench and the EES simulation model are only capable of simulating a purely radial rotating pipe. The simulation model is not capable of handling a rotating-pipe with any deviations in the axial or theta directions. However, with minor adjustments to the existing simulation programme a variable-area, non-radial rotating-pipe can also be simulated.
- It was decided that the rotational speed of the disc will be limited to between 2000 and 5000 rpm. These constraints on the rotational speed of the disc also limit the range of the data obtained from the experimental test bench and simulation model.
- This study only focused on the steady-state behaviour of a rotating disc with radial cooling passages. At the moment no conclusions can be made

about the transient response of the fluid-flow and heat transfer parameters associated with the rotating disc system.

7.3. Suggestions for further research

7.3.1. Experimental

- In order to be able to verify more extensive simulation results the experimental test bench must be capable of measuring the temperature at various locations. Temperature measurements that need to be made, include the inlet and outlet temperature of the rotating pipe, radial temperature distribution in the rotating pipe and the surface temperature distribution of the rotating disc.
- The rotational speed of the disc must be increased to about 10000 rpm. This will allow a broader range of experimental data.
- The internal geometry of the rotating pipe should be varied. This is necessary to simulate the complex internal cooling passages of turbine blades. It is recommended that another rotating disc be constructed that has a rotating pipe with a deviation in the radial, axial and theta directions.
- With respect to the fluid flow measurements, it will be wise to acquire a more accurate flowmeter. For low flow rates there is a decline in the accuracy of the current flowmeter. The current flowmeter is also only capable of measuring flow rates up to 1280 L/min. Therefore the current flowmeter will not be capable of measuring flow rates of rotational speeds higher than 5000 rpm.

7.3.2. Simulation model

- A detailed survey of the theory of vortices needs to be done in order to obtain a mathematical model for the vortex located in the rotating cylindrical cavity. It is highly recommended to incorporate a more complex model for both the inlet and outlet vortices in the EES simulation model. The current model considers the vortices to be steady-state, inviscid and incompressible.
- The next step is to simulate a more complex internal rotating channel. Therefore it is also necessary to expand the current theory for purely radial rotating channels to include more complex rotating channels.
- The current simulation should also be capable of performing transient simulations of the rotating disc with radial cooling passages.
- It was also found that to produce a more uniform temperature contour of the rotating disc, it is necessary to increase the number of pipe increments.

REFERENCES

ABU-HIJLEH, B.A.K., HEILEN, W.N. 1998. Correlation for laminar mixed convection from a rotating cylinder. *Int. Comm. Heat and Mass Transfer,* **25(6)**: 875-884.

ANDERSON, T., SAUNDERS, O.A. 1953. Convection from an Isolated Heated Horizontal Cylinder rotating about its Axis. *Proc. Roy. Soc. of London, England, A,* **217**: 555-562.

BECKER, K.M. 1963. *International Journal of Heat and Mass Transfer,* **6**: 1053.

BIRD, R.B., STEWART, W.E., LIGHTFOOT, E.N. 1960. *Transport Phenomena*. 5th ed. New-York: John Wiley & Sons. 739 p.

CHEN, J.X., GAN, X., OWEN, J.M. 1994. Flow and heat transfer in enclosed rotor-stator systems. (**In:** International Heat Transfer Conference 10th. Brighton, England), **3**: 161-166.

COBB, E.C., SAUNDERS, O.A. 1956. Heat transfer from a rotating disk. *Proc.Roy.Soc.A*, 236, 343-351.

COHEN, H., ROGERS, G.F.C., SARAVANAMUTTOO, H.I.H. 1987. *Gas turbine theory, 3rd ed.* Longman Group Ltd.

DROPKIN, D., CARMI, A. 1957. *Trans. ASME,* **80**: 70.

ETEMAD, G.A., BUFFALO, N.Y. 1955. Free-Convection Heat Transfer from a Rotating Horizontal Cylinder to Ambient Air with Interferometric Study of Flow. *Trans. ASME,* **77**: 1283-1289.

FANN, S., YANG, WJ. 1992. Hydrodynamically and thermal developing laminar flow through rotating channels having isothermal walls. *Journal of Numerical Heat Transfer, A*, **22(3)**: 257-288.

GREENSPAN, H.P. 1968. *The Theory of Rotating Fluids.* Cambridge Monographs on Mechanics & Applied Mathematics: Cambridge at the University Press. 327 p.

GREYVENSTEIN, R. 2002. *Modeling the Flow in a Rotating Pipe.* Potchefstroom: Potchefstroom University for Christian higher education. (Final Year Project – B.Eng.). 114 p.

HARASGAMA, S.P., MORRIS, W.D. 1988. The influence of Rotation on the Heat Transfer Characteristics of Circular, Triangular, and Square-Sectioned Coolant Passages of Gas Turbine Rotor Blades. *Journal of Turbomachinery*, **110(1)**: 44-50.

ITO, H., NANBU, K. 1971. Flow in rotating straight pipes of circular cross section. *Journal of Basic Engineering,* 93(3): 383-394.

INCROPERA, F.P., DEWITT, D.P., 1996. *Fundamentals of Heat and Mass Transfer.* 4th ed. New-York: John Wiley & Sons. 886 p.

KARABAY, H., WILSON, M., OWEN, J.M. 2000. Predictions of effect of swirl on flow and heat transfer in a rotating cavity. *International Journal of Heat and Fluid Flow,* 22: 143-155.

KENDOUSH, A.A. 1996. An approximate solution of the convective heat transfer from an isothermal rotating cylinder. *Int. J. Heat and Fluid Flow,* **17**: 439-441.

KOTRBA, V. 1990. Flow and Heat Transfer in Radial Channels of Electric Machines. *Journal of Electric and Power Machines,* **18**: 83-96.

KREITH, F., TAYLOR, J.H., CHONG, J.P. 1959. Heat and mass transfer from a rotating disc. *ASME Journal of Heat and Mass Transfer,* **81**: 95-105.

LONG, C.A., OWEN, J.M. 1986. The Effect of Inlet Conditions on Heat Transfer in a Rotating Cavity with a Radial Outflow of Fluid. *Journal of Turbomachinery*, **108**: 145-152.

McCOMAS, S.T., HARTNETT, J.P. 1970. Temperature profiles associated with a single disk rotating in still air. 4th Int. Heat Transfer Conf., Versailles, III, F.C.7.7.

MEDWELL, J.O., MORRIS, W.D., XIA, J.Y., TAYLOR, C. 1991. An Investigation of Convective Heat Transfer in a Rotating Coolant Channel. *Journal of Turbomachinery*, **113(3)**: 354-359.

MIRZAEE, I., GAN, X., WILSON, M., OWEN, J.M. 1998. Heat transfer in a Rotating Cavity with a Peripheral Inflow and Outflow of cooling air. *Journal of turbomachinery,* **120**: 818-823.

MIRZAEE, I., QUINN, P., WILSON, M., OWEN, J.M. 1999. Heat Transfer in a Rotating Cavity with a Stationary Stepped Casing. *Journal of turbomachinery,* **121**: 281-287.

MORRIS, W.D., CHANG. S.W. 1997. An experimental study of heat transfer in a simulated turbine blade cooling passage. *International Journal of heat and mass transfer,* **40**: 3703-3716.

NESREDDINE, H., NGUYEN, C.T., VO-NGOC, D. 1995. Laminar flow between a stationary and a rotating disk with radial throughflow. *Journal of Numerical Heat Transfer, Part A*, 27: 537-557.

NORTHROP, A., OWEN, J.M. 1988b. Heat transfer measurements in rotating-disc systems Part 1: The rotating free disc. *The International Journal of Heat and Fluid Flow,* **9(1)**: 19-26.

NORTHROP, A., OWEN, J.M. 1988a. Heat transfer measurements in rotating-disc systems Part 2: The rotating cavity with a radial outflow of cooling air. *The International Journal of Heat and Fluid Flow,* **9(1)**: 27-36.

ONG, C.L., OWEN, J.M. 1991. Prediction of Heat Transfer in a Rotating Cavity with a Radial Outflow. *Journal of Turbomachinery,* **113**: 115-122.

OWEN, J.M., BILIMORIA, E.D. 1977. Heat transfer in rotating cylindrical cavities. *Journal of Mechanical engineering science,* 19: 175-187.

OWEN, J.M., HAYNES, C.M., BAYLEY, F.J. 1974. Heat transfer from an air-cooled rotating disk. *Proc.Roy.Soc.A*, 336, 453-473.

OWEN, J.M., ONUR, H.S. 1983. Convective Heat Transfer in a Rotating Cylindrical Cavity. *Journal of engineering for power,* **105**: 265-271.

OWEN, J.M., ROGERS, R.H., 1995. *Flow and Heat Transfer in Rotating-Disc Systems Volume 2 – Rotating Cavities.* 1st ed. West Sussex : John Wiley & Sons. 295 p.

OWEN, J.M., ROGERS, R.H., 1989. *Flow and Heat Transfer in Rotating-Disc Systems Volume 1 – Rotor Stator Systems.* 1st ed. West Sussex : John Wiley & Sons. 278 p.

OZERDEM, B. 2000. Measurement of convective heat transfer coefficient for a horizontal cylinder rotating in quiescent air. *Int. Comm. Heat and Mass Transfer,* **27(3)**: 389-395.

PILBROW, R., KARABAY, H., WILSON, M., OWEN, J.M. 1999. Heat transfer in a "Cover Plate" pre-swirl rotating disk system. *Journal of Turbomachinery,* 121: 249-256.

QURESHI, G., NGUYEN, M.H., SAAD, N.R., TADROS, R.N. 1989. Heat transfer measurements for rotating turbine discs. (**In:** Gas Turbine and Aeroengine Congress and Exposition held on 4-8 June 1989. Toronto, Ontario, Canada. **p. 1-8.**)

SHAMES, I.H. 1992. *Mechanics of fluids*, 3rd ed. McGraw-Hill.

SHIMADA, R., et al. 1991. *Trans. ASME,* **57**: 210.

SOONG, C.Y., NG, E.Y.K., LIU, Z.Y. 2000. Heat and Flow evaluation in rotating circular disks passage with a CFD approach. *Journal of Numerical Heat Transfer, Part A,* **38**: 611-626.

TUCKER, P.G., LONG, C.A. 1998. Fluid Temperature Distributions in a rotating cavity with an axial throughflow. *Int. Comm. Heat Mass Transfer,* **25**(4): 511-520.

WAGNER, J.H., JOHNSON, B.V., HAJEK, T.J. 1991a. Heat Transfer in Rotating Passages with Smooth Walls and Radial Outward Flow. *Journal of Turbomachinery*, **113(1)**: 42-51.

WAGNER, J.H., JOHNSON, B.V., KOPPER, F.C. 1991b. Heat Transfer in Rotating Serpentine Passages with smooth walls. *Journal of Turbomachinery*, **113(3)**: 321-330.

YANG, H.Q., YANG. K.T., LLOYD. J.R. 1988. Rotational Effects on Natural Convection in a Horizontal Cylinder. *AIChE Journal,* **34**(10): 1627-1633.

APPENDIX A: Derivation of fluid flow conservation equations

A.1. Rotating pipe

A.1.1. Preliminaries

A.1.1.1. Geometry

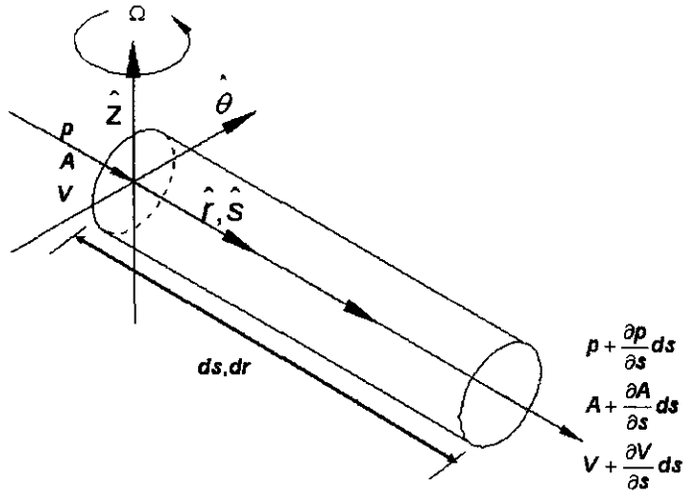

Figure A.1: Geometry of an infinitesimal control volume situated on a rotating pipe.

Figure A.1 shows the geometry of the infinitesimal control volume situated on a rotating pipe. The reference areas $A+\frac{\partial A}{\partial s}ds$ are perpendicular to the $\hat{r}$ and the $\hat{s}$ unit vector at the inlet and outlet.

The unit vector parallel to the pipe shown in figure B.1 may be written in terms of the unit vectors in the r,θ and z coordinates respectively.

$$\hat{s}=\left|\frac{\partial r}{\partial s}\right|\hat{r}+r\left|\frac{\partial \theta}{\partial s}\right|\hat{\theta}+\left|\frac{\partial z}{\partial s}\right|\hat{z} \qquad \text{(A.1)}$$

The rotating pipe is a purely radial pipe, thus there is no change in the θ and the z coordinates. The $\hat{s}$ unit vector reduces to

$$\hat{s} = \left|\frac{\partial r}{\partial s}\right| ds \tag{A.2}$$

It is also clear that

$$dr = \left|\frac{\partial r}{\partial s}\right| ds \tag{A.3}$$

But

$$\frac{\partial r}{\partial s} = 1 \tag{A.4}$$

Therefore:

$$dr = ds \tag{A.5}$$

The following vector quantities may be defined for a purely radial rotating pipe for rotation around the z-axis:

$$\overline{r} = (r)\hat{r} \tag{A.6}$$

$$\overline{V} = (V)\hat{r} \tag{A.7}$$

$$\overline{\omega} = (\omega)\hat{z} \tag{A.8}$$

$$\overline{r_e} = \left(r + \frac{1}{2}ds\right)\hat{r} \tag{A.9}$$

$$\overline{r_i} = \left(r - \frac{1}{2}ds\right)\hat{r} \tag{A.10}$$

$$\overline{V_e} = \left(\frac{\partial r}{\partial s}V + \frac{1}{2}\frac{\partial}{\partial s}\left(\frac{\partial r}{\partial s}V\right)ds\right)\hat{r} \tag{A.11}$$

$$\overline{V_i} = \left(\frac{\partial r}{\partial s}V - \frac{1}{2}\frac{\partial}{\partial s}\left(\frac{\partial r}{\partial s}V\right)ds\right)\hat{r} \tag{A.12}$$

A.1.1.2. Vector algebra relations

The following relations may also be derived with the help of the definitions given in Section A.1.1.1:

$$2\bar{\omega}\times\bar{V}=\left(-\left|\frac{\partial\theta}{\partial s}\right|2\omega V\right)\hat{r}+\left(\left|\frac{\partial r}{\partial s}\right|2\omega V\right)\hat{\theta} \tag{A.13}$$

$$\bar{\omega}\times\left(\bar{\omega}\times\bar{r}\right)=\left(-\omega^2 r\right)\hat{r} \tag{A.14}$$

$$\bar{r}\times\overline{ds}=\left(-\left|\frac{\partial z}{\partial s}\right|r\right)\hat{\theta}+\left(\left|\frac{\partial\theta}{\partial s}\right|r\right)\hat{z} \tag{A.15}$$

$$\bar{r}\times\left(2\bar{\omega}\times\bar{V}\right)=\left(\left|\frac{\partial r}{\partial s}\right|2\omega r V\right)\hat{z} \tag{A.16}$$

$$\bar{r}\times\left(\bar{\omega}\times\left(\bar{\omega}\times\bar{r}\right)\right)=0 \tag{A.17}$$

A.1.1.3. Fundamental fluid mechanics equations

The total enthalpy h_o is defined by Cohen (1987):

$$h_0=h+\frac{1}{2}C^2 \tag{A.18}$$

where C is the magnitude of the absolute velocity relative to the inertial frame of reference i.e. $C=\left|\bar{C}\right|$. For a rotating pipe the absolute velocity vector $\bar{C}$ may be written as

$$\bar{C}=\bar{V}+\bar{V}_\theta$$

$$\bar{C}=\left(\left|\frac{\partial r}{\partial s}\right|V\right)\hat{r}+\left(\omega r\right)\hat{\theta}$$

The square of the magnitude of $\overline{C}$ is therefore

$$C^2 = \left(\left|\frac{\partial r}{\partial s}\right| V\right)^2 + (\omega r)^2$$

$$C^2 = V^2\left(\left|\frac{\partial r}{\partial s}\right|^2\right) + \omega^2 r^2$$

Therefore we have

$$C^2 = V^2 + \omega^2 r^2 \qquad \text{(A.19)}$$

For compressible and incompressible flow the following equation may be used:

$$h_o = c_p T_o \qquad \text{(A.20)}$$

It follows from Equations (A.18) and (A.20) that

$$c_p T_o = c_p T + \frac{1}{2} C^2$$

and therefore

$$T_o = T + \frac{C^2}{2c_p} \qquad \text{(A.21)}$$

For compressible ideal gas flow the following equation may be used:

$$T_o = T\left(1 + \frac{C^2}{2c_p T}\right)$$

$$T_o = T\left(1 + \frac{(\gamma - 1)C^2}{2\gamma RT}\right)$$

$$T_o = T\left(1 + \frac{(\gamma - 1)}{2}\frac{C^2}{\left(\sqrt{\gamma RT}\right)^2}\right)$$

$$T_o = T\left(1 + \frac{\gamma - 1}{2} M^2\right)$$

Therefore:

$$\frac{T_o}{T} = \left(1 + \frac{\gamma - 1}{2} M^2\right) \tag{A.22}$$

with the mach number defined as

$$M = \frac{C}{\sqrt{\gamma R T}} \tag{A.23}$$

From the isentropic property relations for an ideal gas, the equation may be written as:

$$\frac{T_o}{T} = \left(\frac{p_o}{p}\right)^{\left(\frac{\gamma-1}{\gamma}\right)}$$

and therefore

$$\frac{p_o}{p} = \left(1 + \frac{\gamma - 1}{2} M^2\right)^{\frac{\gamma}{\gamma-1}} \tag{A.24}$$

Using the ideal gas law to determine the density:

$$\rho = \frac{p}{R_{air} T} \tag{A.25}$$

For compressible flow the total pressure loss coefficient is defined by Cohen (1987):

$$K = \frac{\Delta p_o}{p_o - p} \tag{A.26}$$

and therefore

$$\Delta p_o = Kp\left(\left(1 + \frac{\gamma - 1}{2} M^2\right)^{\frac{\gamma}{\gamma-1}} - 1\right) \tag{A.27}$$

A.1.2. Mass conservation

The integral form of the mass conservation equation for a finite control volume is given by Shames (1992):

$$\frac{\partial}{\partial t}\left(\iiint \rho d\forall\right) + \oiint \rho \overline{V} \bullet \overline{dA} = 0 \qquad \text{(A.28)}$$

The first term of Equation (A.28) may be omitted because only steady-state conditions apply.

For the infinitesimal control volume the equation may be written as:

$$\oiint \rho \overline{V} \bullet \overline{dA} = \left(\rho VA + \frac{\partial}{\partial s}(\rho VA)ds\right) - \rho VA$$

$$\oiint \rho \overline{V} \bullet \overline{dA} = \frac{\partial}{\partial s}(\rho VA)ds \qquad \text{(A.29)}$$

Therefore:

$$\frac{1}{A}\frac{\partial}{\partial s}(\rho VA) = 0 \qquad \text{(A.30)}$$

Equation (A.30) may now be integrated over a pipe with finite length L resulting in the final integral form:

$$\left(\rho_e V_e A_e - \rho_i V_i A_i\right) = 0$$

or

$$\dot{m}_e - \dot{m}_i = 0 \qquad \text{(A.31)}$$

A.1.3. Linear momentum conservation

The integral form of the linear momentum conservation equation for a finite non-inertial control volume of which the origin has no linear acceleration is given by Shames (1992):

$$\begin{aligned}
&\oiint \tau \overline{dA} + \iiint \overline{B}\rho d\forall \\
&-\iiint \left(\left(2\overline{\omega} \times \overline{V}\right) + \left(\dot{\overline{\omega}} \times \overline{r}\right) + \left(\overline{\omega} \times \left(\overline{\omega} \times \overline{r}\right)\right) \right) \rho d\forall \\
&= \frac{\partial}{\partial t}\left(\iiint \overline{V} \rho d\forall \right) + \oiint \overline{V}\left(\rho \overline{V} \bullet \overline{dA}\right)
\end{aligned} \tag{A.32}$$

The surface force term for the infinitesimal control volume may now be written as follows:

$$\begin{aligned}
\sum \tau \overline{dA} &= \left(pA\overline{ds} - \left(p + \frac{\partial p}{\partial s} ds\right)\left(A + \frac{\partial A}{\partial s} ds\right) \right) \hat{s} \\
&+ \left(\frac{1}{2}\left(p + \left(p + \frac{\partial p}{\partial s} ds\right)\right)\left(\left(A + \frac{\partial A}{\partial s} ds\right) - A\right) \right) \hat{s} \\
&- \left(\frac{f}{D}\frac{1}{2}\rho |V| V A ds \right) \hat{s} \\
&= \left(-\left(\frac{\partial p}{\partial s} + \frac{f}{D}\frac{1}{2}\rho |V| V \right) A ds \right) \hat{s}
\end{aligned} \tag{A.33}$$

The body force term $\iiint \overline{B}\rho d\forall$ may be omitted due to the fact that the rotating pipe is horizontal. The inlet and the outlet of the pipe are therefore at the same height.

The Coriolis force term is defined as

$$-\left(2\bar{\omega}\times\bar{V}\right)\rho d\forall = \left(\left|\frac{\partial\theta}{\partial s}\right|2\omega V\rho A ds\right)\hat{r} + \left(-\left|\frac{\partial r}{\partial s}\right|2\omega V\rho A ds\right)\hat{\theta}$$
$$= \left(\left|\frac{\partial\theta}{\partial s}\right|2\omega V\rho A ds\right)\left(\left|\frac{\partial r}{\partial s}\right|\right)\hat{s} + \left(-\left|\frac{\partial r}{\partial s}\right|2\omega V\rho A ds\right)\left(\left|\frac{\partial\theta}{\partial s}\right|\right)\hat{s} \qquad \text{(A.34)}$$
$$= (0)\hat{s}$$

The rotational acceleration term $\iiint\left(\dot{\bar{\omega}}\times\bar{r}\right)\rho d\forall$ may be omitted due to the fact that only steady-state conditions are considered.

The centrifugal force term may be written as

$$-\left(\bar{\omega}\times\left(\bar{\omega}\times\bar{r}\right)\right)\rho d\forall = \left(\omega^2 r\rho A ds\right)\hat{r} = \left(\left|\frac{\partial r}{\partial s}\right|\omega^2 r\rho A ds\right)\hat{s} \qquad \text{(A.35)}$$

The rate of change of momentum within the control volume is taken as zero because of the steady-state conditions.

The net outflow of momentum from the control volume is

$$\sum\bar{V}\left(\rho\bar{V}\bullet\overline{dA}\right) = \begin{pmatrix}\left(V+\frac{\partial V}{\partial s}ds\right)\left(\rho VA+\frac{\partial}{\partial s}(\rho VA)ds\right)\\ -V(\rho VA)\end{pmatrix}\hat{s} \qquad \text{(A.36)}$$
$$\sum\bar{V}\left(\rho\bar{V}\bullet\overline{dA}\right) = \left(\frac{\partial}{\partial s}\left(V(\rho VA)\right)ds\right)\hat{s}$$

By substituting Equations (A.33) to (A.36) in Equation (A.32) for an infinitesimal control volume, the following is obtained:

$$\left|\frac{\partial r}{\partial s}\right|\rho\omega^2 r = \frac{\partial p}{\partial s} + \frac{f}{D}\frac{1}{2}\rho|V|V + \frac{1}{A}\frac{\partial}{\partial s}\left(V(\rho VA)\right) \qquad \text{(A.37)}$$

The last term of the preceding equation may be developed as follows:

$$\frac{1}{A}\frac{\partial}{\partial s}\left(V\left(\rho VA\right)\right)=V\left(\frac{\partial}{\partial s}\left(\rho VA\right)\right)+\rho\left(V\frac{\partial V}{\partial s}\right)$$

$$\frac{1}{A}\frac{\partial}{\partial s}\left(V\left(\rho VA\right)\right)=\rho V\frac{\partial V}{\partial s}$$

provided that mass conservation is satisfied as prescribed by Equation (A.30) Therefore:

$$\left|\frac{\partial r}{\partial s}\right|\rho\omega^2 r=\frac{\partial p}{\partial s}+\frac{f}{D}\frac{1}{2}\rho|V|V+\rho V\frac{\partial V}{\partial s} \qquad \text{(A.38)}$$

Equation (A.38) is valid for both incompressible and compressible flow in a rotating pipe.

A.1.3.1. Compressible flow

For compressible flow it can be shown that[1]:

$$\rho C\frac{\partial C}{\partial s}+\frac{\partial p}{\partial s}=\frac{p}{p_o}\frac{\partial p_o}{\partial s}+\frac{1}{2}\rho C^2\frac{1}{T_o}\frac{\partial T_o}{\partial s} \qquad \text{(A.39)}$$

or

$$\frac{1}{2}\rho\frac{\partial}{\partial s}\left(C^2\right)+\frac{\partial p}{\partial s}=\frac{p}{p_o}\frac{\partial p_o}{\partial s}+\frac{1}{2}\rho C^2\frac{1}{T_o}\frac{\partial T_o}{\partial s}$$

By inserting the definition of C^2 from Equation (A.19) into the preceding equation, the following is obtained:

$$\frac{1}{2}\rho\frac{\partial}{\partial s}\left(V^2+\omega^2r^2\right)+\frac{\partial p}{\partial s}=\frac{p}{p_o}\frac{\partial p_o}{\partial s}+\frac{1}{2}\rho C^2\frac{1}{T_o}\frac{\partial T_o}{\partial s}$$

After manipulation this leads to

$$\rho V\frac{\partial V}{\partial s}+\frac{\partial p}{\partial s}=\frac{p}{p_o}\frac{\partial p_o}{\partial s}+\frac{1}{2}\rho C^2\frac{1}{T_o}\frac{\partial T_o}{\partial s}-\frac{1}{2}\rho\frac{\partial}{\partial s}\left(\omega^2r^2\right) \qquad \text{(A.40)}$$

[1] See Appendix B

By inserting Equation (A.40) into Equation (A.38), the following is obtained:

$$\left|\frac{\partial r}{\partial s}\right|\rho\omega^2 r+\frac{1}{2}\rho\frac{\partial}{\partial s}\left(\omega^2 r^2\right)=\frac{p}{p_o}\frac{\partial p_o}{\partial s}+\frac{f}{D}\frac{1}{2}\rho|V|V +\frac{1}{2}\rho C^2\frac{1}{T_o}\frac{\partial T_o}{\partial s} \tag{A.41}$$

Equation (A.41) may also be written as

$$\left|\frac{\partial r}{\partial s}\right|\rho\omega^2 r ds+\frac{1}{2}\rho\omega^2\frac{\partial}{\partial s}\left(r^2\right)ds=\frac{p}{p_o}\frac{\partial p_o}{\partial s}ds+\frac{f}{D}\frac{1}{2}\rho|V|Vds +\frac{1}{2}\rho C^2\frac{1}{T_o}\frac{\partial T_o}{\partial s}ds$$

or

$$\rho\omega^2 r ds+\frac{1}{2}\rho\omega^2\frac{\partial}{\partial s}\left(r^2\right)ds=\frac{p}{p_o}\frac{\partial p_o}{\partial s}ds+\frac{f}{D}\frac{1}{2}\rho|V|Vds +\frac{1}{2}\rho C^2\frac{1}{T_o}\frac{\partial T_o}{\partial s}ds$$

which, after integration over a finite pipe length L, leads to

$$\frac{1}{2}\tilde{\rho}\omega^2\left(r_e^2-r_i^2\right)+\frac{1}{2}\tilde{\rho}\omega^2\left(r_e^2-r_i^2\right)=\frac{\tilde{p}}{\tilde{p}_o}\left(p_{oe}-p_{oi}\right)+\frac{\tilde{f}L}{\tilde{D}}\frac{1}{2}\tilde{\rho}\left|\tilde{V}\right|\tilde{V} +\frac{1}{2}\tilde{\rho}C^2\frac{1}{\tilde{T}_o}\left(T_{oe}-T_{oi}\right)$$

Terms for the change in total pressure due to secondary losses within the pipe at the inlet and outlet, may now be added.

The coefficient of friction for a rotating pipe will be discussed in section 3.5.

The final integral form of the equation is as follows:

$$\tilde{\rho}\omega^2\left(r_e^2 - r_i^2\right) = \frac{\tilde{p}}{\tilde{p}_o}\left(p_{oe} - p_{oi}\right) + \frac{1}{2}\tilde{\rho}C^2\frac{1}{\tilde{T}_o}\left(T_{oe} - T_{oi}\right)$$
$$+\left(\frac{\tilde{f}L}{\tilde{D}} + \sum K\right)\frac{\left|\tilde{\dot{m}}\right|\tilde{\dot{m}}}{2\tilde{\rho}\tilde{A}^2} + K_i p_i\left(\left(1 + \frac{\gamma-1}{2}M_i^2\right)^{\frac{\gamma}{\gamma-1}} - 1\right) \qquad \text{(A.42)}$$
$$+K_e p_e\left(\left(1 + \frac{\gamma-1}{2}M_e^2\right)^{\frac{\gamma}{\gamma-1}} - 1\right)$$

A.1.4. Angular momentum conservation

The integral form of the angular momentum conservation equation for a finite non-inertial control volume of which the origin has no linear acceleration is given by Shames (1992):

$$\oiint \bar{r} \times \tau \overline{dA} + \iiint \bar{r} \times \bar{B}\rho d\forall$$
$$-\iiint\left[\bar{r} \times \left(2\bar{\omega} \times \bar{V}\right) + \bar{r} \times \left(\dot{\bar{\omega}} \times \bar{r}\right) + \bar{r} \times \left(\bar{\omega} \times \left(\bar{\omega} \times \bar{r}\right)\right)\right]\rho d\forall \qquad \text{(A.43)}$$
$$= \frac{\partial}{\partial t}\left(\iiint \bar{r} \times \bar{V}\rho d\forall\right) + \oiint \bar{r} \times \bar{V}\left(\rho\bar{V} \bullet \overline{dA}\right)$$

The first term of Equation (A.43) represents the torque exerted on the fluid by all forces acting on the surface of the fluid control volume. This therefore includes the tangential (shear) and normal (pressure) forces exerted by the pipe walls as well as the pressures acting perpendicular to the inlet and outlet areas of the pipe. The total torque on the infinitesimally small fluid control volume due to the pipe walls are hereby lumped together and written as:

$$\overline{dM} = dM_z\hat{z} \qquad \text{(A.44)}$$

If it is assumed that at the inlet and outlet of the pipe, the areas are perpendicular to the radial direction the pressure forces perpendicular to the inlet and outlet areas will not result in moments around the axis of rotation. Therefore, the total moment due to surface forces becomes:

$$\sum \bar{r} \times \tau \overline{dA} = dM_z \hat{z} \qquad \text{(A.45)}$$

The body force term $\iiint \bar{r} \times \bar{B} \rho d\forall$ may be omitted due to the fact that the rotating pipe is horizontal. The inlet and the outlet of the pipe are therefore at the same height.

The Coriolis force term is:

$$-\bar{r} \times \left(2\bar{\omega} \times \bar{V}\right) \rho d\forall = \left(-\left|\frac{\partial r}{\partial s}\right| 2\omega r V \rho A ds\right) \hat{z} \qquad \text{(A.46)}$$

The rotational acceleration term $-\iiint \bar{r} \times \left(\dot{\bar{\omega}} \times \bar{r}\right) \rho d\forall$ may be omitted due to the fact that only steady-state conditions are considered.

The centrifugal force term is:

$$-\bar{r} \times \left(\bar{\omega} \times \left(\bar{\omega} \times \bar{r}\right)\right) \rho d\forall = 0 \qquad \text{(A.47)}$$

The rate of change of momentum within the control volume is taken as zero because of the steady-state conditions.

The net outflow of angular momentum from the control volume is taken as zero because the rotating pipe is purely radial; therefore there is no change in the θ or the z coordinates.

By substituting Equations (A.44) to (A.47) in Equation (A.43) for an infinitesimal control volume and separating z-coordinate terms that are valid for the axis of rotation, the following is found:

$$\frac{dM_z}{Ads} = \left|\frac{\partial r}{\partial s}\right| 2\rho\omega r V \qquad \text{(A.48)}$$

Equation (A.48) may be written as:

$$dM_z = \left|\frac{\partial r}{\partial s}\right| 2\rho V A\omega r ds$$

$$dM_z = 2\rho V A\omega r dr$$

which after integration over a finite pipe length L leads to:

$$M_z = \tilde{\rho}\tilde{V}\tilde{A}\omega\left(r_e^2 - r_i^2\right)$$

This then leads to the final integral form of the equation in terms of the mass flow rate as follows:

$$M_z = \tilde{\dot{m}}\omega\left(r_e^2 - r_i^2\right) \qquad \text{(A.49)}$$

A.1.5. Energy conservation

The integral form of the energy conservation equation for a finite control volume is given by Shames (1992):

$$\sum Q + \sum W = \frac{\partial}{\partial t}\left(\iiint\left(u + \frac{1}{2}C^2 + gz\right)\rho d\forall\right) + \oiint\left(h + \frac{1}{2}C^2 + gz\right)\rho\overline{V}\bullet\overline{dA} \qquad \text{(A.50)}$$

$\sum Q$ is the total rate of heat transfer to the fluid and $\sum W$ the total rate of work done on the fluid. The rate of change of energy within the infinitesimal control volume will be taken as zero because of the steady-state conditions considered here.

The net outflow of energy from the control volume is:

$$\begin{aligned}
&\oiint\left(h+\frac{1}{2}C^2\right)\rho\vec{V}\bullet\overline{dA}\\
&=\left(\left(h+\frac{1}{2}C^2\right)\rho V+\frac{\partial}{\partial s}\left(\left(h+\frac{1}{2}C^2\right)\rho V\right)ds\right)\left(A+\frac{\partial A}{\partial s}ds\right)\\
&-\left(\left(h+\frac{1}{2}C^2\right)\rho V\right)(A)\\
&=\frac{\partial}{\partial s}\left(\left(h+\frac{1}{2}C^2\right)\rho VA\right)ds
\end{aligned}\qquad \text{(A.51)}$$

The gz term is omitted from the equations because of the horizontal radial rotating pipe condition.

By substituting Equations (A.51) into Equation (A.50) it is found that:

$$\sum dQ+\sum dW=\frac{\partial}{\partial s}\left(\left(h+\frac{1}{2}C^2\right)\rho VA\right)ds$$

The third term in the preceding equation may be written as:

$$\begin{aligned}
&\frac{\partial}{\partial s}\left(\left(h+\frac{1}{2}C^2\right)\rho VA\right)ds\\
&=A\left(h+\frac{1}{2}C^2\right)\left(\frac{1}{A}\frac{\partial}{\partial s}(\rho VA)\right)ds+\rho A\left(V\frac{\partial}{\partial s}\left(h+\frac{1}{2}C^2\right)\right)ds\\
&=\rho VA\frac{\partial}{\partial s}\left(h+\frac{1}{2}C^2\right)ds
\end{aligned}$$

Provided that mass conservation is satisfied as prescribed by Equation (A.30) , the equation may be written as:

$$\sum dQ+\sum dW=\rho VA\frac{\partial}{\partial s}\left(h+\frac{1}{2}C^2\right)ds \qquad \text{(A.52)}$$

Substituting the total enthalpy (defined in Equation (A.18)) into Equation (A.52), the following is obtained:

$$\sum dQ + \sum dW = \rho VA \frac{\partial}{\partial s}(h_o) ds \qquad \text{(A.53)}$$

Equation (A.53) may now be integrated over a pipe with finite length L, resulting in the final integral form as follows:

$$\sum Q + \sum W = \tilde{\rho}\tilde{V}\tilde{A}(h_{oe} - h_{oi})$$

For a rotating pipe the total heat transfer to the fluid is simply equal to the heat transfer from the pipe walls Q_h, while the total work done on the fluid is equal to the torque exerted by the pipe walls M_z (as defined by Equation (A.49)) times the angular velocity ω. Therefore:

$$Q_h + M_z\omega = \tilde{\dot{m}}(h_{oe} - h_{oi}) \qquad \text{(A.54)}$$

APPENDIX B: Compressible flow theorem

$$\rho C\frac{\partial C}{\partial s}+\frac{\partial p}{\partial s}=\rho\frac{1}{2}\frac{\partial}{\partial s}\left(C^2\right)+\frac{\partial}{\partial s}\left(p_o\frac{p}{p_o}\right)$$

$$=\rho C_p\frac{\partial T_o}{\partial s}-\rho C_p\frac{\partial T}{\partial s}+\frac{p}{p_o}\frac{\partial p_o}{\partial s}+p_o\frac{\partial}{\partial s}\left(\frac{p}{p_o}\right)$$

$$=\frac{p}{p_o}\frac{\partial p_o}{\partial s}+\rho C_p\frac{\partial T_o}{\partial s}-\rho C_p\frac{\partial}{\partial s}\left(T_o\frac{T}{T_o}\right)+p_o\frac{\partial}{\partial s}\left(\frac{p}{p_o}\right)$$

$$=\frac{p}{p_o}\frac{\partial p_o}{\partial s}+\rho C_p\frac{\partial T_o}{\partial s}-\rho C_p\frac{T}{T_o}\frac{\partial T_o}{\partial s}-\rho C_pT_o\frac{\partial}{\partial s}\left(\frac{T}{T_o}\right)+p_o\frac{\partial}{\partial s}\left(\frac{p}{p_o}\right)$$

$$=\frac{p}{p_o}\frac{\partial p_o}{\partial s}+\rho C_p\frac{T_o}{T_o}\frac{\partial T_o}{\partial s}-\rho C_p\frac{T}{T_o}\frac{\partial T_o}{\partial s}-\rho C_pT_o\frac{\partial}{\partial s}\left(\left(\frac{p}{p_o}\right)^{\frac{\gamma-1}{\gamma}}\right)+p_o\frac{\partial}{\partial s}\left(\frac{p}{p_o}\right)$$

$$=\frac{p}{p_o}\frac{\partial p_o}{\partial s}+\frac{1}{T_o}\rho\left(C_pT_o-C_pT\right)\frac{\partial T_o}{\partial s}-\rho C_pT_o\frac{\gamma-1}{\gamma}\left(\frac{p}{p_o}\right)^{\frac{\gamma-1}{\gamma}-1}\frac{\partial}{\partial s}\left(\frac{p}{p_o}\right)+p_o\frac{\partial}{\partial s}\left(\frac{p}{p_o}\right)$$

$$=\frac{p}{p_o}\frac{\partial p_o}{\partial s}+\frac{1}{2}\rho C^2\frac{1}{T_o}\frac{\partial T_o}{\partial s}-\rho\frac{R\gamma}{\gamma-1}T_o\frac{\gamma-1}{\gamma}\left(\frac{p}{p_o}\right)^{\frac{\gamma-1}{\gamma}}\left(\frac{p_o}{p}\right)\frac{\partial}{\partial s}\left(\frac{p}{p_o}\right)+p_o\frac{\partial}{\partial s}\left(\frac{p}{p_o}\right)$$

$$=\frac{p}{p_o}\frac{\partial p_o}{\partial s}+\frac{1}{2}\rho C^2\frac{1}{T_o}\frac{\partial T_o}{\partial s}-\rho RT_o\left(\frac{T}{T_o}\right)\left(\frac{p_o}{p}\right)\frac{\partial}{\partial s}\left(\frac{p}{p_o}\right)+p_o\frac{\partial}{\partial s}\left(\frac{p}{p_o}\right)$$

$$=\frac{p}{p_o}\frac{\partial p_o}{\partial s}+\frac{1}{2}\rho C^2\frac{1}{T_o}\frac{\partial T_o}{\partial s}-\rho RT\left(\frac{p_o}{p}\right)\frac{\partial}{\partial s}\left(\frac{p}{p_o}\right)+p_o\frac{\partial}{\partial s}\left(\frac{p}{p_o}\right)$$

$$=\frac{p}{p_o}\frac{\partial p_o}{\partial s}+\frac{1}{2}\rho C^2\frac{1}{T_o}\frac{\partial T_o}{\partial s}-p\left(\frac{p_o}{p}\right)\frac{\partial}{\partial s}\left(\frac{p}{p_o}\right)+p_o\frac{\partial}{\partial s}\left(\frac{p}{p_o}\right)$$

$$=\frac{p}{p_o}\frac{\partial p_o}{\partial s}+\frac{1}{2}\rho C^2\frac{1}{T_o}\frac{\partial T_o}{\partial s}-p_o\frac{\partial}{\partial s}\left(\frac{p}{p_o}\right)+p_o\frac{\partial}{\partial s}\left(\frac{p}{p_o}\right)$$

$$=\frac{p}{p_o}\frac{\partial p_o}{\partial s}+\frac{1}{2}\rho C^2\frac{1}{T_o}\frac{\partial T_o}{\partial s}$$

APPENDIX C: Derivation of the conservation equations for the outlet inviscid free vortex

It is important to mention that the vortex will be modeled as two-dimensional. The free vortex will therefore only be modeled in the (r,θ) coordinate plane and the velocity and pressure effects in the (axial) z coordinate plane will be neglected.

For a steady, incompressible, axially symmetric, laminar, inviscid free vortex, the following mass conservation equation is given by Owen and Rogers (1989:9):

Mass conservation

$$\frac{\partial V_r}{\partial r} + \frac{V_r}{r} = 0$$

$$r\frac{\partial V_r}{\partial r} + V_r = 0$$

$$r\frac{\partial V_r}{\partial r} + V_r \frac{\partial r}{\partial r} = 0$$

$$\frac{\partial}{\partial r}(rV_r) = 0$$

Therefore:

$$rV_r = C_1 \qquad \text{(C.1)}$$

The momentum conservation equation for a free vortex in component form is given by Shames (1992:444):

Momentum conservation

r-component

$$V_r \frac{\partial V_r}{\partial r} - \frac{V_\theta^2}{r} = -\frac{1}{\rho}\frac{\partial P}{\partial r} \qquad \text{(C.2)}$$

θ-component

$$V_r \frac{\partial V_\theta}{\partial r} + \frac{V_r V_\theta}{r} = 0 \qquad \text{(C.3)}$$

By inserting Equation (C.1) into Equation (C.3), the following expression is valid:

$$rV_r \frac{\partial V_\theta}{\partial r} + \frac{C_1}{r} V_\theta = 0$$

$$C_1 \frac{\partial V_\theta}{\partial r} + \frac{C_1}{r} V_\theta = 0$$

$$\frac{\partial V_\theta}{\partial r} + \frac{V_\theta}{r} = 0$$

$$r \frac{\partial V_\theta}{\partial r} + V_\theta \frac{\partial r}{\partial r} = 0$$

$$\frac{\partial}{\partial r}(rV_\theta) = 0$$

Therefore:

$$rV_\theta = C_2 \qquad \text{(C.4)}$$

If Equation (C.1) and Equation (C.4) are substituted into Equation (C.2):

$$\frac{C_1}{r} \frac{\partial V_r}{\partial r} - \frac{C_2^2}{r^3} = -\frac{1}{\rho} \frac{\partial P}{\partial r}$$

and

$$\frac{\partial V_r}{\partial r} = -\frac{C_1}{r^2}$$

Therefore:

$$\frac{C_1}{r}\left(-\frac{C_1}{r^2}\right)-\frac{C_2^2}{r^3}=-\frac{1}{\rho}\frac{\partial P}{\partial r}$$

$$-\frac{C_1^2}{r^3}-\frac{C_2^2}{r^3}=-\frac{1}{\rho}\frac{\partial P}{\partial r}$$

$$\frac{1}{\rho}\frac{\partial P}{\partial r}=\frac{C_1^2+C_2^2}{r^3}$$

$$\frac{1}{\rho}dP=\left(C_1^2+C_2^2\right)\frac{1}{r^3}dr$$

$$\frac{1}{\rho}(P_e-P_i)=-\frac{1}{2}\left(C_1^2+C_2^2\right)\left(\frac{1}{r_e^2}-\frac{1}{r_i^2}\right)$$

Therefore:

$$P_e-P_i=\frac{\rho}{2}\left(C_1^2+C_2^2\right)\left(\frac{1}{r_i^2}-\frac{1}{r_e^2}\right) \qquad \text{(C.5)}$$

These pressures are static pressures. The total pressure is defined as:

$$P_0=P+\frac{1}{2}\rho C^2 \qquad \text{(C.6)}$$

with C the absolute velocity defined by equation A.19 in appendix A. The following is valid:

$$P_{0e}-P_{0i}=P_e-P_i+\frac{1}{2}\rho\left(V_\theta^2+V_r^2\right)_e-\frac{1}{2}\rho\left(V_\theta^2+V_r^2\right)_i$$

The absolute velocity far from the rotating disc will be zero. Therefore the second last term in the previous equation may be omitted:

$$P_e-P_i=P_{0e}-P_{0i}+\frac{1}{2}\rho\left(V_\theta^2+V_r^2\right)_i \qquad \text{(C.7)}$$

By substitution of equation (C.5) into equation (C.7) and noting that $\frac{1}{r_e} \rightarrow 0$ at a distance far away from the disc, the following may be written:

$$P_{0e} - P_{0i} + \frac{1}{2}\rho\left(V_\theta^2 + V_r^2\right)_i = \frac{1}{2}\rho\left(C_1^2 + C_2^2\right)\left(\frac{1}{r_i^2}\right)$$

The following may be written with the help of the definition of C_1 and C_2:

$$P_{0e} - P_{0i} + \frac{1}{2}\rho V_\theta^2 + \frac{1}{2}\rho V_r^2 = \frac{1}{2}\rho V_\theta^2 + \frac{1}{2}\rho V_r^2$$

Thus:

$$P_{0e} = P_{0i} \qquad \text{(C.8)}$$

It is therefore clear that the total pressure must remain constant in the free vortex at the outside of the rotating disc. Thus the outlet loss factor is defined as follows:

$$K_{out} = 0 \qquad \text{(C.9)}$$

ε_{smooth}	Pipe roughness for a smooth pipe	m
$\bar{f}_i / f_{r,rough,i}$	Friction factor for a rotating rough pipe at increment	-
$f_{r,smooth,i}$	Friction factor for a rotating smooth pipe at increment	-
$f_{s,rough,i}$	Friction factor for a stationary rough pipe at increment	-
$f_{s,smooth,i}$	Friction factor for a stationary smooth pipe at increment	-
$f_{sl,i}$	Friction factor for laminar flow in a stationary straight pipe at increment	-
$f_{st,i}$	Friction factor for turbulent flow in a stationary straight pipe at increment	-
$Freq_{motor}$	Frequency of electric motor	Hz
HTA	Heat transfer area of rotating pipe increment	m^2
h	Convection coefficient	$W/m^2 \bullet K$
h_i	Convection coefficient in the rotating pipe at increment	$W/m^2 \bullet K$
$ho_{in,i}$	Inlet enthalpy based on total temperature in the rotating pipe at increment	$J/kg \bullet K$
$ho_{out,i}$	Outlet enthalpy based on total temperature in the rotating pipe at increment	$J/kg \bullet K$
$HT_{effectivns,i}$	Heat transfer effectiveness in the rotating pipe at increment	%
$h_{Unitareabottom}$	Convection coefficient per unit area of the bottom side of the rotating disc	W/K
$h_{Unitareatop}$	Convection coefficient per unit area of the top side of the rotating disc	W/K
inc	Number of increments of the rotating pipe	-

$inlet_{ratio}$	Radial inlet velocity divided by the tangential inlet velocity	-
k	Thermal conductivity of air	$W/m{\bullet}K$
k_i	Thermal conductivity of air in the rotating pipe at increment	$W/m{\bullet}K$
k_j	Thermal conductivity of the aluminium disc	$W/m{\bullet}K$
K_{in}	Inlet loss factor	-
K_{out}	Outlet loss factor	-
$K_{l,i}$	Dimensionless parameter for laminar flow in the rotating pipe at increment	-
$K_{t,i}$	Dimensionless parameter for turbulent flow in the rotating pipe at increment	-
L	Length of the rotating pipe	m
L_{inc}	Length of a radial increment of the rotating pipe	m
$\dot{m}$	Mass flow	kg/s
$\bar{M}_i$	Average mach number in the rotating pipe at radial increment	-
$M_{in,i}$	Inlet mach number in the rotating pipe at increment	-
$M_{out,i}$	Outlet mach number in the rotating pipe at increment	-
N	Rotational speed of the disc	rpm
NTU_i	Number of transfer units in the rotating pipe at increment	-
$Nusselt$	Nusselt number	-
$Nusselt_{pipe,i}$	Nusslet number in the rotating pipe at increment	-
ω	Rotational speed of the disc	rad/s
Pr	Prandtl number	-

Pr_i	Prandtl number in the rotating pipe at increment	-
PR_{total}	Pressure ratio referring to the total pressure	-
$Pulley_{ratio}$	Pulley ratio	-
P	Total pressure	Pa
$\bar{p}_i$	Average static pressure in the rotating pipe at increment	Pa
$p_{in,i}$	Inlet static pressure in the rotating pipe at increment	Pa
$p_{out,i}$	Outlet static pressure in the rotating pipe at increment	Pa
$\bar{po}_i$	Average total pressure in the rotating pipe at increment	Pa
$po_{in,i}$	Inlet total pressure in the rotating pipe at increment	Pa
$po_{out,i}$	Outlet total pressure in the rotating pipe at increment	Pa
$\dot{Q}_i$	Heat transfer rate in the rotating pipe at increment	W
$\dot{Q}_{max,i}$	Maximum heat transfer rate in the rotating pipe at increment	W
q_i	Heat flux in the rotating pipe at increment	W/m^2
r	Increments in the radial direction	-
Re	Rotational Reynolds number	-
$Re_{rot,i}$	Rotational Reynolds number in the rotating pipe at increment	-
$Re_{radial,i}$	Reynolds number based on the mean radial velocity in the rotating pipe at increment	-
$Re_{crit,i}$	Critical Reynolds number indicating the transition between laminar and turbulent flow for the determination of the rotating pipe friction factor at	-

	increment	
ρ	Density of the air	kg/m^3
ρ_j	Density of the aluminium disc	kg/m^3
$\bar{\rho}_i$	Average density in the rotating pipe at increment	kg/m^3
$\rho_{in,i}$	Inlet density in the rotating pipe at increment	kg/m^3
$\rho_{out,i}$	Outlet density in the rotating pipe at increment	kg/m^3
R_{air}	Universal gas constant for air (287)	$J/kg \cdot K$
$ratio_i$	$f_{s,rough,i}/f_{s,smooth,i}$ at increment	-
r_{in}	Rotating cylindrical cavity radius	m
r_{mean}	Mean radius of rotating pipe	m
r_{out}	Outer edge of the disc radius	m
$\bar{r}_i$	Average radius at radial increment	m
$r_{in,i}$	Inlet radius in the rotating pipe of increment	m
$r_{out,i}$	Outlet radius in the rotating pipe of increment	m
$Sec_{loss,i}$	Secondary loss factor at increment	-
Tf	Environmental temperature	K
T	Temperature	K
$\bar{T}_i$	Average static temperature in the rotating pipe at increment	K
$T_{in,i}$	Inlet static temperature in the rotating pipe at increment	K
$T_{out,i}$	Outlet static temperature in the rotating pipe at increment	K
$\bar{To}_i$	Average total temperature in the rotating pipe at increment	K

$To_{in,i}$	Inlet total temperature in the rotating pipe at increment	K
$To_{out,i}$	Outlet total temperature in the rotating pipe at increment	K
$T_{wall,i}$	Wall temperature of the rotating pipe at increment	K
$T_{gem,j}$	Average temperature of node block	K
$T_{x,y}$	Temperature of solid aluminium disc (x=node block=1,2,3,...7) (y=node=1,2,3,...27)	K
UA_i	Overall heat transfer coefficient multiplied by the total heat transfer surface area at increment	W/K
vis	Dynamic viscosity	$kg/m \cdot s$
$\bar{\mu}_i$	Average dynamic viscosity in the rotating pipe at increment	$kg/m \cdot s$
$Volumeflow$	Volume flow rate	$\ell/\min$
$\bar{Vr}_i$	Average radial velocity in the rotating pipe at increment	m/s
$Vr_{in,i}$	Inlet radial velocity in the rotating pipe at increment	m/s
$Vr_{out,i}$	Outlet radial velocity in the rotating pipe at increment	m/s
$\bar{Vtheta}_i$	Average tangential velocity in the rotating pipe at increment	m/s
$Vtheta_{in,i}$	Inlet tangential velocity in the rotating pipe at increment	m/s
$Vtheta_{out,i}$	Outlet tangential velocity in the rotating pipe at increment	m/s
$\bar{Vtotal}_i$	Average total velocity in the rotating pipe at increment	m/s

$Vtotal_{in,i}$	Inlet total velocity in the rotating pipe at increment	m/s
$Vtotal_{out,i}$	Outlet total velocity in the rotating pipe at increment	m/s
$width$	Thickness of the disc	m
$X_{j,i}$	Conduction equations source terms	-
z	Increments in the axial direction	-
$\tau_{ext,i}$	Total torque exerted due to the pipe walls at increment	W
γ_i	Ratio of specific heats in the rotating pipe at increment	-

SUBSCRIPTS

SYMBOL	NAME
top/zt	Top side of the disc
$bottom/zb$	Bottom side of the disc
$inside/ri$	Rotating cylindrical cavity
$outside/ro$	Outside edge of the rotating disc
$r\,i,j$	i=radial position (i=1,2,...9) j=node block (j=1,2,...7)
$z\,i,j$	i=axial position (i=1,2,3) j=node block (j=1,2,...7)
i	Radial position (i=1,2,...9)
j	Node block (i=1,2,...7)

EES Ver. 6.867: #1102: G. P. Greyvenstein, M-Tech Industrial, South Africa

Function $\mathbf{Nusselt_{top}}$ (Re)

If [(Re < 200000) and (Re > 30000)] Then

$Nusselt_{top} := 0.8 \cdot Re^{0.5}$

Else

If [Re > 200000] Then

$Nusselt_{top} := 0.0171 \cdot Re^{0.814}$

Else

$Nusselt_{top} := 0$

EndIf

EndIf

End $\mathbf{Nusselt_{top}}$

Function $\mathbf{Nusselt_{bottom}}$ (Re)

If [(Re < 200000) and (Re > 30000)] Then

$Nusselt_{bottom} := 0.8 \cdot Re^{0.5}$

Else

If [Re > 200000] Then

$Nusselt_{bottom} := 0.0171 \cdot Re^{0.814}$

Else

$Nusselt_{bottom} := 0$

EndIf

EndIf

End $\mathbf{Nusselt_{bottom}}$

Function $\mathbf{Nusselt_{pipe}}$ (Re, Pr)

If [Re < 2300] Then

$Nusselt_{pipe} := 4.36$

Else

$Nusselt_{pipe} := 0.023 \cdot Re^{0.8} \cdot Pr^{0.3}$

EndIf

End $\mathbf{Nusselt_{pipe}}$

Function $\mathbf{Sec_{loss}}$ (i, inc, K_{in}, K_{out}, ρ_{in}, ρ_{out}, p_{in}, p_{out}, γ, M_{in}, M_{out})

If [(i = 1) and (i = inc)] Then

$$Sec_{loss} := K_{in} \cdot p_{in} \cdot \left[\left(1 + \left[\frac{\gamma - 1}{2} \right] \cdot M_{in}^{\,2} \right)^{\left(\frac{\gamma}{\gamma - 1} \right)} - 1 \right] + K_{out} \cdot p_{out} \cdot \left[\left(1 + \left[\frac{\gamma - 1}{2} \right] \cdot M_{out}^{\,2} \right)^{\left(\frac{\gamma}{\gamma - 1} \right)} - 1 \right]$$

Else

If [i = 1] Then

$$Sec_{loss} := K_{in} \cdot p_{in} \cdot \left[\left(1 + \left[\frac{\gamma - 1}{2}\right] \cdot M_{in}^{\,2}\right)^{\left(\frac{\gamma}{\gamma - 1}\right)} - 1\right]$$

Else

If [i = inc] Then

$$Sec_{loss} := K_{out} \cdot p_{out} \cdot \left[\left(1 + \left[\frac{\gamma - 1}{2}\right] \cdot M_{out}^{\,2}\right)^{\left(\frac{\gamma}{\gamma - 1}\right)} - 1\right]$$

Else

$Sec_{loss} := 0$

EndIf

EndIf

EndIf

End **Sec**$_{loss}$

Function **Friction**$_r$ (f_{sl}, f_{st}, K_l, K_t, R, R_{rot}, R_{crit}, eps, D)

If $\left[\left(\left[\left(R < R_{crit}\right) \text{ and } \left(K_l < 10^{7}\right)\right] \text{ and } \left[K_l > 220\right]\right) \text{ and } \left(\frac{R_{rot}}{R} < 0.5\right)\right]$ Then

$$Friction_r := f_{sl} \cdot 0.0883 \cdot K_l^{\,0.25} \cdot \left[1 + 11.2 \cdot K_t^{\,-0.325}\right]$$

Else

If $\left[\left(\left[R > R_{crit}\right] \text{ and } \left[K_t < 500\right]\right) \text{ and } \left(K_t > 1\right)\right]$ Then

$$Friction_r := f_{st} \cdot \left[0.942 + 0.058 \cdot K_t^{\,0.282}\right]$$

Else

If $\left[\left(K_l < 220\right) \text{ and } \left(\frac{R_{rot}}{R} < 0.5\right)\right]$ Then

$$Friction_r := \frac{64}{R}$$

Else

If $[K_t < 1]$ Then

$$Friction_r := \frac{0.25}{\log^2\left[0.27 \cdot \frac{eps}{D} + \frac{5.74}{R^{0.9}}\right]}$$

Else

$$Frictionturb := \frac{0.25}{\log^2\left[0.27 \cdot \frac{eps}{D} + \frac{5.74}{R^{0.9}}\right]}$$

$$Frictionlam := \frac{64}{R}$$

lam := 2000

turb := 5000

$$Friction_r := \left[\frac{Frictionturb - Frictionlam}{turb - lam}\right] \cdot [R - lam] + Frictionlam$$

EndIf

EndIf

EndIf

EndIf

End **Friction$_r$**

Function **Friction$_s$** (R, D, eps)

If [R < 2000] Then

$$Friction_s := \frac{64}{R}$$

Else

If [R > 5000] Then

$$Friction_s := \frac{0.25}{\log^2\left[0.27 \cdot \frac{eps}{D} + \frac{5.74}{R^{0.9}}\right]}$$

Else

$$Frictionturb := \frac{0.25}{\log^2\left[0.27 \cdot \frac{eps}{D} + \frac{5.74}{R^{0.9}}\right]}$$

$$Frictionlam := \frac{64}{R}$$

lam := 2000

turb := 5000

$$Friction_s := \left[\frac{Frictionturb - Frictionlam}{turb - lam}\right] \cdot [R - lam] + Frictionlam$$

EndIf

EndIf

End **Friction$_s$**

***********Input Conditions**********

T_{inside} = 298.15

$T_{outside}$ = 328.15

T_{top} = 328.15

T_{bottom} = 328.15

P_{inside} = 85940

$P_{outside} = 87500$

$P_{top} = 87500$

$P_{bottom} = 87500$

**********Geometry of the pipe**********

$z = 3$

$r = 9$

$b = 7$

$inc = 9$

$r_{in} = 0.023$

$r_{out} = 0.3$

$r_{in,1} = r_{in}$

$r_{out,1} = r_{in,1} + L_{inc}$

$\bar{r}_1 = 0.5 \cdot [r_{in,1} + r_{out,1}]$

$D = 0.0064$

$Width = 0.014$

$$L_{inc} = \frac{L}{inc}$$

$L = r_{out} - r_{in}$

$$A = \pi \cdot \frac{D^2}{4}$$

$HTA = \pi \cdot D \cdot L_{inc}$

$\varepsilon_{rough} = 0.00003$

$\varepsilon_{smooth} = 0$

**********Mass flow**********

**********Properties of fluid medium**********

$R_{air} = 287$

**********Inlet and outlet loss factors**********

$$inlet_{ratio} = \frac{Vr_{in,1}}{Vtheta_{in,1}}$$

$K_{in} = 217 - 206.4 \cdot inlet_{ratio} + 94.13 \cdot inlet_{ratio}^2 - 24.36 \cdot inlet_{ratio}^3 + 3.636 \cdot inlet_{ratio}^4 - 0.291 \cdot inlet_{ratio}^5 + 0.009654 \cdot inlet_{ratio}^6$

$K_{out} = 0$

**********Rotation speed**********

$N = 2000$

$$\omega = 2 \cdot \pi \cdot \frac{N}{60}$$

**********Electric motor variables**********

$Pulley_{ratio} = 2.95$

$$Freq_{motor} = \frac{N}{60 \cdot Pulley_{ratio}}$$

**********Rotating pipe incrementation**********

$r_{in,i} = r_{out,i-1}$ for i = 2 to inc

$r_{out,i} = r_{in,i} + L_{inc}$ for i = 2 to inc

$\bar{r}_i = 0.5 \cdot [r_{in,i} + r_{out,i}]$ for i = 2 to inc

**********Inlet and Outlet Pressures and Temperatures**********

$To_{in,1} = T_{inside}$

$po_{in,1} = P_{inside}$

$po_{out,9} = P_{outside}$

**********Pressure and Temperature Connection**********

$po_{in,i} = po_{out,i-1}$ for i = 2 to inc

$To_{in,i} = To_{out,i-1}$ for i = 2 to inc

**********Compressible Pipe Flow**********

$$\gamma_i = \frac{Cp['Air', T = \bar{T}_i]}{Cv['Air', T = \bar{T}_i]}$$ for i = 1 to inc

$Cp_i = Cp['Air', T = \bar{T}_i]$ for i = 1 to inc

**********Friction factor for a stationary and rotating pipe**********

$f_{r,smooth,i} = Friction_r[f_{st,i}, f_{st,i}, K_{l,i}, K_{t,i}, Re_{radial,i}, Re_{rot,i}, Re_{crit,i}, \varepsilon_{rough}, D]$ for i = 1 to inc

$f_{r,rough,i} = ratio_i \cdot f_{r,smooth,i}$ for i = 1 to inc

$f_{s,rough,i} = Friction_s[Re_{radial,i}, D, \varepsilon_{rough}]$ for i = 1 to inc

$f_{s,smooth,i} = Friction_s[Re_{radial,i}, D, \varepsilon_{smooth}]$ for i = 1 to inc

$\bar{f}_i = f_{r,rough,i}$ for i = 1 to inc

$$ratio_i = \frac{f_{s,rough,i}}{f_{s,smooth,i}}$$ for i = 1 to inc

$$Re_{rot,i} = \frac{\bar{\rho}_i \cdot \omega \cdot D^2}{\bar{\mu}_i}$$ for i = 1 to inc

$Re_{crit,i} = 1070 \cdot Re_{rot,i}^{0.23}$ for i = 1 to inc

**********Laminar flow in a rotating straight pipe**********

$$f_{sl,i} = \frac{64}{Re_{radial,i}}$$ for i = 1 to inc

$K_{l,i} = Re_{rot,i} \cdot Re_{radial,i}$ for i = 1 to inc

**********Turbulent flow in a rotating straight pipe**********

$f_{st,i} = 0.3164 \cdot Re_{radial,i}^{-0.25}$ for i = 1 to inc

$$K_{t,i} = \frac{Re_{rot,i}^{\ 2}}{Re_{radial,i}} \quad \text{for } i = 1 \text{ to inc}$$

**********Inlet**********

$$po_{in,i} = p_{in,i} \cdot \left[\left(1 + \left[\frac{\gamma_i - 1}{2}\right] \cdot M_{in,i}^{\ 2}\right)^{\left(\frac{\gamma_i}{\gamma_i - 1}\right)}\right] \quad \text{for } i = 1 \text{ to inc}$$

$$To_{in,i} = T_{in,i} \cdot \left[1 + \left(\frac{\gamma_i - 1}{2}\right) \cdot M_{in,i}^{\ 2}\right] \quad \text{for } i = 1 \text{ to inc}$$

$$\rho_{in,i} = \frac{p_{in,i}}{R_{air} \cdot T_{in,i}} \quad \text{for } i = 1 \text{ to inc}$$

$$\dot{m} = \rho_{in,i} \cdot Vr_{in,i} \cdot A \quad \text{for } i = 1 \text{ to inc}$$

$$c_{in,i} = \sqrt{\gamma_i \cdot R_{air} \cdot T_{in,i}} \quad \text{for } i = 1 \text{ to inc}$$

$$M_{in,i} = \frac{Vtotal_{in,i}}{c_{in,i}} \quad \text{for } i = 1 \text{ to inc}$$

$$Vtheta_{in,i} = \omega \cdot r_{in,i} \quad \text{for } i = 1 \text{ to inc}$$

$$Vtotal_{in,i}^{\ 2} = Vr_{in,i}^{\ 2} + Vtheta_{in,i}^{\ 2} \quad \text{for } i = 1 \text{ to inc}$$

**********Outlet**********

$$po_{out,i} = p_{out,i} \cdot \left[\left(1 + \left[\frac{\gamma_i - 1}{2}\right] \cdot M_{out,i}^{\ 2}\right)^{\left(\frac{\gamma_i}{\gamma_i - 1}\right)}\right] \quad \text{for } i = 1 \text{ to inc}$$

$$To_{out,i} = T_{out,i} \cdot \left[1 + \left(\frac{\gamma_i - 1}{2}\right) \cdot M_{out,i}^{\ 2}\right] \quad \text{for } i = 1 \text{ to inc}$$

$$\rho_{out,i} = \frac{p_{out,i}}{R_{air} \cdot T_{out,i}} \quad \text{for } i = 1 \text{ to inc}$$

$$\dot{m} = \rho_{out,i} \cdot Vr_{out,i} \cdot A \quad \text{for } i = 1 \text{ to inc}$$

$$c_{out,i} = \sqrt{\gamma_i \cdot R_{air} \cdot T_{out,i}} \quad \text{for } i = 1 \text{ to inc}$$

$$M_{out,i} = \frac{Vtotal_{out,i}}{c_{out,i}} \quad \text{for } i = 1 \text{ to inc}$$

$$Vtheta_{out,i} = \omega \cdot r_{out,i} \quad \text{for } i = 1 \text{ to inc}$$

$$Vtotal_{out,i}^{\ 2} = Vr_{out,i}^{\ 2} + Vtheta_{out,i}^{\ 2} \quad \text{for } i = 1 \text{ to inc}$$

**********Average**********

$$\overline{po}_i = 0.5 \cdot [po_{in,i} + po_{out,i}] \quad \text{for } i = 1 \text{ to inc}$$

$$\overline{po}_i = \overline{p}_i \cdot \left[\left(1 + \left[\frac{\gamma_i - 1}{2}\right] \cdot \overline{M}_i^{\ 2}\right)^{\left(\frac{\gamma_i}{\gamma_i - 1}\right)}\right] \quad \text{for } i = 1 \text{ to inc}$$

$$\overline{To}_i = 0.5 \cdot [To_{in,i} + To_{out,i}] \quad \text{for } i = 1 \text{ to inc}$$

$$\overline{To}_i = \overline{T}_i \cdot \left[1 + \left(\frac{\gamma_i - 1}{2}\right) \cdot \overline{M}_i^{\ 2}\right] \quad \text{for } i = 1 \text{ to inc}$$

$$\overline{\rho}_i = \frac{\overline{p}_i}{R_{air} \cdot \overline{T}_i} \quad \text{for } i = 1 \text{ to inc}$$

$$\dot{m} = \overline{\rho}_i \cdot \overline{Vr}_i \cdot A \quad \text{for } i = 1 \text{ to inc}$$

$$\overline{c}_i = \sqrt{\gamma_i \cdot R_{air} \cdot \overline{T}_i} \quad \text{for } i = 1 \text{ to inc}$$

$\overline{M}_i = \frac{\overline{Vtotal}_i}{\overline{c}_i}$ for i = 1 to inc

$\overline{Vtheta}_i = \omega \cdot \overline{r}_i$ for i = 1 to inc

$\overline{Vtotal}_i^2 = \overline{Vr}_i^2 + \overline{Vtheta}_i^2$ for i = 1 to inc

**********Through-flow Reynolds Number**********

$\overline{\mu}_i$ = **Visc** ['Air' , T = $\overline{T}_i$] for i = 1 to inc

$Re_{radial,i} = \frac{\overline{\rho}_i \cdot \overline{Vr}_i \cdot D}{\overline{\mu}_i}$ for i = 1 to inc

**********LINEAR MOMENTUM CONSERVATION**********

$\overline{\rho}_i \cdot \omega^2 \cdot [r_{out,i}^2 - r_{in,i}^2] = \frac{\overline{p}_i}{\overline{po}_i} \cdot [po_{out,i} - po_{in,i}] + \frac{\overline{\rho}_i \cdot \overline{Vtotal}_i^2}{2 \cdot \overline{To}_i} \cdot [To_{out,i} - To_{in,i}] + \frac{\overline{f}_i \cdot L_{inc}}{D} \cdot \frac{|\dot{m}| \cdot \dot{m}}{2 \cdot \overline{\rho}_i \cdot A^2} + Sec_{loss,i}$

for i = 1 to inc

$Sec_{loss,i}$ = **Sec**$_{loss}$ [i , inc , K_{in} , K_{out} , $\rho_{in,i}$, $\rho_{out,i}$, $p_{in,i}$, $p_{out,i}$, γ_i , $M_{in,i}$, $M_{out,i}$] for i = 1 to inc

**********ANGULAR MOMENTUM CONSERVATION**********

$\tau_{ext,i} = \dot{m} \cdot \omega \cdot [r_{out,i}^2 - r_{in,i}^2]$ for i = 1 to inc

**********ENERGY CONSERVATION**********

$ho_{out,i}$ = **h** ['Air' , T = $To_{out,i}$] for i = 1 to inc

$ho_{in,i}$ = **h** ['Air' , T = $To_{in,i}$] for i = 1 to inc

$\dot{Q}_i + \tau_{ext,i} \cdot \omega = \dot{m} \cdot [ho_{out,i} - ho_{in,i}]$ for i = 1 to inc

**********EFFECTIVENESS NTU FOR PIPE**********

$eps_i = 1 - \exp[-NTU_i]$ for i = 1 to inc

$HT_{effectivns,i} = eps_i \cdot 100$ for i = 1 to inc

Pr_i = **Pr** ['Air' , T = $\overline{T}_i$] for i = 1 to inc

k_i = **k** ['Air' , T = $\overline{T}_i$] for i = 1 to inc

$Nusselt_{pipe,i}$ = **Nusselt**$_{pipe}$ [$Re_{radial,i}$, Pr_i] for i = 1 to inc

$h_i = Nusselt_{pipe,i} \cdot \frac{k_i}{D}$ for i = 1 to inc

$UA_i = h_i \cdot HTA$ for i = 1 to inc

$NTU_i = \frac{UA_i}{\dot{m} \cdot Cp_i}$ for i = 1 to inc

$\dot{Q}_{max,i} = \dot{m} \cdot Cp_i \cdot [T_{wall,i} - \overline{T}_i]$ for i = 1 to inc

$\dot{Q}_i = eps_i \cdot \dot{Q}_{max,i}$ for i = 1 to inc

$Volumeflow = 60000 \cdot \frac{\dot{m}}{0.5 \cdot [\overline{\rho}_9 + \overline{\rho}_1]}$

$PR_{total} = \frac{po_{out,9}}{po_{in,1}}$

**********Connection of Wall Temperatures to the temperature distribution equations**********

$T_{wall,1} = T_{4,2}$

$T_{wall,2} = T_{4,5}$

$T_{wall,3} = T_{4,8}$

$T_{wall,4} = T_{4,11}$

$T_{wall,5} = T_{4,14}$

$T_{wall,6} = T_{4,17}$

$T_{wall,7} = T_{4,20}$

$T_{wall,8} = T_{4,23}$

$T_{wall,9} = T_{4,26}$

**********Program to determine the temperature distribution through**********

**********a 3-dimensional system (cylinder) using derived equations**********

**********Geometry**********

Radial

$$\Delta_r = \frac{r_{out} - r_{in}}{r}$$

$$D2 = \frac{\Delta_r}{2}$$

$$r_1 = \frac{\Delta_r}{2} + r_{in}$$

$r_i = r_{i-1} + \Delta_r$ for i = 2 to r

Axial

$$\Delta_z = \frac{Width}{z}$$

Theta

$$Angle = \frac{60}{b}$$

$$\Delta_\theta = Angle \cdot \frac{\pi}{180}$$

**********Initial Temperatures**********

Radial

$$T_{gem,1} = \frac{\sum_{i=1}^{r*z} [T_{1,i}]}{r \cdot z}$$

$$T_{gem,2} = \frac{\sum_{i=1}^{r*z} [T_{2,i}]}{r \cdot z}$$

$$T_{gem,3} = \frac{\sum_{i=1}^{r*z} [T_{3,i}]}{r \cdot z}$$

$$T_{gem,4} = \frac{\sum_{i=1}^{r*z} [T_{4,i}]}{r \cdot z}$$

$$T_{gem,5} = \frac{\sum_{i=1}^{r*z} [T_{5,i}]}{r \cdot z}$$

$$T_{gem,6} = \frac{\sum_{i=1}^{r*z} [T_{6,i}]}{r \cdot z}$$

$$T_{gem,7} = \frac{\sum_{i=1}^{r*z} [T_{7,i}]}{r \cdot z}$$

****Temperatures used in temp distribution equations****

$Tf_{zb} = T_{bottom}$

$Tf_{zt} = T_{top}$

$Tf_{ri} = T_{inside}$

$Tf_{ro} = T_{outside}$

***********Convection coefficients***********

******Inside******

******For an isothermal rotating cylinder (kendousch)******

$D_{inside} = 2 \cdot r_{in}$

$vis_{inside} = \mathbf{Visc}[\text{'Air'}, T = T_{inside}]$

$k_{inside} = \mathbf{k}[\text{'Air'}, T = T_{inside}]$

$\rho_{inside} = \rho[\text{'Air'}, T = T_{inside}, P = P_{inside}]$

$Pr_{inside} = \mathbf{Pr}[\text{'Air'}, T = T_{inside}]$

$$Re_{inside} = \rho_{inside} \cdot [2 \cdot r_{in}]^2 \cdot \frac{\omega}{2 \cdot vis_{inside}}$$

$$Nusselt_{inside} = 0.6366 \cdot [Re_{Inside} \cdot Pr_{inside}]^{0.5}$$

$$h_{inside} = Nusselt_{inside} \cdot \frac{k_{inside}}{D_{inside}}$$

******Outside******

******For an isothermal rotating cylinder (kendousch)******

$D_{outside} = 2 \cdot r_{out}$

$vis_{outside} = \mathbf{Visc}[\text{'Air'}, T = T_{outside}]$

$k_{outside} = \mathbf{k}['Air', T = T_{outside}]$

$\rho_{outside} = \rho['Air', T = T_{outside}, P = P_{outside}]$

$Pr_{outside} = \mathbf{Pr}['Air', T = T_{outside}]$

$Re_{outside} = \rho_{outside} \cdot [2 \cdot r_{out}]^2 \cdot \frac{\omega}{2 \cdot vis_{outside}}$

$Nusselt_{outside} = 0.6366 \cdot [Re_{outside} \cdot Pr_{outside}]^{0.5}$

$h_{outside} = \pi \cdot Nusselt_{outside} \cdot \frac{k_{outside}}{D_{outside}}$

****Cartesian****

******Top******

******For unheated free disc top and bottom (axial) Owen et al. (1974) Qureshi et al. (1989) ******

$r_{mean} = 0.5 \cdot [r_{out} + r_{in}]$

$A_{top} = \pi \cdot [r_{out}^2 - r_{in}^2]$

$vis_{top} = \mathbf{Visc}['Air', T = T_{top}]$

$k_{top} = \mathbf{k}['Air', T = T_{top}]$

$\rho_{top} = \rho['Air', T = T_{top}, P = P_{top}]$

$Re_{top} = \rho_{top} \cdot \omega \cdot \frac{r_{mean}^2}{vis_{top}}$

$Nusselt_{top} = \mathbf{Nusselt}_{top}[Re_{top}]$

$h_{Unitareatop} = Nusselt_{top} \cdot k_{top} \cdot \pi \cdot [r_{out} + r_{in}]$

$h_{top} = \frac{h_{Unitareatop}}{A_{top}}$

******Bottom******

******For unheated free disc top and bottom (axial) Owen et al. (1974) Qureshi et al. (1989)******

$A_{bottom} = \pi \cdot [r_{out}^2 - r_{in}^2]$

$vis_{bottom} = \mathbf{Visc}['Air', T = T_{bottom}]$

$k_{bottom} = \mathbf{k}['Air', T = T_{bottom}]$

$\rho_{bottom} = \rho['Air', T = T_{bottom}, P = P_{bottom}]$

$Re_{bottom} = \rho_{bottom} \cdot \omega \cdot \frac{r_{mean}^2}{vis_{bottom}}$

$Nusselt_{bottom} = \mathbf{Nusselt}_{bottom}[Re_{bottom}]$

$h_{Unitareabottom} = Nusselt_{bottom} \cdot k_{bottom} \cdot \pi \cdot [r_{out} + r_{in}]$

$h_{bottom} = \frac{h_{Unitareabottom}}{A_{bottom}}$

******Heat Source Terms******

+ Heat

- Cool

$q_{increment}$

$q_1 = \dot{Q}_1$

$q_2 = \dot{Q}_2$

$q_3 = \dot{Q}_3$

$q_4 = \dot{Q}_4$

$q_5 = \dot{Q}_5$

$q_6 = \dot{Q}_6$

$q_7 = \dot{Q}_7$

$q_8 = \dot{Q}_8$

$q_9 = \dot{Q}_9$

**********Material Properties**********

*****BLOCK 1*****

k_1 = **k** ['Aluminium' , $T_{gem,1}$]

ρ_1 = **rho** ['Aluminium' , $T_{gem,1}$]

*****BLOCK 2*****

k_2 = **k** ['Aluminium' , $T_{gem,2}$]

ρ_2 = **rho** ['Aluminium' , $T_{gem,2}$]

*****BLOCK 3*****

k_3 = **k** ['Aluminium' , $T_{gem,3}$]

ρ_3 = **rho** ['Aluminium' , $T_{gem,3}$]

*****BLOCK 4*****

k_4 = **k** ['Aluminium' , $T_{gem,4}$]

ρ_4 = **rho** ['Aluminium' , $T_{gem,4}$]

*****BLOCK 5*****

k_5 = **k** ['Aluminium' , $T_{gem,5}$]

ρ_5 = **rho** ['Aluminium' , $T_{gem,5}$]

*****BLOCK 6*****

k_6 = **k** ['Aluminium' , $T_{gem,6}$]

ρ_6 = **rho** ['Aluminium' , $T_{gem,6}$]

*****BLOCK 7*****

k_7 = **k** ['Aluminium' , $T_{gem,7}$]

ρ_7 = **rho** ['Aluminium' , $T_{gem,7}$]

Radial

*****BLOCK 1*****

$$Cp_{r1,1} = 1000 \cdot c\left['Aluminium', \frac{T_{1,1} + T_{1,2} + T_{1,3}}{3}\right]$$

$$Cp_{r2,1} = 1000 \cdot c\left['Aluminium', \frac{T_{1,4} + T_{1,5} + T_{1,6}}{3}\right]$$

$$Cp_{r3,1} = 1000 \cdot c\left['Aluminium', \frac{T_{1,7} + T_{1,8} + T_{1,9}}{3}\right]$$

$$Cp_{r4,1} = 1000 \cdot c\left['Aluminium', \frac{T_{1,10} + T_{1,11} + T_{1,12}}{3}\right]$$

$$Cp_{r5,1} = 1000 \cdot c\left['Aluminium', \frac{T_{1,13} + T_{1,14} + T_{1,15}}{3}\right]$$

$$Cp_{r6,1} = 1000 \cdot c\left['Aluminium', \frac{T_{1,16} + T_{1,17} + T_{1,18}}{3}\right]$$

$$Cp_{r7,1} = 1000 \cdot c\left['Aluminium', \frac{T_{1,19} + T_{1,20} + T_{1,21}}{3}\right]$$

$$Cp_{r8,1} = 1000 \cdot c\left['Aluminium', \frac{T_{1,22} + T_{1,23} + T_{1,24}}{3}\right]$$

$$Cp_{r9,1} = 1000 \cdot c\left['Aluminium', \frac{T_{1,25} + T_{1,26} + T_{1,27}}{3}\right]$$

*****BLOCK 2*****

$$Cp_{r1,2} = 1000 \cdot c\left['Aluminium', \frac{T_{2,1} + T_{2,2} + T_{2,3}}{3}\right]$$

$$Cp_{r2,2} = 1000 \cdot c\left['Aluminium', \frac{T_{2,4} + T_{2,5} + T_{2,6}}{3}\right]$$

$$Cp_{r3,2} = 1000 \cdot c\left['Aluminium', \frac{T_{2,7} + T_{2,8} + T_{2,9}}{3}\right]$$

$$Cp_{r4,2} = 1000 \cdot c\left['Aluminium', \frac{T_{2,10} + T_{2,11} + T_{2,12}}{3}\right]$$

$$Cp_{r5,2} = 1000 \cdot c\left['Aluminium', \frac{T_{2,13} + T_{2,14} + T_{2,15}}{3}\right]$$

$$Cp_{r6,2} = 1000 \cdot c\left['Aluminium', \frac{T_{2,16} + T_{2,17} + T_{2,18}}{3}\right]$$

$$Cp_{r7,2} = 1000 \cdot c\left['Aluminium', \frac{T_{2,19} + T_{2,20} + T_{2,21}}{3}\right]$$

$$Cp_{r8,2} = 1000 \cdot c\left['Aluminium', \frac{T_{2,22} + T_{2,23} + T_{2,24}}{3}\right]$$

$$Cp_{r9,2} = 1000 \cdot c\left['Aluminium', \frac{T_{2,25} + T_{2,26} + T_{2,27}}{3}\right]$$

*****BLOCK 3*****

$$Cp_{r1,3} = 1000 \cdot c\left['Aluminium', \frac{T_{3,1} + T_{3,2} + T_{3,3}}{3}\right]$$

$$Cp_{r2,3} = 1000 \cdot c\left['Aluminium', \frac{T_{3,4} + T_{3,5} + T_{3,6}}{3}\right]$$

$$Cp_{r3,3} = 1000 \cdot c\left['Aluminium', \frac{T_{3,7} + T_{3,8} + T_{3,9}}{3}\right]$$

$$Cp_{r4,3} = 1000 \cdot c\left['Aluminium', \frac{T_{3,10} + T_{3,11} + T_{3,12}}{3}\right]$$

$$Cp_{r5,3} = 1000 \cdot c\left['Aluminium', \frac{T_{3,13} + T_{3,14} + T_{3,15}}{3}\right]$$

$$Cp_{r6,3} = 1000 \cdot c\left['Aluminium', \frac{T_{3,16} + T_{3,17} + T_{3,18}}{3}\right]$$

$$Cp_{r7,3} = 1000 \cdot c\left['Aluminium', \frac{T_{3,19} + T_{3,20} + T_{3,21}}{3}\right]$$

$$Cp_{r8,3} = 1000 \cdot c\left['Aluminium', \frac{T_{3,22} + T_{3,23} + T_{3,24}}{3}\right]$$

$$Cp_{r9,3} = 1000 \cdot c\left['Aluminium', \frac{T_{3,25} + T_{3,26} + T_{3,27}}{3}\right]$$

*****BLOCK 4*****

$$Cp_{r1,4} = 1000 \cdot c\left['Aluminium', \frac{T_{4,1} + T_{4,2} + T_{4,3}}{3}\right]$$

$$Cp_{r2,4} = 1000 \cdot c\left['Aluminium', \frac{T_{4,4} + T_{4,5} + T_{4,6}}{3}\right]$$

$$Cp_{r3,4} = 1000 \cdot c\left['Aluminium', \frac{T_{4,7} + T_{4,8} + T_{4,9}}{3}\right]$$

$$Cp_{r4,4} = 1000 \cdot c\left['Aluminium', \frac{T_{4,10} + T_{4,11} + T_{4,12}}{3}\right]$$

$$Cp_{r5,4} = 1000 \cdot c\left['Aluminium', \frac{T_{4,13} + T_{4,14} + T_{4,15}}{3}\right]$$

$$Cp_{r6,4} = 1000 \cdot c\left['Aluminium', \frac{T_{4,16} + T_{4,17} + T_{4,18}}{3}\right]$$

$$Cp_{r7,4} = 1000 \cdot c\left['Aluminium', \frac{T_{4,19} + T_{4,20} + T_{4,21}}{3}\right]$$

$$Cp_{r8,4} = 1000 \cdot c\left['Aluminium', \frac{T_{4,22} + T_{4,23} + T_{4,24}}{3}\right]$$

$$Cp_{r9,4} = 1000 \cdot c\left['Aluminium', \frac{T_{4,25} + T_{4,26} + T_{4,27}}{3}\right]$$

*****BLOCK 5*****

$$Cp_{r1,5} = 1000 \cdot c\left['Aluminium', \frac{T_{5,1} + T_{5,2} + T_{5,3}}{3}\right]$$

$$Cp_{r2,5} = 1000 \cdot c\left['Aluminium', \frac{T_{5,4} + T_{5,5} + T_{5,6}}{3}\right]$$

$$Cp_{r3,5} = 1000 \cdot c\left['Aluminium', \frac{T_{5,7} + T_{5,8} + T_{5,9}}{3}\right]$$

$$Cp_{r4,5} = 1000 \cdot c\left['Aluminium', \frac{T_{5,10} + T_{5,11} + T_{5,12}}{3}\right]$$

$$Cp_{r5,5} = 1000 \cdot c\left['Aluminium', \frac{T_{5,13} + T_{5,14} + T_{5,15}}{3}\right]$$

$$Cp_{r6,5} = 1000 \cdot c\left['Aluminium', \frac{T_{5,16} + T_{5,17} + T_{5,18}}{3}\right]$$

$$Cp_{r7,5} = 1000 \cdot c\left['Aluminium', \frac{T_{5,19} + T_{5,20} + T_{5,21}}{3}\right]$$

$$Cp_{r8,5} = 1000 \cdot c\left['Aluminium', \frac{T_{5,22} + T_{5,23} + T_{5,24}}{3}\right]$$

$$Cp_{r9,5} = 1000 \cdot c\left['Aluminium', \frac{T_{5,25} + T_{5,26} + T_{5,27}}{3}\right]$$

*****BLOCK 6*****

$$Cp_{r1,6} = 1000 \cdot c\left['Aluminium', \frac{T_{6,1} + T_{6,2} + T_{6,3}}{3}\right]$$

$$Cp_{r2,6} = 1000 \cdot c\left['Aluminium', \frac{T_{6,4} + T_{6,5} + T_{6,6}}{3}\right]$$

$$Cp_{r3,6} = 1000 \cdot c\left['Aluminium', \frac{T_{6,7} + T_{6,8} + T_{6,9}}{3}\right]$$

$$Cp_{r4,6} = 1000 \cdot c\left['Aluminium', \frac{T_{6,10} + T_{6,11} + T_{6,12}}{3}\right]$$

$$Cp_{r5,6} = 1000 \cdot c\left['Aluminium', \frac{T_{6,13} + T_{6,14} + T_{6,15}}{3}\right]$$

$$Cp_{r6,6} = 1000 \cdot c\left['Aluminium', \frac{T_{6,16} + T_{6,17} + T_{6,18}}{3}\right]$$

$$Cp_{r7,6} = 1000 \cdot c\left['Aluminium', \frac{T_{6,19} + T_{6,20} + T_{6,21}}{3}\right]$$

$$Cp_{r8,6} = 1000 \cdot c\left['Aluminium', \frac{T_{6,22} + T_{6,23} + T_{6,24}}{3}\right]$$

$$Cp_{r9,6} = 1000 \cdot c\left['Aluminium', \frac{T_{6,25} + T_{6,26} + T_{6,27}}{3}\right]$$

*****BLOCK 7*****

$$Cp_{r1,7} = 1000 \cdot c\left['Aluminium', \frac{T_{7,1} + T_{7,2} + T_{7,3}}{3}\right]$$

$$Cp_{r2,7} = 1000 \cdot c\left['Aluminium', \frac{T_{7,4} + T_{7,5} + T_{7,6}}{3}\right]$$

$$Cp_{r3,7} = 1000 \cdot c\left['Aluminium', \frac{T_{7,7} + T_{7,8} + T_{7,9}}{3}\right]$$

$$Cp_{r4,7} = 1000 \cdot c\left['Aluminium', \frac{T_{7,10} + T_{7,11} + T_{7,12}}{3}\right]$$

$$Cp_{r5,7} = 1000 \cdot c\left['Aluminium', \frac{T_{7,13} + T_{7,14} + T_{7,15}}{3}\right]$$

$$Cp_{r6,7} = 1000 \cdot c\left['Aluminium', \frac{T_{7,16} + T_{7,17} + T_{7,18}}{3}\right]$$

$$Cp_{r7,7} = 1000 \cdot c\left['Aluminium', \frac{T_{7,19} + T_{7,20} + T_{7,21}}{3}\right]$$

$$Cp_{r8,7} = 1000 \cdot c\left['Aluminium', \frac{T_{7,22} + T_{7,23} + T_{7,24}}{3}\right]$$

$$Cp_{r9,7} = 1000 \cdot c\left['Aluminium', \frac{T_{7,25} + T_{7,26} + T_{7,27}}{3}\right]$$

Axial

*****BLOCK 1*****

$$Cp_{z1,1} = 1000 \cdot c\left['Aluminium', \frac{T_{1,1} + T_{1,4} + T_{1,7} + T_{1,10} + T_{1,13} + T_{1,16} + T_{1,19} + T_{1,22} + T_{1,25}}{9}\right]$$

$$Cp_{z2,1} = 1000 \cdot c\left['Aluminium', \frac{T_{1,2} + T_{1,5} + T_{1,8} + T_{1,11} + T_{1,14} + T_{1,17} + T_{1,20} + T_{1,23} + T_{1,26}}{9}\right]$$

$$Cp_{z3,1} = 1000 \cdot c\left['Aluminium', \frac{T_{1,3} + T_{1,6} + T_{1,9} + T_{1,12} + T_{1,15} + T_{1,18} + T_{1,21} + T_{1,24} + T_{1,27}}{9}\right]$$

*****BLOCK 2*****

$$Cp_{z1,2} = 1000 \cdot c\left['Aluminium', \frac{T_{2,1} + T_{2,4} + T_{2,7} + T_{2,10} + T_{2,13} + T_{2,16} + T_{2,19} + T_{2,22} + T_{2,25}}{9}\right]$$

$$Cp_{z2,2} = 1000 \cdot c\left['Aluminium', \frac{T_{2,2} + T_{2,5} + T_{2,8} + T_{2,11} + T_{2,14} + T_{2,17} + T_{2,20} + T_{2,23} + T_{2,26}}{9}\right]$$

$$Cp_{z3,2} = 1000 \cdot c\left['Aluminium', \frac{T_{2,3} + T_{2,6} + T_{2,9} + T_{2,12} + T_{2,15} + T_{2,18} + T_{2,21} + T_{2,24} + T_{2,27}}{9}\right]$$

*****BLOCK 3*****

$$Cp_{z1,3} = 1000 \cdot c\left['Aluminium', \frac{T_{3,1} + T_{3,4} + T_{3,7} + T_{3,10} + T_{3,13} + T_{3,16} + T_{3,19} + T_{3,22} + T_{3,25}}{9}\right]$$

$$Cp_{z2,3} = 1000 \cdot c\left['Aluminium', \frac{T_{3,2} + T_{3,5} + T_{3,8} + T_{3,11} + T_{3,14} + T_{3,17} + T_{3,20} + T_{3,23} + T_{3,26}}{9}\right]$$

$$Cp_{z3,3} = 1000 \cdot c\left['Aluminium', \frac{T_{3,3} + T_{3,6} + T_{3,9} + T_{3,12} + T_{3,15} + T_{3,18} + T_{3,21} + T_{3,24} + T_{3,27}}{9}\right]$$

*****BLOCK 4*****

$$Cp_{z1,4} = 1000 \cdot c\left['Aluminium', \frac{T_{4,1} + T_{4,4} + T_{4,7} + T_{4,10} + T_{4,13} + T_{4,16} + T_{4,19} + T_{4,22} + T_{4,25}}{9}\right]$$

$$Cp_{z2,4} = 1000 \cdot c\left['Aluminium', \frac{T_{4,2} + T_{4,5} + T_{4,8} + T_{4,11} + T_{4,14} + T_{4,17} + T_{4,20} + T_{4,23} + T_{4,26}}{9}\right]$$

$$Cp_{z3,4} = 1000 \cdot c\left['Aluminium', \frac{T_{4,3} + T_{4,6} + T_{4,9} + T_{4,12} + T_{4,15} + T_{4,18} + T_{4,21} + T_{4,24} + T_{4,27}}{9}\right]$$

*****BLOCK 5*****

$$Cp_{z1,5} = 1000 \cdot c\left['Aluminium', \frac{T_{5,1} + T_{5,4} + T_{5,7} + T_{5,10} + T_{5,13} + T_{5,16} + T_{5,19} + T_{5,22} + T_{5,25}}{9}\right]$$

$$Cp_{z2,5} = 1000 \cdot c\left['Aluminium', \frac{T_{5,2} + T_{5,5} + T_{5,8} + T_{5,11} + T_{5,14} + T_{5,17} + T_{5,20} + T_{5,23} + T_{5,26}}{9}\right]$$

$$Cp_{z3,5} = 1000 \cdot c\left['Aluminium', \frac{T_{5,3} + T_{5,6} + T_{5,9} + T_{5,12} + T_{5,15} + T_{5,18} + T_{5,21} + T_{5,24} + T_{5,27}}{9}\right]$$

*****BLOCK 6*****

$$Cp_{z1,6} = 1000 \cdot c\left['Aluminium', \frac{T_{6,1} + T_{6,4} + T_{6,7} + T_{6,10} + T_{6,13} + T_{6,16} + T_{6,19} + T_{6,22} + T_{6,25}}{9}\right]$$

$$Cp_{z2,6} = 1000 \cdot c\left['Aluminium', \frac{T_{6,2} + T_{6,5} + T_{6,8} + T_{6,11} + T_{6,14} + T_{6,17} + T_{6,20} + T_{6,23} + T_{6,26}}{9}\right]$$

$$Cp_{z3,6} = 1000 \cdot c\left['Aluminium', \frac{T_{6,3} + T_{6,6} + T_{6,9} + T_{6,12} + T_{6,15} + T_{6,18} + T_{6,21} + T_{6,24} + T_{6,27}}{9}\right]$$

*****BLOCK 7*****

$$Cp_{z1,7} = 1000 \cdot c\left['Aluminium', \frac{T_{7,1} + T_{7,4} + T_{7,7} + T_{7,10} + T_{7,13} + T_{7,16} + T_{7,19} + T_{7,22} + T_{7,25}}{9}\right]$$

$$Cp_{z2,7} = 1000 \cdot c\left['Aluminium', \frac{T_{7,2} + T_{7,5} + T_{7,8} + T_{7,11} + T_{7,14} + T_{7,17} + T_{7,20} + T_{7,23} + T_{7,26}}{9}\right]$$

$$Cp_{z3,7} = 1000 \cdot c\left['Aluminium', \frac{T_{7,3} + T_{7,6} + T_{7,9} + T_{7,12} + T_{7,15} + T_{7,18} + T_{7,21} + T_{7,24} + T_{7,27}}{9}\right]$$

**********Temperature Node Points**********

$T_{theta,Node}$

$Temperature_{(theta\ block)Node\ point]}$

**********BLOCK 1**********

*****NODE*****

1

$$\frac{2}{\rho_1 \cdot Cp_{r1,1} \cdot [(r_1 + D2)^2 - (r_1 - D2)^2]} \cdot \left[r_{in} \cdot h_{inside} \cdot (Tf_{ri} - T_{1,1}) + (r_1 + D2) \cdot k_1 \cdot \left(\frac{T_{1,4} - T_{1,1}}{\Delta_r}\right)\right] + \frac{2}{\rho_1 \cdot Cp_{z1,1} \cdot \Delta_z} \cdot \left[\frac{k_1}{\Delta_z} \cdot (T_{1,2} - T_{1,1}) + h_{bottom} \cdot (Tf_{zb} - T_{1,1})\right] + X_{1,1} = 0$$

$$X_{1,1} = \frac{1}{\rho_1 \cdot Cp_{r1,1} \cdot \Delta_\theta} \cdot -\frac{k_1}{\Delta_\theta} \cdot \left[\frac{T_{1,1} - T_{2,1}}{r_1^{\,2}}\right]$$

2

$$\frac{2}{\rho_1 \cdot Cp_{r1,1} \cdot [(r_1 + D2)^2 - (r_1 - D2)^2]} \cdot \left[r_{in} \cdot h_{inside} \cdot (Tf_{ri} - T_{1,2}) + (r_1 + D2) \cdot k_1 \cdot \left(\frac{T_{1,5} - T_{1,2}}{\Delta_r}\right)\right] + \frac{1}{\rho_1 \cdot Cp_{z2,1} \cdot \Delta_z} \cdot \left[\frac{k_1}{\Delta_z} \cdot (T_{1,3} - T_{1,2}) - \frac{k_1}{\Delta_z} \cdot (T_{1,2} - T_{1,1})\right] + X_{1,2} = 0$$

$$X_{1,2} = \frac{1}{\rho_1 \cdot Cp_{r1,1} \cdot \Delta_\theta} \cdot -\frac{k_1}{\Delta_\theta} \cdot \left[\frac{T_{1,2} - T_{2,2}}{r_1^{\,2}}\right]$$

3

$$\frac{2}{\rho_1 \cdot Cp_{r1,1} \cdot [(r_1 + D2)^2 - (r_1 - D2)^2]} \cdot \left[r_{in} \cdot h_{inside} \cdot (Tf_{ri} - T_{1,3}) + (r_1 + D2) \cdot k_1 \cdot \left(\frac{T_{1,6} - T_{1,3}}{\Delta_r}\right)\right] + \frac{2}{\rho_1 \cdot Cp_{z3,1} \cdot \Delta_z} \cdot \left[\frac{k_1}{\Delta_z} \cdot (T_{1,2} - T_{1,3}) + h_{top} \cdot (Tf_{zt} - T_{1,3})\right] + X_{1,3} = 0$$

$$X_{1,3} = \frac{1}{\rho_1 \cdot Cp_{r1,1} \cdot \Delta_\theta} \cdot -\frac{k_1}{\Delta_\theta} \cdot \left[\frac{T_{1,3} - T_{2,3}}{r_1^{\,2}}\right]$$

4

$$\frac{2 \cdot k_1}{\rho_1 \cdot Cp_{r2,1} \cdot [(r_2 + D2)^2 - (r_2 - D2)^2]} \cdot \left[(T_{1,7} - T_{1,4}) \cdot \left(\frac{r_2 + D2}{\Delta_r}\right) - \left([T_{1,4} - T_{1,1}] \cdot \left[\frac{r_2 - D2}{\Delta_r}\right]\right)\right] + \frac{2}{\rho_1 \cdot Cp_{z1,1} \cdot \Delta_z} \cdot \left[\frac{k_1}{\Delta_z} \cdot (T_{1,5} - T_{1,4}) + h_{bottom} \cdot (Tf_{zb} - T_{1,4})\right] + X_{1,4} = 0$$

$$X_{1,4} = \frac{1}{\rho_1 \cdot Cp_{r2,1} \cdot \Delta_\theta} \cdot -\frac{k_1}{\Delta_\theta} \cdot \left[\frac{T_{1,4} - T_{2,4}}{r_2^{\,2}}\right]$$

5

$$\frac{2 \cdot k_1}{\rho_1 \cdot Cp_{r2,1} \cdot \left[(r_2 + D2)^2 - (r_2 - D2)^2 \right]} \cdot \left[(T_{1,6} - T_{1,5}) \cdot \left(\frac{r_2 + D2}{\Delta_r} \right) - \left(\left[T_{1,5} - T_{1,2} \right] \cdot \left[\frac{r_2 - D2}{\Delta_r} \right] \right) \right] + \frac{1}{\rho_1 \cdot Cp_{z2,1} \cdot \Delta_z} \cdot \left[\frac{k_1}{\Delta_z} \cdot (T_{1,6} - T_{1,5}) - \frac{k_1}{\Delta_z} \cdot (T_{1,5} - T_{1,4}) \right] + X_{1,5} = 0$$

$$X_{1,5} = \frac{1}{\rho_1 \cdot Cp_{r2,1} \cdot \Delta_\theta} \cdot - \frac{k_1}{\Delta_\theta} \cdot \left[\frac{T_{1,5} - T_{2,5}}{r_2^{\,2}} \right]$$

6

$$\frac{2 \cdot k_1}{\rho_1 \cdot Cp_{r2,1} \cdot \left[(r_2 + D2)^2 - (r_2 - D2)^2 \right]} \cdot \left[(T_{1,9} - T_{1,6}) \cdot \left(\frac{r_2 + D2}{\Delta_r} \right) - \left(\left[T_{1,6} - T_{1,3} \right] \cdot \left[\frac{r_2 - D2}{\Delta_r} \right] \right) \right] + \frac{2}{\rho_1 \cdot Cp_{z3,1} \cdot \Delta_z} \cdot \left[\frac{k_1}{\Delta_z} \cdot (T_{1,5} - T_{1,6}) + h_{top} \cdot (Tf_{zt} - T_{1,6}) \right] + X_{1,6} = 0$$

$$X_{1,6} = \frac{1}{\rho_1 \cdot Cp_{r2,1} \cdot \Delta_\theta} \cdot - \frac{k_1}{\Delta_\theta} \cdot \left[\frac{T_{1,6} - T_{2,6}}{r_2^{\,2}} \right]$$

7

$$\frac{2 \cdot k_1}{\rho_1 \cdot Cp_{r3,1} \cdot \left[(r_3 + D2)^2 - (r_3 - D2)^2 \right]} \cdot \left[(T_{1,10} - T_{1,7}) \cdot \left(\frac{r_3 + D2}{\Delta_r} \right) - \left(\left[T_{1,7} - T_{1,4} \right] \cdot \left[\frac{r_3 - D2}{\Delta_r} \right] \right) \right] + \frac{2}{\rho_1 \cdot Cp_{z1,1} \cdot \Delta_z} \cdot \left[\frac{k_1}{\Delta_z} \cdot (T_{1,8} - T_{1,7}) + h_{bottom} \cdot (Tf_{zb} - T_{1,7}) \right] + X_{1,7} = 0$$

$$X_{1,7} = \frac{1}{\rho_1 \cdot Cp_{r3,1} \cdot \Delta_\theta} \cdot - \frac{k_1}{\Delta_\theta} \cdot \left[\frac{T_{1,7} - T_{2,7}}{r_3^{\,2}} \right]$$

8

$$\frac{2 \cdot k_1}{\rho_1 \cdot Cp_{r3,1} \cdot \left[(r_3 + D2)^2 - (r_3 - D2)^2 \right]} \cdot \left[(T_{1,11} - T_{1,8}) \cdot \left(\frac{r_3 + D2}{\Delta_r} \right) - \left(\left[T_{1,8} - T_{1,5} \right] \cdot \left[\frac{r_3 - D2}{\Delta_r} \right] \right) \right] + \frac{1}{\rho_1 \cdot Cp_{z2,1} \cdot \Delta_z} \cdot \left[\frac{k_1}{\Delta_z} \cdot (T_{1,9} - T_{1,8}) - \frac{k_1}{\Delta_z} \cdot (T_{1,8} - T_{1,7}) \right] + X_{1,8} = 0$$

$$X_{1,8} = \frac{1}{\rho_1 \cdot Cp_{r3,1} \cdot \Delta_\theta} \cdot - \frac{k_1}{\Delta_\theta} \cdot \left[\frac{T_{1,8} - T_{2,8}}{r_3^{\,2}} \right]$$

9

$$\frac{2 \cdot k_1}{\rho_1 \cdot Cp_{r3,1} \cdot \left[(r_3 + D2)^2 - (r_3 - D2)^2 \right]} \cdot \left[(T_{1,12} - T_{1,9}) \cdot \left(\frac{r_3 + D2}{\Delta_r} \right) - \left(\left[T_{1,9} - T_{1,6} \right] \cdot \left[\frac{r_3 - D2}{\Delta_r} \right] \right) \right] + \frac{2}{\rho_1 \cdot Cp_{z3,1} \cdot \Delta_z} \cdot \left[\frac{k_1}{\Delta_z} \cdot (T_{1,8} - T_{1,9}) + h_{top} \cdot (Tf_{zt} - T_{1,9}) \right] + X_{1,9} = 0$$

$$X_{1,9} = \frac{1}{\rho_1 \cdot Cp_{r3,1} \cdot \Delta_\theta} \cdot - \frac{k_1}{\Delta_\theta} \cdot \left[\frac{T_{1,9} - T_{2,9}}{r_3^{\,2}} \right]$$

10

$$\frac{2 \cdot k_1}{\rho_1 \cdot Cp_{r4,1} \cdot \left[(r_4 + D2)^2 - (r_4 - D2)^2 \right]} \cdot \left[(T_{1,13} - T_{1,10}) \cdot \left(\frac{r_4 + D2}{\Delta_r} \right) - \left(\left[T_{1,10} - T_{1,7} \right] \cdot \left[\frac{r_4 - D2}{\Delta_r} \right] \right) \right] + \frac{2}{\rho_1 \cdot Cp_{z1,1} \cdot \Delta_z} \cdot \left[\frac{k_1}{\Delta_z} \cdot (T_{1,11} - T_{1,10}) + h_{bottom} \cdot (Tf_{zb} - T_{1,10}) \right] + X_{1,10} = 0$$

$$X_{1,10} = \frac{1}{\rho_1 \cdot Cp_{r4,1} \cdot \Delta_\theta} \cdot - \frac{k_1}{\Delta_\theta} \cdot \left[\frac{T_{1,10} - T_{2,10}}{r_4^{\,2}} \right]$$

11

$$\frac{2 \cdot k_1}{\rho_1 \cdot Cp_{r4,1} \cdot \left[(r_4 + D2)^2 - (r_4 - D2)^2 \right]} \cdot \left[(T_{1,14} - T_{1,11}) \cdot \left(\frac{r_4 + D2}{\Delta_r} \right) - \left(\left[T_{1,11} - T_{1,8} \right] \cdot \left[\frac{r_4 - D2}{\Delta_r} \right] \right) \right] + \frac{1}{\rho_1 \cdot Cp_{z2,1} \cdot \Delta_z} \cdot \left[\frac{k_1}{\Delta_z} \cdot (T_{1,12} - T_{1,11}) - \frac{k_1}{\Delta_z} \cdot (T_{1,11} - T_{1,10}) \right] + X_{1,11} = 0$$

$$X_{1,11} = \frac{1}{\rho_1 \cdot Cp_{r4,1} \cdot \Delta_\theta} \cdot -\frac{k_1}{\Delta_\theta} \cdot \left[\frac{T_{1,11} - T_{2,11}}{r_4^{\,2}}\right]$$

12

$$\frac{2 \cdot k_1}{\rho_1 \cdot Cp_{r4,1} \cdot \left[(r_4 + D2)^2 - (r_4 - D2)^2\right]} \cdot \left[(T_{1,15} - T_{1,12}) \cdot \left(\frac{r_4 + D2}{\Delta_r}\right) - \left([T_{1,12} - T_{1,9}] \cdot \left[\frac{r_4 - D2}{\Delta_r}\right]\right)\right] + \frac{2}{\rho_1 \cdot Cp_{z3,1} \cdot \Delta_z} \cdot \left[\frac{k_1}{\Delta_z} \cdot (T_{1,11} - T_{1,12}) + h_{top} \cdot (Tf_{zt} - T_{1,12})\right] + X_{1,12} = 0$$

$$X_{1,12} = \frac{1}{\rho_1 \cdot Cp_{r4,1} \cdot \Delta_\theta} \cdot -\frac{k_1}{\Delta_\theta} \cdot \left[\frac{T_{1,12} - T_{2,12}}{r_4^{\,2}}\right]$$

13

$$\frac{2 \cdot k_1}{\rho_1 \cdot Cp_{r5,1} \cdot \left[(r_5 + D2)^2 - (r_5 - D2)^2\right]} \cdot \left[(T_{1,16} - T_{1,13}) \cdot \left(\frac{r_5 + D2}{\Delta_r}\right) - \left([T_{1,13} - T_{1,10}] \cdot \left[\frac{r_5 - D2}{\Delta_r}\right]\right)\right] + \frac{2}{\rho_1 \cdot Cp_{z1,1} \cdot \Delta_z} \cdot \left[\frac{k_1}{\Delta_z} \cdot (T_{1,14} - T_{1,13}) + h_{bottom} \cdot (Tf_{zb} - T_{1,13})\right] + X_{1,13} = 0$$

$$X_{1,13} = \frac{1}{\rho_1 \cdot Cp_{r5,1} \cdot \Delta_\theta} \cdot -\frac{k_1}{\Delta_\theta} \cdot \left[\frac{T_{1,13} - T_{2,13}}{r_5^{\,2}}\right]$$

14

$$\frac{2 \cdot k_1}{\rho_1 \cdot Cp_{r5,1} \cdot \left[(r_5 + D2)^2 - (r_5 - D2)^2\right]} \cdot \left[(T_{1,17} - T_{1,14}) \cdot \left(\frac{r_5 + D2}{\Delta_r}\right) - \left([T_{1,14} - T_{1,11}] \cdot \left[\frac{r_5 - D2}{\Delta_r}\right]\right)\right] + \frac{1}{\rho_1 \cdot Cp_{z2,1} \cdot \Delta_z} \cdot \left[\frac{k_1}{\Delta_z} \cdot (T_{1,15} - T_{1,14}) - \frac{k_1}{\Delta_z} \cdot (T_{1,14} - T_{1,13})\right] + X_{1,14} = 0$$

$$X_{1,14} = \frac{1}{\rho_1 \cdot Cp_{r5,1} \cdot \Delta_\theta} \cdot -\frac{k_1}{\Delta_\theta} \cdot \left[\frac{T_{1,14} - T_{2,14}}{r_5^{\,2}}\right]$$

15

$$\frac{2 \cdot k_1}{\rho_1 \cdot Cp_{r5,1} \cdot \left[(r_5 + D2)^2 - (r_5 - D2)^2\right]} \cdot \left[(T_{1,18} - T_{1,15}) \cdot \left(\frac{r_5 + D2}{\Delta_r}\right) - \left([T_{1,15} - T_{1,12}] \cdot \left[\frac{r_5 - D2}{\Delta_r}\right]\right)\right] + \frac{2}{\rho_1 \cdot Cp_{z3,1} \cdot \Delta_z} \cdot \left[\frac{k_1}{\Delta_z} \cdot (T_{1,14} - T_{1,15}) + h_{top} \cdot (Tf_{zt} - T_{1,15})\right] + X_{1,15} = 0$$

$$X_{1,15} = \frac{1}{\rho_1 \cdot Cp_{r5,1} \cdot \Delta_\theta} \cdot -\frac{k_1}{\Delta_\theta} \cdot \left[\frac{T_{1,15} - T_{2,15}}{r_5^{\,2}}\right]$$

16

$$\frac{2 \cdot k_1}{\rho_1 \cdot Cp_{r6,1} \cdot \left[(r_6 + D2)^2 - (r_6 - D2)^2\right]} \cdot \left[(T_{1,19} - T_{1,16}) \cdot \left(\frac{r_6 + D2}{\Delta_r}\right) - \left([T_{1,16} - T_{1,13}] \cdot \left[\frac{r_6 - D2}{\Delta_r}\right]\right)\right] + \frac{2}{\rho_1 \cdot Cp_{z1,1} \cdot \Delta_z} \cdot \left[\frac{k_1}{\Delta_z} \cdot (T_{1,17} - T_{1,16}) + h_{bottom} \cdot (Tf_{zb} - T_{1,16})\right] + X_{1,16} = 0$$

$$X_{1,16} = \frac{1}{\rho_1 \cdot Cp_{r6,1} \cdot \Delta_\theta} \cdot -\frac{k_1}{\Delta_\theta} \cdot \left[\frac{T_{1,16} - T_{2,16}}{r_6^{\,2}}\right]$$

17

$$\frac{2 \cdot k_1}{\rho_1 \cdot Cp_{r6,1} \cdot \left[(r_6 + D2)^2 - (r_6 - D2)^2\right]} \cdot \left[(T_{1,20} - T_{1,17}) \cdot \left(\frac{r_6 + D2}{\Delta_r}\right) - \left([T_{1,17} - T_{1,14}] \cdot \left[\frac{r_6 - D2}{\Delta_r}\right]\right)\right] + \frac{1}{\rho_1 \cdot Cp_{z2,1} \cdot \Delta_z} \cdot \left[\frac{k_1}{\Delta_z} \cdot (T_{1,18} - T_{1,17}) - \frac{k_1}{\Delta_z} \cdot (T_{1,17} - T_{1,16})\right] + X_{1,17} = 0$$

$$X_{1,17} = \frac{1}{\rho_1 \cdot Cp_{r6,1} \cdot \Delta_\theta} \cdot -\frac{k_1}{\Delta_\theta} \cdot \left[\frac{T_{1,17} - T_{2,17}}{r_6^{\,2}}\right]$$

18

$$\frac{2 \cdot k_1}{\rho_1 \cdot Cp_{r6,1} \cdot \left[(r_6 + D2)^2 - (r_6 - D2)^2\right]} \cdot \left[(T_{1,21} - T_{1,18}) \cdot \left(\frac{r_6 + D2}{\Delta_r}\right) - \left([T_{1,18} - T_{1,15}] \cdot \left[\frac{r_6 - D2}{\Delta_r}\right]\right)\right]$$

$$X_{1,18} = \frac{1}{\rho_1 \cdot Cp_{r6,1} \cdot \Delta_\theta} \cdot -\frac{k_1}{\Delta_\theta} \cdot \left[\frac{T_{1,18} - T_{2,18}}{r_6^{\,2}}\right]$$

19

$$\frac{2 \cdot k_1}{\rho_1 \cdot Cp_{r7,1} \cdot \left[(r_7 + D2)^2 - (r_7 - D2)^2\right]} \cdot \left[(T_{1,22} - T_{1,19}) \cdot \left(\frac{r_7 + D2}{\Delta_r}\right) - \left([T_{1,19} - T_{1,16}] \cdot \left[\frac{r_7 - D2}{\Delta_r}\right]\right)\right]$$
$$+ \frac{2}{\rho_1 \cdot Cp_{z1,1} \cdot \Delta_z} \cdot \left[\frac{k_1}{\Delta_z} \cdot (T_{1,20} - T_{1,19}) + h_{bottom} \cdot (Tf_{zb} - T_{1,19})\right] + X_{1,19} = 0$$

$$X_{1,19} = \frac{1}{\rho_1 \cdot Cp_{r7,1} \cdot \Delta_\theta} \cdot -\frac{k_1}{\Delta_\theta} \cdot \left[\frac{T_{1,19} - T_{2,19}}{r_7^{\,2}}\right]$$

20

$$\frac{2 \cdot k_1}{\rho_1 \cdot Cp_{r7,1} \cdot \left[(r_7 + D2)^2 - (r_7 - D2)^2\right]} \cdot \left[(T_{1,23} - T_{1,20}) \cdot \left(\frac{r_7 + D2}{\Delta_r}\right) - \left([T_{1,20} - T_{1,17}] \cdot \left[\frac{r_7 - D2}{\Delta_r}\right]\right)\right]$$
$$+ \frac{1}{\rho_1 \cdot Cp_{z2,1} \cdot \Delta_z} \cdot \left[\frac{k_1}{\Delta_z} \cdot (T_{1,21} - T_{1,20}) - \frac{k_1}{\Delta_z} \cdot (T_{1,20} - T_{1,19})\right] + X_{1,20} = 0$$

$$X_{1,20} = \frac{1}{\rho_1 \cdot Cp_{r7,1} \cdot \Delta_\theta} \cdot -\frac{k_1}{\Delta_\theta} \cdot \left[\frac{T_{1,20} - T_{2,20}}{r_7^{\,2}}\right]$$

21

$$\frac{2 \cdot k_1}{\rho_1 \cdot Cp_{r7,1} \cdot \left[(r_7 + D2)^2 - (r_7 - D2)^2\right]} \cdot \left[(T_{1,24} - T_{1,21}) \cdot \left(\frac{r_7 + D2}{\Delta_r}\right) - \left([T_{1,21} - T_{1,18}] \cdot \left[\frac{r_7 - D2}{\Delta_r}\right]\right)\right]$$
$$+ \frac{2}{\rho_1 \cdot Cp_{z3,1} \cdot \Delta_z} \cdot \left[\frac{k_1}{\Delta_z} \cdot (T_{1,20} - T_{1,21}) + h_{top} \cdot (Tf_{zt} - T_{1,21})\right] + X_{1,21} = 0$$

$$X_{1,21} = \frac{1}{\rho_1 \cdot Cp_{r7,1} \cdot \Delta_\theta} \cdot -\frac{k_1}{\Delta_\theta} \cdot \left[\frac{T_{1,21} - T_{2,21}}{r_7^{\,2}}\right]$$

22

$$\frac{2 \cdot k_1}{\rho_1 \cdot Cp_{r8,1} \cdot \left[(r_8 + D2)^2 - (r_8 - D2)^2\right]} \cdot \left[(T_{1,25} - T_{1,22}) \cdot \left(\frac{r_8 + D2}{\Delta_r}\right) - \left([T_{1,22} - T_{1,19}] \cdot \left[\frac{r_8 - D2}{\Delta_r}\right]\right)\right]$$
$$+ \frac{2}{\rho_1 \cdot Cp_{z1,1} \cdot \Delta_z} \cdot \left[\frac{k_1}{\Delta_z} \cdot (T_{1,23} - T_{1,22}) + h_{bottom} \cdot (Tf_{zb} - T_{1,22})\right] + X_{1,22} = 0$$

$$X_{1,22} = \frac{1}{\rho_1 \cdot Cp_{r8,1} \cdot \Delta_\theta} \cdot -\frac{k_1}{\Delta_\theta} \cdot \left[\frac{T_{1,22} - T_{2,22}}{r_8^{\,2}}\right]$$

23

$$\frac{2 \cdot k_1}{\rho_1 \cdot Cp_{r8,1} \cdot \left[(r_8 + D2)^2 - (r_8 - D2)^2\right]} \cdot \left[(T_{1,26} - T_{1,23}) \cdot \left(\frac{r_8 + D2}{\Delta_r}\right) - \left([T_{1,23} - T_{1,20}] \cdot \left[\frac{r_8 - D2}{\Delta_r}\right]\right)\right]$$
$$+ \frac{1}{\rho_1 \cdot Cp_{z2,1} \cdot \Delta_z} \cdot \left[\frac{k_1}{\Delta_z} \cdot (T_{1,24} - T_{1,23}) - \frac{k_1}{\Delta_z} \cdot (T_{1,23} - T_{1,22})\right] + X_{1,23} = 0$$

$$X_{1,23} = \frac{1}{\rho_1 \cdot Cp_{r6,1} \cdot \Delta_\theta} \cdot -\frac{k_1}{\Delta_\theta} \cdot \left[\frac{T_{1,23} - T_{2,23}}{r_8^{\,2}}\right]$$

24

$$\frac{2 \cdot k_1}{\rho_1 \cdot Cp_{r8,1} \cdot \left[(r_8 + D2)^2 - (r_8 - D2)^2\right]} \cdot \left[(T_{1,27} - T_{1,24}) \cdot \left(\frac{r_8 + D2}{\Delta_r}\right) - \left([T_{1,24} - T_{1,21}] \cdot \left[\frac{r_8 - D2}{\Delta_r}\right]\right)\right]$$
$$+ \frac{2}{\rho_1 \cdot Cp_{z3,1} \cdot \Delta_z} \cdot \left[\frac{k_1}{\Delta_z} \cdot (T_{1,23} - T_{1,24}) + h_{top} \cdot (Tf_{zt} - T_{1,24})\right] + X_{1,24} = 0$$

$$X_{1,24} = \frac{1}{\rho_1 \cdot Cp_{r8,1} \cdot \Delta_\theta} \cdot -\frac{k_1}{\Delta_\theta} \cdot \left[\frac{T_{1,24} - T_{2,24}}{r_8^{\,2}}\right]$$

25

$$+ \frac{2}{\rho_1 \cdot Cp_{z3,1} \cdot \Delta_z} \cdot \left[\frac{k_1}{\Delta_z} \cdot (T_{1,17} - T_{1,18}) + h_{top} \cdot (Tf_{zt} - T_{1,18})\right] + X_{1,18} = 0$$

$$\frac{2}{\rho_1 \cdot Cp_{r9,1} \cdot \left[(r_9 + D2)^2 - (r_9 - D2)^2\right]} \cdot \left[r_{out} \cdot h_{outside} \cdot (Tf_{ro} - T_{1,25}) + (r_9 - D2) \cdot k_1 \cdot \left(\frac{T_{1,22} - T_{1,25}}{\Delta_r}\right)\right] + \frac{2}{\rho_1 \cdot Cp_{z1,1} \cdot \Delta_z} \cdot \left[\frac{k_1}{\Delta_z} \cdot (T_{1,26} - T_{1,25}) + h_{bottom} \cdot (Tf_{zb} - T_{1,25})\right] + X_{1,25} = 0$$

$$X_{1,25} = \frac{1}{\rho_1 \cdot Cp_{r9,1} \cdot \Delta_\theta} \cdot -\frac{k_1}{\Delta_\theta} \cdot \left[\frac{T_{1,25} - T_{2,25}}{r_9^{\,2}}\right]$$

26

$$\frac{2}{\rho_1 \cdot Cp_{r9,1} \cdot \left[(r_9 + D2)^2 - (r_9 - D2)^2\right]} \cdot \left[r_{out} \cdot h_{outside} \cdot (Tf_{ro} - T_{1,26}) + (r_9 - D2) \cdot k_1 \cdot \left(\frac{T_{1,23} - T_{1,26}}{\Delta_r}\right)\right] + \frac{1}{\rho_1 \cdot Cp_{z2,1} \cdot \Delta_z} \cdot \left[\frac{k_1}{\Delta_z} \cdot (T_{1,27} - T_{1,26}) - \frac{k_1}{\Delta_z} \cdot (T_{1,26} - T_{1,25})\right] + X_{1,26} = 0$$

$$X_{1,26} = \frac{1}{\rho_1 \cdot Cp_{r9,1} \cdot \Delta_\theta} \cdot -\frac{k_1}{\Delta_\theta} \cdot \left[\frac{T_{1,26} - T_{2,26}}{r_9^{\,2}}\right]$$

27

$$\frac{2}{\rho_1 \cdot Cp_{r9,1} \cdot \left[(r_9 + D2)^2 - (r_9 - D2)^2\right]} \cdot \left[r_{out} \cdot h_{outside} \cdot (Tf_{ro} - T_{1,27}) + (r_9 - D2) \cdot k_1 \cdot \left(\frac{T_{1,24} - T_{1,27}}{\Delta_r}\right)\right] + \frac{2}{\rho_1 \cdot Cp_{z3,1} \cdot \Delta_z} \cdot \left[\frac{k_1}{\Delta_z} \cdot (T_{1,26} - T_{1,27}) + h_{top} \cdot (Tf_{zt} - T_{1,27})\right] + X_{1,27} = 0$$

$$X_{1,27} = \frac{1}{\rho_1 \cdot Cp_{r9,1} \cdot \Delta_\theta} \cdot -\frac{k_1}{\Delta_\theta} \cdot \left[\frac{T_{1,27} - T_{2,27}}{r_9^{\,2}}\right]$$

**********BLOCK 2**********

*****NODE*****

1

$$\frac{2}{\rho_2 \cdot Cp_{r1,2} \cdot \left[(r_1 + D2)^2 - (r_1 - D2)^2\right]} \cdot \left[r_{in} \cdot h_{inside} \cdot (Tf_{ri} - T_{2,1}) + (r_1 + D2) \cdot k_2 \cdot \left(\frac{T_{2,4} - T_{2,1}}{\Delta_r}\right)\right] + \frac{2}{\rho_2 \cdot Cp_{z1,2} \cdot \Delta_z} \cdot \left[\frac{k_2}{\Delta_z} \cdot (T_{2,2} - T_{2,1}) + h_{bottom} \cdot (Tf_{zb} - T_{2,1})\right] + X_{2,1} = 0$$

$$X_{2,1} = \frac{1}{\rho_2 \cdot Cp_{r1,2} \cdot \Delta_\theta} \cdot \left[\frac{k_2}{\Delta_\theta} \cdot \left(\frac{T_{1,1} - T_{2,1}}{r_1^{\,2}}\right) - \frac{k_2}{\Delta_\theta} \cdot \left(\frac{T_{2,1} - T_{3,1}}{r_1^{\,2}}\right)\right]$$

2

$$\frac{2}{\rho_2 \cdot Cp_{r1,2} \cdot \left[(r_1 + D2)^2 - (r_1 - D2)^2\right]} \cdot \left[r_{in} \cdot h_{inside} \cdot (Tf_{ri} - T_{2,2}) + (r_1 + D2) \cdot k_2 \cdot \left(\frac{T_{2,5} - T_{2,2}}{\Delta_r}\right)\right] + \frac{1}{\rho_2 \cdot Cp_{z2,2} \cdot \Delta_z} \cdot \left[\frac{k_2}{\Delta_z} \cdot (T_{2,3} - T_{2,2}) - \frac{k_2}{\Delta_z} \cdot (T_{2,2} - T_{2,1})\right] + X_{2,2} = 0$$

$$X_{2,2} = \frac{1}{\rho_2 \cdot Cp_{r1,2} \cdot \Delta_\theta} \cdot \left[\frac{k_2}{\Delta_\theta} \cdot \left(\frac{T_{1,2} - T_{2,2}}{r_1^{\,2}}\right) - \frac{k_2}{\Delta_\theta} \cdot \left(\frac{T_{2,2} - T_{3,2}}{r_1^{\,2}}\right)\right]$$

3

$$\frac{2}{\rho_2 \cdot Cp_{r1,2} \cdot \left[(r_1 + D2)^2 - (r_1 - D2)^2\right]} \cdot \left[r_{in} \cdot h_{inside} \cdot (Tf_{ri} - T_{2,3}) + (r_1 + D2) \cdot k_2 \cdot \left(\frac{T_{2,6} - T_{2,3}}{\Delta_r}\right)\right] + \frac{2}{\rho_2 \cdot Cp_{z3,2} \cdot \Delta_z} \cdot \left[\frac{k_2}{\Delta_z} \cdot (T_{2,2} - T_{2,3}) + h_{top} \cdot (Tf_{zt} - T_{2,3})\right] + X_{2,3} = 0$$

$$X_{2,3} = \frac{1}{\rho_2 \cdot Cp_{r1,2} \cdot \Delta_\theta} \cdot \left[\frac{k_2}{\Delta_\theta} \cdot \left(\frac{T_{1,3} - T_{2,3}}{r_1^{\,2}}\right) - \frac{k_2}{\Delta_\theta} \cdot \left(\frac{T_{2,3} - T_{3,3}}{r_1^{\,2}}\right)\right]$$

4

$$\frac{2 \cdot k_2}{\rho_2 \cdot Cp_{r2,2} \cdot \left[(r_2 + D2)^2 - (r_2 - D2)^2 \right]} \cdot \left[(T_{2,7} - T_{2,4}) \cdot \left(\frac{r_2 + D2}{\Delta_r} \right) - \left(\left[T_{2,4} - T_{2,1} \right] \cdot \left[\frac{r_2 - D2}{\Delta_r} \right] \right) \right] + \frac{2}{\rho_2 \cdot Cp_{z1,2} \cdot \Delta_z} \cdot \left[\frac{k_2}{\Delta_z} \cdot (T_{2,5} - T_{2,4}) + h_{bottom} \cdot (Tf_{zb} - T_{2,4}) \right] + X_{2,4} = 0$$

$$X_{2,4} = \frac{1}{\rho_2 \cdot Cp_{r2,2} \cdot \Delta_\theta} \cdot \left[\frac{k_2}{\Delta_\theta} \cdot \left(\frac{T_{1,4} - T_{2,4}}{r_2^2} \right) - \frac{k_2}{\Delta_\theta} \cdot \left(\frac{T_{2,4} - T_{3,4}}{r_2^2} \right) \right]$$

5

$$\frac{2 \cdot k_2}{\rho_2 \cdot Cp_{r2,2} \cdot \left[(r_2 + D2)^2 - (r_2 - D2)^2 \right]} \cdot \left[(T_{2,8} - T_{2,5}) \cdot \left(\frac{r_2 + D2}{\Delta_r} \right) - \left(\left[T_{2,5} - T_{2,2} \right] \cdot \left[\frac{r_2 - D2}{\Delta_r} \right] \right) \right] + \frac{1}{\rho_2 \cdot Cp_{z2,2} \cdot \Delta_z} \cdot \left[\frac{k_2}{\Delta_z} \cdot (T_{2,6} - T_{2,5}) - \frac{k_2}{\Delta_z} \cdot (T_{2,5} - T_{2,4}) \right] + X_{2,5} = 0$$

$$X_{2,5} = \frac{1}{\rho_2 \cdot Cp_{r2,2} \cdot \Delta_\theta} \cdot \left[\frac{k_2}{\Delta_\theta} \cdot \left(\frac{T_{1,5} - T_{2,5}}{r_2^2} \right) - \frac{k_2}{\Delta_\theta} \cdot \left(\frac{T_{2,5} - T_{3,5}}{r_2^2} \right) \right]$$

6

$$\frac{2 \cdot k_2}{\rho_2 \cdot Cp_{r2,2} \cdot \left[(r_2 + D2)^2 - (r_2 - D2)^2 \right]} \cdot \left[(T_{2,9} - T_{2,6}) \cdot \left(\frac{r_2 + D2}{\Delta_r} \right) - \left(\left[T_{2,6} - T_{2,3} \right] \cdot \left[\frac{r_2 - D2}{\Delta_r} \right] \right) \right] + \frac{2}{\rho_2 \cdot Cp_{z3,2} \cdot \Delta_z} \cdot \left[\frac{k_2}{\Delta_z} \cdot (T_{2,5} - T_{2,6}) + h_{top} \cdot (Tf_{zt} - T_{2,6}) \right] + X_{2,6} = 0$$

$$X_{2,6} = \frac{1}{\rho_2 \cdot Cp_{r2,2} \cdot \Delta_\theta} \cdot \left[\frac{k_2}{\Delta_\theta} \cdot \left(\frac{T_{1,6} - T_{2,6}}{r_2^2} \right) - \frac{k_2}{\Delta_\theta} \cdot \left(\frac{T_{2,6} - T_{3,6}}{r_2^2} \right) \right]$$

7

$$\frac{2 \cdot k_2}{\rho_2 \cdot Cp_{r3,2} \cdot \left[(r_3 + D2)^2 - (r_3 - D2)^2 \right]} \cdot \left[(T_{2,10} - T_{2,7}) \cdot \left(\frac{r_3 + D2}{\Delta_r} \right) - \left(\left[T_{2,7} - T_{2,4} \right] \cdot \left[\frac{r_3 - D2}{\Delta_r} \right] \right) \right] + \frac{2}{\rho_2 \cdot Cp_{z1,2} \cdot \Delta_z} \cdot \left[\frac{k_2}{\Delta_z} \cdot (T_{2,8} - T_{2,7}) + h_{bottom} \cdot (Tf_{zb} - T_{2,7}) \right] + X_{2,7} = 0$$

$$X_{2,7} = \frac{1}{\rho_2 \cdot Cp_{r3,2} \cdot \Delta_\theta} \cdot \left[\frac{k_2}{\Delta_\theta} \cdot \left(\frac{T_{1,7} - T_{2,7}}{r_3^2} \right) - \frac{k_2}{\Delta_\theta} \cdot \left(\frac{T_{2,7} - T_{3,7}}{r_3^2} \right) \right]$$

8

$$\frac{2 \cdot k_2}{\rho_2 \cdot Cp_{r3,2} \cdot \left[(r_3 + D2)^2 - (r_3 - D2)^2 \right]} \cdot \left[(T_{2,11} - T_{2,8}) \cdot \left(\frac{r_3 + D2}{\Delta_r} \right) - \left(\left[T_{2,8} - T_{2,5} \right] \cdot \left[\frac{r_3 - D2}{\Delta_r} \right] \right) \right] + \frac{1}{\rho_2 \cdot Cp_{z2,2} \cdot \Delta_z} \cdot \left[\frac{k_2}{\Delta_z} \cdot (T_{2,9} - T_{2,8}) - \frac{k_2}{\Delta_z} \cdot (T_{2,8} - T_{2,7}) \right] + X_{2,8} = 0$$

$$X_{2,8} = \frac{1}{\rho_2 \cdot Cp_{r3,2} \cdot \Delta_\theta} \cdot \left[\frac{k_2}{\Delta_\theta} \cdot \left(\frac{T_{1,8} - T_{2,8}}{r_3^2} \right) - \frac{k_2}{\Delta_\theta} \cdot \left(\frac{T_{2,8} - T_{3,8}}{r_3^2} \right) \right]$$

9

$$\frac{2 \cdot k_2}{\rho_2 \cdot Cp_{r3,2} \cdot \left[(r_3 + D2)^2 - (r_3 - D2)^2 \right]} \cdot \left[(T_{2,12} - T_{2,9}) \cdot \left(\frac{r_3 + D2}{\Delta_r} \right) - \left(\left[T_{2,9} - T_{2,6} \right] \cdot \left[\frac{r_3 - D2}{\Delta_r} \right] \right) \right] + \frac{2}{\rho_2 \cdot Cp_{z3,2} \cdot \Delta_z} \cdot \left[\frac{k_2}{\Delta_z} \cdot (T_{2,8} - T_{2,9}) + h_{top} \cdot (Tf_{zt} - T_{2,9}) \right] + X_{2,9} = 0$$

$$X_{2,9} = \frac{1}{\rho_2 \cdot Cp_{r3,2} \cdot \Delta_\theta} \cdot \left[\frac{k_2}{\Delta_\theta} \cdot \left(\frac{T_{1,9} - T_{2,9}}{r_3^2} \right) - \frac{k_2}{\Delta_\theta} \cdot \left(\frac{T_{2,9} - T_{3,9}}{r_3^2} \right) \right]$$

10

$$\frac{2 \cdot k_2}{\rho_2 \cdot Cp_{r4,2} \cdot \left[(r_4 + D2)^2 - (r_4 - D2)^2 \right]} \cdot \left[(T_{2,13} - T_{2,10}) \cdot \left(\frac{r_4 + D2}{\Delta_r} \right) - \left(\left[T_{2,10} - T_{2,7} \right] \cdot \left[\frac{r_4 - D2}{\Delta_r} \right] \right) \right] + \frac{2}{\rho_2 \cdot Cp_{z1,2} \cdot \Delta_z} \cdot \left[\frac{k_2}{\Delta_z} \cdot (T_{2,11} - T_{2,10}) + h_{bottom} \cdot (Tf_{zb} - T_{2,10}) \right] + X_{2,10} = 0$$

$$X_{2,10} = \frac{1}{\rho_2 \cdot Cp_{r4,2} \cdot \Delta_\theta} \cdot \left[\frac{k_2}{\Delta_\theta} \cdot \left(\frac{T_{1,10} - T_{2,10}}{r_4^2} \right) - \frac{k_2}{\Delta_\theta} \cdot \left(\frac{T_{2,10} - T_{3,10}}{r_4^2} \right) \right]$$

11

$$\frac{2 \cdot k_2}{\rho_2 \cdot Cp_{r4,2} \cdot \left[(r_4 + D2)^2 - (r_4 - D2)^2 \right]} \cdot \left[(T_{2,14} - T_{2,11}) \cdot \left(\frac{r_4 + D2}{\Delta_r} \right) - \left([T_{2,11} - T_{2,8}] \cdot \left[\frac{r_4 - D2}{\Delta_r} \right] \right) \right] + \frac{1}{\rho_2 \cdot Cp_{z2,2} \cdot \Delta_z} \cdot \left[\frac{k_2}{\Delta_z} \cdot (T_{2,12} - T_{2,11}) - \frac{k_2}{\Delta_z} \cdot (T_{2,11} - T_{2,10}) \right] + X_{2,11} = 0$$

$$X_{2,11} = \frac{1}{\rho_2 \cdot Cp_{r4,2} \cdot \Delta_\theta} \cdot \left[\frac{k_2}{\Delta_\theta} \cdot \left(\frac{T_{1,11} - T_{2,11}}{r_4^2} \right) - \frac{k_2}{\Delta_\theta} \cdot \left(\frac{T_{2,11} - T_{3,11}}{r_4^2} \right) \right]$$

12

$$\frac{2 \cdot k_2}{\rho_2 \cdot Cp_{r4,2} \cdot \left[(r_4 + D2)^2 - (r_4 - D2)^2 \right]} \cdot \left[(T_{2,15} - T_{2,12}) \cdot \left(\frac{r_4 + D2}{\Delta_r} \right) - \left([T_{2,12} - T_{2,9}] \cdot \left[\frac{r_4 - D2}{\Delta_r} \right] \right) \right] + \frac{2}{\rho_2 \cdot Cp_{z3,2} \cdot \Delta_z} \cdot \left[\frac{k_2}{\Delta_z} \cdot (T_{2,11} - T_{2,12}) + h_{top} \cdot (Tf_{zt} - T_{2,12}) \right] + X_{2,12} = 0$$

$$X_{2,12} = \frac{1}{\rho_2 \cdot Cp_{r4,2} \cdot \Delta_\theta} \cdot \left[\frac{k_2}{\Delta_\theta} \cdot \left(\frac{T_{1,12} - T_{2,12}}{r_4^2} \right) - \frac{k_2}{\Delta_\theta} \cdot \left(\frac{T_{2,12} - T_{3,12}}{r_4^2} \right) \right]$$

13

$$\frac{2 \cdot k_2}{\rho_2 \cdot Cp_{r5,2} \cdot \left[(r_5 + D2)^2 - (r_5 - D2)^2 \right]} \cdot \left[(T_{2,16} - T_{2,13}) \cdot \left(\frac{r_5 + D2}{\Delta_r} \right) - \left([T_{2,13} - T_{2,10}] \cdot \left[\frac{r_5 - D2}{\Delta_r} \right] \right) \right] + \frac{2}{\rho_2 \cdot Cp_{z1,2} \cdot \Delta_z} \cdot \left[\frac{k_2}{\Delta_z} \cdot (T_{2,14} - T_{2,13}) + h_{bottom} \cdot (Tf_{zb} - T_{2,13}) \right] + X_{2,13} = 0$$

$$X_{2,13} = \frac{1}{\rho_2 \cdot Cp_{r5,2} \cdot \Delta_\theta} \cdot \left[\frac{k_2}{\Delta_\theta} \cdot \left(\frac{T_{1,13} - T_{2,13}}{r_5^2} \right) - \frac{k_2}{\Delta_\theta} \cdot \left(\frac{T_{2,13} - T_{3,13}}{r_5^2} \right) \right]$$

14

$$\frac{2 \cdot k_2}{\rho_2 \cdot Cp_{r5,2} \cdot \left[(r_5 + D2)^2 - (r_5 - D2)^2 \right]} \cdot \left[(T_{2,17} - T_{2,14}) \cdot \left(\frac{r_5 + D2}{\Delta_r} \right) - \left([T_{2,14} - T_{2,11}] \cdot \left[\frac{r_5 - D2}{\Delta_r} \right] \right) \right] + \frac{1}{\rho_2 \cdot Cp_{z2,2} \cdot \Delta_z} \cdot \left[\frac{k_2}{\Delta_z} \cdot (T_{2,15} - T_{2,14}) - \frac{k_2}{\Delta_z} \cdot (T_{2,14} - T_{2,13}) \right] + X_{2,14} = 0$$

$$X_{2,14} = \frac{1}{\rho_2 \cdot Cp_{r5,2} \cdot \Delta_\theta} \cdot \left[\frac{k_2}{\Delta_\theta} \cdot \left(\frac{T_{1,14} - T_{2,14}}{r_5^2} \right) - \frac{k_2}{\Delta_\theta} \cdot \left(\frac{T_{2,14} - T_{3,14}}{r_5^2} \right) \right]$$

15

$$\frac{2 \cdot k_2}{\rho_2 \cdot Cp_{r5,2} \cdot \left[(r_5 + D2)^2 - (r_5 - D2)^2 \right]} \cdot \left[(T_{2,18} - T_{2,15}) \cdot \left(\frac{r_5 + D2}{\Delta_r} \right) - \left([T_{2,15} - T_{2,12}] \cdot \left[\frac{r_5 - D2}{\Delta_r} \right] \right) \right] + \frac{2}{\rho_2 \cdot Cp_{z3,2} \cdot \Delta_z} \cdot \left[\frac{k_2}{\Delta_z} \cdot (T_{2,14} - T_{2,15}) + h_{top} \cdot (Tf_{zt} - T_{2,15}) \right] + X_{2,15} = 0$$

$$X_{2,15} = \frac{1}{\rho_2 \cdot Cp_{r5,2} \cdot \Delta_\theta} \cdot \left[\frac{k_2}{\Delta_\theta} \cdot \left(\frac{T_{1,15} - T_{2,15}}{r_5^2} \right) - \frac{k_2}{\Delta_\theta} \cdot \left(\frac{T_{2,15} - T_{3,15}}{r_5^2} \right) \right]$$

16

$$\frac{2 \cdot k_2}{\rho_2 \cdot Cp_{r6,2} \cdot \left[(r_6 + D2)^2 - (r_6 - D2)^2 \right]} \cdot \left[(T_{2,19} - T_{2,16}) \cdot \left(\frac{r_6 + D2}{\Delta_r} \right) - \left([T_{2,16} - T_{2,13}] \cdot \left[\frac{r_6 - D2}{\Delta_r} \right] \right) \right] + \frac{2}{\rho_2 \cdot Cp_{z1,2} \cdot \Delta_z} \cdot \left[\frac{k_2}{\Delta_z} \cdot (T_{2,17} - T_{2,16}) + h_{bottom} \cdot (Tf_{zb} - T_{2,16}) \right] + X_{2,16} = 0$$

$$X_{2,16} = \frac{1}{\rho_2 \cdot Cp_{r6,2} \cdot \Delta_\theta} \cdot \left[\frac{k_2}{\Delta_\theta} \cdot \left(\frac{T_{1,16} - T_{2,16}}{r_6^2} \right) - \frac{k_2}{\Delta_\theta} \cdot \left(\frac{T_{2,16} - T_{3,16}}{r_6^2} \right) \right]$$

17

$$\frac{2 \cdot k_2}{\rho_2 \cdot Cp_{r6,2} \cdot \left[(r_6 + D2)^2 - (r_6 - D2)^2 \right]} \cdot \left[(T_{2,20} - T_{2,17}) \cdot \left(\frac{r_6 + D2}{\Delta_r} \right) - \left([T_{2,17} - T_{2,14}] \cdot \left[\frac{r_6 - D2}{\Delta_r} \right] \right) \right] + \frac{1}{\rho_2 \cdot Cp_{z2,2} \cdot \Delta_z} \cdot \left[\frac{k_2}{\Delta_z} \cdot (T_{2,18} - T_{2,17}) - \frac{k_2}{\Delta_z} \cdot (T_{2,17} - T_{2,16}) \right] + X_{2,17} = 0$$

$$X_{2,17} = \frac{1}{\rho_2 \cdot Cp_{r6,2} \cdot \Delta_\theta} \cdot \left[\frac{k_2}{\Delta_\theta} \cdot \left(\frac{T_{1,17} - T_{2,17}}{r_6^{\,2}} \right) - \frac{k_2}{\Delta_\theta} \cdot \left(\frac{T_{2,17} - T_{3,17}}{r_6^{\,2}} \right) \right]$$

18

$$\frac{2 \cdot k_2}{\rho_2 \cdot Cp_{r6,2} \cdot \left[(r_6 + D2)^2 - (r_6 - D2)^2 \right]} \cdot \left[(T_{2,21} - T_{2,18}) \cdot \left(\frac{r_6 + D2}{\Delta_r} \right) - \left([T_{2,18} - T_{2,15}] \cdot \left[\frac{r_6 - D2}{\Delta_r} \right] \right) \right] + \frac{2}{\rho_2 \cdot Cp_{z3,2} \cdot \Delta_z} \cdot \left[\frac{k_2}{\Delta_z} \cdot (T_{2,17} - T_{2,18}) + h_{top} \cdot (Tf_{zt} - T_{2,18}) \right] + X_{2,18} = 0$$

$$X_{2,18} = \frac{1}{\rho_2 \cdot Cp_{r6,2} \cdot \Delta_\theta} \cdot \left[\frac{k_2}{\Delta_\theta} \cdot \left(\frac{T_{1,18} - T_{2,18}}{r_6^{\,2}} \right) - \frac{k_2}{\Delta_\theta} \cdot \left(\frac{T_{2,18} - T_{3,18}}{r_6^{\,2}} \right) \right]$$

19

$$\frac{2 \cdot k_2}{\rho_2 \cdot Cp_{r7,2} \cdot \left[(r_7 + D2)^2 - (r_7 - D2)^2 \right]} \cdot \left[(T_{2,22} - T_{2,19}) \cdot \left(\frac{r_7 + D2}{\Delta_r} \right) - \left([T_{2,19} - T_{2,16}] \cdot \left[\frac{r_7 - D2}{\Delta_r} \right] \right) \right] + \frac{2}{\rho_2 \cdot Cp_{z1,2} \cdot \Delta_z} \cdot \left[\frac{k_2}{\Delta_z} \cdot (T_{2,20} - T_{2,19}) + h_{bottom} \cdot (Tf_{zb} - T_{2,19}) \right] + X_{2,19} = 0$$

$$X_{2,19} = \frac{1}{\rho_2 \cdot Cp_{r7,2} \cdot \Delta_\theta} \cdot \left[\frac{k_2}{\Delta_\theta} \cdot \left(\frac{T_{1,19} - T_{2,19}}{r_7^{\,2}} \right) - \frac{k_2}{\Delta_\theta} \cdot \left(\frac{T_{2,19} - T_{3,19}}{r_7^{\,2}} \right) \right]$$

20

$$\frac{2 \cdot k_2}{\rho_2 \cdot Cp_{r7,2} \cdot \left[(r_7 + D2)^2 - (r_7 - D2)^2 \right]} \cdot \left[(T_{2,23} - T_{2,20}) \cdot \left(\frac{r_7 + D2}{\Delta_r} \right) - \left([T_{2,20} - T_{2,17}] \cdot \left[\frac{r_7 - D2}{\Delta_r} \right] \right) \right] + \frac{1}{\rho_2 \cdot Cp_{z2,2} \cdot \Delta_z} \cdot \left[\frac{k_2}{\Delta_z} \cdot (T_{2,21} - T_{2,20}) - \frac{k_2}{\Delta_z} \cdot (T_{2,20} - T_{2,19}) \right] + X_{2,20} = 0$$

$$X_{2,20} = \frac{1}{\rho_2 \cdot Cp_{r7,2} \cdot \Delta_\theta} \cdot \left[\frac{k_2}{\Delta_\theta} \cdot \left(\frac{T_{1,20} - T_{2,20}}{r_7^{\,2}} \right) - \frac{k_2}{\Delta_\theta} \cdot \left(\frac{T_{2,20} - T_{3,20}}{r_7^{\,2}} \right) \right]$$

21

$$\frac{2 \cdot k_2}{\rho_2 \cdot Cp_{r7,2} \cdot \left[(r_7 + D2)^2 - (r_7 - D2)^2 \right]} \cdot \left[(T_{2,24} - T_{2,21}) \cdot \left(\frac{r_7 + D2}{\Delta_r} \right) - \left([T_{2,21} - T_{2,18}] \cdot \left[\frac{r_7 - D2}{\Delta_r} \right] \right) \right] + \frac{2}{\rho_2 \cdot Cp_{z3,2} \cdot \Delta_z} \cdot \left[\frac{k_2}{\Delta_z} \cdot (T_{2,20} - T_{2,21}) + h_{top} \cdot (Tf_{zt} - T_{2,21}) \right] + X_{2,21} = 0$$

$$X_{2,21} = \frac{1}{\rho_2 \cdot Cp_{r7,2} \cdot \Delta_\theta} \cdot \left[\frac{k_2}{\Delta_\theta} \cdot \left(\frac{T_{1,21} - T_{2,21}}{r_7^{\,2}} \right) - \frac{k_2}{\Delta_\theta} \cdot \left(\frac{T_{2,21} - T_{3,21}}{r_7^{\,2}} \right) \right]$$

22

$$\frac{2 \cdot k_2}{\rho_2 \cdot Cp_{r8,2} \cdot \left[(r_8 + D2)^2 - (r_8 - D2)^2 \right]} \cdot \left[(T_{2,25} - T_{2,22}) \cdot \left(\frac{r_8 + D2}{\Delta_r} \right) - \left([T_{2,22} - T_{2,19}] \cdot \left[\frac{r_8 - D2}{\Delta_r} \right] \right) \right] + \frac{2}{\rho_2 \cdot Cp_{z1,2} \cdot \Delta_z} \cdot \left[\frac{k_2}{\Delta_z} \cdot (T_{2,23} - T_{2,22}) + h_{bottom} \cdot (Tf_{zb} - T_{2,22}) \right] + X_{2,22} = 0$$

$$X_{2,22} = \frac{1}{\rho_2 \cdot Cp_{r8,2} \cdot \Delta_\theta} \cdot \left[\frac{k_2}{\Delta_\theta} \cdot \left(\frac{T_{1,22} - T_{2,22}}{r_8^{\,2}} \right) - \frac{k_2}{\Delta_\theta} \cdot \left(\frac{T_{2,22} - T_{3,22}}{r_8^{\,2}} \right) \right]$$

23

$$\frac{2 \cdot k_2}{\rho_2 \cdot Cp_{r8,2} \cdot \left[(r_8 + D2)^2 - (r_8 - D2)^2 \right]} \cdot \left[(T_{2,26} - T_{2,23}) \cdot \left(\frac{r_8 + D2}{\Delta_r} \right) - \left([T_{2,23} - T_{2,20}] \cdot \left[\frac{r_8 - D2}{\Delta_r} \right] \right) \right] + \frac{1}{\rho_2 \cdot Cp_{z2,2} \cdot \Delta_z} \cdot \left[\frac{k_2}{\Delta_z} \cdot (T_{2,24} - T_{2,23}) - \frac{k_2}{\Delta_z} \cdot (T_{2,23} - T_{2,22}) \right] + X_{2,23} = 0$$

$$X_{2,23} = \frac{1}{\rho_2 \cdot Cp_{r8,2} \cdot \Delta_\theta} \cdot \left[\frac{k_2}{\Delta_\theta} \cdot \left(\frac{T_{1,23} - T_{2,23}}{r_8^{\,2}} \right) - \frac{k_2}{\Delta_\theta} \cdot \left(\frac{T_{2,23} - T_{3,23}}{r_8^{\,2}} \right) \right]$$

24

$$\frac{2 \cdot k_2}{\rho_2 \cdot Cp_{r8,2} \cdot \left[(r_8 + D2)^2 - (r_8 - D2)^2 \right]} \cdot \left[(T_{2,27} - T_{2,24}) \cdot \left(\frac{r_8 + D2}{\Delta_r} \right) - \left(\left[T_{2,24} - T_{2,21} \right] \cdot \left[\frac{r_8 - D2}{\Delta_r} \right] \right) \right]$$
$$+ \frac{2}{\rho_2 \cdot Cp_{z3,2} \cdot \Delta_z} \cdot \left[\frac{k_2}{\Delta_z} \cdot (T_{2,23} - T_{2,24}) + h_{top} \cdot (Tf_{zt} - T_{2,24}) \right] + X_{2,24} = 0$$

$$X_{2,24} = \frac{1}{\rho_2 \cdot Cp_{r8,2} \cdot \Delta_\theta} \cdot \left[\frac{k_2}{\Delta_\theta} \cdot \left(\frac{T_{1,24} - T_{2,24}}{r_8^2} \right) - \frac{k_2}{\Delta_\theta} \cdot \left(\frac{T_{2,24} - T_{3,24}}{r_8^2} \right) \right]$$

25

$$\frac{2}{\rho_2 \cdot Cp_{r9,2} \cdot \left[(r_9 + D2)^2 - (r_9 - D2)^2 \right]} \cdot \left[r_{out} \cdot h_{outside} \cdot (Tf_{ro} - T_{2,25}) + (r_9 - D2) \cdot k_2 \cdot \left(\frac{T_{2,22} - T_{2,25}}{\Delta_r} \right) \right]$$
$$+ \frac{2}{\rho_2 \cdot Cp_{z1,2} \cdot \Delta_z} \cdot \left[\frac{k_2}{\Delta_z} \cdot (T_{2,26} - T_{2,25}) + h_{bottom} \cdot (Tf_{zb} - T_{2,25}) \right] + X_{2,25} = 0$$

$$X_{2,25} = \frac{1}{\rho_2 \cdot Cp_{r9,2} \cdot \Delta_\theta} \cdot \left[\frac{k_2}{\Delta_\theta} \cdot \left(\frac{T_{1,25} - T_{2,25}}{r_9^2} \right) - \frac{k_2}{\Delta_\theta} \cdot \left(\frac{T_{2,25} - T_{3,25}}{r_9^2} \right) \right]$$

26

$$\frac{2}{\rho_2 \cdot Cp_{r9,2} \cdot \left[(r_9 + D2)^2 - (r_9 - D2)^2 \right]} \cdot \left[r_{out} \cdot h_{outside} \cdot (Tf_{ro} - T_{2,26}) + (r_9 - D2) \cdot k_2 \cdot \left(\frac{T_{2,23} - T_{2,26}}{\Delta_r} \right) \right]$$
$$+ \frac{1}{\rho_2 \cdot Cp_{z2,2} \cdot \Delta_z} \cdot \left[\frac{k_2}{\Delta_z} \cdot (T_{2,27} - T_{2,26}) - \frac{k_2}{\Delta_z} \cdot (T_{2,26} - T_{2,25}) \right] + X_{2,26} = 0$$

$$X_{2,26} = \frac{1}{\rho_2 \cdot Cp_{r9,2} \cdot \Delta_\theta} \cdot \left[\frac{k_2}{\Delta_\theta} \cdot \left(\frac{T_{1,26} - T_{2,26}}{r_9^2} \right) - \frac{k_2}{\Delta_\theta} \cdot \left(\frac{T_{2,26} - T_{3,26}}{r_9^2} \right) \right]$$

27

$$\frac{2}{\rho_2 \cdot Cp_{r9,2} \cdot \left[(r_9 + D2)^2 - (r_9 - D2)^2 \right]} \cdot \left[r_{out} \cdot h_{outside} \cdot (Tf_{ro} - T_{2,27}) + (r_9 - D2) \cdot k_2 \cdot \left(\frac{T_{2,24} - T_{2,27}}{\Delta_r} \right) \right]$$
$$+ \frac{2}{\rho_2 \cdot Cp_{z3,2} \cdot \Delta_z} \cdot \left[\frac{k_2}{\Delta_z} \cdot (T_{2,26} - T_{2,27}) + h_{top} \cdot (Tf_{zt} - T_{2,27}) \right] + X_{2,27} = 0$$

$$X_{2,27} = \frac{1}{\rho_2 \cdot Cp_{r9,2} \cdot \Delta_\theta} \cdot \left[\frac{k_2}{\Delta_\theta} \cdot \left(\frac{T_{1,27} - T_{2,27}}{r_9^2} \right) - \frac{k_2}{\Delta_\theta} \cdot \left(\frac{T_{2,27} - T_{3,27}}{r_9^2} \right) \right]$$

**********BLOCK 3**********

*****NODE*****

1

$$\frac{2}{\rho_3 \cdot Cp_{r1,3} \cdot \left[(r_1 + D2)^2 - (r_1 - D2)^2 \right]} \cdot \left[r_{out} \cdot h_{inside} \cdot (Tf_{ri} - T_{3,1}) + (r_1 + D2) \cdot k_3 \cdot \left(\frac{T_{3,4} - T_{3,1}}{\Delta_r} \right) \right]$$
$$+ \frac{2}{\rho_3 \cdot Cp_{z1,3} \cdot \Delta_z} \cdot \left[\frac{k_3}{\Delta_z} \cdot (T_{3,2} - T_{3,1}) + h_{bottom} \cdot (Tf_{zb} - T_{3,1}) \right] + X_{3,1} = 0$$

$$X_{3,1} = \frac{1}{\rho_3 \cdot Cp_{r1,3} \cdot \Delta_\theta} \cdot \left[\frac{k_3}{\Delta_\theta} \cdot \left(\frac{T_{2,1} - T_{3,1}}{r_1^2} \right) - \frac{k_3}{\Delta_\theta} \cdot \left(\frac{T_{3,1} - T_{4,1}}{r_1^2} \right) \right]$$

2

$$\frac{2}{\rho_3 \cdot Cp_{r1,3} \cdot \left[(r_1 + D2)^2 - (r_1 - D2)^2 \right]} \cdot \left[r_{out} \cdot h_{inside} \cdot (Tf_{ri} - T_{3,2}) + (r_1 + D2) \cdot k_3 \cdot \left(\frac{T_{3,5} - T_{3,2}}{\Delta_r} \right) \right]$$
$$+ \frac{1}{\rho_3 \cdot Cp_{z2,3} \cdot \Delta_z} \cdot \left[\frac{k_3}{\Delta_z} \cdot (T_{3,3} - T_{3,2}) - \frac{k_3}{\Delta_z} \cdot (T_{3,2} - T_{3,1}) \right] + X_{3,2} = 0$$

$$X_{3,2} = \frac{1}{\rho_3 \cdot Cp_{r1,3} \cdot \Delta_\theta} \cdot \left[\frac{k_3}{\Delta_\theta} \cdot \left(\frac{T_{2,2} - T_{3,2}}{r_1^2} \right) - \frac{k_3}{\Delta_\theta} \cdot \left(\frac{T_{3,2} - T_{4,2}}{r_1^2} \right) \right]$$

3

$$\frac{2}{\rho_3 \cdot Cp_{r1,3} \cdot \left[(r_1 + D2)^2 - (r_1 - D2)^2 \right]} \cdot \left[r_{out} \cdot h_{inside} \cdot (Tf_{ri} - T_{3,3}) + (r_1 + D2) \cdot k_3 \cdot \left(\frac{T_{3,6} - T_{3,3}}{\Delta_r} \right) \right]$$

$$X_{3,3} = \frac{1}{\rho_3 \cdot Cp_{r1,3} \cdot \Delta_\theta} \cdot \left[\frac{k_3}{\Delta_\theta} \cdot \left(\frac{T_{2,3} - T_{3,3}}{r_1^{\,2}} \right) - \frac{k_3}{\Delta_\theta} \cdot \left(\frac{T_{3,3} - T_{4,3}}{r_1^{\,2}} \right) \right]$$

4

$$\frac{2 \cdot k_3}{\rho_3 \cdot Cp_{r2,3} \cdot \left[(r_2 + D2)^2 - (r_2 - D2)^2 \right]} \cdot \left[(T_{3,7} - T_{3,4}) \cdot \left(\frac{r_2 + D2}{\Delta_r} \right) - \left(\left[T_{3,4} - T_{3,1} \right] \cdot \left[\frac{r_2 - D2}{\Delta_r} \right] \right) \right] + \frac{2}{\rho_3 \cdot Cp_{z1,3} \cdot \Delta_z} \cdot \left[\frac{k_3}{\Delta_z} \cdot (T_{3,5} - T_{3,4}) + h_{bottom} \cdot (Tf_{zb} - T_{3,4}) \right] + X_{3,4} = 0$$

$$X_{3,4} = \frac{1}{\rho_3 \cdot Cp_{r2,3} \cdot \Delta_\theta} \cdot \left[\frac{k_3}{\Delta_\theta} \cdot \left(\frac{T_{2,4} - T_{3,4}}{r_2^{\,2}} \right) - \frac{k_3}{\Delta_\theta} \cdot \left(\frac{T_{3,4} - T_{4,4}}{r_2^{\,2}} \right) \right]$$

5

$$\frac{2 \cdot k_3}{\rho_3 \cdot Cp_{r2,3} \cdot \left[(r_2 + D2)^2 - (r_2 - D2)^2 \right]} \cdot \left[(T_{3,8} - T_{3,5}) \cdot \left(\frac{r_2 + D2}{\Delta_r} \right) - \left(\left[T_{3,5} - T_{3,2} \right] \cdot \left[\frac{r_2 - D2}{\Delta_r} \right] \right) \right] + \frac{1}{\rho_3 \cdot Cp_{z2,3} \cdot \Delta_z} \cdot \left[\frac{k_3}{\Delta_z} \cdot (T_{3,6} - T_{3,5}) - \frac{k_3}{\Delta_z} \cdot (T_{3,5} - T_{3,4}) \right] + X_{3,5} = 0$$

$$X_{3,5} = \frac{1}{\rho_3 \cdot Cp_{r2,3} \cdot \Delta_\theta} \cdot \left[\frac{k_3}{\Delta_\theta} \cdot \left(\frac{T_{2,5} - T_{3,5}}{r_2^{\,2}} \right) - \frac{k_3}{\Delta_\theta} \cdot \left(\frac{T_{3,5} - T_{4,5}}{r_2^{\,2}} \right) \right]$$

6

$$\frac{2 \cdot k_3}{\rho_3 \cdot Cp_{r2,3} \cdot \left[(r_2 + D2)^2 - (r_2 - D2)^2 \right]} \cdot \left[(T_{3,9} - T_{3,6}) \cdot \left(\frac{r_2 + D2}{\Delta_r} \right) - \left(\left[T_{3,6} - T_{3,3} \right] \cdot \left[\frac{r_2 - D2}{\Delta_r} \right] \right) \right] + \frac{2}{\rho_3 \cdot Cp_{z3,3} \cdot \Delta_z} \cdot \left[\frac{k_3}{\Delta_z} \cdot (T_{3,5} - T_{3,6}) + h_{top} \cdot (Tf_{zt} - T_{3,6}) \right] + X_{3,6} = 0$$

$$X_{3,6} = \frac{1}{\rho_3 \cdot Cp_{r2,3} \cdot \Delta_\theta} \cdot \left[\frac{k_3}{\Delta_\theta} \cdot \left(\frac{T_{2,6} - T_{3,6}}{r_2^{\,2}} \right) - \frac{k_3}{\Delta_\theta} \cdot \left(\frac{T_{3,6} - T_{4,6}}{r_2^{\,2}} \right) \right]$$

7

$$\frac{2 \cdot k_3}{\rho_3 \cdot Cp_{r3,3} \cdot \left[(r_3 + D2)^2 - (r_3 - D2)^2 \right]} \cdot \left[(T_{3,10} - T_{3,7}) \cdot \left(\frac{r_3 + D2}{\Delta_r} \right) - \left(\left[T_{3,7} - T_{3,4} \right] \cdot \left[\frac{r_3 - D2}{\Delta_r} \right] \right) \right] + \frac{2}{\rho_3 \cdot Cp_{z1,3} \cdot \Delta_z} \cdot \left[\frac{k_3}{\Delta_z} \cdot (T_{3,8} - T_{3,7}) + h_{bottom} \cdot (Tf_{zb} - T_{3,7}) \right] + X_{3,7} = 0$$

$$X_{3,7} = \frac{1}{\rho_3 \cdot Cp_{r3,3} \cdot \Delta_\theta} \cdot \left[\frac{k_3}{\Delta_\theta} \cdot \left(\frac{T_{2,7} - T_{3,7}}{r_3^{\,2}} \right) - \frac{k_3}{\Delta_\theta} \cdot \left(\frac{T_{3,7} - T_{4,7}}{r_3^{\,2}} \right) \right]$$

8

$$\frac{2 \cdot k_3}{\rho_3 \cdot Cp_{r3,3} \cdot \left[(r_3 + D2)^2 - (r_3 - D2)^2 \right]} \cdot \left[(T_{3,11} - T_{3,8}) \cdot \left(\frac{r_3 + D2}{\Delta_r} \right) - \left(\left[T_{3,8} - T_{3,5} \right] \cdot \left[\frac{r_3 - D2}{\Delta_r} \right] \right) \right] + \frac{1}{\rho_3 \cdot Cp_{z2,3} \cdot \Delta_z} \cdot \left[\frac{k_3}{\Delta_z} \cdot (T_{3,9} - T_{3,8}) - \frac{k_3}{\Delta_z} \cdot (T_{3,8} - T_{3,7}) \right] + X_{3,8} = 0$$

$$X_{3,8} = \frac{1}{\rho_3 \cdot Cp_{r3,3} \cdot \Delta_\theta} \cdot \left[\frac{k_3}{\Delta_\theta} \cdot \left(\frac{T_{2,8} - T_{3,8}}{r_3^{\,2}} \right) - \frac{k_3}{\Delta_\theta} \cdot \left(\frac{T_{3,8} - T_{4,8}}{r_3^{\,2}} \right) \right]$$

9

$$\frac{2 \cdot k_3}{\rho_3 \cdot Cp_{r3,3} \cdot \left[(r_3 + D2)^2 - (r_3 - D2)^2 \right]} \cdot \left[(T_{3,12} - T_{3,9}) \cdot \left(\frac{r_3 + D2}{\Delta_r} \right) - \left(\left[T_{3,9} - T_{3,6} \right] \cdot \left[\frac{r_3 - D2}{\Delta_r} \right] \right) \right] + \frac{2}{\rho_3 \cdot Cp_{z3,3} \cdot \Delta_z} \cdot \left[\frac{k_3}{\Delta_z} \cdot (T_{3,6} - T_{3,9}) + h_{top} \cdot (Tf_{zt} - T_{3,9}) \right] + X_{3,9} = 0$$

$$X_{3,9} = \frac{1}{\rho_3 \cdot Cp_{r3,3} \cdot \Delta_\theta} \cdot \left[\frac{k_3}{\Delta_\theta} \cdot \left(\frac{T_{2,9} - T_{3,9}}{r_3^{\,2}} \right) - \frac{k_3}{\Delta_\theta} \cdot \left(\frac{T_{3,9} - T_{4,9}}{r_3^{\,2}} \right) \right]$$

10

$$\frac{2}{\rho_3 \cdot Cp_{z3,3} \cdot \Delta_z} \cdot \left[\frac{k_3}{\Delta_z} \cdot (T_{3,2} - T_{3,3}) + h_{top} \cdot (Tf_{zt} - T_{3,3}) \right] + X_{3,3} = 0$$

$$\frac{2 \cdot k_3}{\rho_3 \cdot Cp_{r4,3} \cdot \left[(r_4 + D2)^2 - (r_4 - D2)^2 \right]} \cdot \left[(T_{3,13} - T_{3,10}) \cdot \left(\frac{r_4 + D2}{\Delta_r} \right) - \left([T_{3,10} - T_{3,7}] \cdot \left[\frac{r_4 - D2}{\Delta_r} \right] \right) \right]$$
$$+ \frac{2}{\rho_3 \cdot Cp_{z1,3} \cdot \Delta_z} \cdot \left[\frac{k_3}{\Delta_z} \cdot (T_{3,11} - T_{3,10}) + h_{bottom} \cdot (Tf_{zb} - T_{3,10}) \right] + X_{3,10} = 0$$

$$X_{3,10} = \frac{1}{\rho_3 \cdot Cp_{r4,3} \cdot \Delta_\theta} \cdot \left[\frac{k_3}{\Delta_\theta} \cdot \left(\frac{T_{2,10} - T_{3,10}}{r_4^{\,2}} \right) - \frac{k_3}{\Delta_\theta} \cdot \left(\frac{T_{3,10} - T_{4,10}}{r_4^{\,2}} \right) \right]$$

11

$$\frac{2 \cdot k_3}{\rho_3 \cdot Cp_{r4,3} \cdot \left[(r_4 + D2)^2 - (r_4 - D2)^2 \right]} \cdot \left[(T_{3,14} - T_{3,11}) \cdot \left(\frac{r_4 + D2}{\Delta_r} \right) - \left([T_{3,11} - T_{3,8}] \cdot \left[\frac{r_4 - D2}{\Delta_r} \right] \right) \right]$$
$$+ \frac{1}{\rho_3 \cdot Cp_{z2,3} \cdot \Delta_z} \cdot \left[\frac{k_3}{\Delta_z} \cdot (T_{3,12} - T_{3,11}) - \frac{k_3}{\Delta_z} \cdot (T_{3,11} - T_{3,10}) \right] + X_{3,11} = 0$$

$$X_{3,11} = \frac{1}{\rho_3 \cdot Cp_{r4,3} \cdot \Delta_\theta} \cdot \left[\frac{k_3}{\Delta_\theta} \cdot \left(\frac{T_{2,11} - T_{3,11}}{r_4^{\,2}} \right) - \frac{k_3}{\Delta_\theta} \cdot \left(\frac{T_{3,11} - T_{4,11}}{r_4^{\,2}} \right) \right]$$

12

$$\frac{2 \cdot k_3}{\rho_3 \cdot Cp_{r4,3} \cdot \left[(r_4 + D2)^2 - (r_4 - D2)^2 \right]} \cdot \left[(T_{3,15} - T_{3,12}) \cdot \left(\frac{r_4 + D2}{\Delta_r} \right) - \left([T_{3,12} - T_{3,9}] \cdot \left[\frac{r_4 - D2}{\Delta_r} \right] \right) \right]$$
$$+ \frac{2}{\rho_3 \cdot Cp_{z3,3} \cdot \Delta_z} \cdot \left[\frac{k_3}{\Delta_z} \cdot (T_{3,11} - T_{3,12}) + h_{top} \cdot (Tf_{zt} - T_{3,12}) \right] + X_{3,12} = 0$$

$$X_{3,12} = \frac{1}{\rho_3 \cdot Cp_{r4,3} \cdot \Delta_\theta} \cdot \left[\frac{k_3}{\Delta_\theta} \cdot \left(\frac{T_{2,12} - T_{3,12}}{r_4^{\,2}} \right) - \frac{k_3}{\Delta_\theta} \cdot \left(\frac{T_{3,12} - T_{4,12}}{r_4^{\,2}} \right) \right]$$

13

$$\frac{2 \cdot k_3}{\rho_3 \cdot Cp_{r5,3} \cdot \left[(r_5 + D2)^2 - (r_5 - D2)^2 \right]} \cdot \left[(T_{3,16} - T_{3,13}) \cdot \left(\frac{r_5 + D2}{\Delta_r} \right) - \left([T_{3,13} - T_{3,10}] \cdot \left[\frac{r_5 - D2}{\Delta_r} \right] \right) \right]$$
$$+ \frac{2}{\rho_3 \cdot Cp_{z1,3} \cdot \Delta_z} \cdot \left[\frac{k_3}{\Delta_z} \cdot (T_{3,14} - T_{3,13}) + h_{bottom} \cdot (Tf_{zb} - T_{3,13}) \right] + X_{3,13} = 0$$

$$X_{3,13} = \frac{1}{\rho_3 \cdot Cp_{r5,3} \cdot \Delta_\theta} \cdot \left[\frac{k_3}{\Delta_\theta} \cdot \left(\frac{T_{2,13} - T_{3,13}}{r_5^{\,2}} \right) - \frac{k_3}{\Delta_\theta} \cdot \left(\frac{T_{3,13} - T_{4,13}}{r_5^{\,2}} \right) \right]$$

14

$$\frac{2 \cdot k_3}{\rho_3 \cdot Cp_{r5,3} \cdot \left[(r_5 + D2)^2 - (r_5 - D2)^2 \right]} \cdot \left[(T_{3,17} - T_{3,14}) \cdot \left(\frac{r_5 + D2}{\Delta_r} \right) - \left([T_{3,14} - T_{3,11}] \cdot \left[\frac{r_5 - D2}{\Delta_r} \right] \right) \right]$$
$$+ \frac{1}{\rho_3 \cdot Cp_{z2,3} \cdot \Delta_z} \cdot \left[\frac{k_3}{\Delta_z} \cdot (T_{3,15} - T_{3,14}) - \frac{k_3}{\Delta_z} \cdot (T_{3,14} - T_{3,13}) \right] + X_{3,14} = 0$$

$$X_{3,14} = \frac{1}{\rho_3 \cdot Cp_{r5,3} \cdot \Delta_\theta} \cdot \left[\frac{k_3}{\Delta_\theta} \cdot \left(\frac{T_{2,14} - T_{3,14}}{r_5^{\,2}} \right) - \frac{k_3}{\Delta_\theta} \cdot \left(\frac{T_{3,14} - T_{4,14}}{r_5^{\,2}} \right) \right]$$

15
$$\frac{2 \cdot k_3}{\rho_3 \cdot Cp_{r5,3} \cdot \left[(r_5 + D2)^2 - (r_5 - D2)^2 \right]} \cdot \left[(T_{3,18} - T_{3,15}) \cdot \left(\frac{r_5 + D2}{\Delta_r} \right) - \left([T_{3,15} - T_{3,12}] \cdot \left[\frac{r_5 - D2}{\Delta_r} \right] \right) \right]$$
$$+ \frac{2}{\rho_3 \cdot Cp_{z3,3} \cdot \Delta_z} \cdot \left[\frac{k_3}{\Delta_z} \cdot (T_{3,14} - T_{3,15}) + h_{top} \cdot (Tf_{zt} - T_{3,15}) \right] + X_{3,15} = 0$$

$$X_{3,15} = \frac{1}{\rho_3 \cdot Cp_{r5,3} \cdot \Delta_\theta} \cdot \left[\frac{k_3}{\Delta_\theta} \cdot \left(\frac{T_{2,15} - T_{3,15}}{r_5^{\,2}} \right) - \frac{k_3}{\Delta_\theta} \cdot \left(\frac{T_{3,15} - T_{4,15}}{r_5^{\,2}} \right) \right]$$

16

$$\frac{2 \cdot k_3}{\rho_3 \cdot Cp_{r6,3} \cdot \left[(r_6 + D2)^2 - (r_6 - D2)^2 \right]} \cdot \left[(T_{3,19} - T_{3,16}) \cdot \left(\frac{r_6 + D2}{\Delta_r} \right) - \left([T_{3,16} - T_{3,13}] \cdot \left[\frac{r_6 - D2}{\Delta_r} \right] \right) \right]$$
$$+ \frac{2}{\rho_3 \cdot Cp_{z1,3} \cdot \Delta_z} \cdot \left[\frac{k_3}{\Delta_z} \cdot (T_{3,17} - T_{3,16}) + h_{bottom} \cdot (Tf_{zb} - T_{3,16}) \right] + X_{3,16} = 0$$

$$X_{3,16} = \frac{1}{\rho_3 \cdot Cp_{r6,3} \cdot \Delta_\theta} \cdot \left[\frac{k_3}{\Delta_\theta} \cdot \left(\frac{T_{2,16} - T_{3,16}}{r_6^{\,2}} \right) - \frac{k_3}{\Delta_\theta} \cdot \left(\frac{T_{3,16} - T_{4,16}}{r_6^{\,2}} \right) \right]$$

17

$$\frac{2 \cdot k_3}{\rho_3 \cdot Cp_{r6,3} \cdot \left[(r_6 + D2)^2 - (r_6 - D2)^2 \right]} \cdot \left[(T_{3,20} - T_{3,17}) \cdot \left(\frac{r_6 + D2}{\Delta_r} \right) - \left([T_{3,17} - T_{3,14}] \cdot \left[\frac{r_6 - D2}{\Delta_r} \right] \right) \right]$$
$$+ \frac{1}{\rho_3 \cdot Cp_{z2,3} \cdot \Delta_z} \cdot \left[\frac{k_3}{\Delta_z} \cdot (T_{3,18} - T_{3,17}) - \frac{k_3}{\Delta_z} \cdot (T_{3,17} - T_{3,16}) \right] + X_{3,17} = 0$$

$$X_{3,17} = \frac{1}{\rho_3 \cdot Cp_{r6,3} \cdot \Delta_\theta} \cdot \left[\frac{k_3}{\Delta_\theta} \cdot \left(\frac{T_{2,17} - T_{3,17}}{r_6^{\,2}} \right) - \frac{k_3}{\Delta_\theta} \cdot \left(\frac{T_{3,17} - T_{4,17}}{r_6^{\,2}} \right) \right]$$

18

$$\frac{2 \cdot k_3}{\rho_3 \cdot Cp_{r6,3} \cdot \left[(r_6 + D2)^2 - (r_6 - D2)^2 \right]} \cdot \left[(T_{3,21} - T_{3,18}) \cdot \left(\frac{r_6 + D2}{\Delta_r} \right) - \left([T_{3,18} - T_{3,15}] \cdot \left[\frac{r_6 - D2}{\Delta_r} \right] \right) \right]$$
$$+ \frac{2}{\rho_3 \cdot Cp_{z3,3} \cdot \Delta_z} \cdot \left[\frac{k_3}{\Delta_z} \cdot (T_{3,17} - T_{3,18}) + h_{top} \cdot (Tf_{zt} - T_{3,18}) \right] + X_{3,18} = 0$$

$$X_{3,18} = \frac{1}{\rho_3 \cdot Cp_{r6,3} \cdot \Delta_\theta} \cdot \left[\frac{k_3}{\Delta_\theta} \cdot \left(\frac{T_{2,18} - T_{3,18}}{r_6^{\,2}} \right) - \frac{k_3}{\Delta_\theta} \cdot \left(\frac{T_{3,18} - T_{4,18}}{r_6^{\,2}} \right) \right]$$

19

$$\frac{2 \cdot k_3}{\rho_3 \cdot Cp_{r7,3} \cdot \left[(r_7 + D2)^2 - (r_7 - D2)^2 \right]} \cdot \left[(T_{3,22} - T_{3,19}) \cdot \left(\frac{r_7 + D2}{\Delta_r} \right) - \left([T_{3,19} - T_{3,16}] \cdot \left[\frac{r_7 - D2}{\Delta_r} \right] \right) \right]$$
$$+ \frac{2}{\rho_3 \cdot Cp_{z1,3} \cdot \Delta_z} \cdot \left[\frac{k_3}{\Delta_z} \cdot (T_{3,20} - T_{3,19}) + h_{bottom} \cdot (Tf_{zb} - T_{3,19}) \right] + X_{3,19} = 0$$

$$X_{3,19} = \frac{1}{\rho_3 \cdot Cp_{r7,3} \cdot \Delta_\theta} \cdot \left[\frac{k_3}{\Delta_\theta} \cdot \left(\frac{T_{2,19} - T_{3,19}}{r_7^{\,2}} \right) - \frac{k_3}{\Delta_\theta} \cdot \left(\frac{T_{3,19} - T_{4,19}}{r_7^{\,2}} \right) \right]$$

20

$$\frac{2 \cdot k_3}{\rho_3 \cdot Cp_{r7,3} \cdot \left[(r_7 + D2)^2 - (r_7 - D2)^2 \right]} \cdot \left[(T_{3,23} - T_{3,20}) \cdot \left(\frac{r_7 + D2}{\Delta_r} \right) - \left([T_{3,20} - T_{3,17}] \cdot \left[\frac{r_7 - D2}{\Delta_r} \right] \right) \right]$$
$$+ \frac{1}{\rho_3 \cdot Cp_{z2,3} \cdot \Delta_z} \cdot \left[\frac{k_3}{\Delta_z} \cdot (T_{3,21} - T_{3,20}) - \frac{k_3}{\Delta_z} \cdot (T_{3,20} - T_{3,19}) \right] + X_{3,20} = 0$$

$$X_{3,20} = \frac{1}{\rho_3 \cdot Cp_{r7,3} \cdot \Delta_\theta} \cdot \left[\frac{k_3}{\Delta_\theta} \cdot \left(\frac{T_{2,20} - T_{3,20}}{r_7^{\,2}} \right) - \frac{k_3}{\Delta_\theta} \cdot \left(\frac{T_{3,20} - T_{4,20}}{r_7^{\,2}} \right) \right]$$

21

$$\frac{2 \cdot k_3}{\rho_3 \cdot Cp_{r7,3} \cdot \left[(r_7 + D2)^2 - (r_7 - D2)^2 \right]} \cdot \left[(T_{3,24} - T_{3,21}) \cdot \left(\frac{r_7 + D2}{\Delta_r} \right) - \left([T_{3,21} - T_{3,18}] \cdot \left[\frac{r_7 - D2}{\Delta_r} \right] \right) \right]$$
$$+ \frac{2}{\rho_3 \cdot Cp_{z3,3} \cdot \Delta_z} \cdot \left[\frac{k_3}{\Delta_z} \cdot (T_{3,20} - T_{3,21}) + h_{top} \cdot (Tf_{zt} - T_{3,21}) \right] + X_{3,21} = 0$$

$$X_{3,21} = \frac{1}{\rho_3 \cdot Cp_{r7,3} \cdot \Delta_\theta} \cdot \left[\frac{k_3}{\Delta_\theta} \cdot \left(\frac{T_{2,21} - T_{3,21}}{r_7^{\,2}} \right) - \frac{k_3}{\Delta_\theta} \cdot \left(\frac{T_{3,21} - T_{4,21}}{r_7^{\,2}} \right) \right]$$

22

$$\frac{2 \cdot k_3}{\rho_3 \cdot Cp_{r8,3} \cdot \left[(r_8 + D2)^2 - (r_8 - D2)^2 \right]} \cdot \left[(T_{3,25} - T_{3,22}) \cdot \left(\frac{r_8 + D2}{\Delta_r} \right) - \left([T_{3,22} - T_{3,19}] \cdot \left[\frac{r_8 - D2}{\Delta_r} \right] \right) \right]$$
$$+ \frac{2}{\rho_3 \cdot Cp_{z1,3} \cdot \Delta_z} \cdot \left[\frac{k_3}{\Delta_z} \cdot (T_{3,23} - T_{3,22}) + h_{bottom} \cdot (Tf_{zb} - T_{3,22}) \right] + X_{3,22} = 0$$

$$X_{3,22} = \frac{1}{\rho_3 \cdot Cp_{r8,3} \cdot \Delta_\theta} \cdot \left[\frac{k_3}{\Delta_\theta} \cdot \left(\frac{T_{2,22} - T_{3,22}}{r_6^{\,2}} \right) - \frac{k_3}{\Delta_\theta} \cdot \left(\frac{T_{3,22} - T_{4,22}}{r_8^{\,2}} \right) \right]$$

23

$$\frac{2 \cdot k_3}{\rho_3 \cdot Cp_{r8,3} \cdot \left[(r_8 + D2)^2 - (r_8 - D2)^2 \right]} \cdot \left[(T_{3,26} - T_{3,23}) \cdot \left(\frac{r_8 + D2}{\Delta_r} \right) - \left([T_{3,23} - T_{3,20}] \cdot \left[\frac{r_8 - D2}{\Delta_r} \right] \right) \right]$$
$$+ \frac{1}{\rho_3 \cdot Cp_{z2,3} \cdot \Delta_z} \cdot \left[\frac{k_3}{\Delta_z} \cdot (T_{3,24} - T_{3,23}) - \frac{k_3}{\Delta_z} \cdot (T_{3,23} - T_{3,22}) \right] + X_{3,23} = 0$$

$$X_{3,23} = \frac{1}{\rho_3 \cdot Cp_{r8,3} \cdot \Delta_\theta} \cdot \left[\frac{k_3}{\Delta_\theta} \cdot \left(\frac{T_{2,23} - T_{3,23}}{r_8^{\,2}} \right) - \frac{k_3}{\Delta_\theta} \cdot \left(\frac{T_{3,23} - T_{4,23}}{r_8^{\,2}} \right) \right]$$

24

$$\frac{2 \cdot k_3}{\rho_3 \cdot Cp_{r8,3} \cdot \left[(r_8 + D2)^2 - (r_8 - D2)^2 \right]} \cdot \left[(T_{3,27} - T_{3,24}) \cdot \left(\frac{r_8 + D2}{\Delta_r} \right) - \left([T_{3,24} - T_{3,21}] \cdot \left[\frac{r_8 - D2}{\Delta_r} \right] \right) \right]$$
$$+ \frac{2}{\rho_3 \cdot Cp_{z3,3} \cdot \Delta_z} \cdot \left[\frac{k_3}{\Delta_z} \cdot (T_{3,23} - T_{3,24}) + h_{top} \cdot (Tf_{zt} - T_{3,24}) \right] + X_{3,24} = 0$$

$$X_{3,24} = \frac{1}{\rho_3 \cdot Cp_{r8,3} \cdot \Delta_\theta} \cdot \left[\frac{k_3}{\Delta_\theta} \cdot \left(\frac{T_{2,24} - T_{3,24}}{r_8^{\,2}} \right) - \frac{k_3}{\Delta_\theta} \cdot \left(\frac{T_{3,24} - T_{4,24}}{r_8^{\,2}} \right) \right]$$

25

$$\frac{2}{\rho_3 \cdot Cp_{r9,3} \cdot \left[(r_9 + D2)^2 - (r_9 - D2)^2 \right]} \cdot \left[r_{out} \cdot h_{outside} \cdot (Tf_{ro} - T_{3,25}) + (r_9 - D2) \cdot k_3 \cdot \left(\frac{T_{3,22} - T_{3,25}}{\Delta_r} \right) \right]$$
$$+ \frac{2}{\rho_3 \cdot Cp_{z1,3} \cdot \Delta_z} \cdot \left[\frac{k_3}{\Delta_z} \cdot (T_{3,26} - T_{3,25}) + h_{bottom} \cdot (Tf_{zb} - T_{3,25}) \right] + X_{3,25} = 0$$

$$X_{3,25} = \frac{1}{\rho_3 \cdot Cp_{r9,3} \cdot \Delta_\theta} \cdot \left[\frac{k_3}{\Delta_\theta} \cdot \left(\frac{T_{2,25} - T_{3,25}}{r_9^{\,2}} \right) - \frac{k_3}{\Delta_\theta} \cdot \left(\frac{T_{3,25} - T_{4,25}}{r_9^{\,2}} \right) \right]$$

26

$$\frac{2}{\rho_3 \cdot Cp_{r9,3} \cdot \left[(r_9 + D2)^2 - (r_9 - D2)^2 \right]} \cdot \left[r_{out} \cdot h_{outside} \cdot (Tf_{ro} - T_{3,26}) + (r_9 - D2) \cdot k_3 \cdot \left(\frac{T_{3,23} - T_{3,26}}{\Delta_r} \right) \right]$$
$$+ \frac{1}{\rho_3 \cdot Cp_{z2,3} \cdot \Delta_z} \cdot \left[\frac{k_3}{\Delta_z} \cdot (T_{3,27} - T_{3,26}) - \frac{k_3}{\Delta_z} \cdot (T_{3,26} - T_{3,25}) \right] + X_{3,26} = 0$$

$$X_{3,26} = \frac{1}{\rho_3 \cdot Cp_{r9,3} \cdot \Delta_\theta} \cdot \left[\frac{k_3}{\Delta_\theta} \cdot \left(\frac{T_{2,26} - T_{3,26}}{r_9^{\,2}} \right) - \frac{k_3}{\Delta_\theta} \cdot \left(\frac{T_{3,26} - T_{4,26}}{r_9^{\,2}} \right) \right]$$

27

$$\frac{2}{\rho_3 \cdot Cp_{r9,3} \cdot \left[(r_9 + D2)^2 - (r_9 - D2)^2 \right]} \cdot \left[r_{out} \cdot h_{outside} \cdot (Tf_{ro} - T_{3,27}) + (r_9 - D2) \cdot k_3 \cdot \left(\frac{T_{3,24} - T_{3,27}}{\Delta_r} \right) \right]$$
$$+ \frac{2}{\rho_3 \cdot Cp_{z3,3} \cdot \Delta_z} \cdot \left[\frac{k_3}{\Delta_z} \cdot (T_{3,26} - T_{3,27}) + h_{top} \cdot (Tf_{zt} - T_{3,27}) \right] + X_{3,27} = 0$$

$$X_{3,27} = \frac{1}{\rho_3 \cdot Cp_{r9,3} \cdot \Delta_\theta} \cdot \left[\frac{k_3}{\Delta_\theta} \cdot \left(\frac{T_{2,27} - T_{3,27}}{r_9^{\,2}} \right) - \frac{k_3}{\Delta_\theta} \cdot \left(\frac{T_{3,27} - T_{4,27}}{r_9^{\,2}} \right) \right]$$

**********BLOCK 4**********

*****NODE*****

1

$$\frac{2}{\rho_4 \cdot Cp_{r1,4} \cdot \left[(r_1 + D2)^2 - (r_1 - D2)^2 \right]} \cdot \left[r_{in} \cdot h_{inside} \cdot (Tf_{ri} - T_{4,1}) + (r_1 + D2) \cdot k_4 \cdot \left(\frac{T_{4,4} - T_{4,1}}{\Delta_r} \right) \right] + \frac{2}{\rho_4 \cdot Cp_{z1,4} \cdot \Delta_z}$$
$$\cdot \left[\frac{k_4}{\Delta_z} \cdot (T_{4,2} - T_{4,1}) + h_{bottom} \cdot (Tf_{zb} - T_{4,1}) \right] + X_{4,1} = 0$$

$$X_{4,1} = \frac{1}{\rho_4 \cdot Cp_{r1,4} \cdot \Delta_\theta} \cdot \left[\frac{k_4}{\Delta_\theta} \cdot \left(\frac{T_{3,1} - T_{4,1}}{r_1^{\,2}} \right) - \frac{k_4}{\Delta_\theta} \cdot \left(\frac{T_{4,1} - T_{5,1}}{r_1^{\,2}} \right) \right]$$

2

$$\frac{2}{\rho_4 \cdot Cp_{r1,4} \cdot \left[(r_1 + D2)^2 - (r_1 - D2)^2 \right]} \cdot \left[r_{in} \cdot h_{inside} \cdot (Tf_{ri} - T_{4,2}) + (r_1 + D2) \cdot k_4 \cdot \left(\frac{T_{4,5} - T_{4,2}}{\Delta_r} \right) \right] + \frac{1}{\rho_4 \cdot Cp_{z2,4} \cdot \Delta_z}$$
$$\cdot \left[\frac{k_4}{\Delta_z} \cdot (T_{4,3} - T_{4,2}) - \frac{k_4}{\Delta_z} \cdot (T_{4,2} - T_{4,1}) \right] + X_{4,2} = -q_1$$

$$X_{4,2} = \frac{1}{\rho_4 \cdot Cp_{r1,4} \cdot \Delta_\theta} \cdot \left[\frac{k_4}{\Delta_\theta} \cdot \left(\frac{T_{3,2} - T_{4,2}}{r_1^{\,2}} \right) - \frac{k_4}{\Delta_\theta} \cdot \left(\frac{T_{4,2} - T_{5,2}}{r_1^{\,2}} \right) \right]$$

3

$$\frac{2}{\rho_4 \cdot Cp_{r1,4} \cdot [(r_1 + D2)^2 - (r_1 - D2)^2]} \cdot \left[r_{in} \cdot h_{inside} \cdot (Tf_{ri} - T_{4,3}) + (r_1 + D2) \cdot k_4 \cdot \left(\frac{T_{4,6} - T_{4,3}}{\Delta_r} \right) \right] + \frac{2}{\rho_4 \cdot Cp_{z3,4} \cdot \Delta_z} \cdot \left[\frac{k_4}{\Delta_z} \cdot (T_{4,2} - T_{4,3}) + h_{top} \cdot (Tf_{zt} - T_{4,3}) \right] + X_{4,3} = 0$$

$$X_{4,3} = \frac{1}{\rho_4 \cdot Cp_{r1,4} \cdot \Delta_\theta} \cdot \left[\frac{k_4}{\Delta_\theta} \cdot \left(\frac{T_{3,3} - T_{4,3}}{r_1^2} \right) - \frac{k_4}{\Delta_\theta} \cdot \left(\frac{T_{4,3} - T_{5,3}}{r_1^2} \right) \right]$$

4

$$\frac{2 \cdot k_4}{\rho_4 \cdot Cp_{r2,4} \cdot [(r_2 + D2)^2 - (r_2 - D2)^2]} \cdot \left[(T_{4,7} - T_{4,4}) \cdot \left(\frac{r_2 + D2}{\Delta_r} \right) - \left([T_{4,4} - T_{4,1}] \cdot \left[\frac{r_2 - D2}{\Delta_r} \right] \right) \right] + \frac{2}{\rho_4 \cdot Cp_{z1,4} \cdot \Delta_z} \cdot \left[\frac{k_4}{\Delta_z} \cdot (T_{4,5} - T_{4,4}) + h_{bottom} \cdot (Tf_{zb} - T_{4,4}) \right] + X_{4,4} = 0$$

$$X_{4,4} = \frac{1}{\rho_4 \cdot Cp_{r2,4} \cdot \Delta_\theta} \cdot \left[\frac{k_4}{\Delta_\theta} \cdot \left(\frac{T_{3,4} - T_{4,4}}{r_2^2} \right) - \frac{k_4}{\Delta_\theta} \cdot \left(\frac{T_{4,4} - T_{5,4}}{r_2^2} \right) \right]$$

5

$$\frac{2 \cdot k_4}{\rho_4 \cdot Cp_{r2,4} \cdot [(r_2 + D2)^2 - (r_2 - D2)^2]} \cdot \left[(T_{4,8} - T_{4,5}) \cdot \left(\frac{r_2 + D2}{\Delta_r} \right) - \left([T_{4,5} - T_{4,2}] \cdot \left[\frac{r_2 - D2}{\Delta_r} \right] \right) \right] + \frac{1}{\rho_4 \cdot Cp_{z2,4} \cdot \Delta_z} \cdot \left[\frac{k_4}{\Delta_z} \cdot (T_{4,6} - T_{4,5}) - \frac{k_4}{\Delta_z} \cdot (T_{4,5} - T_{4,4}) \right] + X_{4,5} = -q_2$$

$$X_{4,5} = \frac{1}{\rho_4 \cdot Cp_{r2,4} \cdot \Delta_\theta} \cdot \left[\frac{k_4}{\Delta_\theta} \cdot \left(\frac{T_{3,5} - T_{4,5}}{r_2^2} \right) - \frac{k_4}{\Delta_\theta} \cdot \left(\frac{T_{4,5} - T_{5,5}}{r_2^2} \right) \right]$$

6

$$\frac{2 \cdot k_4}{\rho_4 \cdot Cp_{r2,4} \cdot [(r_2 + D2)^2 - (r_2 - D2)^2]} \cdot \left[(T_{4,9} - T_{4,6}) \cdot \left(\frac{r_2 + D2}{\Delta_r} \right) - \left([T_{4,6} - T_{4,3}] \cdot \left[\frac{r_2 - D2}{\Delta_r} \right] \right) \right] + \frac{2}{\rho_4 \cdot Cp_{z3,4} \cdot \Delta_z} \cdot \left[\frac{k_4}{\Delta_z} \cdot (T_{4,5} - T_{4,6}) + h_{top} \cdot (Tf_{zt} - T_{4,6}) \right] + X_{4,6} = 0$$

$$X_{4,6} = \frac{1}{\rho_4 \cdot Cp_{r2,4} \cdot \Delta_\theta} \cdot \left[\frac{k_4}{\Delta_\theta} \cdot \left(\frac{T_{3,6} - T_{4,6}}{r_2^2} \right) - \frac{k_4}{\Delta_\theta} \cdot \left(\frac{T_{4,6} - T_{5,6}}{r_2^2} \right) \right]$$

7

$$\frac{2 \cdot k_4}{\rho_4 \cdot Cp_{r3,4} \cdot [(r_3 + D2)^2 - (r_3 - D2)^2]} \cdot \left[(T_{4,10} - T_{4,7}) \cdot \left(\frac{r_3 + D2}{\Delta_r} \right) - \left([T_{4,7} - T_{4,4}] \cdot \left[\frac{r_3 - D2}{\Delta_r} \right] \right) \right] + \frac{2}{\rho_4 \cdot Cp_{z1,4} \cdot \Delta_z} \cdot \left[\frac{k_4}{\Delta_z} \cdot (T_{4,8} - T_{4,7}) + h_{bottom} \cdot (Tf_{zb} - T_{4,7}) \right] + X_{4,7} = 0$$

$$X_{4,7} = \frac{1}{\rho_4 \cdot Cp_{r3,4} \cdot \Delta_\theta} \cdot \left[\frac{k_4}{\Delta_\theta} \cdot \left(\frac{T_{3,7} - T_{4,7}}{r_3^2} \right) - \frac{k_4}{\Delta_\theta} \cdot \left(\frac{T_{4,7} - T_{5,7}}{r_3^2} \right) \right]$$

8

$$\frac{2 \cdot k_4}{\rho_4 \cdot Cp_{r3,4} \cdot [(r_3 + D2)^2 - (r_3 - D2)^2]} \cdot \left[(T_{4,11} - T_{4,8}) \cdot \left(\frac{r_3 + D2}{\Delta_r} \right) - \left([T_{4,8} - T_{4,5}] \cdot \left[\frac{r_3 - D2}{\Delta_r} \right] \right) \right] + \frac{1}{\rho_4 \cdot Cp_{z2,4} \cdot \Delta_z} \cdot \left[\frac{k_4}{\Delta_z} \cdot (T_{4,9} - T_{4,8}) - \frac{k_4}{\Delta_z} \cdot (T_{4,8} - T_{4,7}) \right] + X_{4,8} = -q_3$$

$$X_{4,8} = \frac{1}{\rho_4 \cdot Cp_{r3,4} \cdot \Delta_\theta} \cdot \left[\frac{k_4}{\Delta_\theta} \cdot \left(\frac{T_{3,8} - T_{4,8}}{r_3^2} \right) - \frac{k_4}{\Delta_\theta} \cdot \left(\frac{T_{4,8} - T_{5,8}}{r_3^2} \right) \right]$$

9

$$\frac{2 \cdot k_4}{\rho_4 \cdot Cp_{r3,4} \cdot [(r_3 + D2)^2 - (r_3 - D2)^2]} \cdot \left[(T_{4,12} - T_{4,9}) \cdot \left(\frac{r_3 + D2}{\Delta_r} \right) - \left([T_{4,9} - T_{4,6}] \cdot \left[\frac{r_3 - D2}{\Delta_r} \right] \right) \right] + \frac{2}{\rho_4 \cdot Cp_{z3,4} \cdot \Delta_z} \cdot \left[\frac{k_4}{\Delta_z} \cdot (T_{4,8} - T_{4,9}) + h_{top} \cdot (Tf_{zt} - T_{4,9}) \right] + X_{4,9} = 0$$

$$X_{4,9} = \frac{1}{\rho_4 \cdot Cp_{r3,4} \cdot \Delta_\theta} \cdot \left[\frac{k_4}{\Delta_\theta} \cdot \left(\frac{T_{3,9} - T_{4,9}}{r_3^{\,2}} \right) - \frac{k_4}{\Delta_\theta} \cdot \left(\frac{T_{4,9} - T_{5,9}}{r_3^{\,2}} \right) \right]$$

10

$$\frac{2 \cdot k_4}{\rho_4 \cdot Cp_{r4,4} \cdot \left[(r_4 + D2)^2 - (r_4 - D2)^2 \right]} \cdot \left[(T_{4,13} - T_{4,10}) \cdot \left(\frac{r_4 + D2}{\Delta_r} \right) - \left([T_{4,10} - T_{4,7}] \cdot \left[\frac{r_4 - D2}{\Delta_r} \right] \right) \right]$$
$$+ \frac{2}{\rho_4 \cdot Cp_{z1,4} \cdot \Delta_z} \cdot \left[\frac{k_4}{\Delta_z} \cdot (T_{4,11} - T_{4,10}) + h_{bottom} \cdot (Tf_{zb} - T_{4,10}) \right] + X_{4,10} = 0$$

$$X_{4,10} = \frac{1}{\rho_4 \cdot Cp_{r4,4} \cdot \Delta_\theta} \cdot \left[\frac{k_4}{\Delta_\theta} \cdot \left(\frac{T_{3,10} - T_{4,10}}{r_4^{\,2}} \right) - \frac{k_4}{\Delta_\theta} \cdot \left(\frac{T_{4,10} - T_{5,10}}{r_4^{\,2}} \right) \right]$$

11

$$\frac{2 \cdot k_4}{\rho_4 \cdot Cp_{r4,4} \cdot \left[(r_4 + D2)^2 - (r_4 - D2)^2 \right]} \cdot \left[(T_{4,14} - T_{4,11}) \cdot \left(\frac{r_4 + D2}{\Delta_r} \right) - \left([T_{4,11} - T_{4,8}] \cdot \left[\frac{r_4 - D2}{\Delta_r} \right] \right) \right]$$
$$+ \frac{1}{\rho_4 \cdot Cp_{z2,4} \cdot \Delta_z} \cdot \left[\frac{k_4}{\Delta_z} \cdot (T_{4,12} - T_{4,11}) - \frac{k_4}{\Delta_z} \cdot (T_{4,11} - T_{4,10}) \right] + X_{4,11} = -q_4$$

$$X_{4,11} = \frac{1}{\rho_4 \cdot Cp_{r4,4} \cdot \Delta_\theta} \cdot \left[\frac{k_4}{\Delta_\theta} \cdot \left(\frac{T_{3,11} - T_{4,11}}{r_4^{\,2}} \right) - \frac{k_4}{\Delta_\theta} \cdot \left(\frac{T_{4,11} - T_{5,11}}{r_4^{\,2}} \right) \right]$$

12

$$\frac{2 \cdot k_4}{\rho_4 \cdot Cp_{r4,4} \cdot \left[(r_4 + D2)^2 - (r_4 - D2)^2 \right]} \cdot \left[(T_{4,15} - T_{4,12}) \cdot \left(\frac{r_4 + D2}{\Delta_r} \right) - \left([T_{4,12} - T_{4,9}] \cdot \left[\frac{r_4 - D2}{\Delta_r} \right] \right) \right]$$
$$+ \frac{2}{\rho_4 \cdot Cp_{z3,4} \cdot \Delta_z} \cdot \left[\frac{k_4}{\Delta_z} \cdot (T_{4,11} - T_{4,12}) + h_{top} \cdot (Tf_{zt} - T_{4,12}) \right] + X_{4,12} = 0$$

$$X_{4,12} = \frac{1}{\rho_4 \cdot Cp_{r4,4} \cdot \Delta_\theta} \cdot \left[\frac{k_4}{\Delta_\theta} \cdot \left(\frac{T_{3,12} - T_{4,12}}{r_4^{\,2}} \right) - \frac{k_4}{\Delta_\theta} \cdot \left(\frac{T_{4,12} - T_{5,12}}{r_4^{\,2}} \right) \right]$$

13

$$\frac{2 \cdot k_4}{\rho_4 \cdot Cp_{r5,4} \cdot \left[(r_5 + D2)^2 - (r_5 - D2)^2 \right]} \cdot \left[(T_{4,16} - T_{4,13}) \cdot \left(\frac{r_5 + D2}{\Delta_r} \right) - \left([T_{4,13} - T_{4,10}] \cdot \left[\frac{r_5 - D2}{\Delta_r} \right] \right) \right]$$
$$+ \frac{2}{\rho_4 \cdot Cp_{z1,4} \cdot \Delta_z} \cdot \left[\frac{k_4}{\Delta_z} \cdot (T_{4,14} - T_{4,13}) + h_{bottom} \cdot (Tf_{zb} - T_{4,13}) \right] + X_{4,13} = 0$$

$$X_{4,13} = \frac{1}{\rho_4 \cdot Cp_{r5,4} \cdot \Delta_\theta} \cdot \left[\frac{k_4}{\Delta_\theta} \cdot \left(\frac{T_{3,13} - T_{4,13}}{r_5^{\,2}} \right) - \frac{k_4}{\Delta_\theta} \cdot \left(\frac{T_{4,13} - T_{5,13}}{r_5^{\,2}} \right) \right]$$

14

$$\frac{2 \cdot k_4}{\rho_4 \cdot Cp_{r5,4} \cdot \left[(r_5 + D2)^2 - (r_5 - D2)^2 \right]} \cdot \left[(T_{4,17} - T_{4,14}) \cdot \left(\frac{r_5 + D2}{\Delta_r} \right) - \left([T_{4,14} - T_{4,11}] \cdot \left[\frac{r_5 - D2}{\Delta_r} \right] \right) \right]$$
$$+ \frac{1}{\rho_4 \cdot Cp_{z2,4} \cdot \Delta_z} \cdot \left[\frac{k_4}{\Delta_z} \cdot (T_{4,15} - T_{4,14}) - \frac{k_4}{\Delta_z} \cdot (T_{4,14} - T_{4,13}) \right] + X_{4,14} = -q_5$$

$$X_{4,14} = \frac{1}{\rho_4 \cdot Cp_{r5,4} \cdot \Delta_\theta} \cdot \left[\frac{k_4}{\Delta_\theta} \cdot \left(\frac{T_{3,14} - T_{4,14}}{r_5^{\,2}} \right) - \frac{k_4}{\Delta_\theta} \cdot \left(\frac{T_{4,14} - T_{5,14}}{r_5^{\,2}} \right) \right]$$

15

$$\frac{2 \cdot k_4}{\rho_4 \cdot Cp_{r5,4} \cdot \left[(r_5 + D2)^2 - (r_5 - D2)^2 \right]} \cdot \left[(T_{4,18} - T_{4,15}) \cdot \left(\frac{r_5 + D2}{\Delta_r} \right) - \left([T_{4,15} - T_{4,12}] \cdot \left[\frac{r_5 - D2}{\Delta_r} \right] \right) \right]$$
$$+ \frac{2}{\rho_4 \cdot Cp_{z3,4} \cdot \Delta_z} \cdot \left[\frac{k_4}{\Delta_z} \cdot (T_{4,14} - T_{4,15}) + h_{top} \cdot (Tf_{zt} - T_{4,15}) \right] + X_{4,15} = 0$$

$$X_{4,15} = \frac{1}{\rho_4 \cdot Cp_{r5,4} \cdot \Delta_\theta} \cdot \left[\frac{k_4}{\Delta_\theta} \cdot \left(\frac{T_{3,15} - T_{4,15}}{r_5^{\,2}} \right) - \frac{k_4}{\Delta_\theta} \cdot \left(\frac{T_{4,15} - T_{5,15}}{r_5^{\,2}} \right) \right]$$

16

$$\frac{2 \cdot k_4}{\rho_4 \cdot Cp_{r6,4} \cdot \left[(r_6 + D2)^2 - (r_6 - D2)^2 \right]} \cdot \left[(T_{4,19} - T_{4,16}) \cdot \left(\frac{r_6 + D2}{\Delta_r} \right) - \left(\left[T_{4,16} - T_{4,13} \right] \cdot \left[\frac{r_6 - D2}{\Delta_r} \right] \right) \right]$$
$$+ \frac{2}{\rho_4 \cdot Cp_{z1,4} \cdot \Delta_z} \cdot \left[\frac{k_4}{\Delta_z} \cdot (T_{4,17} - T_{4,16}) + h_{bottom} \cdot (Tf_{zb} - T_{4,16}) \right] + X_{4,16} = 0$$

$$X_{4,16} = \frac{1}{\rho_4 \cdot Cp_{r6,4} \cdot \Delta_\theta} \cdot \left[\frac{k_4}{\Delta_\theta} \cdot \left(\frac{T_{3,16} - T_{4,16}}{r_6^{\,2}} \right) - \frac{k_4}{\Delta_\theta} \cdot \left(\frac{T_{4,16} - T_{5,16}}{r_6^{\,2}} \right) \right]$$

17

$$\frac{2 \cdot k_4}{\rho_4 \cdot Cp_{r6,4} \cdot \left[(r_6 + D2)^2 - (r_6 - D2)^2 \right]} \cdot \left[(T_{4,20} - T_{4,17}) \cdot \left(\frac{r_6 + D2}{\Delta_r} \right) - \left(\left[T_{4,17} - T_{4,14} \right] \cdot \left[\frac{r_6 - D2}{\Delta_r} \right] \right) \right]$$
$$+ \frac{1}{\rho_4 \cdot Cp_{z2,4} \cdot \Delta_z} \cdot \left[\frac{k_4}{\Delta_z} \cdot (T_{4,18} - T_{4,17}) - \frac{k_4}{\Delta_z} \cdot (T_{4,17} - T_{4,16}) \right] + X_{4,17} = -q_6$$

$$X_{4,17} = \frac{1}{\rho_4 \cdot Cp_{r6,4} \cdot \Delta_\theta} \cdot \left[\frac{k_4}{\Delta_\theta} \cdot \left(\frac{T_{3,17} - T_{4,17}}{r_6^{\,2}} \right) - \frac{k_4}{\Delta_\theta} \cdot \left(\frac{T_{4,17} - T_{5,17}}{r_6^{\,2}} \right) \right]$$

18

$$\frac{2 \cdot k_4}{\rho_4 \cdot Cp_{r6,4} \cdot \left[(r_6 + D2)^2 - (r_6 - D2)^2 \right]} \cdot \left[(T_{4,21} - T_{4,18}) \cdot \left(\frac{r_6 + D2}{\Delta_r} \right) - \left(\left[T_{4,18} - T_{4,15} \right] \cdot \left[\frac{r_6 - D2}{\Delta_r} \right] \right) \right]$$
$$+ \frac{2}{\rho_4 \cdot Cp_{z3,4} \cdot \Delta_z} \cdot \left[\frac{k_4}{\Delta_z} \cdot (T_{4,17} - T_{4,18}) + h_{top} \cdot (Tf_{zt} - T_{4,18}) \right] + X_{4,18} = 0$$

$$X_{4,18} = \frac{1}{\rho_4 \cdot Cp_{r6,4} \cdot \Delta_\theta} \cdot \left[\frac{k_4}{\Delta_\theta} \cdot \left(\frac{T_{3,18} - T_{4,18}}{r_6^{\,2}} \right) - \frac{k_4}{\Delta_\theta} \cdot \left(\frac{T_{4,18} - T_{5,18}}{r_6^{\,2}} \right) \right]$$

19

$$\frac{2 \cdot k_4}{\rho_4 \cdot Cp_{r7,4} \cdot \left[(r_7 + D2)^2 - (r_7 - D2)^2 \right]} \cdot \left[(T_{4,22} - T_{4,19}) \cdot \left(\frac{r_7 + D2}{\Delta_r} \right) - \left(\left[T_{4,19} - T_{4,16} \right] \cdot \left[\frac{r_7 - D2}{\Delta_r} \right] \right) \right]$$
$$+ \frac{2}{\rho_4 \cdot Cp_{z1,4} \cdot \Delta_z} \cdot \left[\frac{k_4}{\Delta_z} \cdot (T_{4,20} - T_{4,19}) + h_{bottom} \cdot (Tf_{zb} - T_{4,19}) \right] + X_{4,19} = 0$$

$$X_{4,19} = \frac{1}{\rho_4 \cdot Cp_{r7,4} \cdot \Delta_\theta} \cdot \left[\frac{k_4}{\Delta_\theta} \cdot \left(\frac{T_{3,19} - T_{4,19}}{r_7^{\,2}} \right) - \frac{k_4}{\Delta_\theta} \cdot \left(\frac{T_{4,19} - T_{5,19}}{r_7^{\,2}} \right) \right]$$

20

$$\frac{2 \cdot k_4}{\rho_4 \cdot Cp_{r7,4} \cdot \left[(r_7 + D2)^2 - (r_7 - D2)^2 \right]} \cdot \left[(T_{4,23} - T_{4,20}) \cdot \left(\frac{r_7 + D2}{\Delta_r} \right) - \left(\left[T_{4,20} - T_{4,17} \right] \cdot \left[\frac{r_7 - D2}{\Delta_r} \right] \right) \right]$$
$$+ \frac{1}{\rho_4 \cdot Cp_{z2,4} \cdot \Delta_z} \cdot \left[\frac{k_4}{\Delta_z} \cdot (T_{4,21} - T_{4,20}) - \frac{k_4}{\Delta_z} \cdot (T_{4,20} - T_{4,19}) \right] + X_{4,20} = -q_7$$

$$X_{4,20} = \frac{1}{\rho_4 \cdot Cp_{r7,4} \cdot \Delta_\theta} \cdot \left[\frac{k_4}{\Delta_\theta} \cdot \left(\frac{T_{3,20} - T_{4,20}}{r_7^{\,2}} \right) - \frac{k_4}{\Delta_\theta} \cdot \left(\frac{T_{4,20} - T_{5,20}}{r_7^{\,2}} \right) \right]$$

21

$$\frac{2 \cdot k_4}{\rho_4 \cdot Cp_{r7,4} \cdot \left[(r_7 + D2)^2 - (r_7 - D2)^2 \right]} \cdot \left[(T_{4,24} - T_{4,21}) \cdot \left(\frac{r_7 + D2}{\Delta_r} \right) - \left(\left[T_{4,21} - T_{4,18} \right] \cdot \left[\frac{r_7 - D2}{\Delta_r} \right] \right) \right]$$
$$+ \frac{2}{\rho_4 \cdot Cp_{z3,4} \cdot \Delta_z} \cdot \left[\frac{k_4}{\Delta_z} \cdot (T_{4,20} - T_{4,21}) + h_{top} \cdot (Tf_{zt} - T_{4,21}) \right] + X_{4,21} = 0$$

$$X_{4,21} = \frac{1}{\rho_4 \cdot Cp_{r7,4} \cdot \Delta_\theta} \cdot \left[\frac{k_4}{\Delta_\theta} \cdot \left(\frac{T_{3,21} - T_{4,21}}{r_7^{\,2}} \right) - \frac{k_4}{\Delta_\theta} \cdot \left(\frac{T_{4,21} - T_{5,21}}{r_7^{\,2}} \right) \right]$$

22

$$\frac{2 \cdot k_4}{\rho_4 \cdot Cp_{r8,4} \cdot \left[(r_8 + D2)^2 - (r_8 - D2)^2 \right]} \cdot \left[(T_{4,25} - T_{4,22}) \cdot \left(\frac{r_8 + D2}{\Delta_r} \right) - \left(\left[T_{4,22} - T_{4,19} \right] \cdot \left[\frac{r_8 - D2}{\Delta_r} \right] \right) \right]$$
$$+ \frac{2}{\rho_4 \cdot Cp_{z1,4} \cdot \Delta_z} \cdot \left[\frac{k_4}{\Delta_z} \cdot (T_{4,23} - T_{4,22}) + h_{bottom} \cdot (Tf_{zb} - T_{4,22}) \right] + X_{4,22} = 0$$

$$X_{4,22} = \frac{1}{\rho_4 \cdot Cp_{r8,4} \cdot \Delta_\theta} \cdot \left[\frac{k_4}{\Delta_\theta} \cdot \left(\frac{T_{3,22} - T_{4,22}}{r_8^{\,2}} \right) - \frac{k_4}{\Delta_\theta} \cdot \left(\frac{T_{4,22} - T_{5,22}}{r_8^{\,2}} \right) \right]$$

23

$$\frac{2 \cdot k_4}{\rho_4 \cdot Cp_{r8,4} \cdot \left[(r_8 + D2)^2 - (r_8 - D2)^2 \right]} \cdot \left[(T_{4,26} - T_{4,23}) \cdot \left(\frac{r_8 + D2}{\Delta_r} \right) - \left([T_{4,23} - T_{4,20}] \cdot \left[\frac{r_8 - D2}{\Delta_r} \right] \right) \right] + \frac{1}{\rho_4 \cdot Cp_{z2,4} \cdot \Delta_z} \cdot \left[\frac{k_4}{\Delta_z} \cdot (T_{4,24} - T_{4,23}) - \frac{k_4}{\Delta_z} \cdot (T_{4,23} - T_{4,22}) \right] + X_{4,23} = -q_8$$

$$X_{4,23} = \frac{1}{\rho_4 \cdot Cp_{r8,4} \cdot \Delta_\theta} \cdot \left[\frac{k_4}{\Delta_\theta} \cdot \left(\frac{T_{3,23} - T_{4,23}}{r_8^2} \right) - \frac{k_4}{\Delta_\theta} \cdot \left(\frac{T_{4,23} - T_{5,23}}{r_8^2} \right) \right]$$

24

$$\frac{2 \cdot k_4}{\rho_4 \cdot Cp_{r8,4} \cdot \left[(r_8 + D2)^2 - (r_8 - D2)^2 \right]} \cdot \left[(T_{4,27} - T_{4,24}) \cdot \left(\frac{r_8 + D2}{\Delta_r} \right) - \left([T_{4,24} - T_{4,21}] \cdot \left[\frac{r_8 - D2}{\Delta_r} \right] \right) \right] + \frac{2}{\rho_4 \cdot Cp_{z3,4} \cdot \Delta_z} \cdot \left[\frac{k_4}{\Delta_z} \cdot (T_{4,23} - T_{4,24}) + h_{top} \cdot (Tf_{zt} - T_{4,24}) \right] + X_{4,24} = 0$$

$$X_{4,24} = \frac{1}{\rho_4 \cdot Cp_{r8,4} \cdot \Delta_\theta} \cdot \left[\frac{k_4}{\Delta_\theta} \cdot \left(\frac{T_{3,24} - T_{4,24}}{r_8^2} \right) - \frac{k_4}{\Delta_\theta} \cdot \left(\frac{T_{4,24} - T_{5,24}}{r_8^2} \right) \right]$$

25

$$\frac{2}{\rho_4 \cdot Cp_{r9,4} \cdot \left[(r_9 + D2)^2 - (r_9 - D2)^2 \right]} \cdot \left[r_{out} \cdot h_{outside} \cdot (Tf_{ro} - T_{4,25}) + (r_9 - D2) \cdot k_4 \cdot \left(\frac{T_{4,22} - T_{4,25}}{\Delta_r} \right) \right] + \frac{2}{\rho_4 \cdot Cp_{z1,4} \cdot \Delta_z} \cdot \left[\frac{k_4}{\Delta_z} \cdot (T_{4,26} - T_{4,25}) + h_{bottom} \cdot (Tf_{zb} - T_{4,25}) \right] + X_{4,25} = 0$$

$$X_{4,25} = \frac{1}{\rho_4 \cdot Cp_{r9,4} \cdot \Delta_\theta} \cdot \left[\frac{k_4}{\Delta_\theta} \cdot \left(\frac{T_{3,25} - T_{4,25}}{r_9^2} \right) - \frac{k_4}{\Delta_\theta} \cdot \left(\frac{T_{4,25} - T_{5,25}}{r_9^2} \right) \right]$$

26

$$\frac{2}{\rho_4 \cdot Cp_{r9,4} \cdot \left[(r_9 + D2)^2 - (r_9 - D2)^2 \right]} \cdot \left[r_{out} \cdot h_{outside} \cdot (Tf_{ro} - T_{4,26}) + (r_9 - D2) \cdot k_4 \cdot \left(\frac{T_{4,23} - T_{4,26}}{\Delta_r} \right) \right] + \frac{1}{\rho_4 \cdot Cp_{z2,4} \cdot \Delta_z} \cdot \left[\frac{k_4}{\Delta_z} \cdot (T_{4,27} - T_{4,26}) - \frac{k_4}{\Delta_z} \cdot (T_{4,26} - T_{4,25}) \right] + X_{4,26} = -q_9$$

$$X_{4,26} = \frac{1}{\rho_4 \cdot Cp_{r8,4} \cdot \Delta_\theta} \cdot \left[\frac{k_4}{\Delta_\theta} \cdot \left(\frac{T_{3,26} - T_{4,26}}{r_9^2} \right) - \frac{k_4}{\Delta_\theta} \cdot \left(\frac{T_{4,26} - T_{5,26}}{r_9^2} \right) \right]$$

27

$$\frac{2}{\rho_4 \cdot Cp_{r9,4} \cdot \left[(r_9 + D2)^2 - (r_9 - D2)^2 \right]} \cdot \left[r_{out} \cdot h_{outside} \cdot (Tf_{ro} - T_{4,27}) + (r_9 - D2) \cdot k_4 \cdot \left(\frac{T_{4,24} - T_{4,27}}{\Delta_r} \right) \right] + \frac{2}{\rho_4 \cdot Cp_{z3,4} \cdot \Delta_z} \cdot \left[\frac{k_4}{\Delta_z} \cdot (T_{4,26} - T_{4,27}) + h_{top} \cdot (Tf_{zt} - T_{4,27}) \right] + X_{4,27} = 0$$

$$X_{4,27} = \frac{1}{\rho_4 \cdot Cp_{r9,4} \cdot \Delta_\theta} \cdot \left[\frac{k_4}{\Delta_\theta} \cdot \left(\frac{T_{3,27} - T_{4,27}}{r_9^2} \right) - \frac{k_4}{\Delta_\theta} \cdot \left(\frac{T_{4,27} - T_{5,27}}{r_9^2} \right) \right]$$

**********BLOCK 5**********

*****NODE*****

1

$$\frac{2}{\rho_5 \cdot Cp_{r1,5} \cdot \left[(r_1 + D2)^2 - (r_1 - D2)^2 \right]} \cdot \left[r_{in} \cdot h_{inside} \cdot (Tf_{ri} - T_{5,1}) + (r_1 + D2) \cdot k_5 \cdot \left(\frac{T_{5,4} - T_{5,1}}{\Delta_r} \right) \right] + \frac{2}{\rho_5 \cdot Cp_{z1,5} \cdot \Delta_z} \cdot \left[\frac{k_5}{\Delta_z} \cdot (T_{5,2} - T_{5,1}) + h_{bottom} \cdot (Tf_{zb} - T_{5,1}) \right] + X_{5,1} = 0$$

$$X_{5,1} = \frac{1}{\rho_5 \cdot Cp_{r1,5} \cdot \Delta_\theta} \cdot \left[\frac{k_5}{\Delta_\theta} \cdot \left(\frac{T_{4,1} - T_{5,1}}{r_1^2} \right) - \frac{k_5}{\Delta_\theta} \cdot \left(\frac{T_{5,1} - T_{6,1}}{r_1^2} \right) \right]$$

2

9

$$\frac{2 \cdot k_5}{\rho_5 \cdot Cp_{r3,5} \cdot \left[(r_3 + D2)^2 - (r_3 - D2)^2 \right]} \cdot \left[(T_{5,12} - T_{5,9}) \cdot \left(\frac{r_3 + D2}{\Delta_r} \right) - \left([T_{5,9} - T_{5,6}] \cdot \left[\frac{r_3 - D2}{\Delta_r} \right] \right) \right] + \frac{2}{\rho_5 \cdot Cp_{z3,5} \cdot \Delta_z} \cdot \left[\frac{k_5}{\Delta_z} \cdot (T_{5,6} - T_{5,9}) + h_{top} \cdot (Tf_{zt} - T_{5,9}) \right] + X_{5,9} = 0$$

$$X_{5,9} = \frac{1}{\rho_5 \cdot Cp_{r3,5} \cdot \Delta_\theta} \cdot \left[\frac{k_5}{\Delta_\theta} \cdot \left(\frac{T_{4,9} - T_{5,9}}{r_3^{\,2}} \right) - \frac{k_5}{\Delta_\theta} \cdot \left(\frac{T_{5,9} - T_{6,9}}{r_3^{\,2}} \right) \right]$$

10

$$\frac{2 \cdot k_5}{\rho_5 \cdot Cp_{r4,5} \cdot \left[(r_4 + D2)^2 - (r_4 - D2)^2 \right]} \cdot \left[(T_{5,13} - T_{5,10}) \cdot \left(\frac{r_4 + D2}{\Delta_r} \right) - \left([T_{5,10} - T_{5,7}] \cdot \left[\frac{r_4 - D2}{\Delta_r} \right] \right) \right] + \frac{2}{\rho_5 \cdot Cp_{z1,5} \cdot \Delta_z} \cdot \left[\frac{k_5}{\Delta_z} \cdot (T_{5,11} - T_{5,10}) + h_{bottom} \cdot (Tf_{zb} - T_{5,10}) \right] + X_{5,10} = 0$$

$$X_{5,10} = \frac{1}{\rho_5 \cdot Cp_{r4,5} \cdot \Delta_\theta} \cdot \left[\frac{k_5}{\Delta_\theta} \cdot \left(\frac{T_{4,10} - T_{5,10}}{r_4^{\,2}} \right) - \frac{k_5}{\Delta_\theta} \cdot \left(\frac{T_{5,10} - T_{6,10}}{r_4^{\,2}} \right) \right]$$

11

$$\frac{2 \cdot k_5}{\rho_5 \cdot Cp_{r4,5} \cdot \left[(r_4 + D2)^2 - (r_4 - D2)^2 \right]} \cdot \left[(T_{5,14} - T_{5,11}) \cdot \left(\frac{r_4 + D2}{\Delta_r} \right) - \left([T_{5,11} - T_{5,8}] \cdot \left[\frac{r_4 - D2}{\Delta_r} \right] \right) \right] + \frac{1}{\rho_5 \cdot Cp_{z2,5} \cdot \Delta_z} \cdot \left[\frac{k_5}{\Delta_z} \cdot (T_{5,12} - T_{5,11}) - \frac{k_5}{\Delta_z} \cdot (T_{5,11} - T_{5,10}) \right] + X_{5,11} = 0$$

$$X_{5,11} = \frac{1}{\rho_5 \cdot Cp_{r4,5} \cdot \Delta_\theta} \cdot \left[\frac{k_5}{\Delta_\theta} \cdot \left(\frac{T_{4,11} - T_{5,11}}{r_4^{\,2}} \right) - \frac{k_5}{\Delta_\theta} \cdot \left(\frac{T_{5,11} - T_{6,11}}{r_4^{\,2}} \right) \right]$$

12

$$\frac{2 \cdot k_5}{\rho_5 \cdot Cp_{r4,5} \cdot \left[(r_4 + D2)^2 - (r_4 - D2)^2 \right]} \cdot \left[(T_{5,15} - T_{5,12}) \cdot \left(\frac{r_4 + D2}{\Delta_r} \right) - \left([T_{5,12} - T_{5,9}] \cdot \left[\frac{r_4 - D2}{\Delta_r} \right] \right) \right] + \frac{2}{\rho_5 \cdot Cp_{z3,5} \cdot \Delta_z} \cdot \left[\frac{k_5}{\Delta_z} \cdot (T_{5,11} - T_{5,12}) + h_{top} \cdot (Tf_{zt} - T_{5,12}) \right] + X_{5,12} = 0$$

$$X_{5,12} = \frac{1}{\rho_5 \cdot Cp_{r4,5} \cdot \Delta_\theta} \cdot \left[\frac{k_5}{\Delta_\theta} \cdot \left(\frac{T_{4,12} - T_{5,12}}{r_4^{\,2}} \right) - \frac{k_5}{\Delta_\theta} \cdot \left(\frac{T_{5,12} - T_{6,12}}{r_4^{\,2}} \right) \right]$$

13

$$\frac{2 \cdot k_5}{\rho_5 \cdot Cp_{r5,5} \cdot \left[(r_5 + D2)^2 - (r_5 - D2)^2 \right]} \cdot \left[(T_{5,16} - T_{5,13}) \cdot \left(\frac{r_5 + D2}{\Delta_r} \right) - \left([T_{5,13} - T_{5,10}] \cdot \left[\frac{r_5 - D2}{\Delta_r} \right] \right) \right] + \frac{2}{\rho_5 \cdot Cp_{z1,5} \cdot \Delta_z} \cdot \left[\frac{k_5}{\Delta_z} \cdot (T_{5,14} - T_{5,13}) + h_{bottom} \cdot (Tf_{zb} - T_{5,13}) \right] + X_{5,13} = 0$$

$$X_{5,13} = \frac{1}{\rho_5 \cdot Cp_{r5,5} \cdot \Delta_\theta} \cdot \left[\frac{k_5}{\Delta_\theta} \cdot \left(\frac{T_{4,13} - T_{5,13}}{r_5^{\,2}} \right) - \frac{k_5}{\Delta_\theta} \cdot \left(\frac{T_{5,13} - T_{6,13}}{r_5^{\,2}} \right) \right]$$

14

$$\frac{2 \cdot k_5}{\rho_5 \cdot Cp_{r5,5} \cdot \left[(r_5 + D2)^2 - (r_5 - D2)^2 \right]} \cdot \left[(T_{5,17} - T_{5,14}) \cdot \left(\frac{r_5 + D2}{\Delta_r} \right) - \left([T_{5,14} - T_{5,11}] \cdot \left[\frac{r_5 - D2}{\Delta_r} \right] \right) \right] + \frac{1}{\rho_5 \cdot Cp_{z2,5} \cdot \Delta_z} \cdot \left[\frac{k_5}{\Delta_z} \cdot (T_{5,15} - T_{5,14}) - \frac{k_5}{\Delta_z} \cdot (T_{5,14} - T_{5,13}) \right] + X_{5,14} = 0$$

$$X_{5,14} = \frac{1}{\rho_5 \cdot Cp_{r5,5} \cdot \Delta_\theta} \cdot \left[\frac{k_5}{\Delta_\theta} \cdot \left(\frac{T_{4,14} - T_{5,14}}{r_5^{\,2}} \right) - \frac{k_5}{\Delta_\theta} \cdot \left(\frac{T_{5,14} - T_{6,14}}{r_5^{\,2}} \right) \right]$$

15

$$\frac{2 \cdot k_5}{\rho_5 \cdot Cp_{r5,5} \cdot \left[(r_5 + D2)^2 - (r_5 - D2)^2 \right]} \cdot \left[(T_{5,18} - T_{5,15}) \cdot \left(\frac{r_5 + D2}{\Delta_r} \right) - \left([T_{5,15} - T_{5,12}] \cdot \left[\frac{r_5 - D2}{\Delta_r} \right] \right) \right] + \frac{2}{\rho_5 \cdot Cp_{z3,5} \cdot \Delta_z} \cdot \left[\frac{k_5}{\Delta_z} \cdot (T_{5,14} - T_{5,15}) + h_{top} \cdot (Tf_{zt} - T_{5,15}) \right] + X_{5,15} = 0$$

$$X_{5,15} = \frac{1}{\rho_5 \cdot Cp_{r5,5} \cdot \Delta_\theta} \cdot \left[\frac{k_5}{\Delta_\theta} \cdot \left(\frac{T_{4,15} - T_{5,15}}{r_5^{\,2}} \right) - \frac{k_5}{\Delta_\theta} \cdot \left(\frac{T_{5,15} - T_{6,15}}{r_5^{\,2}} \right) \right]$$

16

$$\frac{2 \cdot k_5}{\rho_5 \cdot Cp_{r6,5} \cdot \left[(r_6 + D2)^2 - (r_6 - D2)^2 \right]} \cdot \left[(T_{5,19} - T_{5,16}) \cdot \left(\frac{r_6 + D2}{\Delta_r} \right) - \left(\left[T_{5,16} - T_{5,13} \right] \cdot \left[\frac{r_6 - D2}{\Delta_r} \right] \right) \right]$$
$$+ \frac{2}{\rho_5 \cdot Cp_{z1,5} \cdot \Delta_z} \cdot \left[\frac{k_5}{\Delta_z} \cdot (T_{5,17} - T_{5,16}) + h_{bottom} \cdot (Tf_{zb} - T_{5,16}) \right] + X_{5,16} = 0$$

$$X_{5,16} = \frac{1}{\rho_5 \cdot Cp_{r6,5} \cdot \Delta_\theta} \cdot \left[\frac{k_5}{\Delta_\theta} \cdot \left(\frac{T_{4,16} - T_{5,16}}{r_6^{\,2}} \right) - \frac{k_5}{\Delta_\theta} \cdot \left(\frac{T_{5,16} - T_{6,16}}{r_6^{\,2}} \right) \right]$$

17

$$\frac{2 \cdot k_5}{\rho_5 \cdot Cp_{r6,5} \cdot \left[(r_6 + D2)^2 - (r_6 - D2)^2 \right]} \cdot \left[(T_{5,20} - T_{5,17}) \cdot \left(\frac{r_6 + D2}{\Delta_r} \right) - \left(\left[T_{5,17} - T_{5,14} \right] \cdot \left[\frac{r_6 - D2}{\Delta_r} \right] \right) \right]$$
$$+ \frac{1}{\rho_5 \cdot Cp_{z2,5} \cdot \Delta_z} \cdot \left[\frac{k_5}{\Delta_z} \cdot (T_{5,18} - T_{5,17}) - \frac{k_5}{\Delta_z} \cdot (T_{5,17} - T_{5,16}) \right] + X_{5,17} = 0$$

$$X_{5,17} = \frac{1}{\rho_5 \cdot Cp_{r6,5} \cdot \Delta_\theta} \cdot \left[\frac{k_5}{\Delta_\theta} \cdot \left(\frac{T_{4,17} - T_{5,17}}{r_6^{\,2}} \right) - \frac{k_5}{\Delta_\theta} \cdot \left(\frac{T_{5,17} - T_{6,17}}{r_6^{\,2}} \right) \right]$$

18

$$\frac{2 \cdot k_5}{\rho_5 \cdot Cp_{r6,5} \cdot \left[(r_6 + D2)^2 - (r_6 - D2)^2 \right]} \cdot \left[(T_{5,21} - T_{5,18}) \cdot \left(\frac{r_6 + D2}{\Delta_r} \right) - \left(\left[T_{5,18} - T_{5,15} \right] \cdot \left[\frac{r_6 - D2}{\Delta_r} \right] \right) \right]$$
$$+ \frac{2}{\rho_5 \cdot Cp_{z3,5} \cdot \Delta_z} \cdot \left[\frac{k_5}{\Delta_z} \cdot (T_{5,17} - T_{5,18}) + h_{top} \cdot (Tf_{zt} - T_{5,18}) \right] + X_{5,18} = 0$$

$$X_{5,18} = \frac{1}{\rho_5 \cdot Cp_{r6,5} \cdot \Delta_\theta} \cdot \left[\frac{k_5}{\Delta_\theta} \cdot \left(\frac{T_{4,18} - T_{5,18}}{r_6^{\,2}} \right) - \frac{k_5}{\Delta_\theta} \cdot \left(\frac{T_{5,18} - T_{6,18}}{r_6^{\,2}} \right) \right]$$

19

$$\frac{2 \cdot k_5}{\rho_5 \cdot Cp_{r7,5} \cdot \left[(r_7 + D2)^2 - (r_7 - D2)^2 \right]} \cdot \left[(T_{5,22} - T_{5,19}) \cdot \left(\frac{r_7 + D2}{\Delta_r} \right) - \left(\left[T_{5,19} - T_{5,16} \right] \cdot \left[\frac{r_7 - D2}{\Delta_r} \right] \right) \right]$$
$$+ \frac{2}{\rho_5 \cdot Cp_{z1,5} \cdot \Delta_z} \cdot \left[\frac{k_5}{\Delta_z} \cdot (T_{5,20} - T_{5,19}) + h_{bottom} \cdot (Tf_{zb} - T_{5,19}) \right] + X_{5,19} = 0$$

$$X_{5,19} = \frac{1}{\rho_5 \cdot Cp_{r7,5} \cdot \Delta_\theta} \cdot \left[\frac{k_5}{\Delta_\theta} \cdot \left(\frac{T_{4,19} - T_{5,19}}{r_7^{\,2}} \right) - \frac{k_5}{\Delta_\theta} \cdot \left(\frac{T_{5,19} - T_{6,19}}{r_7^{\,2}} \right) \right]$$

20

$$\frac{2 \cdot k_5}{\rho_5 \cdot Cp_{r7,5} \cdot \left[(r_7 + D2)^2 - (r_7 - D2)^2 \right]} \cdot \left[(T_{5,23} - T_{5,20}) \cdot \left(\frac{r_7 + D2}{\Delta_r} \right) - \left(\left[T_{5,20} - T_{5,17} \right] \cdot \left[\frac{r_7 - D2}{\Delta_r} \right] \right) \right]$$
$$+ \frac{1}{\rho_5 \cdot Cp_{z2,5} \cdot \Delta_z} \cdot \left[\frac{k_5}{\Delta_z} \cdot (T_{5,21} - T_{5,20}) - \frac{k_5}{\Delta_z} \cdot (T_{5,20} - T_{5,19}) \right] + X_{5,20} = 0$$

$$X_{5,20} = \frac{1}{\rho_5 \cdot Cp_{r7,5} \cdot \Delta_\theta} \cdot \left[\frac{k_5}{\Delta_\theta} \cdot \left(\frac{T_{4,20} - T_{5,20}}{r_7^{\,2}} \right) - \frac{k_5}{\Delta_\theta} \cdot \left(\frac{T_{5,20} - T_{6,20}}{r_7^{\,2}} \right) \right]$$

21

$$\frac{2 \cdot k_5}{\rho_5 \cdot Cp_{r7,5} \cdot \left[(r_7 + D2)^2 - (r_7 - D2)^2 \right]} \cdot \left[(T_{5,24} - T_{5,21}) \cdot \left(\frac{r_7 + D2}{\Delta_r} \right) - \left(\left[T_{5,21} - T_{5,18} \right] \cdot \left[\frac{r_7 - D2}{\Delta_r} \right] \right) \right]$$
$$+ \frac{2}{\rho_5 \cdot Cp_{z3,5} \cdot \Delta_z} \cdot \left[\frac{k_5}{\Delta_z} \cdot (T_{5,20} - T_{5,21}) + h_{top} \cdot (Tf_{zt} - T_{5,21}) \right] + X_{5,21} = 0$$

$$X_{5,21} = \frac{1}{\rho_5 \cdot Cp_{r7,5} \cdot \Delta_\theta} \cdot \left[\frac{k_5}{\Delta_\theta} \cdot \left(\frac{T_{4,21} - T_{5,21}}{r_7^{\,2}} \right) - \frac{k_5}{\Delta_\theta} \cdot \left(\frac{T_{5,21} - T_{6,21}}{r_7^{\,2}} \right) \right]$$

22

$$\frac{2 \cdot k_5}{\rho_5 \cdot Cp_{r8,5} \cdot \left[(r_8 + D2)^2 - (r_8 - D2)^2 \right]} \cdot \left[(T_{5,25} - T_{5,22}) \cdot \left(\frac{r_8 + D2}{\Delta_r} \right) - \left([T_{5,22} - T_{5,19}] \cdot \left[\frac{r_8 - D2}{\Delta_r} \right] \right) \right]$$
$$+ \frac{2}{\rho_5 \cdot Cp_{z1,5} \cdot \Delta_z} \cdot \left[\frac{k_5}{\Delta_z} \cdot (T_{5,23} - T_{5,22}) + h_{bottom} \cdot (Tf_{zb} - T_{5,22}) \right] + X_{5,22} = 0$$

$$X_{5,22} = \frac{1}{\rho_5 \cdot Cp_{r8,5} \cdot \Delta_\theta} \cdot \left[\frac{k_5}{\Delta_\theta} \cdot \left(\frac{T_{4,22} - T_{5,22}}{r_8^2} \right) - \frac{k_5}{\Delta_\theta} \cdot \left(\frac{T_{5,22} - T_{6,22}}{r_8^2} \right) \right]$$

23

$$\frac{2 \cdot k_5}{\rho_5 \cdot Cp_{r8,5} \cdot \left[(r_8 + D2)^2 - (r_8 - D2)^2 \right]} \cdot \left[(T_{5,26} - T_{5,23}) \cdot \left(\frac{r_8 + D2}{\Delta_r} \right) - \left([T_{5,23} - T_{5,20}] \cdot \left[\frac{r_8 - D2}{\Delta_r} \right] \right) \right]$$
$$+ \frac{1}{\rho_5 \cdot Cp_{z2,5} \cdot \Delta_z} \cdot \left[\frac{k_5}{\Delta_z} \cdot (T_{5,24} - T_{5,23}) - \frac{k_5}{\Delta_z} \cdot (T_{5,23} - T_{5,22}) \right] + X_{5,23} = 0$$

$$X_{5,23} = \frac{1}{\rho_5 \cdot Cp_{r8,5} \cdot \Delta_\theta} \cdot \left[\frac{k_5}{\Delta_\theta} \cdot \left(\frac{T_{4,23} - T_{5,23}}{r_8^2} \right) - \frac{k_5}{\Delta_\theta} \cdot \left(\frac{T_{5,23} - T_{6,23}}{r_8^2} \right) \right]$$

24

$$\frac{2 \cdot k_5}{\rho_5 \cdot Cp_{r8,5} \cdot \left[(r_8 + D2)^2 - (r_8 - D2)^2 \right]} \cdot \left[(T_{5,27} - T_{5,24}) \cdot \left(\frac{r_8 + D2}{\Delta_r} \right) - \left([T_{5,24} - T_{5,21}] \cdot \left[\frac{r_8 - D2}{\Delta_r} \right] \right) \right]$$
$$+ \frac{2}{\rho_5 \cdot Cp_{z3,5} \cdot \Delta_z} \cdot \left[\frac{k_5}{\Delta_z} \cdot (T_{5,23} - T_{5,24}) + h_{top} \cdot (Tf_{zt} - T_{5,24}) \right] + X_{5,24} = 0$$

$$X_{5,24} = \frac{1}{\rho_5 \cdot Cp_{r8,5} \cdot \Delta_\theta} \cdot \left[\frac{k_5}{\Delta_\theta} \cdot \left(\frac{T_{4,24} - T_{5,24}}{r_8^2} \right) - \frac{k_5}{\Delta_\theta} \cdot \left(\frac{T_{5,24} - T_{6,24}}{r_8^2} \right) \right]$$

25

$$\frac{2}{\rho_5 \cdot Cp_{r9,5} \cdot \left[(r_9 + D2)^2 - (r_9 - D2)^2 \right]} \cdot \left[r_{out} \cdot h_{outside} \cdot (Tf_{ro} - T_{5,25}) + (r_9 - D2) \cdot k_5 \cdot \left(\frac{T_{5,22} - T_{5,25}}{\Delta_r} \right) \right]$$
$$+ \frac{2}{\rho_5 \cdot Cp_{z1,5} \cdot \Delta_z} \cdot \left[\frac{k_5}{\Delta_z} \cdot (T_{5,26} - T_{5,25}) + h_{bottom} \cdot (Tf_{zb} - T_{5,25}) \right] + X_{5,25} = 0$$

$$X_{5,25} = \frac{1}{\rho_5 \cdot Cp_{r9,5} \cdot \Delta_\theta} \cdot \left[\frac{k_5}{\Delta_\theta} \cdot \left(\frac{T_{4,25} - T_{5,25}}{r_9^2} \right) - \frac{k_5}{\Delta_\theta} \cdot \left(\frac{T_{5,25} - T_{6,25}}{r_9^2} \right) \right]$$

26

$$\frac{2}{\rho_5 \cdot Cp_{r9,5} \cdot \left[(r_9 + D2)^2 - (r_9 - D2)^2 \right]} \cdot \left[r_{out} \cdot h_{outside} \cdot (Tf_{ro} - T_{5,26}) + (r_9 - D2) \cdot k_5 \cdot \left(\frac{T_{5,23} - T_{5,26}}{\Delta_r} \right) \right]$$
$$+ \frac{1}{\rho_5 \cdot Cp_{z2,5} \cdot \Delta_z} \cdot \left[\frac{k_5}{\Delta_z} \cdot (T_{5,27} - T_{5,26}) - \frac{k_5}{\Delta_z} \cdot (T_{5,26} - T_{5,25}) \right] + X_{5,26} = 0$$

$$X_{5,26} = \frac{1}{\rho_5 \cdot Cp_{r9,5} \cdot \Delta_\theta} \cdot \left[\frac{k_5}{\Delta_\theta} \cdot \left(\frac{T_{4,26} - T_{5,26}}{r_9^2} \right) - \frac{k_5}{\Delta_\theta} \cdot \left(\frac{T_{5,26} - T_{6,26}}{r_9^2} \right) \right]$$

27

$$\frac{2}{\rho_5 \cdot Cp_{r9,5} \cdot \left[(r_9 + D2)^2 - (r_9 - D2)^2 \right]} \cdot \left[r_{out} \cdot h_{outside} \cdot (Tf_{ro} - T_{5,27}) + (r_9 - D2) \cdot k_5 \cdot \left(\frac{T_{5,24} - T_{5,27}}{\Delta_r} \right) \right]$$
$$+ \frac{2}{\rho_5 \cdot Cp_{z3,5} \cdot \Delta_z} \cdot \left[\frac{k_5}{\Delta_z} \cdot (T_{5,26} - T_{5,27}) + h_{top} \cdot (Tf_{zt} - T_{5,27}) \right] + X_{5,27} = 0$$

$$X_{5,27} = \frac{1}{\rho_5 \cdot Cp_{r9,5} \cdot \Delta_\theta} \cdot \left[\frac{k_5}{\Delta_\theta} \cdot \left(\frac{T_{4,27} - T_{5,27}}{r_9^2} \right) - \frac{k_5}{\Delta_\theta} \cdot \left(\frac{T_{5,27} - T_{6,27}}{r_9^2} \right) \right]$$

**********BLOCK 6**********

*****NODE*****

1

$$\frac{2}{\rho_6 \cdot Cp_{r1,6} \cdot \left[(r_1 + D2)^2 - (r_1 - D2)^2 \right]} \cdot \left[r_{in} \cdot h_{inside} \cdot (Tf_{ri} - T_{6,1}) + (r_1 + D2) \cdot k_6 \cdot \left(\frac{T_{6,4} - T_{6,1}}{\Delta_r} \right) \right] + \frac{2}{\rho_6 \cdot Cp_{z1,6} \cdot \Delta_z}$$

$$X_{6,1} = \frac{1}{\rho_6 \cdot Cp_{r1,6} \cdot \Delta_\theta} \cdot \left[\frac{k_6}{\Delta_\theta} \cdot \left(\frac{T_{5,1} - T_{6,1}}{r_1^{\,2}} \right) - \frac{k_6}{\Delta_\theta} \cdot \left(\frac{T_{6,1} - T_{7,1}}{r_1^{\,2}} \right) \right]$$

2

$$\frac{2}{\rho_6 \cdot Cp_{r1,6} \cdot \left[(r_1 + D2)^2 - (r_1 - D2)^2 \right]} \cdot \left[r_{in} \cdot h_{inside} \cdot (Tf_{ri} - T_{6,2}) + (r_1 + D2) \cdot k_6 \cdot \left(\frac{T_{6,5} - T_{6,2}}{\Delta_r} \right) \right] + \frac{1}{\rho_6 \cdot Cp_{z2,6} \cdot \Delta_z} \cdot \left[\frac{k_6}{\Delta_z} \cdot (T_{6,3} - T_{6,2}) - \frac{k_6}{\Delta_z} \cdot (T_{6,2} - T_{6,1}) \right] + X_{6,2} = 0$$

$$X_{6,2} = \frac{1}{\rho_6 \cdot Cp_{r1,6} \cdot \Delta_\theta} \cdot \left[\frac{k_6}{\Delta_\theta} \cdot \left(\frac{T_{5,2} - T_{6,2}}{r_1^{\,2}} \right) - \frac{k_6}{\Delta_\theta} \cdot \left(\frac{T_{6,2} - T_{7,2}}{r_1^{\,2}} \right) \right]$$

3

$$\frac{2}{\rho_6 \cdot Cp_{r1,6} \cdot \left[(r_1 + D2)^2 - (r_1 - D2)^2 \right]} \cdot \left[r_{in} \cdot h_{inside} \cdot (Tf_{ri} - T_{6,3}) + (r_1 + D2) \cdot k_6 \cdot \left(\frac{T_{6,6} - T_{6,3}}{\Delta_r} \right) \right] + \frac{2}{\rho_6 \cdot Cp_{z3,6} \cdot \Delta_z} \cdot \left[\frac{k_6}{\Delta_z} \cdot (T_{6,2} - T_{6,3}) + h_{top} \cdot (Tf_{zt} - T_{6,3}) \right] + X_{6,3} = 0$$

$$X_{6,3} = \frac{1}{\rho_6 \cdot Cp_{r1,6} \cdot \Delta_\theta} \cdot \left[\frac{k_6}{\Delta_\theta} \cdot \left(\frac{T_{5,3} - T_{6,3}}{r_1^{\,2}} \right) - \frac{k_6}{\Delta_\theta} \cdot \left(\frac{T_{6,3} - T_{7,3}}{r_1^{\,2}} \right) \right]$$

4

$$\frac{2 \cdot k_6}{\rho_6 \cdot Cp_{r2,6} \cdot \left[(r_2 + D2)^2 - (r_2 - D2)^2 \right]} \cdot \left[(T_{6,7} - T_{6,4}) \cdot \left(\frac{r_2 + D2}{\Delta_r} \right) - \left(\left[T_{6,4} - T_{6,1} \right] \cdot \left[\frac{r_2 - D2}{\Delta_r} \right] \right) \right] + \frac{2}{\rho_6 \cdot Cp_{z1,6} \cdot \Delta_z} \cdot \left[\frac{k_6}{\Delta_z} \cdot (T_{6,5} - T_{6,4}) + h_{bottom} \cdot (Tf_{zb} - T_{6,4}) \right] + X_{6,4} = 0$$

$$X_{6,4} = \frac{1}{\rho_6 \cdot Cp_{r2,6} \cdot \Delta_\theta} \cdot \left[\frac{k_6}{\Delta_\theta} \cdot \left(\frac{T_{5,4} - T_{6,4}}{r_2^{\,2}} \right) - \frac{k_6}{\Delta_\theta} \cdot \left(\frac{T_{6,4} - T_{7,4}}{r_2^{\,2}} \right) \right]$$

5

$$\frac{2 \cdot k_6}{\rho_6 \cdot Cp_{r2,6} \cdot \left[(r_2 + D2)^2 - (r_2 - D2)^2 \right]} \cdot \left[(T_{6,8} - T_{6,5}) \cdot \left(\frac{r_2 + D2}{\Delta_r} \right) - \left(\left[T_{6,5} - T_{6,2} \right] \cdot \left[\frac{r_2 - D2}{\Delta_r} \right] \right) \right] + \frac{1}{\rho_6 \cdot Cp_{z2,6} \cdot \Delta_z} \cdot \left[\frac{k_6}{\Delta_z} \cdot (T_{6,6} - T_{6,5}) - \frac{k_6}{\Delta_z} \cdot (T_{6,5} - T_{6,4}) \right] + X_{6,5} = 0$$

$$X_{6,5} = \frac{1}{\rho_6 \cdot Cp_{r2,6} \cdot \Delta_\theta} \cdot \left[\frac{k_6}{\Delta_\theta} \cdot \left(\frac{T_{5,5} - T_{6,5}}{r_2^{\,2}} \right) - \frac{k_6}{\Delta_\theta} \cdot \left(\frac{T_{6,5} - T_{7,5}}{r_2^{\,2}} \right) \right]$$

6

$$\frac{2 \cdot k_6}{\rho_6 \cdot Cp_{r2,6} \cdot \left[(r_2 + D2)^2 - (r_2 - D2)^2 \right]} \cdot \left[(T_{6,9} - T_{6,6}) \cdot \left(\frac{r_2 + D2}{\Delta_r} \right) - \left(\left[T_{6,6} - T_{6,3} \right] \cdot \left[\frac{r_2 - D2}{\Delta_r} \right] \right) \right] + \frac{2}{\rho_6 \cdot Cp_{z3,6} \cdot \Delta_z} \cdot \left[\frac{k_6}{\Delta_z} \cdot (T_{6,5} - T_{6,6}) + h_{top} \cdot (Tf_{zt} - T_{6,6}) \right] + X_{6,6} = 0$$

$$X_{6,6} = \frac{1}{\rho_6 \cdot Cp_{r2,6} \cdot \Delta_\theta} \cdot \left[\frac{k_6}{\Delta_\theta} \cdot \left(\frac{T_{5,6} - T_{6,6}}{r_2^{\,2}} \right) - \frac{k_6}{\Delta_\theta} \cdot \left(\frac{T_{6,6} - T_{7,6}}{r_2^{\,2}} \right) \right]$$

7

$$\frac{2 \cdot k_6}{\rho_6 \cdot Cp_{r3,6} \cdot \left[(r_3 + D2)^2 - (r_3 - D2)^2 \right]} \cdot \left[(T_{6,10} - T_{6,7}) \cdot \left(\frac{r_3 + D2}{\Delta_r} \right) - \left(\left[T_{6,7} - T_{6,4} \right] \cdot \left[\frac{r_3 - D2}{\Delta_r} \right] \right) \right] + \frac{2}{\rho_6 \cdot Cp_{z1,6} \cdot \Delta_z} \cdot \left[\frac{k_6}{\Delta_z} \cdot (T_{6,8} - T_{6,7}) + h_{bottom} \cdot (Tf_{zb} - T_{6,7}) \right] + X_{6,7} = 0$$

$$X_{6,7} = \frac{1}{\rho_6 \cdot Cp_{r3,6} \cdot \Delta_\theta} \cdot \left[\frac{k_6}{\Delta_\theta} \cdot \left(\frac{T_{5,7} - T_{6,7}}{r_3^{\,2}} \right) - \frac{k_6}{\Delta_\theta} \cdot \left(\frac{T_{6,7} - T_{7,7}}{r_3^{\,2}} \right) \right]$$

8 $$\cdot \left[\frac{k_6}{\Delta_z} \cdot (T_{6,2} - T_{6,1}) + h_{bottom} \cdot (Tf_{zb} - T_{6,1}) \right] + X_{6,1} = 0$$

$$\frac{2 \cdot k_6}{\rho_6 \cdot Cp_{r3,6} \cdot \left[(r_3 + D2)^2 - (r_3 - D2)^2 \right]} \cdot \left[(T_{6,11} - T_{6,8}) \cdot \left(\frac{r_3 + D2}{\Delta_r} \right) - \left([T_{6,8} - T_{6,5}] \cdot \left[\frac{r_3 - D2}{\Delta_r} \right] \right) \right]$$
$$+ \frac{1}{\rho_6 \cdot Cp_{z2,6} \cdot \Delta_z} \cdot \left[\frac{k_6}{\Delta_z} \cdot (T_{6,9} - T_{6,8}) - \frac{k_6}{\Delta_z} \cdot (T_{6,8} - T_{6,7}) \right] + X_{6,8} = 0$$

$$X_{6,8} = \frac{1}{\rho_6 \cdot Cp_{r3,6} \cdot \Delta_\theta} \cdot \left[\frac{k_6}{\Delta_\theta} \cdot \left(\frac{T_{5,8} - T_{6,8}}{r_3^{\,2}} \right) - \frac{k_6}{\Delta_\theta} \cdot \left(\frac{T_{6,8} - T_{7,8}}{r_3^{\,2}} \right) \right]$$

9

$$\frac{2 \cdot k_6}{\rho_6 \cdot Cp_{r3,6} \cdot \left[(r_3 + D2)^2 - (r_3 - D2)^2 \right]} \cdot \left[(T_{6,12} - T_{6,9}) \cdot \left(\frac{r_3 + D2}{\Delta_r} \right) - \left([T_{6,9} - T_{6,6}] \cdot \left[\frac{r_3 - D2}{\Delta_r} \right] \right) \right]$$
$$+ \frac{2}{\rho_6 \cdot Cp_{z3,6} \cdot \Delta_z} \cdot \left[\frac{k_6}{\Delta_z} \cdot (T_{6,8} - T_{6,9}) + h_{top} \cdot (Tf_{zt} - T_{6,9}) \right] + X_{6,9} = 0$$

$$X_{6,9} = \frac{1}{\rho_6 \cdot Cp_{r3,6} \cdot \Delta_\theta} \cdot \left[\frac{k_6}{\Delta_\theta} \cdot \left(\frac{T_{5,9} - T_{6,9}}{r_3^{\,2}} \right) - \frac{k_6}{\Delta_\theta} \cdot \left(\frac{T_{6,9} - T_{7,9}}{r_3^{\,2}} \right) \right]$$

10

$$\frac{2 \cdot k_6}{\rho_6 \cdot Cp_{r4,6} \cdot \left[(r_4 + D2)^2 - (r_4 - D2)^2 \right]} \cdot \left[(T_{6,13} - T_{6,10}) \cdot \left(\frac{r_4 + D2}{\Delta_r} \right) - \left([T_{6,10} - T_{6,7}] \cdot \left[\frac{r_4 - D2}{\Delta_r} \right] \right) \right]$$
$$+ \frac{2}{\rho_6 \cdot Cp_{z1,6} \cdot \Delta_z} \cdot \left[\frac{k_6}{\Delta_z} \cdot (T_{6,11} - T_{6,10}) + h_{bottom} \cdot (Tf_{zb} - T_{6,10}) \right] + X_{6,10} = 0$$

$$X_{6,10} = \frac{1}{\rho_6 \cdot Cp_{r4,6} \cdot \Delta_\theta} \cdot \left[\frac{k_6}{\Delta_\theta} \cdot \left(\frac{T_{5,10} - T_{6,10}}{r_4^{\,2}} \right) - \frac{k_6}{\Delta_\theta} \cdot \left(\frac{T_{6,10} - T_{7,10}}{r_4^{\,2}} \right) \right]$$

11

$$\frac{2 \cdot k_6}{\rho_6 \cdot Cp_{r4,6} \cdot \left[(r_4 + D2)^2 - (r_4 - D2)^2 \right]} \cdot \left[(T_{6,14} - T_{6,11}) \cdot \left(\frac{r_4 + D2}{\Delta_r} \right) - \left([T_{6,11} - T_{6,8}] \cdot \left[\frac{r_4 - D2}{\Delta_r} \right] \right) \right]$$
$$+ \frac{1}{\rho_6 \cdot Cp_{z2,6} \cdot \Delta_z} \cdot \left[\frac{k_6}{\Delta_z} \cdot (T_{6,12} - T_{6,11}) - \frac{k_6}{\Delta_z} \cdot (T_{6,11} - T_{6,10}) \right] + X_{6,11} = 0$$

$$X_{6,11} = \frac{1}{\rho_6 \cdot Cp_{r4,6} \cdot \Delta_\theta} \cdot \left[\frac{k_6}{\Delta_\theta} \cdot \left(\frac{T_{5,11} - T_{6,11}}{r_4^{\,2}} \right) - \frac{k_6}{\Delta_\theta} \cdot \left(\frac{T_{6,11} - T_{7,11}}{r_4^{\,2}} \right) \right]$$

12

$$\frac{2 \cdot k_6}{\rho_6 \cdot Cp_{r4,6} \cdot \left[(r_4 + D2)^2 - (r_4 - D2)^2 \right]} \cdot \left[(T_{6,15} - T_{6,12}) \cdot \left(\frac{r_4 + D2}{\Delta_r} \right) - \left([T_{6,12} - T_{6,9}] \cdot \left[\frac{r_4 - D2}{\Delta_r} \right] \right) \right]$$
$$+ \frac{2}{\rho_6 \cdot Cp_{z3,6} \cdot \Delta_z} \cdot \left[\frac{k_6}{\Delta_z} \cdot (T_{6,11} - T_{6,12}) + h_{top} \cdot (Tf_{zt} - T_{6,12}) \right] + X_{6,12} = 0$$

$$X_{6,12} = \frac{1}{\rho_6 \cdot Cp_{r4,6} \cdot \Delta_\theta} \cdot \left[\frac{k_6}{\Delta_\theta} \cdot \left(\frac{T_{5,12} - T_{6,12}}{r_4^{\,2}} \right) - \frac{k_6}{\Delta_\theta} \cdot \left(\frac{T_{6,12} - T_{7,12}}{r_4^{\,2}} \right) \right]$$

13

$$\frac{2 \cdot k_6}{\rho_6 \cdot Cp_{r5,6} \cdot \left[(r_5 + D2)^2 - (r_5 - D2)^2 \right]} \cdot \left[(T_{6,16} - T_{6,13}) \cdot \left(\frac{r_5 + D2}{\Delta_r} \right) - \left([T_{6,13} - T_{6,10}] \cdot \left[\frac{r_5 - D2}{\Delta_r} \right] \right) \right]$$
$$+ \frac{2}{\rho_6 \cdot Cp_{z1,6} \cdot \Delta_z} \cdot \left[\frac{k_6}{\Delta_z} \cdot (T_{6,14} - T_{6,13}) + h_{bottom} \cdot (Tf_{zb} - T_{6,13}) \right] + X_{6,13} = 0$$

$$X_{6,13} = \frac{1}{\rho_6 \cdot Cp_{r5,6} \cdot \Delta_\theta} \cdot \left[\frac{k_6}{\Delta_\theta} \cdot \left(\frac{T_{5,13} - T_{6,13}}{r_5^{\,2}} \right) - \frac{k_6}{\Delta_\theta} \cdot \left(\frac{T_{6,13} - T_{7,13}}{r_5^{\,2}} \right) \right]$$

14

$$\frac{2 \cdot k_6}{\rho_6 \cdot Cp_{r5,6} \cdot \left[(r_5 + D2)^2 - (r_5 - D2)^2 \right]} \cdot \left[(T_{6,17} - T_{6,14}) \cdot \left(\frac{r_5 + D2}{\Delta_r} \right) - \left([T_{6,14} - T_{6,11}] \cdot \left[\frac{r_5 - D2}{\Delta_r} \right] \right) \right]$$
$$+ \frac{1}{\rho_6 \cdot Cp_{z2,6} \cdot \Delta_z} \cdot \left[\frac{k_6}{\Delta_z} \cdot (T_{6,15} - T_{6,14}) - \frac{k_6}{\Delta_z} \cdot (T_{6,14} - T_{6,13}) \right] + X_{6,14} = 0$$

$$X_{6,14} = \frac{1}{\rho_6 \cdot Cp_{r5,6} \cdot \Delta_\theta} \cdot \left[\frac{k_6}{\Delta_\theta} \cdot \left(\frac{T_{5,14} - T_{6,14}}{r_5^{\,2}} \right) - \frac{k_6}{\Delta_\theta} \cdot \left(\frac{T_{6,14} - T_{7,14}}{r_5^{\,2}} \right) \right]$$

15

$$\frac{2 \cdot k_6}{\rho_6 \cdot Cp_{r5,6} \cdot \left[(r_5 + D2)^2 - (r_5 - D2)^2 \right]} \cdot \left[(T_{6,16} - T_{6,15}) \cdot \left(\frac{r_5 + D2}{\Delta_r} \right) - \left([T_{6,15} - T_{6,12}] \cdot \left[\frac{r_5 - D2}{\Delta_r} \right] \right) \right]$$
$$+ \frac{2}{\rho_6 \cdot Cp_{z3,6} \cdot \Delta_z} \cdot \left[\frac{k_6}{\Delta_z} \cdot (T_{6,14} - T_{6,15}) + h_{top} \cdot (Tf_{zt} - T_{6,15}) \right] + X_{6,15} = 0$$

$$X_{6,15} = \frac{1}{\rho_6 \cdot Cp_{r5,6} \cdot \Delta_\theta} \cdot \left[\frac{k_6}{\Delta_\theta} \cdot \left(\frac{T_{5,15} - T_{6,15}}{r_5^{\,2}} \right) - \frac{k_6}{\Delta_\theta} \cdot \left(\frac{T_{6,15} - T_{7,15}}{r_5^{\,2}} \right) \right]$$

16

$$\frac{2 \cdot k_6}{\rho_6 \cdot Cp_{r6,6} \cdot \left[(r_6 + D2)^2 - (r_6 - D2)^2 \right]} \cdot \left[(T_{6,17} - T_{6,16}) \cdot \left(\frac{r_6 + D2}{\Delta_r} \right) - \left([T_{6,16} - T_{6,13}] \cdot \left[\frac{r_6 - D2}{\Delta_r} \right] \right) \right]$$
$$+ \frac{2}{\rho_6 \cdot Cp_{z1,6} \cdot \Delta_z} \cdot \left[\frac{k_6}{\Delta_z} \cdot (T_{6,17} - T_{6,16}) + h_{bottom} \cdot (Tf_{zb} - T_{6,16}) \right] + X_{6,16} = 0$$

$$X_{6,16} = \frac{1}{\rho_6 \cdot Cp_{r6,6} \cdot \Delta_\theta} \cdot \left[\frac{k_6}{\Delta_\theta} \cdot \left(\frac{T_{5,16} - T_{6,16}}{r_6^{\,2}} \right) - \frac{k_6}{\Delta_\theta} \cdot \left(\frac{T_{6,16} - T_{7,16}}{r_6^{\,2}} \right) \right]$$

17

$$\frac{2 \cdot k_6}{\rho_6 \cdot Cp_{r6,6} \cdot \left[(r_6 + D2)^2 - (r_6 - D2)^2 \right]} \cdot \left[(T_{6,20} - T_{6,17}) \cdot \left(\frac{r_6 + D2}{\Delta_r} \right) - \left([T_{6,17} - T_{6,14}] \cdot \left[\frac{r_6 - D2}{\Delta_r} \right] \right) \right]$$
$$+ \frac{1}{\rho_6 \cdot Cp_{z2,6} \cdot \Delta_z} \cdot \left[\frac{k_6}{\Delta_z} \cdot (T_{6,18} - T_{6,17}) - \frac{k_6}{\Delta_z} \cdot (T_{6,17} - T_{6,16}) \right] + X_{6,17} = 0$$

$$X_{6,17} = \frac{1}{\rho_6 \cdot Cp_{r6,6} \cdot \Delta_\theta} \cdot \left[\frac{k_6}{\Delta_\theta} \cdot \left(\frac{T_{5,17} - T_{6,17}}{r_6^{\,2}} \right) - \frac{k_6}{\Delta_\theta} \cdot \left(\frac{T_{6,17} - T_{7,17}}{r_6^{\,2}} \right) \right]$$

18

$$\frac{2 \cdot k_6}{\rho_6 \cdot Cp_{r6,6} \cdot \left[(r_6 + D2)^2 - (r_6 - D2)^2 \right]} \cdot \left[(T_{6,21} - T_{6,18}) \cdot \left(\frac{r_6 + D2}{\Delta_r} \right) - \left([T_{6,18} - T_{6,15}] \cdot \left[\frac{r_6 - D2}{\Delta_r} \right] \right) \right]$$
$$+ \frac{2}{\rho_6 \cdot Cp_{z3,6} \cdot \Delta_z} \cdot \left[\frac{k_6}{\Delta_z} \cdot (T_{6,17} - T_{6,18}) + h_{top} \cdot (Tf_{zt} - T_{6,18}) \right] + X_{6,18} = 0$$

$$X_{6,18} = \frac{1}{\rho_6 \cdot Cp_{r6,6} \cdot \Delta_\theta} \cdot \left[\frac{k_6}{\Delta_\theta} \cdot \left(\frac{T_{5,18} - T_{6,18}}{r_6^{\,2}} \right) - \frac{k_6}{\Delta_\theta} \cdot \left(\frac{T_{6,18} - T_{7,18}}{r_6^{\,2}} \right) \right]$$

19

$$\frac{2 \cdot k_6}{\rho_6 \cdot Cp_{r7,6} \cdot \left[(r_7 + D2)^2 - (r_7 - D2)^2 \right]} \cdot \left[(T_{6,22} - T_{6,19}) \cdot \left(\frac{r_7 + D2}{\Delta_r} \right) - \left([T_{6,19} - T_{6,16}] \cdot \left[\frac{r_7 - D2}{\Delta_r} \right] \right) \right]$$
$$+ \frac{2}{\rho_6 \cdot Cp_{z1,6} \cdot \Delta_z} \cdot \left[\frac{k_6}{\Delta_z} \cdot (T_{6,20} - T_{6,19}) + h_{bottom} \cdot (Tf_{zb} - T_{6,19}) \right] + X_{6,19} = 0$$

$$X_{6,19} = \frac{1}{\rho_6 \cdot Cp_{r7,6} \cdot \Delta_\theta} \cdot \left[\frac{k_6}{\Delta_\theta} \cdot \left(\frac{T_{5,19} - T_{6,19}}{r_7^{\,2}} \right) - \frac{k_6}{\Delta_\theta} \cdot \left(\frac{T_{6,19} - T_{7,19}}{r_7^{\,2}} \right) \right]$$

20

$$\frac{2 \cdot k_6}{\rho_6 \cdot Cp_{r7,6} \cdot \left[(r_7 + D2)^2 - (r_7 - D2)^2 \right]} \cdot \left[(T_{6,23} - T_{6,20}) \cdot \left(\frac{r_7 + D2}{\Delta_r} \right) - \left([T_{6,20} - T_{6,17}] \cdot \left[\frac{r_7 - D2}{\Delta_r} \right] \right) \right]$$
$$+ \frac{1}{\rho_6 \cdot Cp_{z2,6} \cdot \Delta_z} \cdot \left[\frac{k_6}{\Delta_z} \cdot (T_{6,21} - T_{6,20}) - \frac{k_6}{\Delta_z} \cdot (T_{6,20} - T_{6,19}) \right] + X_{6,20} = 0$$

$$X_{6,20} = \frac{1}{\rho_6 \cdot Cp_{r7,6} \cdot \Delta_\theta} \cdot \left[\frac{k_6}{\Delta_\theta} \cdot \left(\frac{T_{5,20} - T_{6,20}}{r_7^{\,2}} \right) - \frac{k_6}{\Delta_\theta} \cdot \left(\frac{T_{6,20} - T_{7,20}}{r_7^{\,2}} \right) \right]$$

21

$$\frac{2 \cdot k_6}{\rho_6 \cdot Cp_{r7,6} \cdot \left[(r_7 + D2)^2 - (r_7 - D2)^2 \right]} \cdot \left[(T_{6,24} - T_{6,21}) \cdot \left(\frac{r_7 + D2}{\Delta_r} \right) - \left([T_{6,21} - T_{6,18}] \cdot \left[\frac{r_7 - D2}{\Delta_r} \right] \right) \right]$$

$$X_{6,21} = \frac{1}{\rho_6 \cdot Cp_{r7,6} \cdot \Delta_\theta} \cdot \left[\frac{k_6}{\Delta_\theta} \cdot \left(\frac{T_{5,21} - T_{6,21}}{r_7^{\,2}} \right) - \frac{k_6}{\Delta_\theta} \cdot \left(\frac{T_{6,21} - T_{7,21}}{r_7^{\,2}} \right) \right]$$

22

$$\frac{2 \cdot k_6}{\rho_6 \cdot Cp_{r8,6} \cdot \left[(r_8 + D2)^2 - (r_8 - D2)^2 \right]} \cdot \left[(T_{6,25} - T_{6,22}) \cdot \left(\frac{r_8 + D2}{\Delta_r} \right) - \left([T_{6,22} - T_{6,19}] \cdot \left[\frac{r_8 - D2}{\Delta_r} \right] \right) \right]$$
$$+ \frac{2}{\rho_6 \cdot Cp_{z1,6} \cdot \Delta_z} \cdot \left[\frac{k_6}{\Delta_z} \cdot (T_{6,23} - T_{6,22}) + h_{bottom} \cdot (Tf_{zb} - T_{6,22}) \right] + X_{6,22} = 0$$

$$X_{6,22} = \frac{1}{\rho_6 \cdot Cp_{r8,6} \cdot \Delta_\theta} \cdot \left[\frac{k_6}{\Delta_\theta} \cdot \left(\frac{T_{5,22} - T_{6,22}}{r_8^{\,2}} \right) - \frac{k_6}{\Delta_\theta} \cdot \left(\frac{T_{6,22} - T_{7,22}}{r_8^{\,2}} \right) \right]$$

23

$$\frac{2 \cdot k_6}{\rho_6 \cdot Cp_{r8,6} \cdot \left[(r_8 + D2)^2 - (r_8 - D2)^2 \right]} \cdot \left[(T_{6,26} - T_{6,23}) \cdot \left(\frac{r_8 + D2}{\Delta_r} \right) - \left([T_{6,23} - T_{6,20}] \cdot \left[\frac{r_8 - D2}{\Delta_r} \right] \right) \right]$$
$$+ \frac{1}{\rho_6 \cdot Cp_{z2,6} \cdot \Delta_z} \cdot \left[\frac{k_6}{\Delta_z} \cdot (T_{6,24} - T_{6,23}) - \frac{k_6}{\Delta_z} \cdot (T_{6,23} - T_{6,22}) \right] + X_{6,23} = 0$$

$$X_{6,23} = \frac{1}{\rho_6 \cdot Cp_{r8,6} \cdot \Delta_\theta} \cdot \left[\frac{k_6}{\Delta_\theta} \cdot \left(\frac{T_{5,23} - T_{6,23}}{r_8^{\,2}} \right) - \frac{k_6}{\Delta_\theta} \cdot \left(\frac{T_{6,23} - T_{7,23}}{r_8^{\,2}} \right) \right]$$

24

$$\frac{2 \cdot k_6}{\rho_6 \cdot Cp_{r8,6} \cdot \left[(r_8 + D2)^2 - (r_8 - D2)^2 \right]} \cdot \left[(T_{6,27} - T_{6,24}) \cdot \left(\frac{r_8 + D2}{\Delta_r} \right) - \left([T_{6,24} - T_{6,21}] \cdot \left[\frac{r_8 - D2}{\Delta_r} \right] \right) \right]$$
$$+ \frac{2}{\rho_6 \cdot Cp_{z3,6} \cdot \Delta_z} \cdot \left[\frac{k_6}{\Delta_z} \cdot (T_{6,23} - T_{6,24}) + h_{top} \cdot (Tf_{zt} - T_{6,24}) \right] + X_{6,24} = 0$$

$$X_{6,24} = \frac{1}{\rho_6 \cdot Cp_{r8,6} \cdot \Delta_\theta} \cdot \left[\frac{k_6}{\Delta_\theta} \cdot \left(\frac{T_{5,24} - T_{6,24}}{r_8^{\,2}} \right) - \frac{k_6}{\Delta_\theta} \cdot \left(\frac{T_{6,24} - T_{7,24}}{r_8^{\,2}} \right) \right]$$

25

$$\frac{2}{\rho_6 \cdot Cp_{r9,6} \cdot \left[(r_9 + D2)^2 - (r_9 - D2)^2 \right]} \cdot \left[r_{out} \cdot h_{outside} \cdot (Tf_{ro} - T_{6,25}) + (r_9 - D2) \cdot k_6 \cdot \left(\frac{T_{6,22} - T_{6,25}}{\Delta_r} \right) \right]$$
$$+ \frac{2}{\rho_6 \cdot Cp_{z1,6} \cdot \Delta_z} \cdot \left[\frac{k_6}{\Delta_z} \cdot (T_{6,26} - T_{6,25}) + h_{bottom} \cdot (Tf_{zb} - T_{6,25}) \right] + X_{6,25} = 0$$

$$X_{6,25} = \frac{1}{\rho_6 \cdot Cp_{r9,6} \cdot \Delta_\theta} \cdot \left[\frac{k_6}{\Delta_\theta} \cdot \left(\frac{T_{5,25} - T_{6,25}}{r_9^{\,2}} \right) - \frac{k_6}{\Delta_\theta} \cdot \left(\frac{T_{6,25} - T_{7,25}}{r_9^{\,2}} \right) \right]$$

26

$$\frac{2}{\rho_6 \cdot Cp_{r9,6} \cdot \left[(r_9 + D2)^2 - (r_9 - D2)^2 \right]} \cdot \left[r_{out} \cdot h_{outside} \cdot (Tf_{ro} - T_{6,26}) + (r_9 - D2) \cdot k_6 \cdot \left(\frac{T_{6,23} - T_{6,26}}{\Delta_r} \right) \right]$$
$$+ \frac{1}{\rho_6 \cdot Cp_{z2,6} \cdot \Delta_z} \cdot \left[\frac{k_6}{\Delta_z} \cdot (T_{6,27} - T_{6,26}) - \frac{k_6}{\Delta_z} \cdot (T_{6,26} - T_{6,25}) \right] + X_{6,26} = 0$$

$$X_{6,26} = \frac{1}{\rho_6 \cdot Cp_{r9,6} \cdot \Delta_\theta} \cdot \left[\frac{k_6}{\Delta_\theta} \cdot \left(\frac{T_{5,26} - T_{6,26}}{r_9^{\,2}} \right) - \frac{k_6}{\Delta_\theta} \cdot \left(\frac{T_{6,26} - T_{7,26}}{r_9^{\,2}} \right) \right]$$

27

$$\frac{2}{\rho_6 \cdot Cp_{r9,6} \cdot \left[(r_9 + D2)^2 - (r_9 - D2)^2 \right]} \cdot \left[r_{out} \cdot h_{outside} \cdot (Tf_{ro} - T_{6,27}) + (r_9 - D2) \cdot k_6 \cdot \left(\frac{T_{6,24} - T_{6,27}}{\Delta_r} \right) \right]$$
$$+ \frac{2}{\rho_6 \cdot Cp_{z3,6} \cdot \Delta_z} \cdot \left[\frac{k_6}{\Delta_z} \cdot (T_{6,26} - T_{6,27}) + h_{top} \cdot (Tf_{zt} - T_{6,27}) \right] + X_{6,27} = 0$$

$$X_{6,27} = \frac{1}{\rho_6 \cdot Cp_{r9,6} \cdot \Delta_\theta} \cdot \left[\frac{k_6}{\Delta_\theta} \cdot \left(\frac{T_{5,27} - T_{6,27}}{r_9^{\,2}} \right) - \frac{k_6}{\Delta_\theta} \cdot \left(\frac{T_{6,27} - T_{7,27}}{r_9^{\,2}} \right) \right]$$

**********BLOCK 7**********

$$+ \frac{2}{\rho_6 \cdot Cp_{z3,6} \cdot \Delta_z} \cdot \left[\frac{k_6}{\Delta_z} \cdot (T_{6,20} - T_{6,21}) + h_{top} \cdot (Tf_{zt} - T_{6,21}) \right] + X_{6,21} = 0$$

*****NODE*****

1

$$\frac{2}{\rho_7 \cdot Cp_{r1,7} \cdot [(r_1 + D2)^2 - (r_1 - D2)^2]} \cdot \left[r_{in} \cdot h_{inside} \cdot (Tf_{ri} - T_{7,1}) + (r_1 + D2) \cdot k_7 \cdot \left(\frac{T_{7,4} - T_{7,1}}{\Delta_r} \right) \right] + \frac{2}{\rho_7 \cdot Cp_{z1,7} \cdot \Delta_z} \cdot \left[\frac{k_7}{\Delta_z} \cdot (T_{7,2} - T_{7,1}) + h_{bottom} \cdot (Tf_{zb} - T_{7,1}) \right] + X_{7,1} = 0$$

$$X_{7,1} = \frac{1}{\rho_7 \cdot Cp_{r1,7} \cdot \Delta_\theta} \cdot \frac{k_7}{\Delta_\theta} \cdot \left[\frac{T_{6,1} - T_{7,1}}{r_1^2} \right]$$

2

$$\frac{2}{\rho_7 \cdot Cp_{r1,7} \cdot [(r_1 + D2)^2 - (r_1 - D2)^2]} \cdot \left[r_{in} \cdot h_{inside} \cdot (Tf_{ri} - T_{7,2}) + (r_1 + D2) \cdot k_7 \cdot \left(\frac{T_{7,5} - T_{7,2}}{\Delta_r} \right) \right] + \frac{1}{\rho_7 \cdot Cp_{z2,7} \cdot \Delta_z} \cdot \left[\frac{k_7}{\Delta_z} \cdot (T_{7,3} - T_{7,2}) - \frac{k_7}{\Delta_z} \cdot (T_{7,2} - T_{7,1}) \right] + X_{7,2} = 0$$

$$X_{7,2} = \frac{1}{\rho_7 \cdot Cp_{r1,7} \cdot \Delta_\theta} \cdot \frac{k_7}{\Delta_\theta} \cdot \left[\frac{T_{6,2} - T_{7,2}}{r_1^2} \right]$$

3

$$\frac{2}{\rho_7 \cdot Cp_{r1,7} \cdot [(r_1 + D2)^2 - (r_1 - D2)^2]} \cdot \left[r_{in} \cdot h_{inside} \cdot (Tf_{ri} - T_{7,3}) + (r_1 + D2) \cdot k_7 \cdot \left(\frac{T_{7,6} - T_{7,3}}{\Delta_r} \right) \right] + \frac{2}{\rho_7 \cdot Cp_{z3,7} \cdot \Delta_z} \cdot \left[\frac{k_7}{\Delta_z} \cdot (T_{7,2} - T_{7,3}) + h_{top} \cdot (Tf_{zt} - T_{7,3}) \right] + X_{7,3} = 0$$

$$X_{7,3} = \frac{1}{\rho_7 \cdot Cp_{r1,7} \cdot \Delta_\theta} \cdot \frac{k_7}{\Delta_\theta} \cdot \left[\frac{T_{6,3} - T_{7,3}}{r_1^2} \right]$$

4

$$\frac{2 \cdot k_7}{\rho_7 \cdot Cp_{r2,7} \cdot [(r_2 + D2)^2 - (r_2 - D2)^2]} \cdot \left[(T_{7,7} - T_{7,4}) \cdot \left(\frac{r_2 + D2}{\Delta_r} \right) - \left([T_{7,4} - T_{7,1}] \cdot \left[\frac{r_2 - D2}{\Delta_r} \right] \right) \right] + \frac{2}{\rho_7 \cdot Cp_{z1,7} \cdot \Delta_z} \cdot \left[\frac{k_7}{\Delta_z} \cdot (T_{7,5} - T_{7,4}) + h_{bottom} \cdot (Tf_{zb} - T_{7,4}) \right] + X_{7,4} = 0$$

$$X_{7,4} = \frac{1}{\rho_7 \cdot Cp_{r2,7} \cdot \Delta_\theta} \cdot \frac{k_7}{\Delta_\theta} \cdot \left[\frac{T_{6,4} - T_{7,4}}{r_2^2} \right]$$

5

$$\frac{2 \cdot k_7}{\rho_7 \cdot Cp_{r2,7} \cdot [(r_2 + D2)^2 - (r_2 - D2)^2]} \cdot \left[(T_{7,8} - T_{7,5}) \cdot \left(\frac{r_2 + D2}{\Delta_r} \right) - \left([T_{7,5} - T_{7,2}] \cdot \left[\frac{r_2 - D2}{\Delta_r} \right] \right) \right] + \frac{1}{\rho_7 \cdot Cp_{z2,7} \cdot \Delta_z} \cdot \left[\frac{k_7}{\Delta_z} \cdot (T_{7,6} - T_{7,5}) - \frac{k_7}{\Delta_z} \cdot (T_{7,5} - T_{7,4}) \right] + X_{7,5} = 0$$

$$X_{7,5} = \frac{1}{\rho_7 \cdot Cp_{r2,7} \cdot \Delta_\theta} \cdot \frac{k_7}{\Delta_\theta} \cdot \left[\frac{T_{6,5} - T_{7,5}}{r_2^2} \right]$$

6

$$\frac{2 \cdot k_7}{\rho_7 \cdot Cp_{r2,7} \cdot [(r_2 + D2)^2 - (r_2 - D2)^2]} \cdot \left[(T_{7,9} - T_{7,6}) \cdot \left(\frac{r_2 + D2}{\Delta_r} \right) - \left([T_{7,6} - T_{7,3}] \cdot \left[\frac{r_2 - D2}{\Delta_r} \right] \right) \right] + \frac{2}{\rho_7 \cdot Cp_{z3,7} \cdot \Delta_z} \cdot \left[\frac{k_7}{\Delta_z} \cdot (T_{7,5} - T_{7,6}) + h_{top} \cdot (Tf_{zt} - T_{7,6}) \right] + X_{7,6} = 0$$

$$X_{7,6} = \frac{1}{\rho_7 \cdot Cp_{r2,7} \cdot \Delta_\theta} \cdot \frac{k_7}{\Delta_\theta} \cdot \left[\frac{T_{6,6} - T_{7,6}}{r_2^2} \right]$$

7

$$\frac{2 \cdot k_7}{\rho_7 \cdot Cp_{r3,7} \cdot \left[(r_3 + D2)^2 - (r_3 - D2)^2\right]} \cdot \left[(T_{7,10} - T_{7,7}) \cdot \left(\frac{r_3 + D2}{\Delta_r}\right) - \left([T_{7,7} - T_{7,4}] \cdot \left[\frac{r_3 - D2}{\Delta_r}\right]\right)\right] + \frac{2}{\rho_7 \cdot Cp_{z1,7} \cdot \Delta_z} \cdot \left[\frac{k_7}{\Delta_z} \cdot (T_{7,8} - T_{7,7}) + h_{bottom} \cdot (Tf_{zb} - T_{7,7})\right] + X_{7,7} = 0$$

$$X_{7,7} = \frac{1}{\rho_7 \cdot Cp_{r3,7} \cdot \Delta_\theta} \cdot \frac{k_7}{\Delta_\theta} \cdot \left[\frac{T_{6,7} - T_{7,7}}{r_3^{\,2}}\right]$$

8

$$\frac{2 \cdot k_7}{\rho_7 \cdot Cp_{r3,7} \cdot \left[(r_3 + D2)^2 - (r_3 - D2)^2\right]} \cdot \left[(T_{7,11} - T_{7,8}) \cdot \left(\frac{r_3 + D2}{\Delta_r}\right) - \left([T_{7,8} - T_{7,5}] \cdot \left[\frac{r_3 - D2}{\Delta_r}\right]\right)\right] + \frac{1}{\rho_7 \cdot Cp_{z2,7} \cdot \Delta_z} \cdot \left[\frac{k_7}{\Delta_z} \cdot (T_{7,9} - T_{7,8}) - \frac{k_7}{\Delta_z} \cdot (T_{7,8} - T_{7,7})\right] + X_{7,8} = 0$$

$$X_{7,8} = \frac{1}{\rho_7 \cdot Cp_{r3,7} \cdot \Delta_\theta} \cdot \frac{k_7}{\Delta_\theta} \cdot \left[\frac{T_{6,8} - T_{7,8}}{r_3^{\,2}}\right]$$

9

$$\frac{2 \cdot k_7}{\rho_7 \cdot Cp_{r3,7} \cdot \left[(r_3 + D2)^2 - (r_3 - D2)^2\right]} \cdot \left[(T_{7,12} - T_{7,9}) \cdot \left(\frac{r_3 + D2}{\Delta_r}\right) - \left([T_{7,9} - T_{7,6}] \cdot \left[\frac{r_3 - D2}{\Delta_r}\right]\right)\right] + \frac{2}{\rho_7 \cdot Cp_{z3,7} \cdot \Delta_z} \cdot \left[\frac{k_7}{\Delta_z} \cdot (T_{7,8} - T_{7,9}) + h_{top} \cdot (Tf_{zt} - T_{7,9})\right] + X_{7,9} = 0$$

$$X_{7,9} = \frac{1}{\rho_7 \cdot Cp_{r3,7} \cdot \Delta_\theta} \cdot \frac{k_7}{\Delta_\theta} \cdot \left[\frac{T_{6,9} - T_{7,9}}{r_3^{\,2}}\right]$$

10

$$\frac{2 \cdot k_7}{\rho_7 \cdot Cp_{r4,7} \cdot \left[(r_4 + D2)^2 - (r_4 - D2)^2\right]} \cdot \left[(T_{7,13} - T_{7,10}) \cdot \left(\frac{r_4 + D2}{\Delta_r}\right) - \left([T_{7,10} - T_{7,7}] \cdot \left[\frac{r_4 - D2}{\Delta_r}\right]\right)\right] + \frac{2}{\rho_7 \cdot Cp_{z1,7} \cdot \Delta_z} \cdot \left[\frac{k_7}{\Delta_z} \cdot (T_{7,11} - T_{7,10}) + h_{bottom} \cdot (Tf_{zb} - T_{7,10})\right] + X_{7,10} = 0$$

$$X_{7,10} = \frac{1}{\rho_7 \cdot Cp_{r4,7} \cdot \Delta_\theta} \cdot \frac{k_7}{\Delta_\theta} \cdot \left[\frac{T_{6,10} - T_{7,10}}{r_4^{\,2}}\right]$$

11

$$\frac{2 \cdot k_7}{\rho_7 \cdot Cp_{r4,7} \cdot \left[(r_4 + D2)^2 - (r_4 - D2)^2\right]} \cdot \left[(T_{7,14} - T_{7,11}) \cdot \left(\frac{r_4 + D2}{\Delta_r}\right) - \left([T_{7,11} - T_{7,8}] \cdot \left[\frac{r_4 - D2}{\Delta_r}\right]\right)\right] + \frac{1}{\rho_7 \cdot Cp_{z2,7} \cdot \Delta_z} \cdot \left[\frac{k_7}{\Delta_z} \cdot (T_{7,12} - T_{7,11}) - \frac{k_7}{\Delta_z} \cdot (T_{7,11} - T_{7,10})\right] + X_{7,11} = 0$$

$$X_{7,11} = \frac{1}{\rho_7 \cdot Cp_{r4,7} \cdot \Delta_\theta} \cdot \frac{k_7}{\Delta_\theta} \cdot \left[\frac{T_{6,11} - T_{7,11}}{r_4^{\,2}}\right]$$

12

$$\frac{2 \cdot k_7}{\rho_7 \cdot Cp_{r4,7} \cdot \left[(r_4 + D2)^2 - (r_4 - D2)^2\right]} \cdot \left[(T_{7,15} - T_{7,12}) \cdot \left(\frac{r_4 + D2}{\Delta_r}\right) - \left([T_{7,12} - T_{7,9}] \cdot \left[\frac{r_4 - D2}{\Delta_r}\right]\right)\right] + \frac{2}{\rho_7 \cdot Cp_{z3,7} \cdot \Delta_z} \cdot \left[\frac{k_7}{\Delta_z} \cdot (T_{7,11} - T_{7,12}) + h_{top} \cdot (Tf_{zt} - T_{7,12})\right] + X_{7,12} = 0$$

$$X_{7,12} = \frac{1}{\rho_7 \cdot Cp_{r4,7} \cdot \Delta_\theta} \cdot \frac{k_7}{\Delta_\theta} \cdot \left[\frac{T_{6,12} - T_{7,12}}{r_4^{\,2}}\right]$$

13

$$\frac{2 \cdot k_7}{\rho_7 \cdot Cp_{r5,7} \cdot \left[(r_5 + D2)^2 - (r_5 - D2)^2\right]} \cdot \left[(T_{7,16} - T_{7,13}) \cdot \left(\frac{r_5 + D2}{\Delta_r}\right) - \left([T_{7,13} - T_{7,10}] \cdot \left[\frac{r_5 - D2}{\Delta_r}\right]\right)\right] + \frac{2}{\rho_7 \cdot Cp_{z1,7} \cdot \Delta_z} \cdot \left[\frac{k_7}{\Delta_z} \cdot (T_{7,14} - T_{7,13}) + h_{bottom} \cdot (Tf_{zb} - T_{7,13})\right] + X_{7,13} = 0$$

$$X_{7,13} = \frac{1}{\rho_7 \cdot Cp_{r5,7} \cdot \Delta_\theta} \cdot \frac{k_7}{\Delta_\theta} \cdot \left[\frac{T_{6,13} - T_{7,13}}{r_5^{\,2}}\right]$$

14

$$\frac{2 \cdot k_7}{\rho_7 \cdot Cp_{r5,7} \cdot \left[(r_5 + D2)^2 - (r_5 - D2)^2 \right]} \cdot \left[(T_{7,17} - T_{7,14}) \cdot \left(\frac{r_5 + D2}{\Delta_r} \right) - \left(\left[T_{7,14} - T_{7,11} \right] \cdot \left[\frac{r_5 - D2}{\Delta_r} \right] \right) \right] + \frac{1}{\rho_7 \cdot Cp_{z2,7} \cdot \Delta_z} \cdot \left[\frac{k_7}{\Delta_z} \cdot (T_{7,15} - T_{7,14}) - \frac{k_7}{\Delta_z} \cdot (T_{7,14} - T_{7,13}) \right] + X_{7,14} = 0$$

$$X_{7,14} = \frac{1}{\rho_7 \cdot Cp_{r5,7} \cdot \Delta_\theta} \cdot \frac{k_7}{\Delta_\theta} \cdot \left[\frac{T_{6,14} - T_{7,14}}{r_5^2} \right]$$

15

$$\frac{2 \cdot k_7}{\rho_7 \cdot Cp_{r5,7} \cdot \left[(r_5 + D2)^2 - (r_5 - D2)^2 \right]} \cdot \left[(T_{7,18} - T_{7,15}) \cdot \left(\frac{r_5 + D2}{\Delta_r} \right) - \left(\left[T_{7,15} - T_{7,12} \right] \cdot \left[\frac{r_5 - D2}{\Delta_r} \right] \right) \right] + \frac{2}{\rho_7 \cdot Cp_{z3,7} \cdot \Delta_z} \cdot \left[\frac{k_7}{\Delta_z} \cdot (T_{7,14} - T_{7,15}) + h_{top} \cdot (Tf_{zt} - T_{7,15}) \right] + X_{7,15} = 0$$

$$X_{7,15} = \frac{1}{\rho_7 \cdot Cp_{r5,7} \cdot \Delta_\theta} \cdot \frac{k_7}{\Delta_\theta} \cdot \left[\frac{T_{6,15} - T_{7,15}}{r_5^2} \right]$$

16

$$\frac{2 \cdot k_7}{\rho_7 \cdot Cp_{r6,7} \cdot \left[(r_6 + D2)^2 - (r_6 - D2)^2 \right]} \cdot \left[(T_{7,19} - T_{7,16}) \cdot \left(\frac{r_6 + D2}{\Delta_r} \right) - \left(\left[T_{7,16} - T_{7,13} \right] \cdot \left[\frac{r_6 - D2}{\Delta_r} \right] \right) \right] + \frac{2}{\rho_7 \cdot Cp_{z1,7} \cdot \Delta_z} \cdot \left[\frac{k_7}{\Delta_z} \cdot (T_{7,17} - T_{7,16}) + h_{bottom} \cdot (Tf_{zb} - T_{7,16}) \right] + X_{7,16} = 0$$

$$X_{7,16} = \frac{1}{\rho_7 \cdot Cp_{r6,7} \cdot \Delta_\theta} \cdot \frac{k_7}{\Delta_\theta} \cdot \left[\frac{T_{6,16} - T_{7,16}}{r_6^2} \right]$$

17

$$\frac{2 \cdot k_7}{\rho_7 \cdot Cp_{r6,7} \cdot \left[(r_6 + D2)^2 - (r_6 - D2)^2 \right]} \cdot \left[(T_{7,20} - T_{7,17}) \cdot \left(\frac{r_6 + D2}{\Delta_r} \right) - \left(\left[T_{7,17} - T_{7,14} \right] \cdot \left[\frac{r_6 - D2}{\Delta_r} \right] \right) \right] + \frac{1}{\rho_7 \cdot Cp_{z2,7} \cdot \Delta_z} \cdot \left[\frac{k_7}{\Delta_z} \cdot (T_{7,18} - T_{7,17}) - \frac{k_7}{\Delta_z} \cdot (T_{7,17} - T_{7,16}) \right] + X_{7,17} = 0$$

$$X_{7,17} = \frac{1}{\rho_7 \cdot Cp_{r6,7} \cdot \Delta_\theta} \cdot \frac{k_7}{\Delta_\theta} \cdot \left[\frac{T_{6,17} - T_{7,17}}{r_6^2} \right]$$

18

$$\frac{2 \cdot k_7}{\rho_7 \cdot Cp_{r6,7} \cdot \left[(r_6 + D2)^2 - (r_6 - D2)^2 \right]} \cdot \left[(T_{7,21} - T_{7,18}) \cdot \left(\frac{r_6 + D2}{\Delta_r} \right) - \left(\left[T_{7,18} - T_{7,15} \right] \cdot \left[\frac{r_6 - D2}{\Delta_r} \right] \right) \right] + \frac{2}{\rho_7 \cdot Cp_{z3,7} \cdot \Delta_z} \cdot \left[\frac{k_7}{\Delta_z} \cdot (T_{7,17} - T_{7,18}) + h_{top} \cdot (Tf_{zt} - T_{7,18}) \right] + X_{7,18} = 0$$

$$X_{7,18} = \frac{1}{\rho_7 \cdot Cp_{r6,7} \cdot \Delta_\theta} \cdot \frac{k_7}{\Delta_\theta} \cdot \left[\frac{T_{6,18} - T_{7,18}}{r_6^2} \right]$$

19

$$\frac{2 \cdot k_7}{\rho_7 \cdot Cp_{r7,7} \cdot \left[(r_7 + D2)^2 - (r_7 - D2)^2 \right]} \cdot \left[(T_{7,22} - T_{7,19}) \cdot \left(\frac{r_7 + D2}{\Delta_r} \right) - \left(\left[T_{7,19} - T_{7,16} \right] \cdot \left[\frac{r_7 - D2}{\Delta_r} \right] \right) \right] + \frac{2}{\rho_7 \cdot Cp_{z1,7} \cdot \Delta_z} \cdot \left[\frac{k_7}{\Delta_z} \cdot (T_{7,20} - T_{7,19}) + h_{bottom} \cdot (Tf_{zb} - T_{7,19}) \right] + X_{7,19} = 0$$

$$X_{7,19} = \frac{1}{\rho_7 \cdot Cp_{r7,7} \cdot \Delta_\theta} \cdot \frac{k_7}{\Delta_\theta} \cdot \left[\frac{T_{6,19} - T_{7,19}}{r_7^2} \right]$$

20

$$\frac{2 \cdot k_7}{\rho_7 \cdot Cp_{r7,7} \cdot \left[(r_7 + D2)^2 - (r_7 - D2)^2 \right]} \cdot \left[(T_{7,23} - T_{7,20}) \cdot \left(\frac{r_7 + D2}{\Delta_r} \right) - \left(\left[T_{7,20} - T_{7,17} \right] \cdot \left[\frac{r_7 - D2}{\Delta_r} \right] \right) \right] + \frac{1}{\rho_7 \cdot Cp_{z2,7} \cdot \Delta_z} \cdot \left[\frac{k_7}{\Delta_z} \cdot (T_{7,21} - T_{7,20}) - \frac{k_7}{\Delta_z} \cdot (T_{7,20} - T_{7,19}) \right] + X_{7,20} = 0$$

$$X_{7,20} = \frac{1}{\rho_7 \cdot Cp_{r7,7} \cdot \Delta_\theta} \cdot \frac{k_7}{\Delta_\theta} \cdot \left[\frac{T_{6,20} - T_{7,20}}{r_7^{\,2}}\right]$$

21

$$\frac{2 \cdot k_7}{\rho_7 \cdot Cp_{r7,7} \cdot \left[(r_7 + D2)^2 - (r_7 - D2)^2\right]} \cdot \left[(T_{7,24} - T_{7,21}) \cdot \left(\frac{r_7 + D2}{\Delta_r}\right) - \left([T_{7,21} - T_{7,18}] \cdot \left[\frac{r_7 - D2}{\Delta_r}\right]\right)\right]$$
$$+ \frac{2}{\rho_7 \cdot Cp_{z3,7} \cdot \Delta_z} \cdot \left[\frac{k_7}{\Delta_z} \cdot (T_{7,20} - T_{7,21}) + h_{top} \cdot (Tf_{zt} - T_{7,21})\right] + X_{7,21} = 0$$

$$X_{7,21} = \frac{1}{\rho_7 \cdot Cp_{r7,7} \cdot \Delta_\theta} \cdot \frac{k_7}{\Delta_\theta} \cdot \left[\frac{T_{6,21} - T_{7,21}}{r_7^{\,2}}\right]$$

22

$$\frac{2 \cdot k_7}{\rho_7 \cdot Cp_{r8,7} \cdot \left[(r_8 + D2)^2 - (r_8 - D2)^2\right]} \cdot \left[(T_{7,25} - T_{7,22}) \cdot \left(\frac{r_8 + D2}{\Delta_r}\right) - \left([T_{7,22} - T_{7,19}] \cdot \left[\frac{r_8 - D2}{\Delta_r}\right]\right)\right]$$
$$+ \frac{2}{\rho_7 \cdot Cp_{z1,7} \cdot \Delta_z} \cdot \left[\frac{k_7}{\Delta_z} \cdot (T_{7,23} - T_{7,22}) + h_{bottom} \cdot (Tf_{zb} - T_{7,22})\right] + X_{7,22} = 0$$

$$X_{7,22} = \frac{1}{\rho_7 \cdot Cp_{r8,7} \cdot \Delta_\theta} \cdot \frac{k_7}{\Delta_\theta} \cdot \left[\frac{T_{6,22} - T_{7,22}}{r_8^{\,2}}\right]$$

23

$$\frac{2 \cdot k_7}{\rho_7 \cdot Cp_{r8,7} \cdot \left[(r_8 + D2)^2 - (r_8 - D2)^2\right]} \cdot \left[(T_{7,26} - T_{7,23}) \cdot \left(\frac{r_8 + D2}{\Delta_r}\right) - \left([T_{7,23} - T_{7,20}] \cdot \left[\frac{r_8 - D2}{\Delta_r}\right]\right)\right]$$
$$+ \frac{1}{\rho_7 \cdot Cp_{z2,7} \cdot \Delta_z} \cdot \left[\frac{k_7}{\Delta_z} \cdot (T_{7,24} - T_{7,23}) - \frac{k_7}{\Delta_z} \cdot (T_{7,23} - T_{7,22})\right] + X_{7,23} = 0$$

$$X_{7,23} = \frac{1}{\rho_7 \cdot Cp_{r8,7} \cdot \Delta_\theta} \cdot \frac{k_7}{\Delta_\theta} \cdot \left[\frac{T_{6,23} - T_{7,23}}{r_8^{\,2}}\right]$$

24

$$\frac{2 \cdot k_7}{\rho_7 \cdot Cp_{r8,7} \cdot \left[(r_8 + D2)^2 - (r_8 - D2)^2\right]} \cdot \left[(T_{7,27} - T_{7,24}) \cdot \left(\frac{r_8 + D2}{\Delta_r}\right) - \left([T_{7,24} - T_{7,21}] \cdot \left[\frac{r_8 - D2}{\Delta_r}\right]\right)\right]$$
$$+ \frac{2}{\rho_7 \cdot Cp_{z3,7} \cdot \Delta_z} \cdot \left[\frac{k_7}{\Delta_z} \cdot (T_{7,23} - T_{7,24}) + h_{top} \cdot (Tf_{zt} - T_{7,24})\right] + X_{7,24} = 0$$

$$X_{7,24} = \frac{1}{\rho_7 \cdot Cp_{r8,7} \cdot \Delta_\theta} \cdot \frac{k_7}{\Delta_\theta} \cdot \left[\frac{T_{6,24} - T_{7,24}}{r_8^{\,2}}\right]$$

25

$$\frac{2}{\rho_7 \cdot Cp_{r9,7} \cdot \left[(r_9 + D2)^2 - (r_9 - D2)^2\right]} \cdot \left[r_{out} \cdot h_{outside} \cdot (Tf_{ro} - T_{7,25}) + (r_9 - D2) \cdot k_7 \cdot \left(\frac{T_{7,22} - T_{7,25}}{\Delta_r}\right)\right]$$
$$+ \frac{2}{\rho_7 \cdot Cp_{z1,7} \cdot \Delta_z} \cdot \left[\frac{k_7}{\Delta_z} \cdot (T_{7,26} - T_{7,25}) + h_{bottom} \cdot (Tf_{zb} - T_{7,25})\right] + X_{7,25} = 0$$

$$X_{7,25} = \frac{1}{\rho_7 \cdot Cp_{r9,7} \cdot \Delta_\theta} \cdot \frac{k_7}{\Delta_\theta} \cdot \left[\frac{T_{6,25} - T_{7,25}}{r_9^{\,2}}\right]$$

26

$$\frac{2}{\rho_7 \cdot Cp_{r9,7} \cdot \left[(r_9 + D2)^2 - (r_9 - D2)^2\right]} \cdot \left[r_{out} \cdot h_{outside} \cdot (Tf_{ro} - T_{7,26}) + (r_9 - D2) \cdot k_7 \cdot \left(\frac{T_{7,23} - T_{7,26}}{\Delta_r}\right)\right]$$
$$+ \frac{1}{\rho_7 \cdot Cp_{z2,7} \cdot \Delta_z} \cdot \left[\frac{k_7}{\Delta_z} \cdot (T_{7,27} - T_{7,26}) - \frac{k_7}{\Delta_z} \cdot (T_{7,26} - T_{7,25})\right] + X_{7,26} = 0$$

$$X_{7,26} = \frac{1}{\rho_7 \cdot Cp_{r8,7} \cdot \Delta_\theta} \cdot \frac{k_7}{\Delta_\theta} \cdot \left[\frac{T_{6,26} - T_{7,26}}{r_9^{\,2}}\right]$$

27

$$\frac{2}{\rho_7 \cdot Cp_{r9,7} \cdot \left[(r_9 + D2)^2 - (r_9 - D2)^2 \right]} \cdot \left[r_{out} \cdot h_{outside} \cdot (Tf_{ro} - T_{7,27}) + (r_9 - D2) \cdot k_7 \cdot \left(\frac{T_{7,24} - T_{7,27}}{\Delta_r} \right) \right]$$
$$+ \frac{2}{\rho_7 \cdot Cp_{z3,7} \cdot \Delta_z} \cdot \left[\frac{k_7}{\Delta_z} \cdot (T_{7,26} - T_{7,27}) + h_{top} \cdot (Tf_{zt} - T_{7,27}) \right] + X_{7,27} = 0$$

$$X_{7,27} = \frac{1}{\rho_7 \cdot Cp_{r9,7} \cdot \Delta_\theta} \cdot \frac{k_7}{\Delta_\theta} \cdot \left[\frac{T_{6,27} - T_{7,27}}{r_9^{\,2}} \right]$$

APPENDIX E: Discretisation of the conduction equations

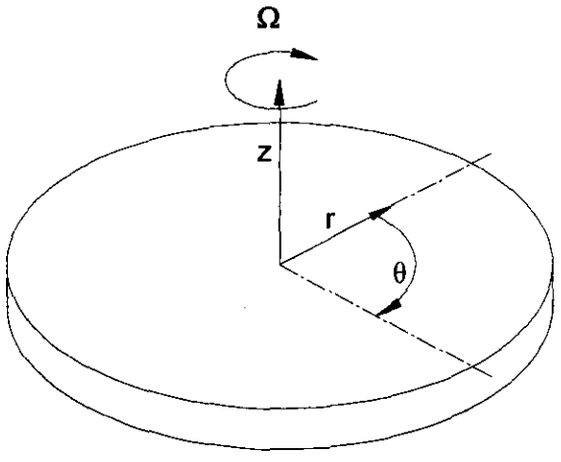

Figure E.1: Coordinate system for conduction equations.

As stated in chapter 3, the equation of energy in terms of the transport properties for Newtonian fluids of a constant density and conduction coefficient can be given in the form: (Bird et al. (1960:319))

r θ z

$$\rho\overline{C_v}\left(\frac{\partial T}{\partial t}\right)=k\left[\frac{1}{r}\frac{\partial}{\partial r}\left(r\frac{\partial T}{\partial r}\right)+\frac{1}{r^2}\frac{\partial^2 T}{\partial \theta^2}+\frac{\partial^2 T}{\partial z^2}\right]$$

We will derive the integral form of the equation in three component parts.

1. r-Coordinate
2. θ-Coordinate
3. z-Coordinate

A control volume is defined as follows:

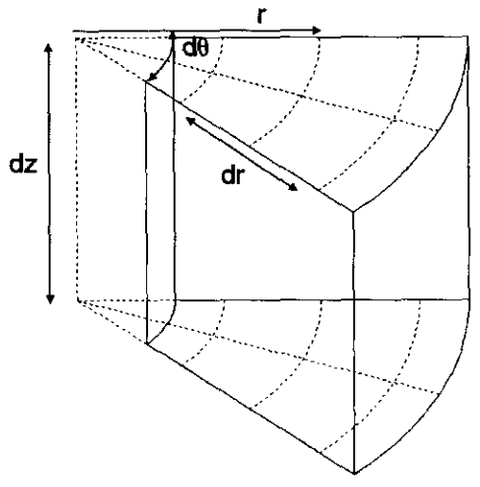

Figure E.2: Control volume definition.

Where

$$dV = rd\theta dzdr$$

r-Coordinate Component

Internal node

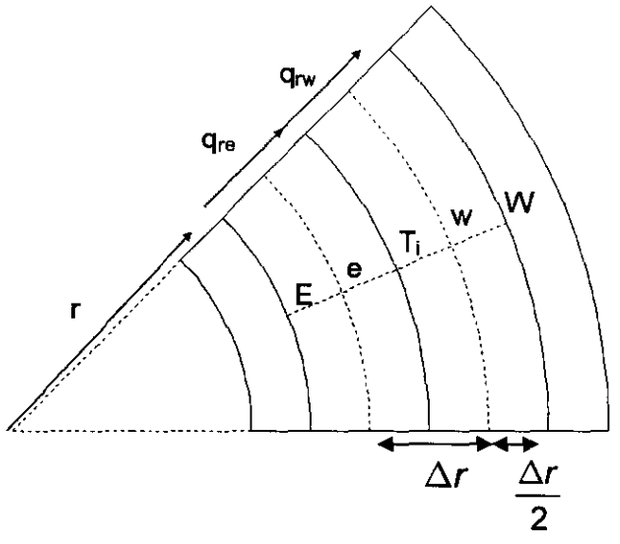

Figure E.3: Radial internal node definition.

Mathematical relationships

$$r_e = r - \frac{\Delta r}{2}$$

$$r_w = r + \frac{\Delta r}{2}$$

$$\Delta r = r_{i+1} - r_i = r_i - r_{i-1}$$

$$r_E = r_{i-1}$$

$$r_W = r_{i+1}$$

$$E = i - 1$$

$$W = i + 1$$

$$T_i = i$$

$$r = r_i$$

$$\rho\overline{C_v}\left(\frac{\partial T}{\partial t}\right) = \frac{k}{r}\frac{\partial}{\partial r}\left(r\frac{\partial T}{\partial r}\right)$$

$$\int \rho\overline{C_v}\left(\frac{\partial T}{\partial t}\right)dV = \int \frac{k}{r}\frac{\partial}{\partial r}\left(r\frac{\partial T}{\partial r}\right)dV$$

$$\rho\overline{C_v}\left(\frac{\partial T}{\partial t}\right)\iiint rd\theta drdz = \iiint \frac{k}{r}\frac{\partial}{\partial r}\left(r\frac{\partial T}{\partial r}\right)rd\theta drdz$$

$$\rho\overline{C_v}\left(\frac{\partial T}{\partial t}\right)\Delta\theta\Delta z\int rdr = -k\Delta\theta\Delta z\int \frac{\partial}{\partial r}\left(r\frac{\partial T}{\partial r}\right)dr$$

$$\rho\overline{C_v}\left(\frac{\partial T}{\partial t}\right)\frac{\left(r_w^2 - r_e^2\right)}{2} = k\left[\left(r\frac{\partial T}{\partial r}\right)_w - \left(r\frac{\partial T}{\partial r}\right)_e\right]$$

$$\frac{\rho\overline{C_v}}{2k}\left(\frac{\partial T}{\partial t}\right)\left(r_w^2 - r_e^2\right) = \left(\frac{r_w}{r_W - r_i}\left(T_W - T_i\right)\right) - \left(\frac{r_e}{r_i - r_E}\left(T_i - T_E\right)\right)$$

$$\left(\frac{\partial T}{\partial t}\right)_i = \frac{2k}{\rho_i \overline{C_{vi}}\left(\left(r+\frac{\Delta r}{2}\right)^2 - \left(r-\frac{\Delta r}{2}\right)^2\right)}\left[\frac{\left(r+\frac{\Delta r}{2}\right)}{(r_{i+1}-r_i)}(T_{i+1}-T_i) - \frac{\left(r-\frac{\Delta r}{2}\right)}{(r_i-r_{i-1})}(T_i-T_{i-1})\right]$$

Omitting the transient term yields

$$\frac{2k}{\rho_i \overline{C_{vi}}\left(\left(r+\frac{\Delta r}{2}\right)^2 - \left(r-\frac{\Delta r}{2}\right)^2\right)}\left[\frac{\left(r+\frac{\Delta r}{2}\right)}{(r_{i+1}-r_i)}(T_{i+1}-T_i) - \frac{\left(r-\frac{\Delta r}{2}\right)}{(r_i-r_{i-1})}(T_i-T_{i-1})\right] = 0$$

Inner node

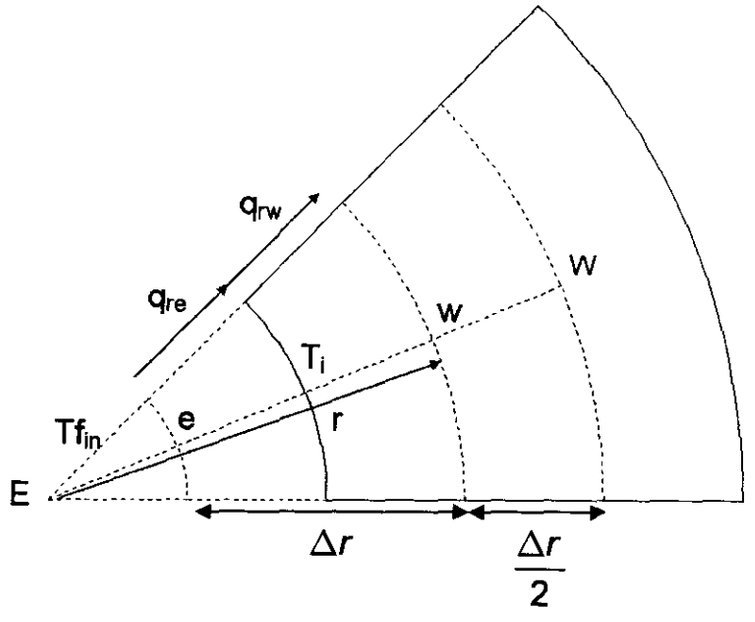

Figure E.4: Radial inner node definition.

Mathematical relationships

$$q_{re} = h\left(Tf_{in} - T_i\right)$$

$$q_{rw} = -k\left.\frac{\partial T}{\partial r}\right|_w$$

$$r_e = r - \frac{\Delta r}{2}$$

$$r_w = r + \frac{\Delta r}{2}$$

$$\Delta r = r_{i+1} - r_i = r_i - r_{i-1}$$

$$r_E = r_{i-1}$$

$$r_W = r_{i+1}$$

$$dV = rd\theta dz\frac{dr}{2}$$

$$E = i - 1$$

$$W = i + 1$$

$$T_i = i$$

$$r = r_i$$

Now for a node on the inner surface of the cylindrical rotating cavity, follows:

$$\rho\overline{C_v}\left(\frac{\partial T}{\partial t}\right) = -\frac{1}{r}\frac{\partial}{\partial r}(rq_r)$$

$$\int \rho\overline{C_v}\left(\frac{\partial T}{\partial t}\right)dV = -\int \frac{1}{r}\frac{\partial}{\partial r}(rq_r)dV$$

$$\rho\overline{C_v}\left(\frac{\partial T}{\partial t}\right)\iiint rd\theta\frac{dr}{2}dz = -\iiint \frac{1}{r}\frac{\partial}{\partial r}(rq_r)rd\theta\frac{dr}{2}dz$$

$$\rho\overline{C_v}\left(\frac{\partial T}{\partial t}\right)\Delta\theta\Delta z\int\frac{r}{2}dr=-\frac{\Delta\theta\Delta z}{2}\int\frac{\partial}{\partial r}(rq_r)dr$$

$$\rho\overline{C_v}\left(\frac{\partial T}{\partial t}\right)\frac{\left(r_w^2-r_e^2\right)}{4}=-\frac{1}{2}\left[(rq_r)_w-(rq_r)_e\right]$$

$$\frac{\rho\overline{C_v}}{4}\left(\frac{\partial T}{\partial t}\right)\left(r_w^2-r_e^2\right)=-\frac{1}{2}\left[-rh(Tf_{in}-T_i)+r_w\left(-k\frac{\partial T}{\partial r}\bigg|_w\right)\right]$$

$$\frac{\rho\overline{C_v}}{4}\left(\frac{\partial T}{\partial t}\right)\left(r_w^2-r_e^2\right)=-\frac{1}{2}\left[-rh(Tf_{in}-T_i)-r_wk\left(\frac{T_W-T_i}{\Delta r}\right)\right]$$

$$\frac{\rho\overline{C_v}}{4}\left(\frac{\partial T}{\partial t}\right)\left(\left(r+\frac{\Delta r}{2}\right)^2-\left(r-\frac{\Delta r}{2}\right)^2\right)=\frac{1}{2}rh(Tf_{in}-T_i)+\frac{1}{2}k\left(r+\frac{\Delta r}{2}\right)\left(\frac{T_W-T_i}{\Delta r}\right)$$

$$\left(\frac{\partial T}{\partial t}\right)=\frac{2}{\rho\overline{C_v}\left(\left(r+\frac{\Delta r}{2}\right)^2-\left(r-\frac{\Delta r}{2}\right)^2\right)}\left[rh(Tf_{in}-T_i)+k\left(r+\frac{\Delta r}{2}\right)\left(\frac{T_W-T_i}{\Delta r}\right)\right]$$

$$\left(\frac{\partial T}{\partial t}\right)_i=\frac{2}{\rho_i\overline{C_{vi}}\left(\left(r+\frac{\Delta r}{2}\right)^2-\left(r-\frac{\Delta r}{2}\right)^2\right)}\left[rh(Tf_{in}-T_i)+k\left(r+\frac{\Delta r}{2}\right)\left(\frac{T_{i+1}-T_i}{r_{i+1}-r_i}\right)\right]$$

Omitting the transient term yields

$$\frac{2}{\rho_i\overline{C_{vi}}\left(\left(r+\frac{\Delta r}{2}\right)^2-\left(r-\frac{\Delta r}{2}\right)^2\right)}\left[rh(Tf_{in}-T_i)+k\left(r+\frac{\Delta r}{2}\right)\left(\frac{T_{i+1}-T_i}{r_{i+1}-r_i}\right)\right]=0$$

Outer node

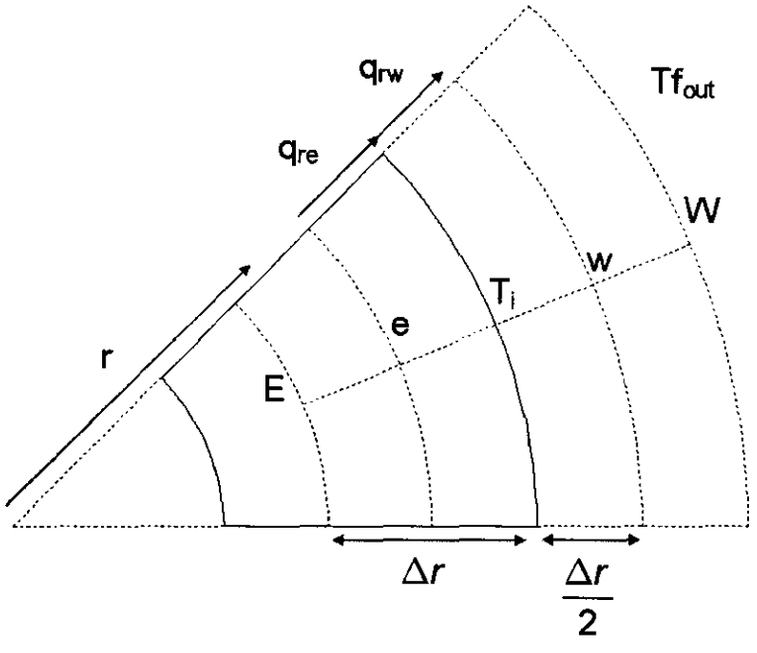

Figure E.5: Radial outer node definition.

Mathematical relationships

$$q_{rw} = h\left(T_i - Tf_{out}\right)$$

$$q_{re} = -k\left.\frac{\partial T}{\partial r}\right|_e$$

$$r_e = r - \frac{\Delta r}{2}$$

$$r_w = r + \frac{\Delta r}{2}$$

$$\Delta r = r_{i+1} - r_i = r_i - r_{i-1}$$

$$r_E = r_{i-1}$$

$$r_W = r_{i+1}$$

$$dV = rd\theta dz\frac{dr}{2}$$

$$E = i-1$$

$$W = i+1$$

$$T_i = i$$

$$r = r_i$$

$$\rho\overline{C_v}\left(\frac{\partial T}{\partial t}\right) = -\frac{1}{r}\frac{\partial}{\partial r}(rq_r)$$

$$\int \rho\overline{C_v}\left(\frac{\partial T}{\partial t}\right)dV = -\int \frac{1}{r}\frac{\partial}{\partial r}(rq_r)dV$$

$$\rho\overline{C_v}\left(\frac{\partial T}{\partial t}\right)\iiint rd\theta\frac{dr}{2}dz = -\iiint \frac{1}{r}\frac{\partial}{\partial r}(rq_r)rd\theta\frac{dr}{2}dz$$

$$\rho\overline{C_v}\left(\frac{\partial T}{\partial t}\right)\Delta\theta\Delta z\int \frac{r}{2}dr = -\frac{\Delta\theta\Delta z}{2}\int \frac{\partial}{\partial r}(rq_r)dr$$

$$\rho\overline{C_v}\left(\frac{\partial T}{\partial t}\right)\frac{\left(r_w^2 - r_e^2\right)}{4} = -\frac{1}{2}\left[(rq_r)_w - (rq_r)_e\right]$$

$$\frac{\rho\overline{C_v}}{4}\left(\frac{\partial T}{\partial t}\right)\left(r_w^2 - r_e^2\right) = -\frac{1}{2}\left[rh\left(T_i - Tf_{out}\right) - r_e\left(-k\frac{\partial T}{\partial r}\bigg|_e\right)\right]$$

$$\frac{\rho\overline{C_v}}{4}\left(\frac{\partial T}{\partial t}\right)\left(r_w^2 - r_e^2\right) = -\frac{1}{2}\left[rh\left(T_i - Tf_{out}\right) + r_e k\left(\frac{T_i - T_E}{\Delta r}\right)\right]$$

$$\frac{\rho\overline{C_v}}{4}\left(\frac{\partial T}{\partial t}\right)\left(\left(r+\frac{\Delta r}{2}\right)^2 - \left(r-\frac{\Delta r}{2}\right)^2\right) = -\frac{1}{2}rh\left(T_i - Tf_{out}\right) - \frac{1}{2}k\left(r-\frac{\Delta r}{2}\right)\left(\frac{T_i - T_E}{\Delta r}\right)$$

$$\left(\frac{\partial T}{\partial t}\right)=\frac{2}{\rho\overline{C_v}\left(\left(r+\frac{\Delta r}{2}\right)^2-\left(r-\frac{\Delta r}{2}\right)^2\right)}\left[-rh\left(T_i-Tf_{out}\right)-k\left(r-\frac{\Delta r}{2}\right)\left(\frac{T_i-T_E}{\Delta r}\right)\right]$$

$$\left(\frac{\partial T}{\partial t}\right)_i=\frac{2}{\rho_i\overline{C_{vi}}\left(\left(r+\frac{\Delta r}{2}\right)^2-\left(r-\frac{\Delta r}{2}\right)^2\right)}\left[rh\left(Tf_{out}-T_i\right)+k\left(r-\frac{\Delta r}{2}\right)\left(\frac{T_{i-1}-T_i}{r_{i+1}-r_i}\right)\right]$$

Omitting the transient term yields

$$\frac{2}{\rho_n\overline{C_{vn}}\left(\left(r+\frac{\Delta r}{2}\right)^2-\left(r-\frac{\Delta r}{2}\right)^2\right)}\left[rh\left(Tf_{out}-T_i\right)+k\left(r-\frac{\Delta r}{2}\right)\left(\frac{T_{i-1}-T_i}{r_{i+1}-r_i}\right)\right]=0$$

θ-Coordinate Component

Internal node

The temperature distribution of the disc will only be simulated for a 60 degree segment of the disc. The axisymmetric nature of the disc allows the use of a segment of the disc to simulate the temperature distribution of the disc as a whole.

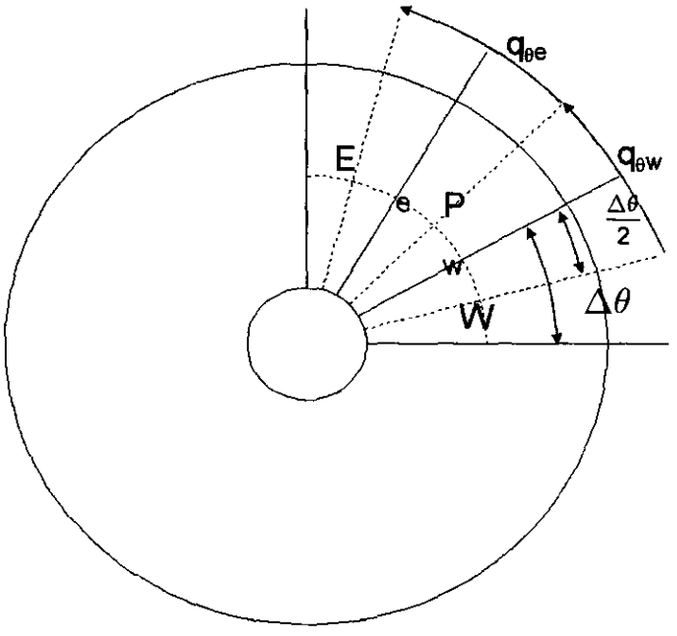

Figure E.6: Theta internal node definition.

Mathematical relationships

$$\Delta\theta = \theta_{i+1} - \theta_{\ i} = \theta_i - \theta_{i-1}$$

$$E = i - 1$$

$$W = i + 1$$

$$P = i$$

$$r_E = r_{i-1}$$

$$r_W = r_{i+1}$$

$$r = r_i = r_{i+1} = r_{i-1}$$

$$\rho\overline{C_v}\left(\frac{\partial T}{\partial t}\right)=\frac{k}{r^2}\left(\frac{\partial^2 T}{\partial \theta^2}\right)$$

$$\rho\overline{C_v}\left(\frac{\partial T}{\partial t}\right)=\frac{\partial}{\partial \theta}\left(\frac{k}{r^2}\frac{\partial T}{\partial \theta}\right)$$

$$\rho\overline{C_v}\left(\frac{\partial T}{\partial t}\right)=\frac{\frac{k_E}{r_E^2}\left[\left.\frac{\partial T}{\partial \theta}\right|_E\right]-\frac{k_W}{r_W^2}\left[\left.\frac{\partial T}{\partial \theta}\right|_W\right]}{\Delta\theta}$$

$$\rho\overline{C_v}\left(\frac{\partial T}{\partial t}\right)=\frac{\frac{k_E}{r_E^2}\left[\frac{T_E-T_P}{\theta_E-\theta_P}\right]-\frac{k_W}{r_W^2}\left[\frac{T_P-T_W}{\theta_P-\theta_W}\right]}{\Delta\theta}$$

thus the following can be derived

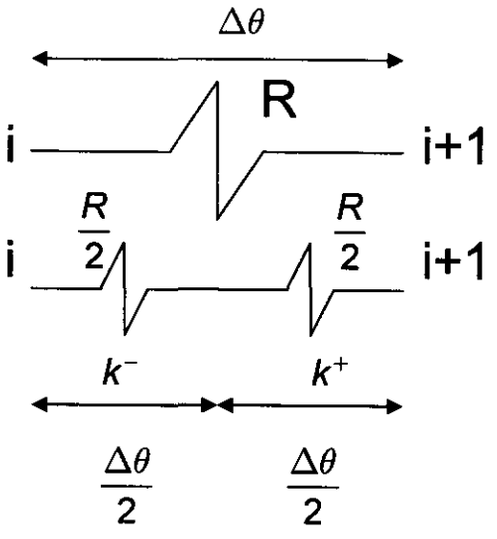

$$\frac{\Delta\theta}{k}=\frac{\Delta\theta^-}{k^-}+\frac{\Delta\theta^+}{k^+}$$

$$\frac{k}{\Delta\theta}=\left[\frac{\Delta\theta^-}{k^-}+\frac{\Delta\theta^+}{k^+}\right]^{-1}$$

$$\frac{k}{\Delta\theta}=\left[\frac{\Delta\theta}{2k^-}+\frac{\Delta\theta}{2k^+}\right]^{-1}$$

$$\left.\frac{k}{\Delta\theta}\right|_{i+1} = 2\left[\left.\frac{\Delta\theta}{k}\right|_{i} + \left.\frac{\Delta\theta}{k}\right|_{i+1}\right]^{-1}$$

$$\left.\frac{k}{\Delta\theta}\right|_{i-1} = 2\left[\left.\frac{\Delta\theta}{k}\right|_{i-1} + \left.\frac{\Delta\theta}{k}\right|_{i}\right]^{-1}$$

therefore

$$\rho\overline{C_v}\left(\frac{\partial T}{\partial t}\right) = \frac{\left.\frac{k}{\Delta\theta}\right|_{i-1}\left[\frac{T_E - T_P}{r_E^2}\right] - \left.\frac{k}{\Delta\theta}\right|_{i+1}\left[\frac{T_P - T_W}{r_W^2}\right]}{\Delta\theta}$$

now for an internal node it follows

$$\left(\frac{\partial T}{\partial t}\right)_i = \frac{1}{\rho_i\overline{C_{vi}}\Delta\theta}\left[\left.\frac{k}{\Delta\theta}\right|_{i-1}\left[\frac{T_{i-1} - T_i}{r_{i-1}^2}\right] - \left.\frac{k}{\Delta\theta}\right|_{i+1}\left[\frac{T_i - T_{i+1}}{r_{i+1}^2}\right]\right]$$

omitting the transient term yields

$$\frac{1}{\rho_i\overline{C_{vi}}\Delta\theta}\left[\left.\frac{k}{\Delta\theta}\right|_{i-1}\left[\frac{T_{i-1} - T_i}{r_{i-1}^2}\right] - \left.\frac{k}{\Delta\theta}\right|_{i+1}\left[\frac{T_i - T_{i+1}}{r_{i+1}^2}\right]\right] = 0$$

The following is also true for the sides of the axisymmetric segments:

Counterclockwise node

Counterclockwise of the middle point P

$$\frac{1}{\rho_i\overline{C_{vi}}\Delta\theta}\left[\left.\frac{k}{\Delta\theta}\right|_{i-1}\left[\frac{T_{i-1} - T_i}{r_{i-1}^2}\right] - 0\right] = 0$$

Clockwise node

Clockwise of the middle point P

$$\frac{1}{\rho_i \overline{C_{vi}} \Delta\theta}\left[0 - \frac{k}{\Delta\theta}\Big|_{i+1}\left[\frac{T_i - T_{i+1}}{r_{i+1}^2}\right]\right] = 0$$

z-Coordinate Component

Internal node

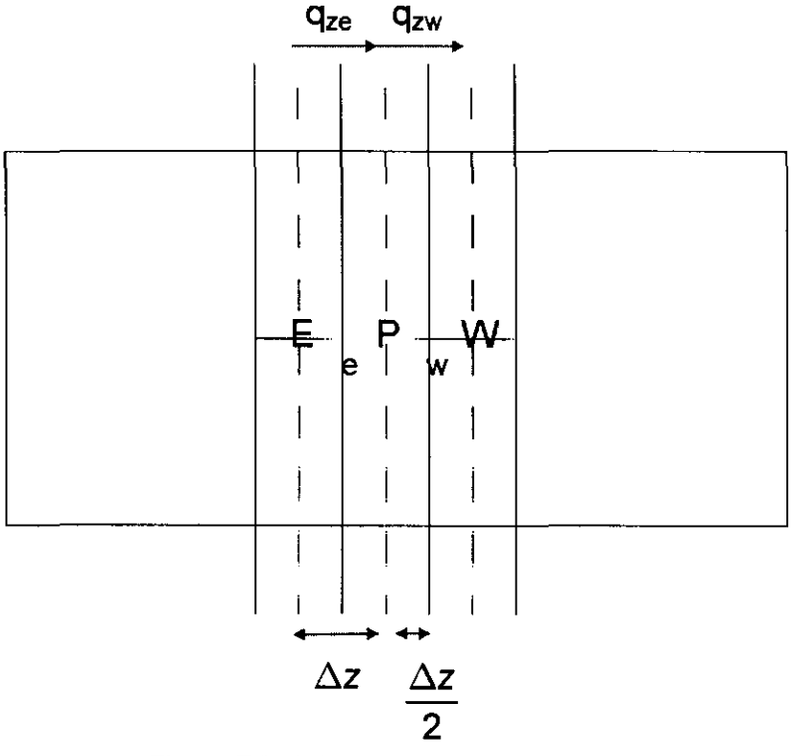

Figure E.7: Axial internal node definition.

Mathematical relationships

$$\Delta z = z_{i+1} - z_{\ i} = z_i - z_{i-1}$$

$$E = i - 1$$

$$W = i+1$$

$$P = i$$

$$z_E = z_{i-1}$$

$$z_W = z_{i+1}$$

$$z_{i+1} = z_{i-1}$$

$$\left.\frac{k}{\Delta z}\right|_{i+1} = 2\left[\left.\frac{\Delta z}{k}\right|_i + \left.\frac{\Delta z}{k}\right|_{i+1}\right]^{-1}$$

$$\left.\frac{k}{\Delta z}\right|_{i-1} = 2\left[\left.\frac{\Delta z}{k}\right|_{i-1} + \left.\frac{\Delta z}{k}\right|_i\right]^{-1}$$

$$\rho\overline{C_v}\left(\frac{\partial T}{\partial t}\right) = k\left(\frac{\partial^2 T}{\partial z^2}\right)$$

$$\rho\overline{C_v}\left(\frac{\partial T}{\partial t}\right) = \frac{\partial}{\partial z}\left(k\frac{\partial T}{\partial z}\right)$$

$$\rho\overline{C_v}\left(\frac{\partial T}{\partial t}\right) = \frac{k_W\left[\left.\frac{\partial T}{\partial z}\right|_W\right] - k_W\left[\left.\frac{\partial T}{\partial z}\right|_E\right]}{\Delta z}$$

$$\rho\overline{C_v}\left(\frac{\partial T}{\partial t}\right) = \frac{k_W\left[\frac{T_W - T_P}{z_W - z_P}\right] - k_E\left[\frac{T_P - T_E}{z_P - z_E}\right]}{\Delta z}$$

using the same relation as the theta component

$$\rho\overline{C_v}\left(\frac{\partial T}{\partial t}\right) = \frac{\left.\frac{k}{\Delta z}\right|_{i+1}[T_W - T_P] - \left.\frac{k}{\Delta z}\right|_{i-1}[T_P - T_E]}{\Delta z}$$

$$\left(\frac{\partial T}{\partial t}\right)_i = \frac{1}{\rho_i \overline{C_{vi}} \Delta z}\left[\left.\frac{k}{\Delta z}\right|_{i+1}\left[T_{i+1}-T_i\right]-\left.\frac{k}{\Delta z}\right|_{i-1}\left[T_i-T_{i-1}\right]\right]$$

$$\frac{1}{\rho_i \overline{C_{vi}} \Delta z}\left[\left.\frac{k}{\Delta z}\right|_{i+1}\left[T_{i+1}-T_i\right]-\left.\frac{k}{\Delta z}\right|_{i-1}\left[T_i-T_{i-1}\right]\right]=0$$

Top and Bottom nodes

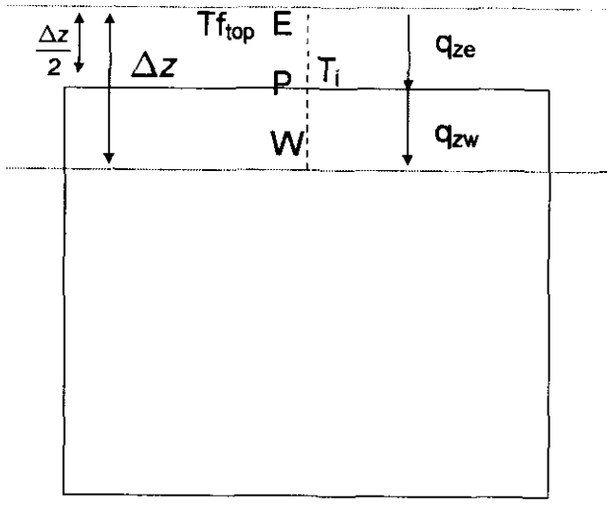

Figure E.8: Axial top node definition.

Mathematical relationships

$$\Delta z = z_{i+1} - z_i = z_i - z_{i-1}$$

$$E = i - 1$$

$$W = i + 1$$

$$P = i$$

$$z_E = z_{i-1}$$

$$z_W = z_{i+1}$$

$$z_{i+1} = z_{i-1}$$

$$\left.\frac{k}{\Delta z}\right|_{i+1} = 2\left[\left.\frac{\Delta z}{k}\right|_{i} + \left.\frac{\Delta z}{k}\right|_{i+1}\right]^{-1}$$

$$\left.\frac{k}{\Delta z}\right|_{i-1} = 2\left[\left.\frac{\Delta z}{k}\right|_{i-1} + \left.\frac{\Delta z}{k}\right|_{i}\right]^{-1}$$

$$\frac{\partial}{\partial z} = \frac{1}{2}\Delta z$$ (Halve of the control volume for the top and bottom)

Top side

$$q_{ze} = h\left(Tf_{top} - T_i\right)$$

$$q_{zw} = -k\left.\frac{\partial T}{\partial z}\right|_{i+1}$$

Bottom side

$$q_{zw} = h\left(Tf_{bottom} - T_i\right)$$

$$q_{ze} = -k\left.\frac{\partial T}{\partial z}\right|_{i-1}$$

$$\rho\overline{C_v}\left(\frac{\partial T}{\partial t}\right) = k\frac{\partial^2 T}{\partial z^2}$$

$$\rho\overline{C_v}\left(\frac{\partial T}{\partial t}\right) = -\frac{\partial}{\partial z}(q_z)$$

$$\rho\overline{C_v}\left(\frac{\partial T}{\partial t}\right) = -\frac{(q_{zw} - q_{ze})}{\frac{\Delta z}{2}}$$

$$\rho\overline{C_v}\left(\frac{\partial T}{\partial t}\right)=-\frac{2}{\Delta z}\left[-k\frac{\partial T}{\partial z}\bigg|_{i+1}-h\left(Tf_{top}-T_i\right)\right]$$

$$\rho\overline{C_v}\left(\frac{\partial T}{\partial t}\right)=\frac{2}{\Delta z}\left[\frac{k}{\Delta z}\bigg|_{i+1}\left(T_W-T_i\right)+h\left(Tf_{top}-T_i\right)\right]$$

$$\left(\frac{\partial T}{\partial t}\right)_i=\frac{2}{\rho_i\overline{C_{vi}}\Delta z}\left[\frac{k}{\Delta z}\bigg|_{i+1}\left(T_{i+1}-T_i\right)+h\left(Tf_{top}-T_i\right)\right]$$

omitting the transient term

$$\frac{2}{\rho_i\overline{C_{vi}}\Delta z}\left[\frac{k}{\Delta z}\bigg|_{i+1}\left(T_{i+1}-T_i\right)+h\left(Tf_{top}-T_i\right)\right]=0$$

The same process can be followed to derive the equation for the bottom side:

$$\frac{2}{\rho_i\overline{C_{vi}}\Delta z}\left[\frac{k}{\Delta z}\bigg|_{i-1}\left(T_{i-1}-T_i\right)+h\left(Tf_{bottom}-T_i\right)\right]=0$$

APPENDIX F: Experimental data

Hz	N (rpm)	P_in (Pa)	Volume flow (% 1280 L/min)	Volume flow (L/min)
11.3	2000	86189.2	17	36.26
		86120.8	15	32.00
		86042.5	13	27.73
		85964.2	11	23.46
		85886.0	9	19.20
12.43	2200	86159.9	24	51.20
		86081.6	22	46.93
		85983.8	20	42.66
		85886.0	18	38.40
		85807.7	16	34.13
		85729.5	14	29.86
		85641.5	12	25.60
		85558.3	10	21.33
		85485.0	8	17.06
13.56	2400	86120.8	30	64.00
		86022.9	28	59.73
		85910.4	26	55.46
		85807.7	24	51.20
		85709.9	22	46.93
		85607.2	20	42.66
		85514.3	18	38.40
		85416.5	16	34.13
		85338.2	14	29.86
		85260.0	12	25.60
		85162.2	10	21.33
		85079.0	8	17.06
14.69	2600	86071.8	35	74.66
		85939.8	33	70.40
		85807.7	31	66.13
		85685.5	29	61.86
		85568.1	27	57.60
		85455.6	25	53.33
		85357.8	23	49.06
		85260.0	21	44.80
		85162.2	19	40.53
		85054.6	17	36.26
		84961.6	15	32.00
		84878.5	13	27.73
		84790.5	11	23.46
		84702.4	9	19.20
15.82	2800	86013.2	40	85.33
		85876.2	38	81.06

		85729.5	36	76.80
		85592.5	34	72.53
		85445.8	32	68.26
		85328.4	30	64.00
		85220.8	28	59.73
		85108.4	26	55.46
		84995.9	24	51.20
		84883.4	22	46.93
		84785.6	20	42.66
		84673.1	18	38.40
		84594.8	16	34.13
		84497.0	14	29.86
		84399.2	12	25.60
		84286.7	10	21.33
		84203.6	8	17.06
16.95	3000	85939.8	44.5	94.93
		85856.6	42.5	90.66
		85714.8	40.5	86.40
		85553.4	38.5	82.13
		85387.1	36.5	77.86
		85254.1	34.5	73.60
		85113.3	32.5	69.33
		84986.1	30.5	65.06
		84868.7	28.5	60.80
		84741.6	26.5	56.53
		84619.3	24.5	52.26
		84506.8	22.5	48.00
		84389.4	20.5	43.73
		84286.6	18.5	39.46
		84188.9	16.5	35.20
		84086.2	14.5	30.93
		83988.4	12.5	26.66
		83890.6	10.5	22.40
		83783.0	8.5	18.13
18.08	3200	85856.6	48.5	103.46
		85758.8	46.5	99.20
		85592.5	44.5	94.93
		85426.3	42.5	90.66
		85260.0	40.5	86.40
		85113.3	38.5	82.13
		84966.5	36.5	77.86
		84795.4	34.5	73.60
		84634.0	32.5	69.33
		84511.7	30.5	65.06
		84399.4	28.5	60.80
		84267.1	26.5	56.53
		84149.8	24.5	52.26
		84032.4	22.5	48.00

		83905.2	20.5	43.73
		83807.4	18.5	39.46
		83694.9	16.5	35.20
		83587.3	14.5	30.93
		83489.5	12.5	26.66
		83381.9	10.5	22.40
		83274.3	8.5	18.13
19.21	3400	85798.0	53	113.06
		85661.0	51	108.80
		85485.0	49	104.53
		85299.1	47	100.26
		85132.8	45	96.00
		84942.1	43	91.73
		84795.4	41	87.46
		84609.5	39	83.20
		84453.0	37	78.93
		84306.3	35	74.66
		84169.3	33	70.40
		84037.3	31	66.13
		83900.3	29	61.86
		83783.0	27	57.60
		83646.0	25	53.33
		83528.6	23	49.06
		83401.5	21	44.80
		83293.9	19	40.53
		83196.1	17	36.26
		83073.8	15	32.00
		82804.8	13	27.73
		82697.2	11	23.46
		82589.6	9	19.20
20.34	3600	85719.7	57	121.6
		85494.7	55	117.33
		85274.6	53	113.06
		85098.6	51	108.80
		84917.6	49	104.53
		84736.7	47	100.26
		84565.5	45	96.00
		84399.2	43	91.73
		84242.7	41	87.46
		84076.4	39	83.20
		83915.0	37	78.93
		83768.3	35	74.66
		83621.6	33	70.40
		83489.5	31	66.13
		83352.6	29	61.86
		83225.4	27	57.60
		83098.3	25	53.33
		82971.1	23	49.06

		82765.7	21	44.80
		82589.6	19	40.53
		82472.2	17	36.26
		82359.7	15	32.00
		82247.3	13	27.73
		82139.7	11	23.46
		82027.2	9	19.20
21.47	3800	85636.6	62	132.26
		85455.6	60	128.00
		85250.2	58	123.73
		85049.7	56	119.46
		84854.0	54	115.20
		84653.5	52	110.93
		84467.7	50	106.66
		84291.6	48	102.40
		84110.6	46	98.13
		83939.5	44	93.86
		83778.1	42	89.60
		83616.7	40	85.33
		83470.0	38	81.06
		83308.6	36	76.80
		83152.1	34	72.53
		83005.3	32	68.26
		82726.6	30	64.00
		82589.6	28	59.73
		82462.5	26	55.46
		82325.5	24	51.20
		82203.2	22	46.93
		82071.2	20	42.66
		81958.7	18	38.40
		81846.2	16	34.13
		81728.8	14	29.86
		81601.7	12	25.60
		81474.5	10	21.33
		81366.9	8	17.06
22.6	4000	85475.2	69	147.20
		85240.4	67	142.93
		85005.7	65	138.66
		84819.8	63	134.40
		84604.6	61	130.13
		84409.0	59	125.86
		84213.3	57	121.60
		84027.5	55	117.33
		83822.1	53	113.06
		83646.0	51	108.80
		83450.4	49	104.53
		83274.3	47	100.26
		83117.8	45	96.00

		82941.7	43	91.73
		82785.2	41	87.46
		82628.7	39	83.20
		82457.6	37	78.93
		82310.8	35	74.66
		82159.2	33	70.40
		82012.5	31	66.13
		81875.6	29	61.86
		81728.8	27	57.60
		81591.9	25	53.33
		81464.7	23	49.00
		81347.4	21	44.80
		81210.4	19	40.53
		81093.0	17	36.26
		80975.7	15	32.00
		80858.3	13	27.73
		80731.1	11	23.46
		80604.0	9	19.20
23.73	4200	85343.1	74	157.86
		85147.5	72	153.60
		84902.9	70	149.33
		84707.3	68	145.06
		84487.2	66	140.80
		84276.9	64	136.53
		84061.7	62	132.26
		83880.8	60	128.00
		83680.3	58	123.73
		83474.8	56	119.46
		83293.9	54	115.20
		83103.1	52	110.93
		82936.9	50	106.66
		82755.9	48	102.40
		82584.7	46	98.13
		82418.4	44	93.86
		82257.0	42	89.60
		82100.5	40	85.33
		81924.5	38	81.06
		81792.4	36	76.80
		81631.0	34	72.53
		81489.2	32	68.26
		81352.2	30	64.00
		81200.6	28	59.73
		81058.8	26	55.46
		80936.5	24	51.20
		80804.5	22	46.93
		80692.0	20	42.66
		80584.4	18	38.40
		80452.3	16	34.13

		80320.3	14	29.86
		80198.0	12	25.60
		80080.6	10	21.33
		79973.0	8	17.06
24.86	4400	85230.6	76.5	163.20
		85005.7	74.5	158.93
		84741.6	72.5	154.66
		84511.7	70.5	150.40
		84286.7	68.5	146.13
		84086.2	66.5	141.86
		83861.2	64.5	137.60
		83660.7	62.5	133.33
		83416.2	60.5	129.06
		83235.2	58.5	124.80
		83039.6	56.5	120.53
		82843.9	54.5	116.26
		82667.9	52.5	112.00
		82486.9	50.5	107.73
		82296.2	48.5	103.46
		82105.4	46.5	99.20
		81944.0	44.5	94.93
		81787.5	42.5	90.66
		81611.5	40.5	86.40
		81445.2	38.5	82.13
		81274.0	36.5	77.86
		81127.3	34.5	73.60
		80965.9	32.5	69.33
		80819.2	30.5	65.06
		80682.2	28.5	60.80
		80545.3	26.5	56.53
		80423.0	24.5	52.26
		80276.3	22.5	48.00
		80158.9	20.5	43.73
		80041.5	18.5	39.46
		79904.6	16.5	35.20
		79792.1	14.5	30.93
		79660.0	12.5	26.66
		79528.0	10.5	22.40
		79415.5	8.5	18.13
25.99	4600	85108.4	79	168.53
		84780.7	77	164.26
		84516.6	75	160.00
		84291.6	73	155.73
		84076.4	71	151.46
		83812.3	69	147.20
		83572.7	67	142.93
		83347.7	65	138.66
		83147.2	63	134.40

		82941.7	61	130.13
		82707.0	59	125.86
		82491.8	57	121.60
		82310.8	55	117.33
		82120.1	53	113.06
		81904.9	51	108.80
		81728.8	49	104.53
		81533.2	47	100.26
		81376.7	45	96.00
		81200.6	43	91.73
		81044.1	41	87.46
		80882.7	39	83.20
		80711.6	37	78.93
		80545.3	35	74.66
		80398.5	33	70.40
		80242.0	31	66.13
		80114.9	29	61.86
		79953.5	27	57.60
		79821.4	25	53.33
		79704.1	23	49.06
		79586.7	21	44.80
		79454.6	19	40.53
		79327.5	17	36.26
		79205.2	15	32.00
		79087.8	13	27.73
		78950.9	11	23.46
		78818.8	9	19.20
27.12	4800	84966.5	83	177.06
		84751.3	81	172.80
		84467.7	79	168.53
		84223.1	77	164.26
		83988.4	75	160.00
		83685.1	73	155.73
		83470.0	71	151.46
		83215.6	69	147.20
		82971.1	67	142.93
		82726.6	65	138.66
		82530.9	63	134.40
		82315.7	61	130.13
		82100.5	59	125.86
		81904.9	57	121.60
		81709.3	55	117.33
		81503.9	53	113.06
		81318.0	51	108.80
		81122.4	49	104.53
		80926.7	47	100.26
		80750.7	45	96.00
		80574.6	43	91.73

		80418.1	41	87.46
		80242.0	39	83.20
		80085.5	37	78.93
		79899.7	35	74.66
		79762.7	33	70.40
		79606.2	31	66.13
		79464.4	29	61.86
		79312.8	27	57.60
		79185.6	25	53.33
		79058.5	23	49.06
		78921.5	21	44.80
		78804.2	19	40.53
		78677.0	17	36.26
		78549.8	15	32.00
		78422.7	13	27.73
		78275.9	11	23.46
		78158.6	9	19.20
28.25	5000	84800.2	86	183.46
		84497.0	84	179.2
		84223.1	82	174.93
		83929.7	80	170.66
		83670.5	78	166.40
		83430.8	76	162.13
		83186.3	74	157.86
		82932.0	72	153.60
		82687.4	70	149.33
		82472.2	68	145.06
		82232.6	66	140.80
		81992.9	64	136.53
		81787.5	62	132.26
		81552.8	60	128.00
		81357.1	58	123.73
		81141.9	56	119.46
		80956.1	54	115.20
		80765.4	52	110.93
		80545.3	50	106.66
		80374.1	48	102.40
		80178.5	46	98.13
		79987.7	44	93.86
		79836.1	42	89.60
		79664.9	40	85.33
		79508.4	38	81.06
		79327.5	36	76.80
		79185.6	34	72.53
		79019.3	32	68.26
		78872.6	30	64.00
		78725.9	28	59.73
		78589.0	26	55.46

		78461.8	24	51.20
		78334.6	22	46.93
		78197.7	20	42.66
		78051.0	18	38.40
		77914.0	16	34.13
		77777.1	14	29.86
		77649.9	12	25.60
		77532.5	10	21.33
		77415.2	8	17.06

Table F.1: Data obtained from the experimental test bench.

APPENDIX G: Additional EES simulation results

The appendix will contain the results obtained from the EES simulation model for higher inlet temperatures.

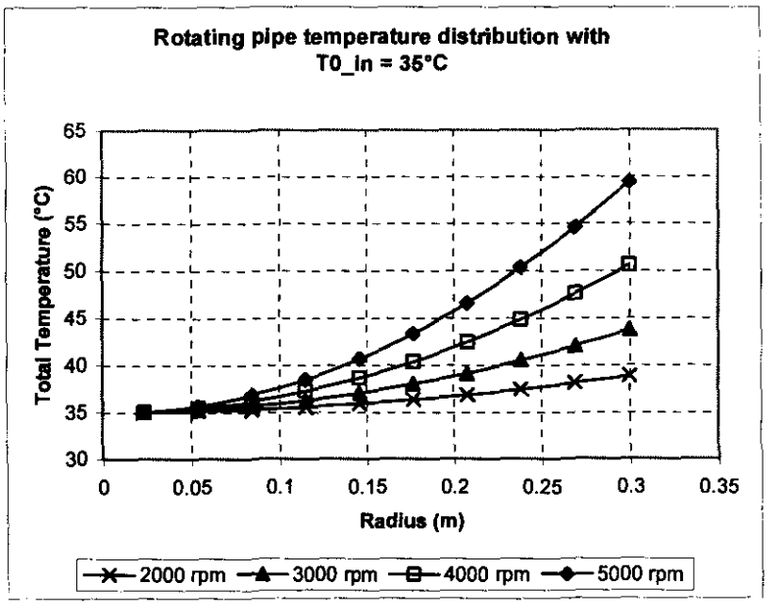

Figure G.1: Rotating pipe temperature distribution for various rotational speeds at an inlet temperature of 35°C.

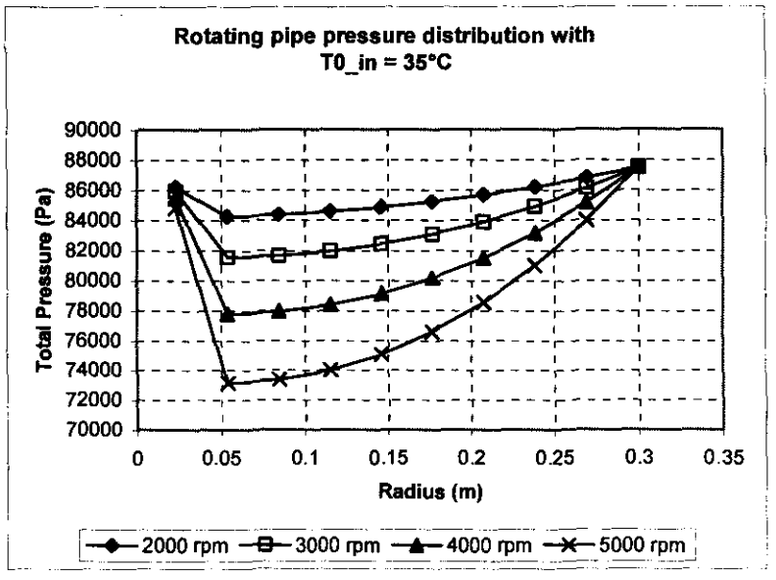

Figure G.2: Rotating pipe pressure distribution for various rotational speeds at an inlet temperature of 35°C.

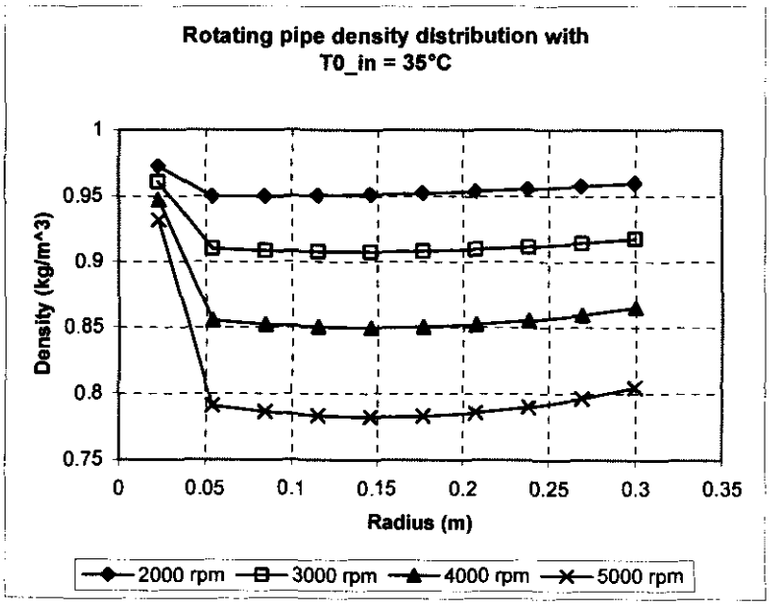

Figure G.3: Rotating pipe density distribution for various rotational speeds at an inlet temperature of 35°C.

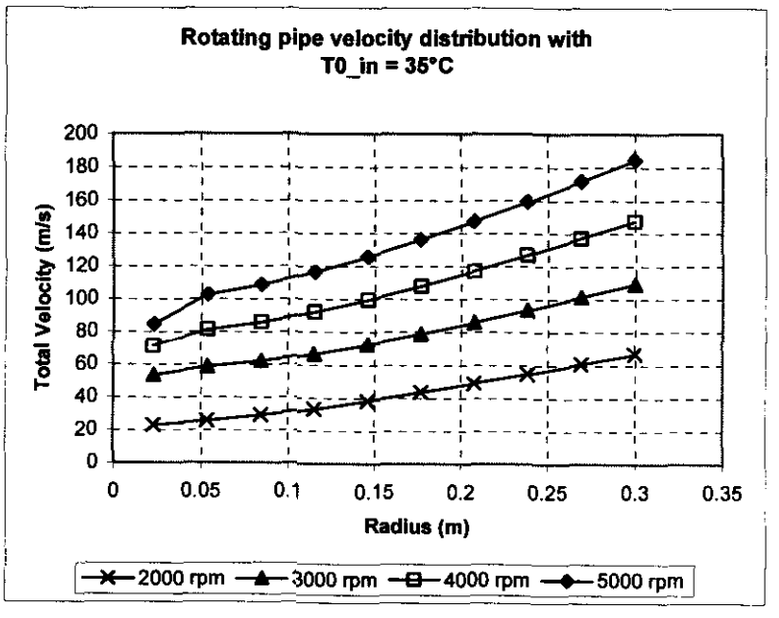

Figure G.4: Rotating pipe velocity distribution for various rotational speeds at an inlet temperature of 35°C.

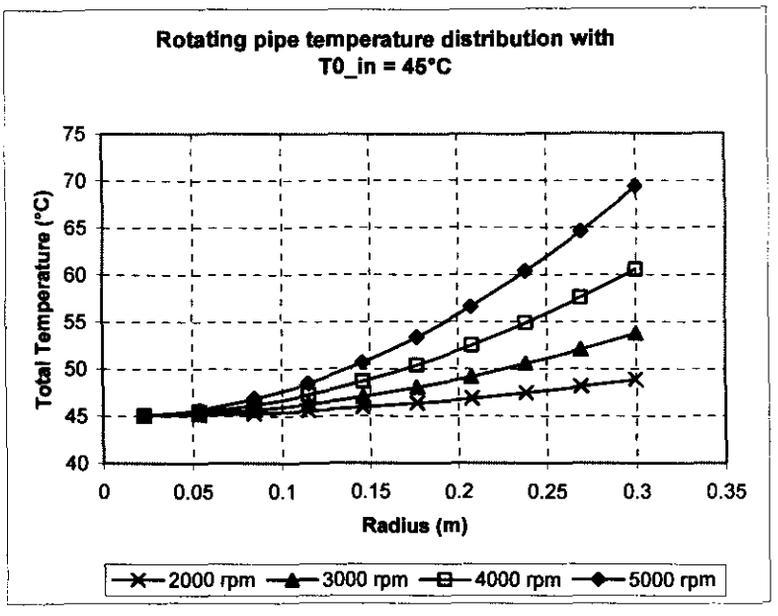

Figure G.5: Rotating pipe temperature distribution for various rotational speeds at an inlet temperature of 45°C.

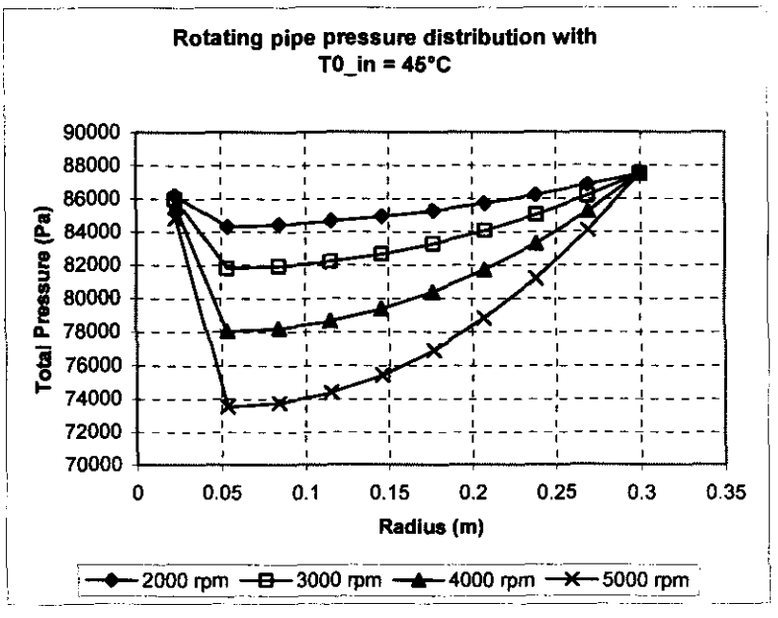

Figure G.6: Rotating pipe pressure distribution for various rotational speeds at an inlet temperature of 45°C.

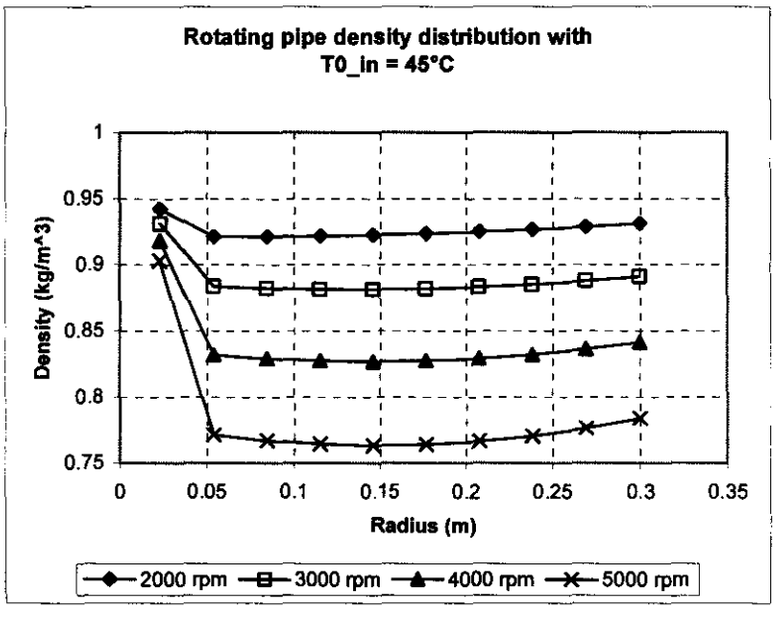

Figure G.7: Rotating pipe density distribution for various rotational speeds at an inlet temperature of 45°C.

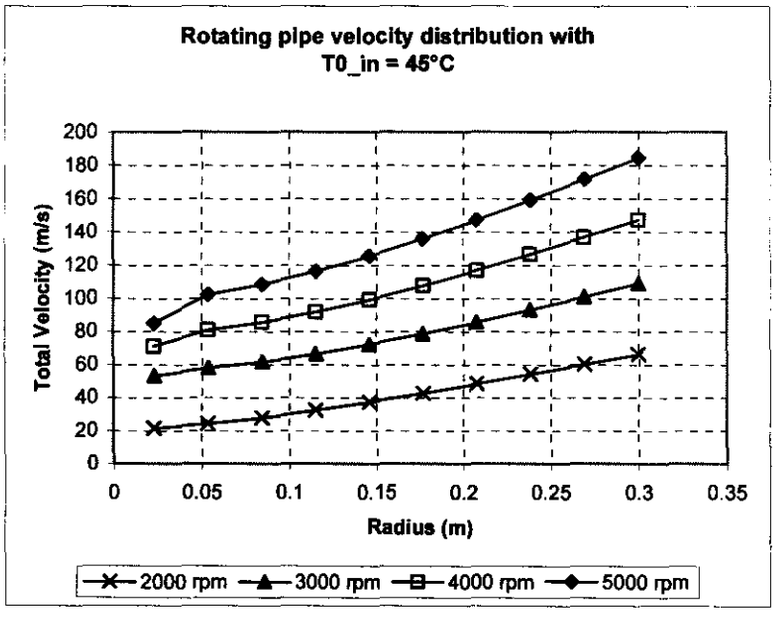

Figure G.8: Rotating pipe velocity distribution for various rotational speeds at an inlet temperature of 45°C.

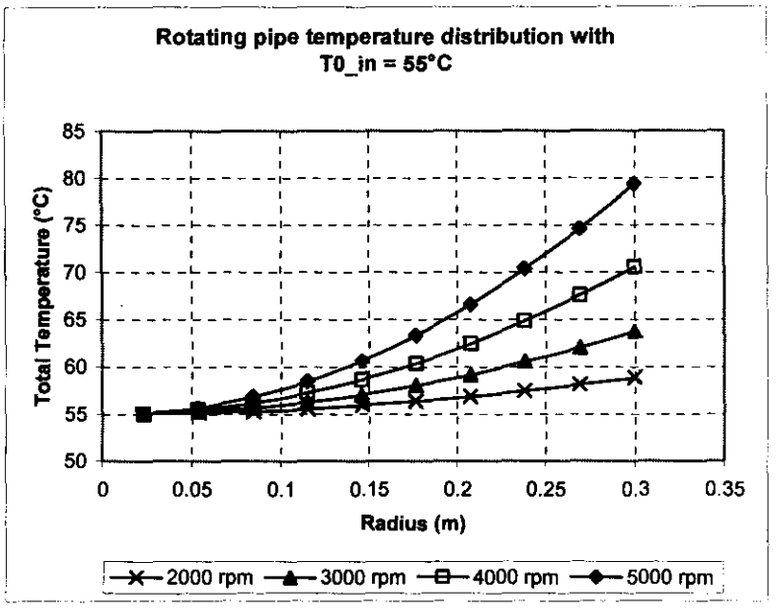

Figure G.9: Rotating pipe temperature distribution for various rotational speeds at an inlet temperature of 55°C.

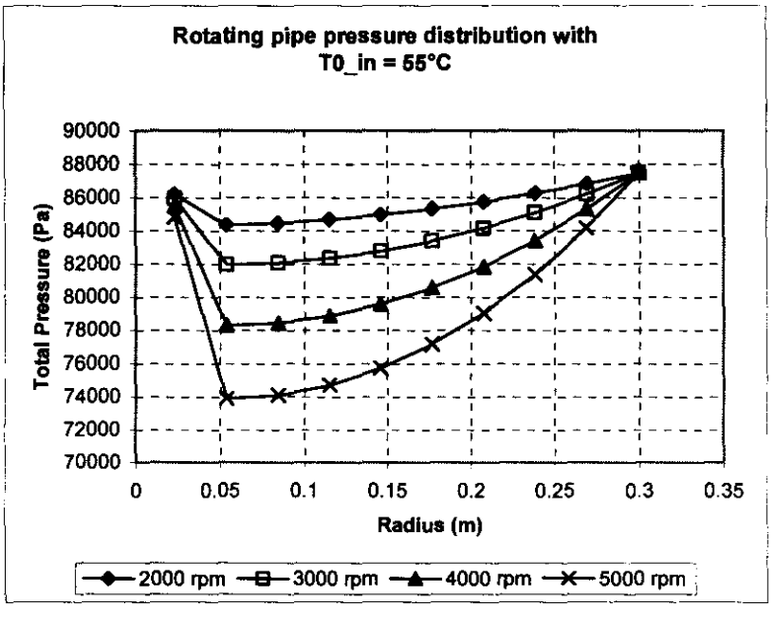

Figure G.10: Rotating pipe pressure distribution for various rotational speeds at an inlet temperature of 55°C.

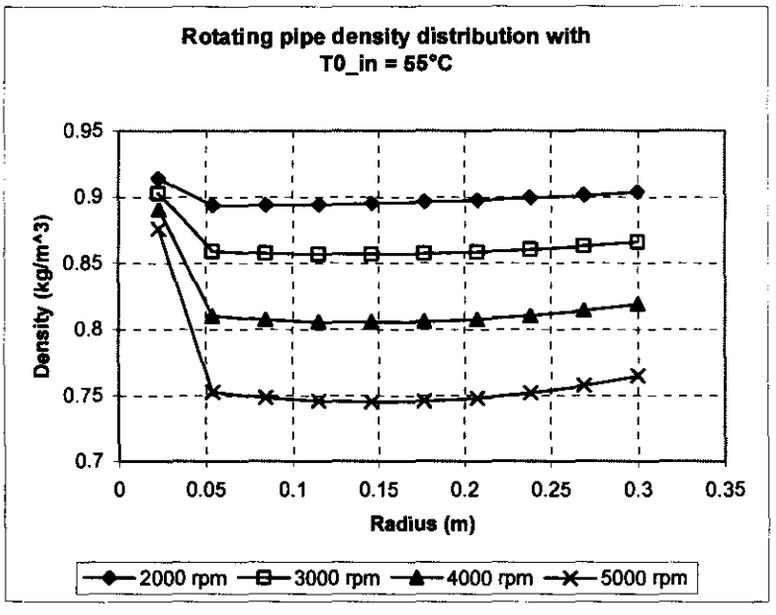

Figure G.11: Rotating pipe density distribution for various rotational speeds at an inlet temperature of 55°C.

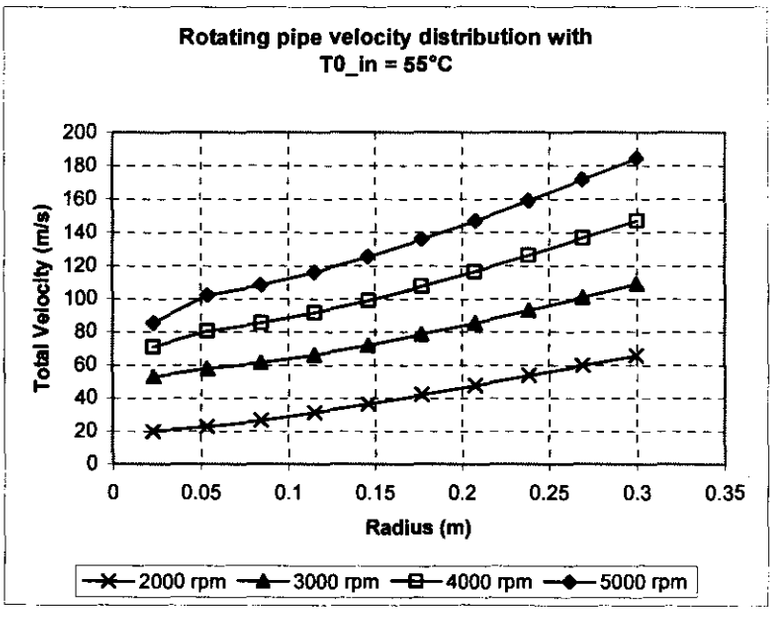

Figure G.12: Rotating pipe velocity distribution for various rotational speeds at an inlet temperature of 55°C.